

New aspects into pathophysiology and molecular diagnostics of myeloproliferative neoplasms

Inaugural Dissertation

zur

Erlangung des Doktorgrades

Dr. nat. med.

der Medizinischen Fakultät

und

der Mathematisch-Naturwissenschaftlichen Fakultät

der Universität zu Köln



vorgelegt von

Dr. med. Dipl. Biol. Udo Siebolts
aus Aurich

Leipzig, 2011

Berichterstatter / Berichterstatterin: Prof. Dr. J. Schultze
Prof. Dr. J. Brüning

Tag der letzten mündlichen Prüfung: 21.12.2011

Erklärung:

Ich versichere, dass ich die von mir vorgelegte Dissertation selbständig angefertigt, die benutzten Quellen und Hilfsmittel vollständig angegeben und die Stellen der Arbeit – einschließlich Tabellen, Karten und Abbildungen –, die anderen Werken im Wortlaut oder dem Sinn nach entnommen sind, in jedem Einzelfall als Entlehnung kenntlich gemacht habe; dass diese Dissertation noch keiner anderen Fakultät oder Universität zur Prüfung vorgelegen hat; dass sie – abgesehen von unten angegebenen Teilpublikationen – noch nicht veröffentlicht worden ist sowie, dass ich eine solche Veröffentlichungen vor Abschluss des Promotionsverfahrens nicht vornehmen werde. Die Bestimmungen dieser Promotionsordnung sind mir bekannt. Die von mir vorgelegte Dissertation ist von Frau Professor Dr. Claudia Wickenhauser betreut worden.



Leipzig, den 21.04.2011

Dr. Udo Siebolts

1. LIST OF PUBLICATIONS	1
1.1 Main publications	1
1.2 Additional publications	2
2. ABSTRACT	3
2. ZUSAMMENFASSUNG	4
3. INTRODUCTION	6
3.1 Myeloproliferative neoplasms	6
3.1.1 Chronic myelogenous leukemia	7
3.1.2 Philadelphia chromosome negative classic myeloproliferative neoplasms	9
3.2 Molecular pathophysiology of Ph- negative myeloproliferative neoplasms	11
3.3 Molecular diagnostics of myeloproliferative neoplasms	13
4. AIMS AND MAJOR FINDINGS OF THIS PhD THESIS	18
4.1 Aims	18
4.2 Major findings	18
5. PRESENT INVESTIGATION	19
5.1 Structural, antigenetic and transcriptional characteristics in peripheral blood CD34+ progenitor cells from polycythemia vera patients: evidence for delayed determination (Wickenhauser C., Perez F., Siebolts U., et al. <i>Int J Oncol.</i> (2003): 23, 437-443)	19
5.2 Quantification of clonal hematopoiesis in polycythemia vera (Siebolts U., Ates M., Spitz R., et al. <i>Virchows Arch.</i> (2005): 447, 947-953)	20
5.3 Dualism of mixed chimerism between hematopoiesis and stroma in chronic idiopathic myelofibrosis after allogeneic stem cell transplantation (Thiele J., Varus E., Siebolts U., et al. <i>Histol Histopathol.</i> (2007): 22, 365-372)	21
5.4 Differences in proportion and dynamics of recipient hematopoiesis following hematopoietic cell transplantation in CML and IMF (Siebolts U., Thiele J., Zander T., et al. <i>Oncol Rep.</i> (2008): 19, 287-292)	23
5.5 Imbalance of DNA-dependent protein kinase subunits in polycythemia vera peripheral blood stem cells (Siebolts U., Breuhahn K., Hennecke A., et al. <i>Int J Cancer.</i> (2009): 124, 600-607)	24
5.6 Tissues from routine pathology archives are suitable for microRNA analyses by quantitative PCR (Siebolts U., Varnholt H., Drebber U., et al. <i>J Clin Pathol.</i> (2009): 62, 84-88)	25
5.7 Allele-specific wild-type blocker quantitative PCR for highly sensitive detection of rare JAK2 p.V617F point mutation in primary myelofibrosis as an appropriate tool for the monitoring of molecular remission following therapy (Siebolts U., Lange T., Niederwieser D., et al. <i>J Clin Pathol.</i> (2010): 63, 370-372)	26

6. PROGRESS AND FURTHER ACTIVITIES DURING THE PhD THESIS	28
6.1 Awards / Talks	29
7. ADDITIONAL PUBLICATIONS DURING THE PhD HESIS	31
8. REFERENCES	34
9. PUBLICATIONS	45
10. ACKNOWLEDGEMENTS	140
11. CURRICULUM VITAE / LIST OF PUBLICATIONS	141

1. List of publications

This PhD thesis is based on the following publications:

1.1 Main publications

Wickenhauser C., Perez F., **Siebolts U.**, Lorenzen J., Varus E., Frimpong S. and Thiele J. Structural, antigenetic and transcriptional characteristics in peripheral blood CD34+ progenitor cells from polycythemia vera patients: evidence for delayed determination. *Int J Oncol.* 2003; 23, 437-43.

Siebolts U., Ates M., Spitz R., Thiele J. and Wickenhauser C. Quantification of clonal hematopoiesis in polycythemia vera. *Virchows Arch.* 2005; 447, 947-53.

Thiele J., Varus E., **Siebolts U.**, Kvasnicka H. M., Wickenhauser C., Metz K. A., Beelen D. W., Ditschkowski M., Zander A. and Kroger N. Dualism of mixed chimerism between hematopoiesis and stroma in chronic idiopathic myelofibrosis after allogeneic stem cell transplantation. *Histol Histopathol.* 2007; 22, 365-72.

Siebolts U., Thiele J., Zander T., Ditschkowski M., Beelen D. W., Kroger N., Fehse B. and Wickenhauser C. Differences in proportion and dynamics of recipient hematopoiesis following hematopoietic cell transplantation in CML and IMF. *Oncol Rep.* 2008; 19, 287-92.

Siebolts U., Breuhahn K., Hennecke A., Schultze J. L. and Wickenhauser C. Imbalance of DNA-dependent protein kinase subunits in polycythemia vera peripheral blood stem cells. *Int J Cancer.* 2009; 124, 600-7.

Siebolts U., Varnholt H., Drebber U., Dienes H. P., Wickenhauser C. and Odenthal M. Tissues from routine pathology archives are suitable for microRNA analyses by quantitative PCR. *J Clin Pathol.* 2009; 62, 84-8.

Siebolts U., Lange T., Niederwieser D. and Wickenhauser C. Allele-specific wild-type blocker quantitative PCR for highly sensitive detection of rare JAK2 p.V617F point mutation in primary myelofibrosis as an appropriate tool for the monitoring of molecular remission following therapy. *J Clin Pathol.* 2010; 63, 370-2.

1.2 Additional publications

Kappert K., Sparwel J., Sandin A., Seiler A., **Siebolts U.**, Leppanen O., Rosenkranz S. and Ostman A. Antioxidants relieve phosphatase inhibition and reduce PDGF signaling in cultured VSMCs and in restenosis. *Arterioscler Thromb Vasc Biol.* 2006: 26, 2644-51.

Gerharz M., Baranowsky A., **Siebolts U.**, Eming S., Nischt R., Krieg T. and Wickenhauser C. Morphometric analysis of murine skin wound healing: standardization of experimental procedures and impact of an advanced multitissue array technique. *Wound Repair Regen.* 2007: 15, 105-12.

Veit G., Zimina E. P., Franzke C. W., Kutsch S., **Siebolts U.**, Gordon M. K., Bruckner-Tuderman L. and Koch M. Shedding of collagen XXIII is mediated by furin and depends on the plasma membrane microenvironment. *J Biol Chem.* 2007: 282, 27424-35.

Odenthal M., **Siebolts U.**, Ernestus K., Disse D., Dienes H. P. and Wickenhauser C. Immunoglobulin heavy chain gene analysis in bone marrow biopsies and corresponding lymph node specimens: dependency on pre-treatment, histological subtype and extension of B-cell lymphoma. *Int J Mol Med.* 2008: 21, 569-76.

Markert E.*, **Siebolts U.***, Odenthal M., Kreuzer K. A. and Wickenhauser C. High diagnostic value of morphologic examination and molecular analysis of bone marrow biopsies in a case of BCR-ABL+ CML with clusters of blasts. *Int J Hematol.* 2009: 89, 294-7.

Markert E.*, **Siebolts U.***, Habbig S., Odenthal M., Dienes H. P., Stippel D. L., Hoppe B. and Wickenhauser C. Evolution of PTLTD following renal transplantation in a child. *Pediatr Transplant.* 2009: 13, 379-83.

Utermohlen O., Baschuk N., Abdullah Z., Engelmann A., **Siebolts U.**, Wickenhauser C., Stocking C. and Kronke M. Immunologic hurdles of therapeutic stem cell transplantation. *Biol Chem.* 2009: 390, 977-83.

* Both authors contributed equally

2. Abstract

The Philadelphia chromosome negative myeloproliferative neoplasms (MPN) comprise diverse entities of hematopoietic stem cell disorders with hematopoietic stem cell transplantation as the only curative therapeutic option. A collective finding of some subgroups is the activating point mutation of *JAK2* p.V617F, important for diagnosis and detection of minimal residual disease (MRD) but a rather late event in the course of MPN.

In this study, we first focused on characteristics of the neoplastic peripheral blood CD34-positive stem cell fraction. Thus, we could reveal a characteristic aberrant morphology and phenotype, and performing cDNA- array analysis most notably an imbalance of DNA-dependent protein kinase subunits which may contribute to the accumulation of chromosomal aberrations, accumulation of hematopoietic cell, and prolongation of CD34- positive peripheral blood stem cells life span (Wickenhauser, Perez, et al. 2003; Siebolts, Breuhahn, et al. 2009). Moreover, there is evidence of a distinct, non-neoplastic, CD34- positive peripheral blood stem cell population which may offer perspectives in treatment of the diseases (Siebolts, Ates, et al. 2005).

The CD34- positive stem cell fraction, as the underlying source of the malignancy, is of course of particular importance, not only for understanding of the pathophysiological process but also for understanding of relapse and regenerative incidents. Performing fluorescence in situ hybridization on bone marrow biopsies, we found an almost complete chimerism following stem cell transplantation concerning the differentiated hematopoiesis, whereas CD34- positive cells remained of recipient origin to a higher proportion (Thiele, Varus, et al. 2007; Siebolts, Thiele, et al. 2008).

Since hematopoietic stem cell transplantation, especially after invention of reduced intensity conditioning (RIC) is a feasible curative option for an increasing number of MPN patients, reliable detection of the specific *JAK2* p.V617F mutation as a sign of minimal residual disease (MRD) becomes more and more important. Therefore, we created in combination of a robust QPCR with a wild- type blocking PCR, a powerful tool for reliable detection of MRD in these patients (Siebolts, Lange, et al. 2010).

Future prospects of MPN research will also focus on the newly-discovered field of non-coding RNA. Therefore, we tested the possibility to perform further retrospective analysis on easily accessible paraffin embedded formalin fixed tissue, and could show for the first time that extraction of sufficient amount of miRNA, with subsequent expression analysis is possible even after decalcification and also after decades (Siebolts, Varnholt, et al. 2009).

2. Zusammenfassung

Die Transplantation hämatopoetischer Stammzellen gilt zurzeit als die einzige kurative Therapie der Philadelphia Chromosom negativen myeloproliferativen Neoplasien und die Kontrolle der minimalen Resterkrankung ist somit von besonderem Interesse. Die in viele Fällen nachweisbare aktivierende Punktmutation *JAK2* p.V617F stellt wahrscheinlich nur ein Epiphänomen der Erkrankungen dar, ist aber für die Diagnostik und Nachweis einer minimalen Resterkrankung von besonderer Bedeutung.

Die vorliegende Arbeit zeigte in ersten Untersuchungen einen charakteristischen aberranten Phänotyp der neoplastischen CD34- positiven Stammzellen des peripheren Blutes, zusammen mit einer Unausgewogenheit der verschiedenen Untereinheiten der DNA- abhängigen Proteinkinase. Dies könnte ursächlich zu verschiedenen bekannten Veränderungen im Rahmen der Erkrankung beitragen wie z.B. Anreicherung von genetischen Störungen, Vermehrung der peripheren Blutzellen sowie die Verlängerung der Lebenspanne CD34- positiver hämatopoetischer Stammzellen (Wickenhauser, Perez, et al. 2003; Siebolts, Breuhahn, et al. 2009). Zudem ergeben sich Hinweise auf eine persistierende nicht neoplastische CD34- positive hämatopoetische Stammzellpopulation im peripheren Blut, die zukünftig im Sinne einer Reservepopulation therapeutische Optionen bieten könnte (Siebolts, Ates, et al. 2005).

Weitere Untersuchungen mittels Fluoreszenz in situ Hybridisierung an Knochenmarkbiopsien zeigten, dass nach Stammzelltransplantation ein nahezu vollständiger Spenderchimärismus, vor allem der ausdifferenzierten hämatopoetischen Zellen bei Patienten mit unkompliziertem Verlauf schon früh erreicht wird, jedoch eine signifikante CD34- positive hämatopoetische Stammzellpopulation als mögliches Reservoir für zukünftige Rezidive verbleibt. (Thiele, Varus, et al. 2007; Siebolts, Thiele, et al. 2008).

Im Rahmen der Stammzelltransplantation *JAK2* p.V617F positiver myeloproliferativer Neoplasien ist eine personalisierte Kontrolle der minimalen Resterkrankung auf molekularer Ebene durch Anwendung moderner, hochempfindlicher Methoden möglich geworden. In weiteren Studien im Rahmen dieser Arbeit gelang uns die Entwicklung einer robusten und hochempfindlichen allelspezifischen quantitativen PCR durch die innovative Reduktion des überwiegenden Anteils kompetitiver Wildtyp DNA (Siebolts, Lange, et al. 2010).

Das neu entdeckte Gebiet der nicht kodierenden RNA eröffnet neue Ansätze zur Diagnostik und Therapie möglicherweise auch der myeloproliferativen Neoplasien. Vor diesem Hintergrund konnten wir zeigen, dass die Möglichkeit besteht, aus archiviertem,

formalinfixierten, teils dekalzifizierten und paraffineingebetteten Material auch nach Jahrzehnten ausreichend Material für vergleichende Expressionsanalysen zu gewinnen (Siebolts, Varnholt, et al. 2009).

3. Introduction

This document presents different aspects of the classic myeloproliferative neoplasms (MPN) and in particular about polycythemia vera (PV) and primary myelofibrosis (PMF). Primarily, questions concerning pathophysiology and diagnostic approaches of the classic Ph⁻ MPN were in the spotlight. The following chapter gives a short synopsis about the actual relevant knowledge of pathophysiology, the new field of targeted therapy and molecular diagnostics in MPN.

3.1 *Myeloproliferative neoplasms*

William Damashek was the first to describe the concept of myeloproliferative disorders in 1951, where the classic myeloproliferative disease (chronic myelogenous leukemia (CML), polycythemia vera (PV), essential thrombocythemia (ET) and primary myelofibrosis (PMF) were defined (Dameshek 1951).

In 2001, the World Health Organization (WHO) committee for the classification of myeloid neoplasms, inaugurated the term chronic myeloproliferative diseases (CMPD) which covers additionally the entities of chronic neutrophilic leukemia (CNL), chronic eosinophilic leukemia/ hypereosinophilic syndrome (CEL/HES) and CMPD, unclassifiable, among with the classic MPD (Jaffe ES 2001; Vardiman JW 2001). In the broader context the CMPDs were considered as one of four major categories of chronic myeloid neoplasms, the other three being myelodysplastic syndromes (MDS), MDS/MPD and mast cell diseases (MCD) (Jaffe ES 2001).

The revised 2008 WHO classification system changed the term disease into neoplasm because of the meanwhile accepted clonal origin of these entities. Now these diseases are subdivided in the category of MPN, which was formerly known as CMPD, and MDS/MPN for MDS/MPD. In addition, the MPN category now includes mast cell diseases whereas the previous CMPD subcategory of CEL/HES is now re-organized into HES, CEL not otherwise categorized (CEL-NOC) and myeloid neoplasms associated with eosinophilia and abnormalities of PDGFRA, PDGFRB and FGFR1 (Table 1). The latter group is now assigned a new category of its own, whereas both HES and CEL-NOC remain subcategories of MPNs

(Table 1) (Vardiman JW 2001; Swerdlow SH 2008; Tefferi and Vardiman 2008; Vardiman, Thiele, et al. 2009).

1. Acute myeloid leukemia
2. Myelodysplastic syndromes (MDS)
3. Myeloproliferative neoplasms (MPN)
3.1 Chronic myelogenous leukemia
3.2 Polycythemia vera
3.3 Essential thrombocythemia
3.4 Primary myelofibrosis
3.5 Chronic neutrophilic leukemia
3.6 Chronic eosinophilic leukemia, not otherwise categorized
3.7 Hypereosinophilic syndrome
3.8 Mast cell diseases
3.9 MPNs, unclassifiable
4. MDS/MPN
4.1 Chronic myelomonocytic leukemia
4.2 Juvenile myelomonocytic leukemia
4.3 Atypical chronic myeloid leukemia
4.4 MDS/MPN, unclassifiable
5. Myeloid neoplasms associated with eosinophilia and abnormalities of PDGFRA, PDGFRB, or FGFR1
5.1 Myeloid neoplasms associated with PDGFRA rearrangement
5.2 Myeloid neoplasms associated with PDGFRB rearrangement
5.3 Myeloid neoplasms associated with FGFR1 rearrangement (8p11 myeloproliferative syndrome)
Table 1. The 2008 World Health Organization classification scheme for myeloid neoplasms (Tefferi and Vardiman 2008)

This new classification can be called a paradigm shift, because for the first time genetic information was incorporated with morphologic, cytochemical, immunophenotypic, and clinical information into diagnostic algorithms for the myeloid neoplasms.

Subsequently this PhD thesis will focus on the subgroup of so-called classic myeloproliferative disease or neoplasm, which can be subdivided into Philadelphia Chromosome positive (CML) and negative entities (PV, ET, PMF).

3.1.1 Chronic myelogenous leukemia

Chronic myelogenous leukemia (CML) is a clonal MPN of a pluripotent stem cell with a specific cytogenetic abnormality, the Philadelphia chromosome (Ph), involving myeloid,

erythroid, megakaryocytic, B lymphoid, and sometimes T lymphoid cells, but not marrow fibroblasts (Silver 2003). Concerning the classic MPN, it is by far the most frequent entity with an annual incidence of 1.6 per 100,000 people, with slightly more men than women to be affected.

CML has a biphasic or triphasic clinical course (Medina, Kantarjian, et al. 2003). Approximately 90% of patients are diagnosed in the chronic phase, but the disease eventually evolves to a blast phase unless successfully treated. Approximately two-thirds of patients manifest an accelerated phase. A distinct feature of disease progression, is the appearance of additional cytogenetic abnormalities in the Ph- positive cells. This phenomenon, known as clonal evolution, frequently involves a second Philadelphia chromosome, trisomy of chromosome 8, and isochromosome 17 and other abnormalities of chromosome 17 (Kantarjian, Dixon, et al. 1988), although other abnormalities have been described. Clonal evolution is considered a criterion of accelerated phase, although when it represents the only criterion of transformation, it is associated with a better prognosis than other criteria of the accelerated phase (Cortes, Talpaz, et al. 2003).

CML was the first disease where a single chromosomal abnormality, the Philadelphia chromosome was demonstrated as fundamental to the etiology of the disease (Nowell and Hungerford 1960; Geary 2000). 20 years later De Klein et al. demonstrated that the Abelson oncogene (*ABL*) is translocated from chromosome 9 to chromosome 22 in the formation of the Philadelphia chromosome (de Klein, van Kessel, et al. 1982). Although the position of the breakpoint in chromosome 9 is quite variable, the breakpoint in chromosome 22 is clustered in an area called *BCR* for breakpoint cluster region.

The normal cellular *BCR* gene encodes a 160-kD phosphoprotein associated with serine/threonine kinase activity. The *BCR* gene is the site of different breakpoints of the known alternative forms of the Philadelphia chromosome translocation found in CML and acute lymphocytic leukemia (Groffen, Stephenson, et al. 1984; Shtivelman, Lifshitz, et al. 1985; Hermans, Heisterkamp, et al. 1987). These alternative breakpoints join different exon sets of *BCR* to a common subset of the exons of the *ABL1* gene. This fusion results in mainly two alternative chimeric oncogene products called p210(*BCR-ABL*) and p185(*BCR-ABL*). The activation of *ABL* tyrosine kinase activity is necessary for the oncogenic potential of the chimeric oncogene (Maru and Witte 1991).

CML was one of the first and most successful stories for allogeneic transplantation (Hughes, Morgan, et al. 1991) and it was in this context that molecular monitoring of so-called minimal residual disease (MRD), by sensitive reverse-transcribed polymerase chain reaction (RT-PCR) techniques was found to be predictive of future relapse (Hughes, Morgan, et al. 1991; Lion, Henn, et al. 1993; Radich, Gehly, et al. 1995). Next came the advent of targeted tyrosine kinase inhibitor (TKI) therapy, which has quickly replaced transplantation as front-line therapy for chronic-phase disease. Given the power of molecular monitoring in the transplantation setting, molecular monitoring was used in the TKI trials as a measure of disease responses. Such monitoring is now advocated for the routine clinical care of CML (Radich 2009).

3.1.2 Philadelphia chromosome negative classic myeloproliferative neoplasms

As described above polycythemia vera (PV), essential thrombocythemia (ET) and primary myelofibrosis (PMF) as the classic Ph- negative MPN are clonal myeloproliferative neoplasms arising from a multipotent progenitor cell.

The finding of a loss of heterozygosity (LOH) on chromosome 9p in MPN suggested that 9p harbors a mutation that contributes to the cause of clonal expansion of hematopoietic cells in these diseases. Independently of each other, five groups found that a high proportion of patients with these myeloproliferative disorders carried a dominant gain-of-function somatic p.V617F point mutation in the *JAK2* gene (Baxter, Scott, et al. 2005; James, Ugo, et al. 2005; Kralovics, Passamonti, et al. 2005; Levine, Wadleigh, et al. 2005; Zhao, Xing, et al. 2005).

The Janus family of tyrosine kinases (JAK1, JAK2, JAK3, TYK2) are cytoplasmatic tyrosine kinases that mediate signaling downstream of different receptor tyrosine kinase, such as the erythropoietin receptor and members of the interleukin receptor family. Normal JAK2 signaling is important in a number of key cellular processes, such as erythropoiesis and thrombopoiesis and therefore great excitement was caused by the finding of the distinct *JAK2* p.V617F mutation.

JAK2 p.V617F occurs at a primitive hematopoietic stem cell level in humans (Jamieson, Gotlib, et al. 2006), causes impairment of *JAK2* regulation and results in the constitutive activation of *JAK2*- *STAT5*, phosphatidylinositol-3-kinase (*PI3K*) and mitogen- activated

protein kinase / extracellular signal- regulated kinase (*MAPK / ERK*) downstream signaling pathways in a cytokine- independent or hypersensitive manner (James, Ugo, et al. 2005; Lu, Levine, et al. 2005; Staerk, Kallin, et al. 2005).

The revised WHO diagnostic criteria from 2008 for PV, ET and PMF were instigated by the discovery of *JAK2* mutations in virtually all patients with PV and a major subset of ET and PMF (Tefferi 2007). Due to the fact that *JAK2* p.V617F is myeloid neoplasm-specific and not found in reactive causes of polycythemia, it has lent itself to being a sensitive diagnostic marker for PV (Tefferi 2007). However, in the context of myeloid neoplasms, *JAK2* p.V617F is not specific neither for PV nor for ET and PMF where it is found in approximately 50% of the patients. Additionally, it can also be found in refractory anemia with ringed sideroblasts associated with marked thrombocytosis (RARS-T) (Ceesay, Lea, et al. 2006; Szpurka, Tiu, et al. 2006), and at a lesser frequency in other myeloid neoplasms (Jelinek, Oki, et al. 2005; Kremer, Horn, et al. 2006; Lee, Kim, et al. 2006; Nishii, Nanbu, et al. 2007; Zecca, Bergamaschi, et al. 2007), but not in lymphoid neoplasms (Fiorini, Farina, et al. 2006; Melzner, Weniger, et al. 2006). Therefore, mutation screening for *JAK2* p.V617F cannot be used to distinguish one MPN from another, but it does complement histology in the diagnosis of both ET and PMF by excluding the possibility of reactive thrombocytosis or myelofibrosis. Therefore it was considered as a major criteria in the revised WHO classification from 2008 (Table 2).

As already described above, the attempt of genetic classification and diagnosis in myeloid neoplasms started with the 1960 discovery of the Philadelphia chromosome in CML. Additional pathogenetically relevant mutations have been further described in classic and non-classic MPNs: *JAK2* p.V617F in PV, ET and PMF; *JAK2* exon12 mutations in PV (Scott, Tong, et al. 2007), *MPL* p.W515L/K in ET or PMF (Pikman, Lee, et al. 2006), *PDGFRA*, *PDGFRB* or *FGFR1* rearrangements in molecularly characterized myeloid neoplasms associated with eosinophilia (Golub, Barker, et al. 1994; Xiao, Nalabolu, et al. 1998; Cools, DeAngelo, et al. 2003), *KIT* p.D816V and other *KIT* mutations in mast cell diseases (MCD) (Nagata, Worobec, et al. 1995) and RAS pathway mutations, including *RAS*, *PTPN11* or *NF1*, in juvenile myelomonocytic leukemia (JMML) (Shannon, O'Connell, et al. 1994; Loh, Vattikuti, et al. 2004; Lauchle, Braun, et al. 2006). Such discoveries in the molecular pathogenesis of myeloid neoplasms, will ultimately lead to a predominantly genetic

classification system with disease-specific molecular markers, that are relevant to both diagnosis and treatment (Tefferi and Vardiman 2008).

2008 WHO diagnostic criteria			
	Polycythemia vera ^a	Essential thrombocythemia ^a	Primary myelofibrosis ^a
Major criteria	1 Hgb >18.5 g dl ⁻¹ (men) >16.5 g dl ⁻¹ (women) or Hgb or Hct >99th percentile of reference range for age, sex or altitude of residence or Hgb>17 g dl ⁻¹ (men), or>15 g dl ⁻¹ (women) if associated with a sustained increase of ≥2 g dl ⁻¹ from baseline that cannot be attributed to correction of iron deficiency or Elevated red cell mass >25% above mean normal predicted value	1 Platelet count ≥450 × 10 ⁹ l ⁻¹	1 Megakaryocyte proliferation and atypia ^b accompanied by either reticulin and/or collagen fibrosis, or In the absence of reticulin fibrosis, the megakaryocyte changes must be accompanied by increased marrow cellularity, granulocytic proliferation and often decreased erythropoiesis (i.e. pre-fibrotic PMF).
	2 Presence of JAK2V617F or similar mutation	2 Megakaryocyte proliferation with large and mature morphology. No or little granulocyte or erythroid Proliferation.	2 Not meeting WHO criteria for CML, PV, MDS, or other myeloid neoplasm
		3 Not meeting WHO criteria for CML, PV, PMF, MDS or other myeloid neoplasm	3 Demonstration of JAK2V617F or other clonal marker or no evidence of reactive marrow fibrosis
		4 Demonstration of JAK2V617F or other clonal marker or no evidence of reactive thrombocytosis	
Minor criteria	1 BM trilineage myeloproliferation		1 Leukoerythroblastosis
	2 Subnormal serum Epo level		2 Increased serum LDH
	3 EEC growth		3 Anemia
			4 Palpable splenomegaly

Abbreviations: CML, chronic myelogenous leukemia; EEC, endogenous erythroid colony; Epo, erythropoietin; Hct, hematocrit; Hgb, hemoglobin; LDH, lactate dehydrogenase; MDS, myelodysplastic syndrome; WHO, World Health Organization.

^a Diagnosis of polycythemia vera (PV) requires meeting either both major criteria and one minor criterion or the first major criterion and 2 minor criteria. Diagnosis of essential thrombocythemia requires meeting all four major criteria. Diagnosis of primary myelofibrosis (PMF) requires meeting all three major criteria and two minor criteria.

^b Small to large megakaryocytes with an aberrant nuclear/cytoplasmic ratio and hyperchromatic and irregularly folded nuclei and dense clustering.

Table 2. Diagnostic criteria for the classic Ph- negative MPN from WHO 2008 classification (Tefferi and Vardiman 2008).

3.2 Molecular pathophysiology of Ph- negative myeloproliferative neoplasms

The above mentioned mutations of *JAK2* and *MPL* are gain-of-function abnormalities that conferred growth-factor independency to cells transduced with mutant allele and induced a myeloproliferative disease when expressed in murine transplant models (Cazzola and Skoda 2005; Vannucchi and Guglielmelli 2008).

Furthermore, loss of heterozygosity (LOH) for the *JAK2* p.V617F mutation, which originates from mitotic recombination of the short arm of chromosome 9, is present in approximately 30% of PV or PMF patients as opposed to 2-4% of ET. Variable proportions of wild-type, heterozygous and homozygous progenitors are present in most patients with PV, while homozygous progenitors are reported as being rare in ET. Mutated erythroid progenitors are more sensitive to erythropoietin than normal ones, and most erythropoietin independent erythroid colonies (EEC) are made up of homozygous progenitors. Conceivably, duplication of mutant allele is expected to result in a higher level of *JAK2*/ *STAT* activation, than in cells harboring one mutant and one wild-type allele, possibly because of the loss of competition between normal and mutated allele and/ or impaired interaction of mutant *JAK2* with cellular regulators, such as the suppressor of cytokine signaling-3 (*SOCS3*) (Hookham, Elliott, et al. 2007).

This hypothesis has recently received experimental support, thanks to the successful development of conditional transgenic mice, that expressed variable levels of *JAK2* p.V617F (Tiedt, Hao-Shen, et al. 2008), in which the phenotype closely reflected the ratio between normal and mutated *JAK2* mRNA. Likewise, the p.V617F allele burden correlates with hematologic characteristics and clinical endpoints in MPN patients. However, owing to the wide distribution of individual values, it seems quite unlikely that load of mutant p.V617F allele alone represents the key mechanism at the basis of MPD pleiotropy, although it is likely that changes in p.V617F allele burden correlate with disease progression (Vannucchi, Antonioli, et al. 2008).

There is evidence to support the possibility that disease alleles other than *JAK2* p.V617F or *MPL* p.W515L/K are involved in the pathogenesis of MPNs (Skoda 2007), in addition to the fact that almost 40% of ET or PMF patients still lack a molecular marker. First, discrepancies were found in the size of del(20)q and *JAK2* p.V617F- mutated clones, leading to the suggestion that p.V617F allele had been acquired by a pre-existing del(20q) clone and can be seen as a rather late event in the progress of the malignancy (Kralovics, Teo, et al. 2006). Second, EEC wild-type for *JAK2* have been detected at low frequency in PV patients, which would indicate the *JAK2* mutation is a secondary, not a disease-initiating, genetic event (Nussenzweig, Swierczek, et al. 2007). Third, the incidence of MPNs among relatives is greater than expected in the normal population, but neither the diagnosis of MPN nor the distinct clinical phenotype encountered in these families were invariably associated

with the presence of *JAK2* or *MPL* mutation, suggesting that these mutations might occur as a secondary genetic event on the background of an inherited genetic predisposition (Rumi, Passamonti, et al. 2006). Finally, blast cells of secondary acute myeloid leukemia that developed in patients with a preceding *JAK2* p.V617F-positive MPN are often *JAK2* p.V617F- negative, indicating that they might derive from the transformation of a pre-*JAK2* p.V617F mutated hematopoietic stem cell which was originally at the basis of the MPN itself (Campbell, Baxter, et al. 2006). However, that these *JAK2* p.V617F negative blasts represented the de-novo transformation of a residual normal progenitor cannot be excluded on the basis of available data. After all, it is more unlikely that the *JAK2* un-mutated blasts originated from a single cell, heterozygous for the p.V617F mutation that underwent a reverse mitotic recombination process, leading to an un-mutated *JAK2* genotype. On the contrary, the possibility that the *JAK2* p.V617F and *MPL* mutation alone might be sufficient for causing an MPN is compellingly supported by the results of animal models, including the recently described transgenic mice, that developed phenotypes closely resembling human ET and PV and presented MF-like symptoms as they aged (Xing, Wanting, et al. 2008).

3.3 Molecular diagnostics of myeloproliferative neoplasms

The spectacular finding of the Philadelphia Chromosome in CML opened new avenues in pathophysiological research and was the initiation of molecular diagnostics. The initial molecular diagnosis can be done performing cytogenetics, fluorescence in situ hybridization (FISH), southern or western blot and RT-PCR. Noteworthy to mention, that cytogenetic diagnostics alone is not sensitive enough to detect the Ph in all of the cases, but still remains the gold standard in most cases.

The new field of the merge of diagnostic and therapy called theragnostic for hematologic disease was invented a decade ago with imatinib mesylate in 1998, the first tyrosine kinase inhibitor (TKI) (Hughes and Branford 2009). It received international attention as a promising new "targeted" therapy for disease control in patients with advanced-phase CML and interferon- refractory chronic-phase disease. Targeted therapy is defined as a drug with a focused mechanism that specifically acts on a well-defined target or biological pathway which, when inactivated, causes regression or destruction of the malignant process (Ross, Schenkein, et al. 2004). The obvious advantage of such therapies is that they are less toxic,

with a higher therapeutic index and potentially more effective. Moreover, the application of these therapies is usually limited to patients known to carry the appropriate molecular target in their malignant cells, therefore eliminating the toxic and financial implications of more generalized use. While in some circumstances these new therapies will eliminate the need for traditional chemotherapy regimens, in other cases, it is likely that they will lower the threshold for induction of programmed cell death, thus enhancing the effectiveness of conventional chemotherapy approaches (Hamilton, Gallipoli, et al. 2010).

Imatinib mesylate functions by competitive inhibition of the adenosine triphosphate (ATP) binding site, thereby preventing BCR-ABL autophosphorylation, TK activity and subsequent phosphorylation of downstream target substrates and appears to selectively induce apoptosis in *BCR-ABL*- positive cells. Five year follow-up studies have shown sustained benefit for imatinib mesylate treated patients. Despite the success of Imatinib, a major clinical concern is the observation of molecular resistance, most often attributed to the development of point mutations within the *ABL*- kinase domain. To date, more than 50 kinase mutations have been described in vivo and from in vitro screens (Branford 2007). These include mutations which prevent BCR-ABL from adopting the inactive conformation required for Imatinib binding. In an attempt to overcome Imatinib resistance, a second generation of BCR-ABL inhibitors has been developed. Nilotinib inhibits *ABL*- kinase with a 20-50- fold greater potency than Imatinib. Like Imatinib, Nilotinib binds the inactive form of BCR-ABL, but has alterations in its structure that allow higher binding affinity. Dasatinib is a second- generation TKI for the treatment of Imatinib- resistant or –intolerant patients with Ph- positive leukemias, which was approved by the FDA in 2006 (Talpaz, Shah, et al. 2006). Dasatinib is a potent oral inhibitor of SCR family kinases and BCR-ABL, and has added activity against KIT- receptor, platelet-derived growth factor receptor (PDGFR) and ephrin receptor tyrosine kinase (Lombardo, Lee, et al. 2004). Dasatinib has a 325- fold greater potency than Imatinib against cells expressing wild-type BCR-ABL and is able to bind both the active and inactive conformation of *ABL*-kinase (Tokarski, Newitt, et al. 2006).

Today, Imatinib represents the established front-line therapy for nearly all patients with CML, achieving near- normal survival and quality of life and second-generation TKIs are usually the preferred option in cases of Imatinib failure. The need for frequent ongoing monitoring for these long-term responders now warrants reassessment. However, up to 30% of patients with

CML will have to stop Imatinib therapy due to intolerance and resistance (Jabbour, Cortes, et al.). Therefore close monitoring still has a vital role.

A risk-adapted monitoring strategy is implemented to ensure cost-effective management for all patients. The main aim of monitoring response to TKI therapy is, to identify patients who can be reassured that they have achieved a stable remission and, perhaps more importantly, those who are likely to achieve better long-term outcome, if they are switched to second-line therapy. This may be another TKI or in some specific cases an allogeneic stem cell transplant. Apparent loss of cytogenetic or molecular response can sometimes be attributed to variations in assay values or short-term lapses in compliance (Hughes and Branford 2009).

Monitoring response to TKI therapy relies on (1) bone marrow cytogenetic analysis in the first 12 to 18 months, as well as (2) regular measurement of the *BCR-ABL* transcript levels by reverse transcriptase quantitative PCR (RT-QPCR) assays plus (3) selective testing for *BCR-ABL* kinase domain mutations. Monitoring strategies during first-line therapy have been reviewed recently and reasonable consensus has been achieved (Baccarani, Pane, et al. 2008; Kantarjian, Schiffer, et al. 2008; Hughes and Branford 2009).

In 2006 an international scale (IS) for expressing *BCR-ABL* RT-QPCR results was proposed (Hughes, Deininger, et al. 2006). This was linked to recommendations for optimizing methodology, including a detailed review of the merits of sampling blood versus bone marrow and optimal volume and preparation of blood samples. In-house methods could be continued because local values were converted to the IS, using a conversion factor derived from a comparison between the *BCR-ABL* levels calculated from a set of shared patient samples studied in the local laboratory and a reference laboratory (Branford, Fletcher, et al. 2008). This process has enabled over 50 laboratories to express their results as *BCR-ABL* level (IS). This allows clinicians to determine whether their patient has achieved specific molecular landmarks ($\leq 0.1\%$ = major molecular response [MMR]; 1% is approximately equivalent to a complete cytogenetic response [CCR]). However, reporting *BCR-ABL* values on the IS does not give an indication of the measurement reliability or the sensitivity of the local RT-QPCR assay, issues that will also impact on the clinical value of RT-QPCR assays.

Compared to molecular diagnostics or theragnostics for CML, the situation concerning the classic Ph- negative MPN is in the fledging stages. We are far away from standardization or

certification of molecular diagnostic methods concerning the relevant genomic aberrations of the *JAK2* and *MPL* gene. As mentioned above, the *JAK2* Exon14 p.V617F point mutation will be detected in cases of PV in 82%, ET in 49% and in PMF in 53% (Hussein, Bock, et al. 2007). Many different PCR- based detection methods are described, all of them with their specific limitations mainly concerning sensitivity, because of the competitive situation with the wild type allele.

Currently, a number of agents to inhibit JAK2, such as XL019 (Shah, Olszynski, et al. 2008), INCB018424 (Verstovsek, Kantarjian, et al. 2008), TG101348 (Lasho, Tefferi, et al. 2008; Wernig, Kharas, et al. 2008), CEP-701 (Verstovsek, Tefferi, et al. 2007) and also Erlotinib (Li, Xu, et al. 2007), are in preclinical development and clinical trials. INCB018424 is the clinically most extensively studied JAK2 inhibitor. It is an orally, bioavailable selective inhibitor of JAK1 and JAK2 at nanomolar concentrations, which entered early- phase clinical trials in 2007. Patients treated with INCB018424, demonstrated a significant reduction in spleen size and also other constitutional symptoms, were either resolved or were significantly reduced (Verstovsek, Kantarjian, et al. 2008). CEP-701 (Lestaurtinib) is an orally active small molecule inhibitor of receptor tyrosine kinase, including fms- related tyrosine kinase (FLT3) (Levis, Allebach, et al. 2002) and JAK2, and is currently in phase II clinical trials for patients with PMF and post- PV / ET myelofibrosis who have the *JAK2* p.V617F mutation (Verstovsek, Tefferi, et al. 2007). However, it is of importance that specific inhibitors to mutated JAK2 are generated to minimize general toxicity and long- term side affects. Preliminary studies have shown, that the suppression of the JAK- STAT- pathway can lead to treatment- related thrombocytopenia and anemia (Verstovsek, Kantarjian, et al. 2008). Despite these concerns, targeting JAK2 represents a promising option for the treatment of *BCR-ABL*- negative MPN.

Normally the clinical test for detection of the *JAK2* p.V617F mutation is performed on peripheral blood, bone marrow aspirates or formalin- fixed- paraffin- embedded (FFPE) bone marrow core biopsies. All of them consist of mixed cellular material with just a fraction of *JAK2* p.V617F positive cells, either hetero- or homozygote. This is a serious problem, mainly in the initial stadium of the diseases and in case of myelofibrosis when the malignant tissue is relatively repelled by reactive mesenchymal proliferation. In those cases sanger sequencing with a sensitivity of 20% will produce false negative results (Adamson, Fialkow, et al. 1976; Sanger, Nicklen, et al. 1977). Remaining techniques like restriction fragment length polymorphism (RFLP) PCR, amplification refractory mutation system (ARMS) PCR and

fluorescent probes SNP QPCR, will all fit the necessary sensitivity for reliable initial diagnosis (Kroger, Badbaran, et al. 2007; Shammaa, Bazarbachi, et al. 2010). Also the upcoming method of pyrosequencing is a powerful tool for sensitive detection of point mutations (Ronaghi, Karamohamed, et al. 1996; Ronaghi, Uhlen, et al. 1998; Ronaghi 2001; Hochberg, Miklos, et al. 2003).

This is also true for diagnosis of the *MPL* point mutations, but the in part more complex mutations in *JAK2* Exon12 will require conventional sequencing methods because of possible negative results from PCR probes, since they are designed especially for known aberrations.

The situation dramatically changes in the case of patients after hematopoietic stem cell transplantation, because of the therapy related strong decrease of malignant cells. Here, for detection of minimal residual disease a sensitivity of at least 0.01% is needed, which can be only provided by few assays (Kroger, Badbaran, et al. 2007; Siebolts, Lange, et al. 2010). Future inventions of targeted therapy will surely come back to these sensitive assays. Like in CML, it will be a fundamental goal to define standardized protocols of robust techniques, in international collaborating diagnostic laboratories.

4. Aims and major findings of this PhD thesis

4.1 Aims

One aim of the study performed on this PhD thesis was to shed new light on aspects of the pathophysiology of MPN. Therefore we started with characterization and quantification of CD34- positive progenitor cells from PV as the source of these diseases. Additionally we performed a cDNA- array study on this particular and rare cell type in order to find molecular mechanisms causing PV besides the *JAK2* p.V617F point mutation.

Furthermore we focused on characterization of host hematopoiesis after stem cell transplantation (SCT) in patients suffering from MPN and particular in developing robust and sensitive diagnostic assay for reliable detection of minimal residual disease (MRD).

4.2 Major findings

(1) Primitive hematopoiesis is altered in PV because untreated peripheral blood CD34- positive progenitor cells in this disease display more pleomorphic size and, during in vitro maturation, a delayed expression of differentiation markers.

(2) CDNA microarray analysis on CD34- positive peripheral blood cells of PV patients revealed an imbalance of DNA-dependent protein kinase subunits which may contribute to the accumulation of chromosomal aberrations, accumulation of hematopoietic cells, and prolongation of CD34- positive peripheral blood cells life span.

(3) In untreated PV patients with trisomy eight of nine, CD34- positive peripheral blood cells consisted almost exclusively of neoplastic cells but with the finding of a distinct, cytogenetically normal, CD34- positive progenitor cell population in chronic phase PV which may offer perspectives in treatment of the disease.

(4) After successful hematopoietic stem cell transplantation following reduced intensity conditioning in patients with MPN the hematopoietic compartment revealed an almost complete chimerism of the mature hematopoiesis whereas CD34- positive cells remained of recipient origin to a higher proportion. Furthermore, the recipient CD34- positive cell

population in case of CML disposes of better strategies to escape immune surveillance than in PMF.

(5) Since reliable detection of minimal residual disease becomes more and more important in MPN patients after hematopoietic stem cell transplantation more sensitive assays are urgently needed. In combination of a robust QPCR with increased sensitivity up to 1×10^5 performing wild- type blocking PCR we could invent a powerful tool for detection of MRD.

(6) Broad retrospective research in miRNA expression profile is exclusively possible hark back to the large archives of formalin fixed paraffin embedded material all over the world. Here, we could show for the first time that extraction of sufficient amount of miRNA even on decalcified specimens and after decades is possible.

5. Present investigation

5.1 Structural, antigenetic and transcriptional characteristics in peripheral blood CD34+ progenitor cells from polycythemia vera patients: evidence for delayed determination (Wickenhauser C., Perez F., Siebolts U., et al. Int J Oncol. (2003): 23, 437-443)

Prior to the evidentiary finding of a neoplastic stem cell character of Ph- negative MPN there was a gap of knowledge concerning this fundamental cell compartment. What was known is that PV progenitor cells are hypersensitive to several growth factors although their receptor expression is reduced or absent (Dai, Krantz, et al. 1991; Dai, Krantz, et al. 1992; Dai, Krantz, et al. 1994). To reveal the underlying mechanisms of this peculiarity we compared frequency, morphology, antigen expression, transcription of differentiation markers and proliferation as well as apoptosis rate following short term culture of selected CD34- positive peripheral blood cells from PV patients, healthy donors and patients with secondary polycythemia.

The highest amount of CD34- positive cells was found in the group of patients with secondary polycythemia by simple cell metering while the frequency was slightly lower but more variable in PV. By performing light microscopy, morphometry and transmission electron microscopy we found native PV CD34- positive cells varying in shape and form and a

decrease amount of intracytoplasmatic organelles like mitochondria and a more extended Golgi apparatus while in the other groups they constituted a uniform phenotype. However performing RT-PCR, no transcripts for Glycophorin A (GypA) and CD41b, both markers for advanced erythropoiesis and megakaryopoiesis, could be detected in sorted PV progenitors. Also, coexpression for early acting hematopoietic cytokine receptors IL-3R and KIT and for initial erythropoiesis (GYPC) or megakaryopoiesis (CD61) was similar in the different groups using additional FACS analysis. Performing 96 h cocultures with bone marrow fibroblasts the frequency of CD34- positive cells was elevated, downregulation of IL-3R delayed coexpression of GYPC reduced and proliferative activity higher in the PV group.

In conclusion our results suggest that primitive hematopoiesis is altered in PV because PB CD34- positive cells in this disease are characterized by a maturation dissociation with increased activation in untreated populations and a delayed differentiation in short-term cultures.

Own contributions:

Together with Prof. Dr. Wickenhauser I was involved in study design and conception. Methodically I performed the cell preparation of mononuclear cells and subsequent enrichment of CD34 positive hematopoietic cells by magnetic activated cell sorting (MACS) on fresh blood samples from healthy donors, patients with PV or secondary polycythemia. Moreover, I was involved in analyzing the stained paraffin sections and performing FISH technique with subsequent microscopic examination.

5.2 Quantification of clonal hematopoiesis in polycythemia vera (Siebolts U., Ates M., Spitz R., et al. Virchows Arch. (2005): 447, 947-953)

This work was done before the spectacular awareness of specific genomic aberrations and especially the finding of the distinct point mutation in the *JAK2* gene p.V617F in the pathophysiology of Ph- negative MPN. Until then there was only not proven evidence for the clonal stem cell origin of these entities that causes the accumulation of morphologically normal red cells, white cells, platelets, and their precursors in the absence of a definable

stimulus (Spivak 2002). This study was undertaken not only to estimate for the first time the proportion of the neoplastic cells compared to the residual nonneoplastic CD34- positive cells but also to ascertain new evidence for the clonal origin.

Therefore, we screened peripheral blood mononuclear cells of PV patients in the chronic phase of the disease and looked for chromosomal abnormalities performing comparative genomic hybridization. Two of ten patients under study revealed cytogenetic changes, including trisomy 8 or 9. These findings enabled us to quantify the proportion of abnormal clonal cells by applying fluorescence in situ hybridization (FISH) technique. Ninety percent of the mononuclear cells and up to 79% of PB- derived CD34- positive cells presented three signals for chromosome 8 or 9. Although the probability to detect FISH signals in a certain section plane is reduced, constantly 10 – 15% of the cells revealed three signals. Concerning the CD34- positive cell pool, a distinct population without cytogenetic aberrations exists in these patients. Our data underline the clonal character of PV and additionally quantify the proportion of clonal CD34- positive cells for the first time. Furthermore, the finding of a distinct, not aberrant, CD34- positive cell population in chronic phase PV may offer perspectives in treatment of the disease.

Own contributions:

Initially I performed the cell preparation of mononuclear cells and subsequent enrichment of CD34- positive hematopoietic cells by magnetic activated cell sorting (MACS) on fresh blood samples from healthy donors, patients with PV or secondary polycythemia. Moreover, I was involved in analyzing the stained paraffin sections and performing FISH technique with subsequent microscopic examination.

5.3 Dualism of mixed chimerism between hematopoiesis and stroma in chronic idiopathic myelofibrosis after allogeneic stem cell transplantation (Thiele J., Varus E., Siebolts U., et al. *Histol Histopathol.* (2007): 22, 365-372)

Since hematopoietic stem cell transplantation is the only curative therapeutic approach for patients with Ph- negative MPN scant knowledge exists concerning mixed chimerism

following therapy (Deeg, Gooley, et al. 2003). However, controversy continues about the donor or host origin of stroma constituents following myeloablative therapy and subsequent transplantation (Simmons, Przepiorka, et al. 1987; Athanasou, Quinn, et al. 1990; Santucci, Trabetti, et al. 1992). Because of the gate keeper function of stromal endothelial cells by controlling the trafficking and homing of progenitors the possible neoplastic origin and its frequency of this cell compartment is of special interest (Simmons, Masinovsky, et al. 1992; Mohle, Bautz, et al. 1999).

Following a sex- mismatched peripheral blood stem cell transplantation of PMF patients, a combined immunopheno- and genotyping by FISH was performed on sequential bone marrow biopsies at standardized intervals. Results were compared with PCR based chimerism analysis of corresponding peripheral blood samples in five patients.

According to FISH, pretransplant specimens revealed a gender congruence of more than 99%, while in the first three month the total bone marrow exhibited a persistent fraction of host cells (30% to 40%) with a tendency to decline after about one year. Although the hematopoietic compartment (CD34 and CD61- positive cells) exhibited only very few host-derived cells which states an almost complete chimeric (donor- derived) hematopoiesis and therefore a successful transplantation. Concerning the stromal cells and especially the endothelial cells we could show that the majority of these cells maintained recipient origin. In keeping with the prevalence of donor cells in the hematopoietic compartment, PCR- data of peripheral blood displayed a non- significant degree of mixed chimerism.

Own contributions:

I was involved in analyzing the stained paraffin sections and performed FISH analysis with subsequent microscopic examination.

5.4 Differences in proportion and dynamics of recipient hematopoiesis following hematopoietic cell transplantation in CML and IMF (Siebolts U., Thiele J., Zander T., et al. Oncol Rep. (2008): 19, 287-292)

Since decades myeloablation followed by allogeneic stem cell transplantation offered the only opportunity to cure leukemia patients and only recently the development of STI571 (Imatinib) created a further alternative in CML. Generally, two variations of transplantation regimen exist, hematopoietic stem cell transplantation with antecedent conventional myeloablative or the newly upcoming reduced intensity conditioning (RIC). The application of conventional myeloablative hematopoietic stem cell transplantation has, amongst others, been limited by the age of the recipient because of its possible complications. Therefore, the use for RIC offers an optional curative therapy also for older and fragile patients.

While among all leukemias the conventional transplantation regimen had the best outcome in CML, trials with RIC were rather humbling and recurrence of the neoplastic clone occurred frequently. However, the same therapy in patients with PMF resulted in a more favorable outcome. In an approach to reveal the underlying mechanisms of this discrepancy long-term mixed chimerism was determined on bone marrow biopsies derived from five PMF patients and from eight CML patients of the pre Imatinib era following sex-mismatched transplantation.

Despite nearly complete chimerism after stem cell transplantation in mature hematopoiesis, analysis of late transplant period revealed a concentration of host cells within the CD34-positive cell compartment in both diseases. However, in PMF bone marrow biopsies only up to 8% recipient CD34-positive cells but in CML biopsies up to 26% recipient CD34-positive cells were detected despite the myeloablative regimen in case of CML patients. Taken into account that in CML up to 10% of the host bone marrow CD34-positive cells bear the BCR-ABL translocation, our data suggest that the neoplastic CD34-positive cell population might dispose of better strategies to escape immune surveillance in CML than in IMF.

Own contributions:

Based on the antecedent study I had the idea of a comparative study of RIC and myeloablative regimen. Methodically, I was involved in analyzing the stained paraffin sections and performed FISH analysis with subsequent microscopic examination and further in conception of the study. After all I performed data analysis and graphical illustration.

5.5 Imbalance of DNA-dependent protein kinase subunits in polycythemia vera peripheral blood stem cells (Siebolts U., Breuhahn K., Hennecke A., et al. Int J Cancer. (2009): 124, 600-607)

The above listed publications published within this doctoral thesis are dealing with different aspects of pathophysiology and therapeutic aspects of MPN. The recurrent finding of interesting results together with distinct hints of international scientific literature concerning the CD34- positive progenitor cell compartment again focused our intensified interest on this cell population.

Since the specific *JAK2* p.V617F point mutation represents a rather late event in the disease progression, is not specific for this disease, and is not ascertained in all patients indicating that additional factors contribute to the specific phenotype of PV, we tried to reveal undescribed aberrations (Baxter, Scott, et al. 2005; Kralovics, Passamonti, et al. 2005; Kralovics, Teo, et al. 2006; Nussenzveig, Swierczek, et al. 2007). Therefore, cDNA microarray analyses were performed on CD34- positive peripheral blood stem cells with subsequent evaluation on mRNA and protein level of a larger cohort of PV patients. Microarray analyses revealed a significant dysregulation of 11 genes. *KU86*, a gene coding for a subunit of the DNA-dependent protein kinase (DNA-PK), displayed the strongest upregulation in all patients under study. This peculiarity was accompanied by downregulation of the catalytic *DNA-PK* subunit *DNA-PKcs*. Also *KU86* protein was upregulated and expressed in the vast majority of CD34- positive peripheral blood stem cells nuclei while a weak nuclear expression was detected in only one blood donor. Differential expression of several genes, imbalance of the distinct subunits of *DNA-PK*, and particularly the strong upregulation of *KU86* protein, are new findings in PV CD34- positive peripheral blood stem cells. These factors may contribute to the accumulation of chromosomal aberrations, accumulation of hematopoietic cells

(especially of erythropoiesis), and prolongation of CD34- positive peripheral blood stem cell life span observed in PV.

Own contributions:

Prior to the lab work I have done most of the study conception and design together with Prof. Dr. Wickenhauser. Initially I performed the cell preparation and enrichment of CD34-positive hematopoietic cells by magnetic activated cell sorting (MACS) on fresh blood samples from healthy donors, patients with PV or secondary polycythemia. Moreover, I have done all subsequent steps of DNA, RNA and Protein preparation, reverse transcription, primer design, radioactive cDNA array hybridization, RT-QPCR, Western Blot and all subsequent analysis and graphical illustration of the data inclusive the statistical evaluation. Further I was involved in microscopic examination of the stained paraffin sections.

5.6 Tissues from routine pathology archives are suitable for microRNA analyses by quantitative PCR (Siebolts U., Varnholt H., Drebber U., et al. J Clin Pathol. (2009): 62, 84-88)

Plenty of expert knowledge in handling of decalcified formalin fixed paraffin embedded tissue could be acquired of our group in the last years. Especially the sufficient extraction of RNA, normally highly degenerated, make high demands on staff and laboratory skills.

However, since molecular diagnostics on formalin fixed paraffin embedded (FFPE) material becomes more and more important numerous studies focused on detection of new specific molecular peculiarities suitable for diagnostic purpose. In this context the new finding of so called microRNA (miRNA) invented a new enthusiasm in finding specific dysregulated groups of miRNA which can be used as a diagnostic means since cDNA- array clustering often leads to a dead end.

A prerequisite for using the large archives of FFPE tumor material all over the world for not only scientific but also for diagnostic purpose is the certain accessibility of miRNA out of this particular material even in the challenging case of osseous bone marrow biopsies.

Therefore we tested the accessibility of two representative miRNAs examined by RT-QPCR in 86 human FFPE samples from liver, breast, bone marrow, lymphatic tissue and colon. Murine liver was used to analyze the influence of fixation time and different fixatives.

Briefly, extraction of sufficient amount of miRNA was possible in all cases. Storage of human tissues for up to seven years did not cause a significant deterioration of miRNA. However, miRNA quality in human archival material following routine processing 10 – 20 years ago was decreased but still sufficient for downstream applications. Oxidation by ambient air during storage and fixation in non-buffered formalin is a possible reason for loss of miRNA quality.

Therefore, the assessment of miRNA in readily obtained FFPE samples is a highly promising tool in molecular pathology when similarly treated samples are analyzed.

Own contributions:

Together with Dr. Odenthal and Dr. Varnholt I have participated upon the study conception and design. Mostly I was involved in analysis of miRNA RT-QPCR inclusive the statistical evaluation and graphical illustration of the data.

5.7 Allele-specific wild-type blocker quantitative PCR for highly sensitive detection of rare JAK2 p.V617F point mutation in primary myelofibrosis as an appropriate tool for the monitoring of molecular remission following therapy (Siebolts U., Lange T., Niederwieser D., et al. J Clin Pathol. (2010): 63, 370-372)

Since the invention of reduced intensity conditioning (RIC) regimen prior to hematopoietic stem cell transplantation improved the accessibility for curative therapy to patients with Ph-negative MPN with myelofibrosis it became more and more important to detect minimal residual disease (MRD) as sign of relapse. In case of patients harboring the specific JAK2 p.V617F mutation monitoring of this mutation on peripheral blood or even on formalin fixed paraffin embedded bone marrow biopsies can be utilized for this purpose. Because of the

therapy related strong decrease of malignant cells a prerequisite for detection of MRD is a sensitivity of the methodological approach of at least 0.01% which means 1 mutated allele on a background of 10,000 wildtyp alleles.

In an attempt to achieve the required high sensitivity, specificity and robustness we created an approach applicable also on bone marrow biopsies where we adapted the principle of wild-type blocker PCR with allele- specific QPCR. The significance of the assay was demonstrated on a retrospective series of sequential bone marrow biopsies as diagnosis of molecular relapse now preceded the diagnosis of clinical relapse by far. This method offers the urgently needed tool for a systematic molecular analysis of sequential biopsies in the course of stem cell transplantation to develop guidelines for the management of these patients.

Own contributions:

Initially I have had the idea of using MGB- Taqman Probes for detection of the wild- type and the mutated allele on the same amplified strand together with performing a two step approach with initial wild- type blocking PCR for increased sensitivity. Moreover, I have done all subsequent steps of design, laboratory work and in silico processing.

6. Progress and further activities during the PhD thesis

In addition to my PhD thesis I was further involved in routine diagnostics pathology within my specialist training since 2004 in the Institute of Pathology, University Hospital of Cologne and since 2008 in the Institute of Pathology, University Hospital of Leipzig. However, particular attention was paid to the special subject of molecular pathology and in 2009 I became laboratory head of molecular diagnostics, Institute of Pathology. In this context, I was able to place the invented methods directly into the routine diagnostics and furthermore to develop new methods especially availing the upcoming technology of pyrosequencing.

Together with scientists of the Department of Hematology / Oncology, University Hospital of Leipzig we screened 20 MPN patients for minimal residual disease after stem cell transplantation with the above described technique (Siebolts, Lange, et al. 2010) and tested each sample in the molecular laboratory of the Department of Hematology / Oncology performing ARMS- PCR. The data were correlated not only with the clinical outcome but also with the corresponding information of donor chimerism of the same samples which also were detected in our laboratory. A manuscript of the data currently is submitted for publication.

As described above the entity of mastocytosis, as a part of MPN, is mostly combined with the finding of the *KIT* p.D816V point mutation, which serves also as a diagnostic means. Analogous to the allele- specific wild- type blocking QPCR we tried to design a highly sensitive and reliable method for detection of the *KIT* p.D816V point mutation using the challenging paraffin embedded and decalcified bone marrow biopsy specimen as the DNA-source. Therefore we designed a specific wild- type blocking LNA modified DNA probe applying in a first round PCR. Subsequently a second PCR in preparation of pyrosequencing will be performed. Finally, this approach together with samples without wild- type blocking PCR gives information about the allelic burden of *KIT* p.D816V and also has the necessary sensitivity in case of a low tumor cell burden which is mostly pathognomonic for mastocytosis. Meanwhile, this technical approach has found its way into the routine diagnosis of our Institute.

Another new molecular diagnostics technique under construction in collaboration with the Department of Ophthalmology is the detection of monosomy of chromosome 3 in diagnostic specimen of patients suffering from uveal melanoma. Uveal melanoma is the most common

primary intraocular tumor, with an annual incidence of six per one million. About 50% of uveal melanoma carry chromosome 3 monosomy, which, together with tumor stage and spindle shaped versus epithelioid subtype, has been shown to be a significant predictor of metastatic disease and poor prognosis. To date cytogenetics, comparative genomic hybridization and microsatellite analysis have been used to identify chromosomal aberrations in uveal melanoma. However, these methods are costly, time consuming, difficult to interpret and mostly require ample tumor material, which is hardly to reach by diagnostic fine needle aspirates (FNA). Therefore we want to establish a reliable, easy to use method on FNA with first, evaluation of the histological subtype and second, subsequent DNA extraction and testing for monosomy 3.

In a first step, DNA can be extracted from FNA- smears and from blood of the respective patients. Blood DNA then is screened for informative because heterozygous SNP loci on chromosome 3 performing pyrosequencing. Accordingly, data will be compared with those obtained by tumor DNA analysis. In case of pseudo- homozygous conversion of the tested SNP, allele- loss and therefore monosomy can be stated. For verification of the method further fluorescence in situ hybridisation (FISH) will be performed. This approach of micro-invasive FNA combined with the technique of allele specific SNP pyrosequencing is highly sensitive, reliable, easy to use and interpret, fast to perform and cost- effective. However, in the meantime the described assay employing tissue from eye enucleates is part of the routine molecular diagnostics of our institute.

6.1 Awards / Talks

Siebolts U., Breuhahn K., Schultze J.L., Thiele T., Wickenhauser C. CD34+ cells from polycythemia vera patients reveal dysregulation of regulators of hematopoiesis, apoptosis, cell cycle and DNA repair. First prize poster presentation, Oncology Symposium of the Cologne Fortune Foundation. July 15th, 2003, Cologne.

Siebolts U., Breuhahn K., Schultze J.L. and Wickenhauser C. CD34+ cells from polycythemia vera patients reveal dysregulation of regulators of hematopoiesis, apoptosis, cell cycle and DNA repair. 88th Annual Meeting of the German Society of Pathology (DGP). June 2 – 5, 2004, Rostock.

Siebolts U., Lange T. and Wickenhauser C. Monitoring of patients with *JAK2* p.V617F positive primary myelofibrosis by allele-specific wild-type blocker QPCR. Annual Fall Meeting of the East- German Study Group for Hematology and Oncology (OSHO). November 21 – 22, 2008, Leipzig.

Siebolts U., Al-Ali HK., Niederwieser D., Wickenhauser C. Establishment of a highly sensitive allele specific wild type blocker polymerase chain reaction followed by pyrosequencing for detection of the *KIT* p.D816V point mutation. Annual Meeting of the American Society of Hematology (ASH). Meeting Abstract. December 4 – 8, 2009, New Orleans, Blood 114, 4975.

Lange T., Edelmann A., **Siebolts U.**, Nehring C., Jäckel N., Cross M., Maier J., Niederwieser D., Wickenhauser C. Milestones of Post Transplant Monitoring of *JAK2* p.V617F Positive MPN Patients. Annual Meeting of the American Society of Hematology (ASH). Poster Abstract. December 4 – 8, 2010, Orlando, Blood 116, 3462.

Siebolts U. and Wickenhauser C. Theragnostic – Prerequisite for a personalized medicine. Regulars' Table Life Science of Bio City Leipzig and Chamber of Industry and Commerce Leipzig. September 15, 2010, Leipzig.

Siebolts U., Lange T. and Wickenhauser C. Allele specific PCR for the *JAK2* p.V617F mutation is a valuable approach to detect residual disease in patients after hematopoietic stem cell transplantation. 94th Annual Meeting of the German Society of Pathology (DGP). May 27 – 30, 2010, Berlin.

Siebolts U. and Wickenhauser C. Establishment of a highly sensitive allele specific wild type blocker polymerase chain reaction followed by pyrosequencing for detection of the *KIT* p.D816V point mutation. 3rd Novartis Oncology Advent Symposium. November 19 – 20, 2010, Eisenach.

7. Additional publications during the PhD thesis

During my PhD thesis I took part of diverse scientific collaborations leading to several publications listed below. Mostly I was involved in molecular analysis performing different PCR- based techniques and fluorescence in situ hybridization (FISH). Also, analyzing of stained paraffin sections and interpretation of immunochemistry and furthermore statistical analysis and graphical illustration was part of my contribution.

Kappert K., Sparwel J., Sandin A., Seiler A., **Siebolts U.**, Leppanen O., Rosenkranz S. and Ostman A. Antioxidants relieve phosphatase inhibition and reduce PDGF signaling in cultured VSMCs and in restenosis. *Arterioscler Thromb Vasc Biol.* 2006: 26, 2644-51.

Own contributions:

I was involved in analyzing the stained paraffin sections and semiquantitative analysis of the immunochemistry.

Gerharz M., Baranowsky A., **Siebolts U.**, Eming S., Nischt R., Krieg T. and Wickenhauser C. Morphometric analysis of murine skin wound healing: standardization of experimental procedures and impact of an advanced multitissue array technique. *Wound Repair Regen.* 2007: 15, 105-12.

Own contributions:

I was involved in analyzing the stained paraffin sections and morphometric analysis. Moreover I performed the statistical evaluation and most of the graphical illustration of the data.

Veit G., Zimina E. P., Franzke C. W., Kutsch S., **Siebolts U.**, Gordon M. K., Bruckner-Tuderman L. and Koch M. Shedding of collagen XXIII is mediated by furin and depends on the plasma membrane microenvironment. *J Biol Chem.* 2007: 282, 27424-35.

Own contributions:

I performed RT-QPCR for quantification of collagen XXIII, and all subsequent data analysis and graphical illustration.

Odenthal M., **Siebolts U.**, Ernestus K., Disse D., Dienes H. P. and Wickenhauser C. Immunoglobulin heavy chain gene analysis in bone marrow biopsies and corresponding lymph node specimens: dependency on pre-treatment, histological subtype and extension of B-cell lymphoma. *Int J Mol Med.* 2008: 21, 569-76.

Own contributions:

I was involved in analyzing the stained paraffin sections and analysis of the immunochemistry. Furthermore I analyzed the IgH FR3 PCR and electropherograms and did all of the graphical illustration.

Markert E.*, **Siebolts U.***, Odenthal M., Kreuzer K. A. and Wickenhauser C. High diagnostic value of morphologic examination and molecular analysis of bone marrow biopsies in a case of BCR-ABL+ CML with clusters of blasts. *Int J Hematol.* 2009: 89, 294-7.

* Both authors contributed equally

Own contributions:

I was involved in analyzing the stained paraffin sections and analysis of FISH. Moreover I designed the detection assay for BCR-ABL on formalin fixed and paraffin embedded tissue and furthermore performed the RT-QPCR with all subsequent data analysis and graphical illustration.

Markert E.*, **Siebolts U.***, Habbig S., Odenthal M., Dienes H. P., Stippel D. L., Hoppe B. and Wickenhauser C. Evolution of PTLD following renal transplantation in a child. *Pediatr Transplant*. 2009; 13, 379-83.

* Both authors contributed equally

Own contributions:

I was involved in conception, in analyzing the stained paraffin sections and analysis of the immunochemistry. Furthermore I provided the IgH FR3 PCR and electropherograms and did most of the graphical illustration.

Utermohlen O., Baschuk N., Abdullah Z., Engelmann A., **Siebolts U.**, Wickenhauser C., Stocking C. and Kronke M. Immunologic hurdles of therapeutic stem cell transplantation. *Biol Chem*. 2009; 390, 977-83.

Own contributions:

I was involved in analyzing the stained paraffin sections and analysis of the immunochemistry. Furthermore I participated in making graphical illustration.

8. References

- Adamson J. W., Fialkow P. J., Murphy S., Prchal J. F. and Steinmann L. Polycythemia vera: stem-cell and probable clonal origin of the disease. *N Engl J Med.* 1976: 295, 913-6.
- Athanasou N. A., Quinn J., Brenner M. K., Prentice H. G., Graham A., Taylor S., Flannery D. and McGee J. O. Origin of marrow stromal cells and haemopoietic chimaerism following bone marrow transplantation determined by in situ hybridisation. *Br J Cancer.* 1990: 61, 385-9.
- Baccarani M., Pane F. and Saglio G. Monitoring treatment of chronic myeloid leukemia. *Haematologica.* 2008: 93, 161-9.
- Baxter E. J., et al. Acquired mutation of the tyrosine kinase JAK2 in human myeloproliferative disorders. *Lancet.* 2005: 365, 1054-61.
- Branford S. Chronic myeloid leukemia: molecular monitoring in clinical practice. *Hematology Am Soc Hematol Educ Program.* 2007: 376-83.
- Branford S., et al. Desirable performance characteristics for BCR-ABL measurement on an international reporting scale to allow consistent interpretation of individual patient response and comparison of response rates between clinical trials. *Blood.* 2008: 112, 3330-8.
- Campbell P. J., et al. Mutation of JAK2 in the myeloproliferative disorders: timing, clonality studies, cytogenetic associations, and role in leukemic transformation. *Blood.* 2006: 108, 3548-55.
- Cazzola M. and Skoda R. Gain of function, loss of control - a molecular basis for chronic myeloproliferative disorders. *Haematologica.* 2005: 90, 871-4.
- Ceesay M. M., et al. The JAK2 V617F mutation is rare in RARS but common in RARS-T. *Leukemia.* 2006: 20, 2060-1.
- Cools J., et al. A tyrosine kinase created by fusion of the PDGFRA and FIP1L1 genes as a therapeutic target of imatinib in idiopathic hypereosinophilic syndrome. *N Engl J Med.* 2003: 348, 1201-14.

Cortes J. E., et al. Prognostic significance of cytogenetic clonal evolution in patients with chronic myelogenous leukemia on imatinib mesylate therapy. *Blood*. 2003: 101, 3794-800.

Dai C. H., Krantz S. B., Means R. T., Jr., Horn S. T. and Gilbert H. S. Polycythemia vera blood burst-forming units-erythroid are hypersensitive to interleukin-3. *J Clin Invest*. 1991: 87, 391-6.

Dai C. H., Krantz S. B., Dessypris E. N., Means R. T., Jr., Horn S. T. and Gilbert H. S. Polycythemia vera. II. Hypersensitivity of bone marrow erythroid, granulocyte-macrophage, and megakaryocyte progenitor cells to interleukin-3 and granulocyte-macrophage colony-stimulating factor. *Blood*. 1992: 80, 891-9.

Dai C. H., Krantz S. B., Green W. F. and Gilbert H. S. Polycythaemia vera. III. Burst-forming units-erythroid (BFU-E) response to stem cell factor and c-kit receptor expression. *Br J Haematol*. 1994: 86, 12-21.

Dameshek W. Some speculations on the myeloproliferative syndromes. *Blood*. 1951: 6, 372-5.

de Klein A., van Kessel A. G., Grosveld G., Bartram C. R., Hagemeijer A., Bootsma D., Spurr N. K., Heisterkamp N., Groffen J. and Stephenson J. R. A cellular oncogene is translocated to the Philadelphia chromosome in chronic myelocytic leukaemia. *Nature*. 1982: 300, 765-7.

Deeg H. J., et al. Allogeneic hematopoietic stem cell transplantation for myelofibrosis. *Blood*. 2003: 102, 3912-8.

Fiorini A., et al. Screening of JAK2 V617F mutation in multiple myeloma. *Leukemia*. 2006: 20, 1912-3.

Geary C. G. The story of chronic myeloid leukaemia. *Br J Haematol*. 2000: 110, 2-11.

Golub T. R., Barker G. F., Lovett M. and Gilliland D. G. Fusion of PDGF receptor beta to a novel ets-like gene, tel, in chronic myelomonocytic leukemia with t(5;12) chromosomal translocation. *Cell*. 1994: 77, 307-16.

Groffen J., Stephenson J. R., Heisterkamp N., de Klein A., Bartram C. R. and Grosveld G. Philadelphia chromosomal breakpoints are clustered within a limited region, bcr, on chromosome 22. *Cell*. 1984: 36, 93-9.

Hamilton A., Gallipoli P., Nicholson E. and Holyoake T. L. Targeted therapy in haematological malignancies. *J Pathol*. 2010: 220, 404-18.

Hermans A., Heisterkamp N., von Linden M., van Baal S., Meijer D., van der Plas D., Wiedemann L. M., Groffen J., Bootsma D. and Grosveld G. Unique fusion of bcr and c-abl genes in Philadelphia chromosome positive acute lymphoblastic leukemia. *Cell*. 1987: 51, 33-40.

Hochberg E. P., Miklos D. B., Neuberger D., Eichner D. A., McLaughlin S. F., Mattes-Ritz A., Alyea E. P., Antin J. H., Soiffer R. J. and Ritz J. A novel rapid single nucleotide polymorphism (SNP)-based method for assessment of hematopoietic chimerism after allogeneic stem cell transplantation. *Blood*. 2003: 101, 363-9.

Hookham M. B., Elliott J., Suessmuth Y., Staerk J., Ward A. C., Vainchenker W., Percy M. J., McMullin M. F., Constantinescu S. N. and Johnston J. A. The myeloproliferative disorder-associated JAK2 V617F mutant escapes negative regulation by suppressor of cytokine signaling 3. *Blood*. 2007: 109, 4924-9.

Hughes T., et al. Monitoring CML patients responding to treatment with tyrosine kinase inhibitors: review and recommendations for harmonizing current methodology for detecting BCR-ABL transcripts and kinase domain mutations and for expressing results. *Blood*. 2006: 108, 28-37.

Hughes T. P., Morgan G. J., Martiat P. and Goldman J. M. Detection of residual leukemia after bone marrow transplant for chronic myeloid leukemia: role of polymerase chain reaction in predicting relapse. *Blood*. 1991: 77, 874-8.

Hughes T. P. and Branford S. Monitoring disease response to tyrosine kinase inhibitor therapy in CML. *Hematology Am Soc Hematol Educ Program*. 2009: 477-87.

Hughes T. P. and Branford S. Measuring minimal residual disease in chronic myeloid leukemia: fluorescence in situ hybridization and polymerase chain reaction. *Clin Lymphoma Myeloma*. 2009: 9 Suppl 3, S266-71.

Hussein K., Bock O. and Kreipe H. Histological and molecular classification of chronic myeloproliferative disorders in the age of JAK2: persistence of old questions despite new answers. *Pathobiology*. 2007: 74, 72-80.

Jabbour E., Cortes J. and Kantarjian H. Long-term outcomes in the second-line treatment of chronic myeloid leukemia: a review of tyrosine kinase inhibitors. *Cancer*. 2010: 117, 897-906.

Jaffe ES H. N., Stein H, Vardiman JW World Health Organization Classification of Tumours of Hematopoietic and Lymphoid Tissues. IARC Press. 2001: Lyon, France, 351.

James C., et al. A unique clonal JAK2 mutation leading to constitutive signalling causes polycythaemia vera. *Nature*. 2005: 434, 1144-8.

Jamieson C. H., Gotlib J., Durocher J. A., Chao M. P., Mariappan M. R., Lay M., Jones C., Zehnder J. L., Lilleberg S. L. and Weissman I. L. The JAK2 V617F mutation occurs in hematopoietic stem cells in polycythemia vera and predisposes toward erythroid differentiation. *Proc Natl Acad Sci U S A*. 2006: 103, 6224-9.

Jelinek J., Oki Y., Gharibyan V., Bueso-Ramos C., Prchal J. T., Verstovsek S., Beran M., Estey E., Kantarjian H. M. and Issa J. P. JAK2 mutation 1849G>T is rare in acute leukemias but can be found in CMML, Philadelphia chromosome-negative CML, and megakaryocytic leukemia. *Blood*. 2005: 106, 3370-3.

Kantarjian H., Schiffer C., Jones D. and Cortes J. Monitoring the response and course of chronic myeloid leukemia in the modern era of BCR-ABL tyrosine kinase inhibitors: practical advice on the use and interpretation of monitoring methods. *Blood*. 2008: 111, 1774-80.

Kantarjian H. M., Dixon D., Keating M. J., Talpaz M., Walters R. S., McCredie K. B. and Freireich E. J. Characteristics of accelerated disease in chronic myelogenous leukemia. *Cancer*. 1988: 61, 1441-6.

Kralovics R., Passamonti F., Buser A. S., Teo S. S., Tiedt R., Passweg J. R., Tichelli A., Cazzola M. and Skoda R. C. A gain-of-function mutation of JAK2 in myeloproliferative disorders. *N Engl J Med*. 2005: 352, 1779-90.

Kralovics R., Teo S. S., Li S., Theodorides A., Buser A. S., Tichelli A. and Skoda R. C. Acquisition of the V617F mutation of JAK2 is a late genetic event in a subset of patients with myeloproliferative disorders. *Blood*. 2006: 108, 1377-80.

Kremer M., Horn T., Dechow T., Tzankov A., Quintanilla-Martinez L. and Fend F. The JAK2 V617F mutation occurs frequently in myelodysplastic/myeloproliferative diseases, but is absent in true myelodysplastic syndromes with fibrosis. *Leukemia*. 2006: 20, 1315-6.

Kroger N., Badbaran A., Holler E., Hahn J., Kobbe G., Bornhauser M., Reiter A., Zabelina T., Zander A. R. and Fehse B. Monitoring of the JAK2-V617F mutation by highly sensitive quantitative real-time PCR after allogeneic stem cell transplantation in patients with myelofibrosis. *Blood*. 2007: 109, 1316-21.

Lasho T. L., Tefferi A., Hood J. D., Verstovsek S., Gilliland D. G. and Pardanani A. TG101348, a JAK2-selective antagonist, inhibits primary hematopoietic cells derived from myeloproliferative disorder patients with JAK2V617F, MPLW515K or JAK2 exon 12 mutations as well as mutation negative patients. *Leukemia*. 2008: 22, 1790-2.

Lauchle J. O., Braun B. S., Loh M. L. and Shannon K. Inherited predispositions and hyperactive Ras in myeloid leukemogenesis. *Pediatr Blood Cancer*. 2006: 46, 579-85.

Lee J. W., et al. The JAK2 V617F mutation in de novo acute myelogenous leukemias. *Oncogene*. 2006: 25, 1434-6.

Levine R. L., et al. Activating mutation in the tyrosine kinase JAK2 in polycythemia vera, essential thrombocythemia, and myeloid metaplasia with myelofibrosis. *Cancer Cell*. 2005: 7, 387-97.

Levis M., Allebach J., Tse K. F., Zheng R., Baldwin B. R., Smith B. D., Jones-Bolin S., Ruggeri B., Dionne C. and Small D. A FLT3-targeted tyrosine kinase inhibitor is cytotoxic to leukemia cells in vitro and in vivo. *Blood*. 2002: 99, 3885-91.

Li Z., Xu M., Xing S., Ho W. T., Ishii T., Li Q., Fu X. and Zhao Z. J. Erlotinib effectively inhibits JAK2V617F activity and polycythemia vera cell growth. *J Biol Chem*. 2007: 282, 3428-32.

Lion T., Henn T., Gaiger A., Kalhs P. and Gadner H. Early detection of relapse after bone marrow transplantation in patients with chronic myelogenous leukaemia. *Lancet*. 1993: 341, 275-6.

Loh M. L., et al. Mutations in PTPN11 implicate the SHP-2 phosphatase in leukemogenesis. *Blood*. 2004: 103, 2325-31.

Lombardo L. J., et al. Discovery of N-(2-chloro-6-methyl- phenyl)-2-(6-(4-(2-hydroxyethyl)-piperazin-1-yl)-2-methylpyrimidin-4- ylamino)thiazole-5-carboxamide (BMS-354825), a dual Src/Abl kinase inhibitor with potent antitumor activity in preclinical assays. *J Med Chem*. 2004: 47, 6658-61.

Lu X., Levine R., Tong W., Wernig G., Pikman Y., Zarnegar S., Gilliland D. G. and Lodish H. Expression of a homodimeric type I cytokine receptor is required for JAK2V617F-mediated transformation. *Proc Natl Acad Sci U S A*. 2005: 102, 18962-7.

Maru Y. and Witte O. N. The BCR gene encodes a novel serine/threonine kinase activity within a single exon. *Cell*. 1991: 67, 459-68.

Medina J., Kantarjian H., Talpaz M., O'Brien S., Garcia-Manero G., Giles F., Rios M. B., Hayes K. and Cortes J. Chromosomal abnormalities in Philadelphia chromosome-negative metaphases appearing during imatinib mesylate therapy in patients with Philadelphia chromosome-positive chronic myelogenous leukemia in chronic phase. *Cancer*. 2003: 98, 1905-11.

Melzner I., Weniger M. A., Menz C. K. and Moller P. Absence of the JAK2 V617F activating mutation in classical Hodgkin lymphoma and primary mediastinal B-cell lymphoma. *Leukemia*. 2006: 20, 157-8.

Mohle R., Bautz F., Rafii S., Moore M. A., Brugger W. and Kanz L. Regulation of transendothelial migration of hematopoietic progenitor cells. *Ann N Y Acad Sci*. 1999: 872, 176-85; discussion 185-6.

Nagata H., Worobec A. S., Oh C. K., Chowdhury B. A., Tannenbaum S., Suzuki Y. and Metcalfe D. D. Identification of a point mutation in the catalytic domain of the protooncogene c-kit in peripheral blood mononuclear cells of patients who have mastocytosis with an associated hematologic disorder. *Proc Natl Acad Sci U S A*. 1995: 92, 10560-4.

Nishii K., Nanbu R., Lorenzo V. F., Monma F., Kato K., Ryuu H. and Katayama N. Expression of the JAK2 V617F mutation is not found in de novo AML and MDS but is detected in MDS-derived leukemia of megakaryoblastic nature. *Leukemia*. 2007: 21, 1337-8.

Nowell P. and Hungerford D. A minute chromosome in human chronic granulocytic leukemia. *Science*. 1960: 132, 1497.

Nussenzveig R. H., Swierczek S. I., Jelinek J., Gaikwad A., Liu E., Verstovsek S., Prchal J. F. and Prchal J. T. Polycythemia vera is not initiated by JAK2V617F mutation. *Exp Hematol*. 2007: 35, 32-8.

Pikman Y., et al. MPLW515L is a novel somatic activating mutation in myelofibrosis with myeloid metaplasia. *PLoS Med*. 2006: 3, e270.

Radich J. P., et al. Polymerase chain reaction detection of the BCR-ABL fusion transcript after allogeneic marrow transplantation for chronic myeloid leukemia: results and implications in 346 patients. *Blood*. 1995: 85, 2632-8.

Radich J. P. How I monitor residual disease in chronic myeloid leukemia. *Blood*. 2009: 114, 3376-81.

Ronaghi M., Karamohamed S., Pettersson B., Uhlen M. and Nyren P. Real-time DNA sequencing using detection of pyrophosphate release. *Anal Biochem*. 1996: 242, 84-9.

Ronaghi M., Uhlen M. and Nyren P. A sequencing method based on real-time pyrophosphate. *Science*. 1998: 281, 363, 365.

Ronaghi M. Pyrosequencing sheds light on DNA sequencing. *Genome Res*. 2001: 11, 3-11.

Ross J. S., et al. Targeted therapies for cancer 2004. *Am J Clin Pathol*. 2004: 122, 598-609.

Rumi E., et al. JAK2 (V617F) as an acquired somatic mutation and a secondary genetic event associated with disease progression in familial myeloproliferative disorders. *Cancer*. 2006: 107, 2206-11.

Sanger F., Nicklen S. and Coulson A. R. DNA sequencing with chain-terminating inhibitors. *Proc Natl Acad Sci U S A*. 1977: 74, 5463-7.

Santucci M. A., Trabetti E., Martinelli G., Buzzzi M., Zaccaria A., Pileri S., Farabegoli P., Sabattini E., Tura S. and Pignatti P. F. Host origin of bone marrow fibroblasts following allogeneic bone marrow transplantation for chronic myeloid leukemia. *Bone Marrow Transplant.* 1992: 10, 255-9.

Scott L. M., et al. JAK2 exon 12 mutations in polycythemia vera and idiopathic erythrocytosis. *N Engl J Med.* 2007: 356, 459-68.

Shah N. P., et al. A phase I study of XL019, a selective JAK2 inhibitor, in patients with primary myelofibrosis, post-polycythemia vera, or post-essential thrombocythemia myelofibrosis. *Blood.* 2008: 112, 98.

Shammaa D., Bazarbachi A., Halas H., Greige L. and Mahfouz R. JAK2 V617F mutation detection: laboratory comparison of two kits using RFLP and qPCR. *Genet Test Mol Biomarkers.* 2010: 14, 13-5.

Shannon K. M., O'Connell P., Martin G. A., Paderanga D., Olson K., Dinndorf P. and McCormick F. Loss of the normal NF1 allele from the bone marrow of children with type 1 neurofibromatosis and malignant myeloid disorders. *N Engl J Med.* 1994: 330, 597-601.

Shtivelman E., Lifshitz B., Gale R. P. and Canaani E. Fused transcript of abl and bcr genes in chronic myelogenous leukaemia. *Nature.* 1985: 315, 550-4.

Siebolts U., Ates M., Spitz R., Thiele J. and Wickenhauser C. Quantification of clonal hematopoiesis in polycythemia vera. *Virchows Arch.* 2005: 447, 947-53.

Siebolts U., Thiele J., Zander T., Ditschkowski M., Beelen D. W., Kroger N., Fehse B. and Wickenhauser C. Differences in proportion and dynamics of recipient hematopoiesis following hematopoietic cell transplantation in CML and IMF. *Oncol Rep.* 2008: 19, 287-92.

Siebolts U., Breuhahn K., Hennecke A., Schultze J. L. and Wickenhauser C. Imbalance of DNA-dependent protein kinase subunits in polycythemia vera peripheral blood stem cells. *Int J Cancer.* 2009: 124, 600-7.

Siebolts U., Varnholt H., Drebbler U., Dienes H. P., Wickenhauser C. and Odenthal M. Tissues from routine pathology archives are suitable for microRNA analyses by quantitative PCR. *J Clin Pathol.* 2009: 62, 84-8.

Siebolts U., Lange T., Niederwieser D. and Wickenhauser C. Allele-specific wild-type blocker quantitative PCR for highly sensitive detection of rare JAK2 p.V617F point mutation in primary myelofibrosis as an appropriate tool for the monitoring of molecular remission following therapy. *J Clin Pathol.* 2010: 63, 370-2.

Silver R. T. Chronic myeloid leukemia. *Hematol Oncol Clin North Am.* 2003: 17, 1159-73, vi-vii.

Simmons P. J., Przepiorka D., Thomas E. D. and Torok-Storb B. Host origin of marrow stromal cells following allogeneic bone marrow transplantation. *Nature.* 1987: 328, 429-32.

Simmons P. J., Masinovsky B., Longenecker B. M., Berenson R., Torok-Storb B. and Gallatin W. M. Vascular cell adhesion molecule-1 expressed by bone marrow stromal cells mediates the binding of hematopoietic progenitor cells. *Blood.* 1992: 80, 388-95.

Skoda R. The genetic basis of myeloproliferative disorders. *Hematology Am Soc Hematol Educ Program.* 2007: 1-10.

Spivak J. L. Polycythemia vera: myths, mechanisms, and management. *Blood.* 2002: 100, 4272-90.

Staerk J., Kallin A., Demoulin J. B., Vainchenker W. and Constantinescu S. N. JAK1 and Tyk2 activation by the homologous polycythemia vera JAK2 V617F mutation: cross-talk with IGF1 receptor. *J Biol Chem.* 2005: 280, 41893-9.

Swerdlow SH C. E., Harris NL, Jaffe ES, Pileri SA, Stein H, Thiele J, Vardiman JW WHO Classification of Tumours of Haematopoietic and Lymphoid Tissues. Vardiman JW. 2008: Lyon, France, 441.

Szpurka H., Tiu R., Murugesan G., Aboudola S., Hsi E. D., Theil K. S., Sekeres M. A. and Maciejewski J. P. Refractory anemia with ringed sideroblasts associated with marked thrombocytosis (RARS-T), another myeloproliferative condition characterized by JAK2 V617F mutation. *Blood.* 2006: 108, 2173-81.

Talpaz M., et al. Dasatinib in imatinib-resistant Philadelphia chromosome-positive leukemias. *N Engl J Med.* 2006: 354, 2531-41.

Tefferi A. JAK2 mutations in polycythemia vera--molecular mechanisms and clinical applications. *N Engl J Med*. 2007: 356, 444-5.

Tefferi A. and Vardiman J. W. Classification and diagnosis of myeloproliferative neoplasms: the 2008 World Health Organization criteria and point-of-care diagnostic algorithms. *Leukemia*. 2008: 22, 14-22.

Thiele J., Varus E., Siebolts U., Kvasnicka H. M., Wickenhauser C., Metz K. A., Beelen D. W., Ditschkowski M., Zander A. and Kroger N. Dualism of mixed chimerism between hematopoiesis and stroma in chronic idiopathic myelofibrosis after allogeneic stem cell transplantation. *Histol Histopathol*. 2007: 22, 365-72.

Tiedt R., Hao-Shen H., Sobas M. A., Looser R., Dirnhofer S., Schwaller J. and Skoda R. C. Ratio of mutant JAK2-V617F to wild-type Jak2 determines the MPD phenotypes in transgenic mice. *Blood*. 2008: 111, 3931-40.

Tokarski J. S., et al. The structure of Dasatinib (BMS-354825) bound to activated ABL kinase domain elucidates its inhibitory activity against imatinib-resistant ABL mutants. *Cancer Res*. 2006: 66, 5790-7.

Vannucchi A. M., Antonioli E., Guglielmelli P., Pardanani A. and Tefferi A. Clinical correlates of JAK2V617F presence or allele burden in myeloproliferative neoplasms: a critical reappraisal. *Leukemia*. 2008: 22, 1299-307.

Vannucchi A. M. and Guglielmelli P. Molecular pathophysiology of Philadelphia-negative myeloproliferative disorders: beyond JAK2 and MPL mutations. *Haematologica*. 2008: 93, 972-6.

Vardiman J. W., et al. The 2008 revision of the World Health Organization (WHO) classification of myeloid neoplasms and acute leukemia: rationale and important changes. *Blood*. 2009: 114, 937-51.

Vardiman JW B. R., Harris NL WHO histological classification of chronic myeloproliferative diseases. in: *World Health Organization Classification of Tumors: Tumours of the Haematopoietic and Lymphoid Tissues*. H. N. affe ES, Stein H, Vardiman JW. 2001: Lyon, France, 17-44.

Verstovsek S., Tefferi A., Kornblau S., Thomas D., Cortes J., Ravandi-Kashani F., Garcia-Manero G. and Kantarjian H. Phase II study of CEP701, an orally available JAK2 inhibitor, in patients with primary myelofibrosis and post- polycythemia vera / essential thrombocythemia myelofibrosis. *Blood*. 2007: 110, 3543.

Verstovsek S., Kantarjian H. M., Pardanani A., Thomas D. A., Cortes J. E., Mesa R., Hogan W., Redman J., Levy R. and Tefferi A. A phase I/II study of INCB018424, an oral, selective JAK inhibitor, in patients with primary myelofibrosis (PMF) and post polycythemia vera/essential thrombocythemia myelofibrosis (Post-PV/ET MF). *J Clin Oncol*. 2008: 26, 7004.

Verstovsek S., et al. The JAK inhibitor, INCB018424, demonstrates durable and marked clinical responses in primary myelofibrosis (PMF) and post- Polycythemia / essential thrombocythemia myelofibrosis (post PV / ET-MF). *Blood*. 2008: 112, 1762.

Wernig G., et al. Efficacy of TG101348, a selective JAK2 inhibitor, in treatment of a murine model of JAK2V617F-induced polycythemia vera. *Cancer Cell*. 2008: 13, 311-20.

Wickenhauser C., Perez F., Siebolts U., Lorenzen J., Varus E., Frimpong S. and Thiele J. Structural, antigenetic and transcriptional characteristics in peripheral blood CD34+ progenitor cells from polycythemia vera patients: evidence for delayed determination. *Int J Oncol*. 2003: 23, 437-43.

Xiao S., Nalabolu S. R., Aster J. C., Ma J., Abruzzo L., Jaffe E. S., Stone R., Weissman S. M., Hudson T. J. and Fletcher J. A. FGFR1 is fused with a novel zinc-finger gene, ZNF198, in the t(8;13) leukaemia/lymphoma syndrome. *Nat Genet*. 1998: 18, 84-7.

Xing S., Wanting T. H., Zhao W., Ma J., Wang S., Xu X., Li Q., Fu X., Xu M. and Zhao Z. J. Transgenic expression of JAK2V617F causes myeloproliferative disorders in mice. *Blood*. 2008: 111, 5109-17.

Zecca M., et al. JAK2 V617F mutation is a rare event in juvenile myelomonocytic leukemia. *Leukemia*. 2007: 21, 367-9.

Zhao R., Xing S., Li Z., Fu X., Li Q., Krantz S. B. and Zhao Z. J. Identification of an acquired JAK2 mutation in polycythemia vera. *J Biol Chem*. 2005: 280, 22788-92.

Structural, antigenetic and transcriptional characteristics in peripheral blood CD34⁺ progenitor cells from polycythemia vera patients: Evidence for delayed determination

CLAUDIA WICKENHAUSER¹, FERNANDO PÉREZ¹, UDO SIEBOLTS¹, JOHANN LORENZEN²,
EVA VARUS¹, SEMRA FRIMPONG³ and JÜRGEN THIELE¹

¹Institute of Pathology, University of Cologne; ²Institute of Pathology, University Hospital of RWTH Aachen;

³Institute of Dermatology, University of Cologne, Germany

Received February 24, 2003; Accepted April 11, 2003

Abstract. Polycythemia vera (PV) is a clonal disorder characterized by trilinear hematopoietic proliferation. PV progenitors are hypersensitive to several growth factors although their receptor expression is reduced or absent. In this study selected CD34⁺ peripheral blood (PB) cells from PV patients, PB healthy donors and patients with secondary polycythemia (SP) were investigated and compared concerning frequency, morphology, antigen expression, transcription of differentiation markers and proliferation as well as apoptosis rate following short-term culture. The highest amount of CD34⁺ cells was found in the SP group while the frequency was slightly lower but more variable in PV. Native PV CD34⁺ cells varied in shape and form and developed intracytoplasmatic organelles like mitochondria and a more extended Golgi apparatus while in the other groups they constituted a uniform phenotype. However, no premature transcripts for glycophorin A (GypA) and CD41b, both markers for advanced erythropoiesis and megakaryopoiesis, could be detected in sorted PV progenitors. Also, coexpression for early acting hematopoietic cytokine receptors IL-3R α and c-Kit and for initial erythropoiesis (GypC) or megakaryopoiesis (CD61) was similar in the different groups. Performing 96 h cocultures with bone marrow (BM) fibroblasts the frequency of CD34⁺ cells was elevated, downregulation of IL-3R α delayed, coexpression of GypC reduced and proliferative activity higher in the PV group. Our results suggest that primitive hematopoiesis is altered in PV because PB CD34⁺ cells in this disease are characterized by a maturation dissociation with increased activation in untreated populations and a delayed differentiation in short-term cultures.

Introduction

PV is one of four diseases commonly called the myeloproliferative disorders (MPDs) and is characterized by a panmyelosis implicating a proliferation especially of the erythroid and megakaryocytic cell series (1,2). PV progenitor cells respond abnormally to a number of cytokines (IL-3, GM-CSF, SCF, EPO, IGF-1 and TPO) (3-5). Different targets have been addressed for the disease mechanisms, spanning all the steps of receptor-mediated growth factor cell signaling. Dysregulation of a number of proteins, including the TPO receptor c-mpl and bcl-x_L have been observed in some PV patients (6,7). Platelet dysfunction (8) and differences in oxidative responses of PV cells (9) suggest, that the PV defect is not restricted to cytokine receptor-mediated signal transduction only. Moreover, a low or absent tumor suppressor H19 expression in CD34⁺/CD33⁻ PV BM-derived cells compared to the controls was found (10). Presentation of H19 is supposed to coincide with the commitment of progenitor cells to a single lineage according to the authors and they argue that low levels of this tumor-suppressor gene might contribute to the pathology of the disease. Temerinac *et al* described a hematopoietic cell surface receptor factor only transcribed in mature peripheral blood granulocytes from PV patients but not in healthy donors (11). The corresponding protein, named PRV-1 and potentially identical with the granulocytic activation marker CD177 (12) is expressed in the neoplastic and healthy myeloid lineage and the abnormal transcription in mature PV granulocytes points at an anachronistic, abnormal and prolonged influence of this factor on the myeloid hemato-poiesis. The aim of the present study was to analyze and to compare morphology, immunophenotype and transcription pattern of native and stimulated CD34⁺ progenitor cells from PV patients and patients with SP as well as healthy donors. Our findings support the above mentioned thesis of discordant proliferation and differentiation steps in the pathogenesis of PV.

Materials and methods

Monoclonal antibodies (MoAbs) for immunodetection and cell separation. Anti-IL-3R α -chain MoAbs, clone 32703.11,

Correspondence to: Dr Claudia Wickenhauser, Institut für Pathologie, Klinikum der Universität zu Köln, Joseph-Stelzmann-Str. 9, D-50934 Köln, Germany
E-mail: C.Wickenhauser@uni-koeln.de

Key words: polycythemia rubra vera, CD34⁺ cell differentiation, ultrastructure

IgG1 (R&D Systems Europe Ltd., Abingdon, UK); anti-CD117 MoAbs c-Kit, clone 95C3, IgG1 (An der Grub GmbH, Kaumberg, Austria). Anti-CD34 MoAbs native and fluorescein isothiocyanate (FITC) coupled, clone QBEND10, IgG1; anti-GypC MoAbs, clone Ret40f; IgG1, anti-CD61 MoAbs, clone Y2/51, IgG1; anti-Ki67 MoAbs, clone Ki-S5, IgG1 and anti-leucocyte common antigen (LCA) MoAbs, clone 2B11, IgG1 were all purchased from Dako (Hamburg, Germany). The MoAbs were applied according to the recommendations of the manufacturers. For the FACScan analysis, MoAbs were coupled to biotin employing a biotinylation kit (Sigma Chemical Co., St. Louis, MO, USA).

Patients. PB-derived samples from 17 PV patients (12 males, 5 females) and 3 patients with SP (males) were gained for therapeutic purpose (phlebotomy) after informed consent. The age of the PV patients ranged from 26 to 70 years (mean 55). The duration of the disease ranged from 0.5 to 82 months (mean 38). The diagnosis of PV was ascertained according to the criteria of the Polycythemia Vera Study Group and the WHO classification. Patients were only treated with phlebotomies, no additional myelosuppressive regimens were administered. Among the SP patients, the age ranged from 26 to 63 years (mean 39) and there was a history of heavy smoking. Buffy coats of PB-derived samples were recruited from the Institute of Transfusion Medicine, University of Cologne, from 24 healthy donors.

Cell preparation and enrichment of CD34⁺ hematopoietic progenitor cells by immunoaffinity selection. Blood samples underwent centrifugation over Ficoll-Paque (Pharmacia, Uppsala, Sweden) to obtain a mononuclear cell concentrate. Afterwards cells were incubated in several steps with paramagnetic beads coupled with CD34 antibodies (clone QBEND10) purchased from Miltenyi Biotec (Bergisch Gladbach, Germany), and then passed over MiniMACS separation columns (Miltenyi Biotec) retained in a magnetic field as already described (13). Following short-term culture CD34⁺ cells were obtained performing the same procedure. To separate hematopoietic cells from fibroblast stroma layer cells an enrichment on the basis of LCA protein expression was performed. For RT-PCR experiments, CD34⁺ cells were sorted according to CD34 expression by using a Coulter Elite flow cytometer.

Cellular immunodetection. Enriched CD34⁺ cells were fixed with 100% acetone and then labeled with anti-CD34 followed by an incubation with a biotinylated rabbit anti-mouse antibody and subsequently stained with several components of an ABC staining kit (Dako) and developed with fast red. For evaluation of the proliferation rate, nuclei of the enriched CD34⁺ cell fraction were stained with anti-Ki67 (reviewed in ref. 13).

Examinations of the CD34⁺ cells by fluorescence-activated cell sorting (FACS) analysis. Analytical two-color experiments were performed using a FACScan flow cytometer (Becton Dickinson, San Jose, CA, USA). List mode data for 10,000 cells were collected either ungated or in an electronic gate for cells with intermediate to high forward light scatter and low-to-

intermediate right angle light scatter to exclude dead cells from the analysis. Flow cytometric data were analyzed using Lysys II software (Becton Dickinson). Enriched progenitor cells were pelleted before staining with MoAbs. For double staining, cells were incubated with FITC-conjugated anti-CD34 and biotinylated MoAbs for 20 min on ice and then washed twice. Cells were then incubated with streptavidin coupled PE. For all experiments isotype controls were performed and the data compared with the specifically stained probes. Also, as further controls, unstained cells and cells stained only with secondary antibody were included.

Morphometry. Morphometric evaluation was performed by a manual optic planimeter (Vidas, Zeiss-Kontron) with a semi-automatic computer analyzer of images on cytopspin preparations of CD34⁺ immunostained cells at x1,250 magnification. Six hundred cells from each sample (3 PV patients, 3 SP patients, and 3 healthy donors) were evaluated.

Transmission electron microscopy (TEM) preparation. At least 20,000 CD34⁺ enriched cells from each sample (3 PV patients, 3 SP patients, and 3 healthy donors) were centrifuged and fixed with 2.5% glutaraldehyde containing buffer and postfixed with 1% OsO₄ as described previously (14). After dehydration and embedding in Araldite ultra-thin sections were mounted on 200 mesh nickel grids and stained by uranyl acetate and lead citrate. Grids were examined with an EM 902a microscope (Zeiss, Oberkochen, Germany).

Identification of apoptotic cells. The ISEL technique was applied on cytopspin preparations of enriched CD34⁺ cells using a standard protocol (15).

RNA extraction and reverse transcriptase-polymerase chain reaction (RT-PCR). The method was performed as described previously (16,17). Briefly, at least 1,000 sorted CD34⁺ cells were collected by centrifugation and then lysed in a solution containing guanidinium isothiocyanate and N-laurylsarcosine. After phenol extraction and precipitation, the cellular RNA was dissolved to a final volume of 20 µl. The mRNA was obtained by using oligo (dT)₁₅ (Promega, Mannheim, Germany) as primer and the reverse transcriptase Superscript II (Gibco BRL), according to the instructions of the manufacturer. After reverse transcription, 3 µl of the reaction solution was used for PCR amplification. The sequences of the oligonucleotide sense and antisense primers used for RT-PCR and the expected length of the amplification products are listed in Table I. Primer sequences were obtained from published sources (18-21). Using hot start technique with a touch down temperature protocol, 40 cycles were performed on a thermocycler (Perkin Elmer, Düsseldorf, Germany), using a sample volume of 50 µl. A second round of 40 PCR cycles was performed, using 10 µl of the amplified material and fresh Taq-polymerase. The products were separated on 5% NuSieve agarose gels (Biozym Diagnostic, Hessisch Oldendorf, Germany) containing ethidium bromide and photographed.

Culture of BM-derived fibroblasts. Fibroblasts were selected as described previously (22). Contamination with monocytes

Table I. Sequences of the oligonucleotide primers.

Amplified transcript	Oligonucleotide primer sequence	Amplification product length (bp)
β -actin	5'-GTGGGGCGCCCCAGGCACCA-3' 5'-CTCCTTAATGTCACGCACGATTTC-3'	548
c-Kit	5'-CGGGATCCCCCAAGGACTTGAGGTTTATT-3' 5'-CGGGATCCCTTGGGATAATCTTCCCATT-3'	603
IL-3R α	5'-TCTCCAGCGTTCTCAAAGTTCACATCC-3' 5'-CCCAGACCACCAGCTTGTCTGTTTTGGAAGC-3'	555
GypA	5'-CGCA/AGCT-TATGTATGGAAAAATAATCTT-3' 5'-CGCG/GATC-CTTCTGGAGGGTAAACAGTCT-3'	240
CD41b	5'-CTCGCTGCTCTTTGACCTCC-3' 5'-AATGCGGCTCAGGGTGTTC-3'	265

Table II. Morphometric analysis of PB-derived CD34⁺ progenitor cells after immunoaffinity selection.

CD34 ⁺ cell source	Cells x10 ⁵ /l blood ^a	Total cell area (μm^2) ^b	Mean value of nuclear parameters \pm SD			
			Area (μm^2)	Minimum diameter (μm)	Maximum diameter (μm)	Form factor
PV	2.0 (1.4-5.0)	118.8 \pm 19.7	81.2 \pm 8.8	7.4 \pm 0.7	10.2 \pm 0.6	0.92 \pm 0.05
SP	4.5 (4.2-4.8)	93.9 \pm 10.4	67.2 \pm 7.8	6.6 \pm 0.4	9.7 \pm 0.5	0.94 \pm 0.04
Controls	3.3 (2.6-3.8)	92.0 \pm 9.4	66.1 \pm 7.1	6.4 \pm 0.4	9.5 \pm 0.4	0.95 \pm 0.04

^aMedian values and ranges (within parentheses) are given; ^bmean values \pm SD are given; numbers in bold-face indicate $p < 0.05$.

and macrophages was assessed by CD14 and CD68 antibody staining (Dako) and the non-specific esterase reaction. According to these staining results, the BM-derived fibroblast populations contained very small amounts of these cell lineages (<1%). Fibroblasts of the third or fourth passage from 3 healthy donors were taken for the study.

Fibroblast - CD34⁺ progenitor cell cocultures (FCC). To measure short-term growth, 1,000 to 2,000 cells were plated in 25 mm culture dishes (Nunc Inc., Naperville, IL, USA) containing attenuated α -MEM, 5x10⁻⁵ mol/l 2-mercaptoethanol (Sigma), 300 $\mu\text{g}/\text{ml}$ fully iron-saturated human transferrin (Sigma), 5x10⁻⁸ mol/l sodium selenite (Sigma), 10 $\mu\text{g}/\text{ml}$ lecithin (Sigma), 6 $\mu\text{g}/\text{ml}$ cholesterol (Sigma), 1 $\mu\text{g}/\text{ml}$ bovine pancreas insulin (Sigma). Each well contained a near-confluent layer of fibroblasts. Dishes were incubated at 37°C in a fully humidified atmosphere flushed with a combination of 5% CO₂. After 96 h, the cells of the culture plates were removed. The cells were prepared for purification according to CD34 or LCA expression.

Statistical analysis. p-values were calculated with SigmaStat software (SPSS Inc., Chicago, IL, USA). For statistical

evaluation we employed the χ^2 test, the Wilcoxon-Mann-Whitney U-test and ANOVA on ranks with a level of significance set at $p < 0.05$.

Results

Efficiency and frequency of PB-derived CD34⁺ expressing cells after immunomagnetic separation. Following selection, CD34⁺ cells were immunochemically labeled and subjected to flow cytometry. The purity of the immunomagnetic enriched CD34⁺ cells ranged between 95 and 98%. The mean values and ranges of the numbers of PB-derived CD34⁺ cells for the two patients groups and for the control subjects are given in the left column of Table II. In PV the number of CD34⁺ cells was slightly less, in the SP fraction slightly higher compared with the healthy donors SP patients and controls (not significant as determined by ANOVA).

Size and morphology of PB CD34⁺ progenitor cells. CD34⁺ cells from healthy donors showed a uniform ultrastructure as established by morphometric evaluation and TEM analysis. The nuclei were round or kidney-shaped (mean area of 66.1 μm^2) and euchromatic with dispersed heterochromatin condensation

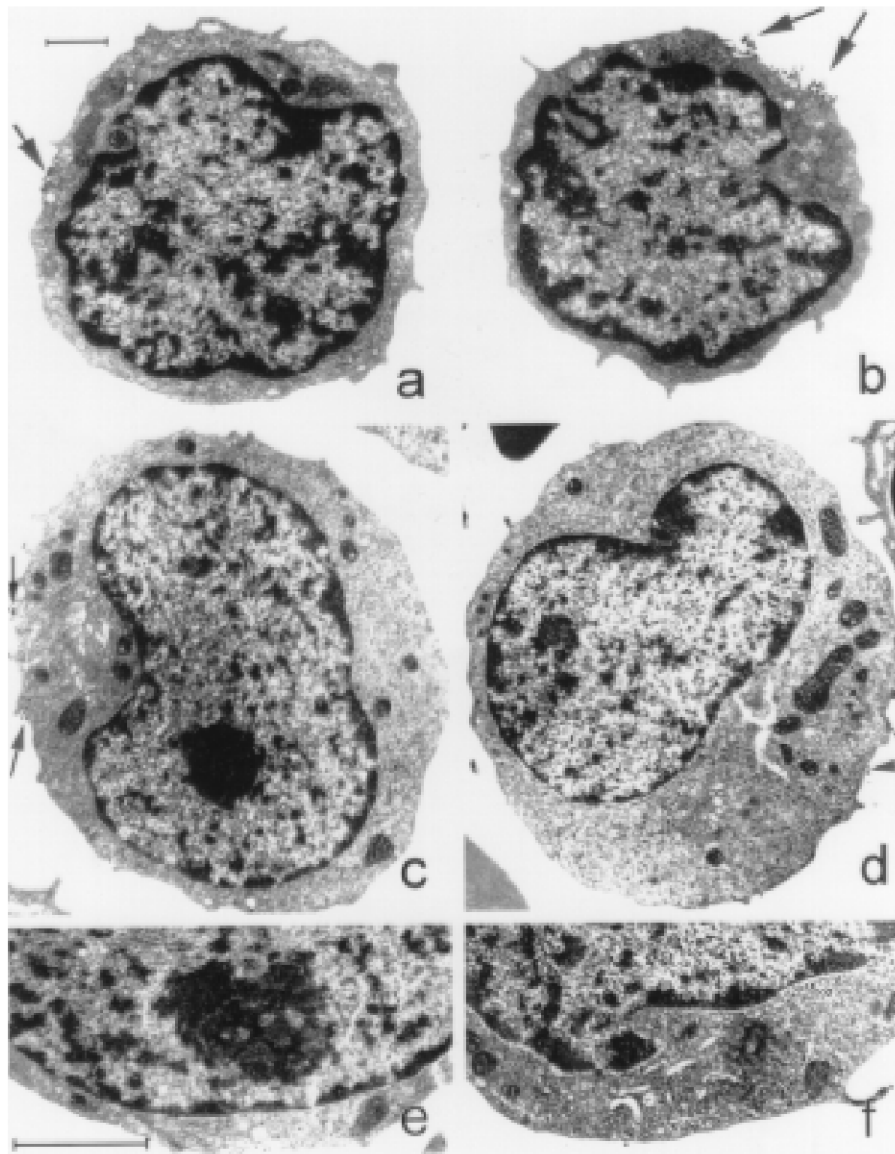


Figure 1. Ultrastructure of freshly prepared CD34⁺ progenitor cells. Iron-coupled anti-CD34 monoclonal antibodies are visible at the cell membranes (and contrasted by arrows). In (a) and (b) cells of the healthy donor group, morphology identical with those of the SP group, are presented with mildly convoluted nuclei and a small cytoplasmic rim. Only few mitochondria are present. In (c) and (d) the PV CD34⁺ cells are more heterogeneous in shape, larger, and display more cell organelles. Mitochondria are more numerous and larger, also a distinctive Golgi apparatus is visible. The nuclei are almost kidney-shaped. In (e) and (f) magnifications of PV CD34⁺ cells are shown to demonstrate the prominent nucleolus (e) and the Golgi apparatus (f) in these cells. Bars indicate 2 μ m.

(Fig. 1a and b). The cytoplasm was reduced to a small inconspicuous rim and poor in organelles (Fig. 1a and b). The entire cell exhibited a mean area of 92.0 μ m² (Table II). CD34⁺ cells from SP patients presented the same features as the CD34⁺ cells of the healthy donor group (not shown). On the contrary, peripheral blood CD34⁺ cells from PV patients varied in size with a preference for larger forms (Table II, Fig. 1c and d). The nuclei (mean area 81.2 μ m²) as well as the entire cell (mean area 118.8 μ m²) showed a significant larger size compared with the CD34⁺ cells of the SP patients and the healthy donor group ($p < 0.05$ in both cases, determined by the Wilcoxon-Mann-Whitney U-test). Progenitors from PV patients had a slightly lower form factor (determined by the Saltykov formula) contrasting both other cell groups. According to ultrastructural data the PV CD34⁺ progenitors

presented many cell organelles including loose clusters of mitochondria and an extended Golgi apparatus (Fig. 1c, d and f). In addition, the CD34⁺ cell nuclei of PV patients, revealed a compact nucleolus with granular and dense fibrillar components (Fig. 1e).

Coexpression of cytokine receptors and differentiation antigens. In FACS analysis CD34⁺ cells were investigated for coexpression of c-Kit and IL-3R α protein as well as for the differentiation markers GypC and CD61. The results are presented in Fig. 2. Only little differences in the overall coexpression of the above mentioned cytokine receptors and differentiation markers could be found in native CD34⁺ cell population between the two tested groups. After serum-free coculture with BM-derived fibroblasts 60% of the PV

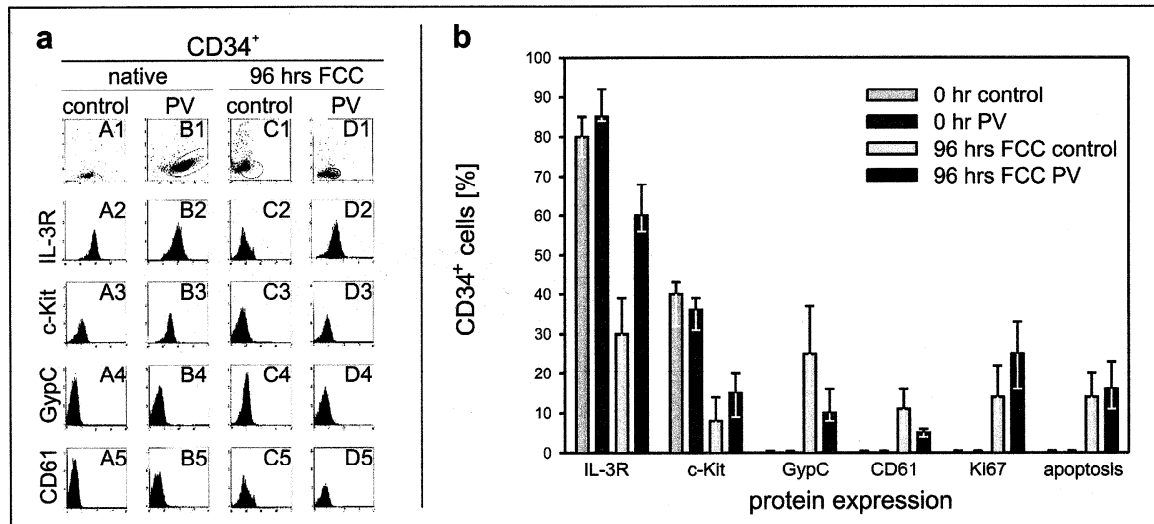


Figure 2. Reactivity with cytokine receptor antibodies and differentiation antibodies as well apoptosis markers of CD34⁺ cells in normal blood samples and blood samples of PV patients. a, Representative FACS analysis of MACS enriched CD34⁺ progenitor cells from one PV patient and one healthy donor sample. For all experiments isotype controls were performed and compared with the stained probes (data not shown). The dot plots demonstrate the light scattering characteristics of the enriched CD34⁺ cells. Dot plots and histograms demonstrate the results on native progenitors (A1-A5 and B1-B5) and following 96 h coculture with BM-derived fibroblasts (FCC; C1-C5 and D1-D5). In (A1-D1) the overall population of hematopoietic cells was investigated. In (A2-D5) the CD34⁺ gated cell fraction was analysed. In (A2-D2) the data for IL-3R α , in (A3-D3) the data for c-Kit, in (A4-D4) data for GypC and in (A5-D5) data for CD61 are demonstrated. b, Results of membranous expression of c-Kit, IL-3R α , GypC, and CD61 as well as proliferation analysis and apoptosis assay (ISEL technique) in CD34⁺ cells. Values from native cells and after 96 h short-term culture with BM-derived fibroblasts (FCC) are presented. Overall values of FACS analysis from 10 PV patients and 10 healthy donors as well as proliferation and apoptosis values from 6 patients each are presented. The data are shown as means with range values.

patient-derived cells remained CD34⁺ compared with 30% in the control group (Fig. 2a, C1 and D1). In addition, after coculture CD34⁺ cells of PV patients presented significantly higher IL-3R α and c-Kit protein expression, meanwhile coexpression for GypC and CD61 was significantly reduced in the PV cell group (Fig. 2b; significance was determined by the χ^2 test in comparison with controls).

Proliferation and apoptosis analysis in CD34⁺ cells. We analyzed proliferation and apoptosis of native and short-term cultured PB-derived CD34⁺ cells by anti-Ki67 immunocytochemical staining and ISEL technique, respectively. The native CD34⁺ fractions of both PV patients and healthy donors presented a low percentage of proliferating cells and also of apoptotic cells (Fig. 2b). CD34⁺ cells cocultured with BM-derived fibroblasts showed 25% of proliferating cells in the PV group compared with 14% in the controls ($p < 0.05$).

Transcription analysis of cytokine receptors and differentiation antigens. A premature transcription of differentiation markers for the advanced erythrocytic and megakaryocytic lineage (18,23) could be excluded using primers for GypA and CD41b (Fig. 3). In addition, mRNA transcription for the cytokine receptors as well as for the differentiation antigens GypA and CD41b was examined within the sorted CD34⁺ cell fraction after coculture with fibroblasts. Again, no premature transcription for GypA or CD41b was found in either fraction. A water control RT-PCR, run simultaneously showed no bands, making carry-over artifact an unlikely explanation for the possibility for the signals detected (data not shown).

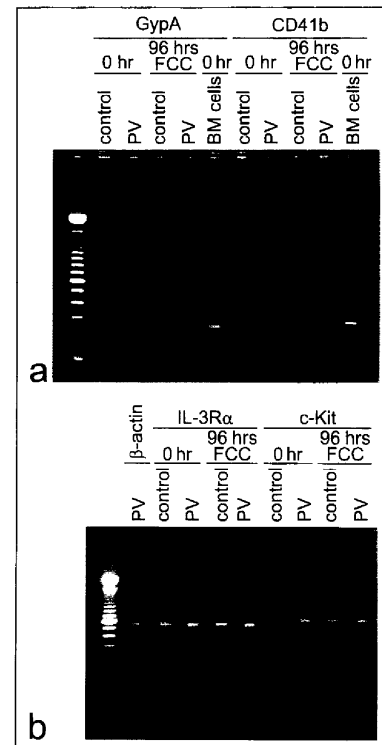


Figure 3. Representative RT-PCR expression analysis of sequences found in native CD34⁺ cells and in CD34⁺ cells following short-term culture. Transcripts for GypA and CD41b (a) as well as for IL-3 receptor (IL-3R α) and the SCF receptor c-Kit (b), were analyzed in sorted CD34⁺ progenitor cells from PV patients and healthy donors performing RT-PCR. (a), bone marrow cells (BM cells) served as control for both transcripts. (b), IL-3R α and c-Kit could be detected in unstimulated cells as well as following coculture with BM-derived fibroblasts (FCC).

Discussion

The underlying cellular and biochemical defects characterizing the pathobiology of PV are still not known and have been the focus of several reviews (24,25). Of particular interest for the interpretation of the presented data is the loss in the expression of H19, a tumor suppressor antigen supposed to coincide with the commitment of progenitor cells to a single lineage, in CD34⁺/CD33⁺ PV bone marrow cells (10). Also, the exclusive transcription of the PRV-1 gene, not only identifiable in myeloid progenitors but also in mature PV granulocytes (11) points to a substantial deviation of maturation in this disorder.

We compared several aspects of the differentiation status of CD34⁺ cells from PV patients, patients with SP and healthy donors. Contrary to others (26) we found slightly lower quantities of CD34⁺ cells in the PV group. This different result is certainly due to the fact that we explicitly used blood from patients in the early polycythemic phase not treated with any cytoreductive drugs and with no evidence for a spent or accelerated phase of the disease. On the other hand, it is well known that high thrombocyte values, typical for PV patients can reduce the recovery rates of CD34⁺ cells in the peripheral blood. Considering the morphology of the control and SP CD34⁺ progenitors ultrastructural findings confirmed the uniform character also reported by our group and others (13,27). In the contrary, the heterogeneity of the PV CD34⁺ cell fraction was conspicuous, and in ultrastructural analysis PV CD34⁺ cells were characterized by numerous cell organelles. Although these findings were suggesting a premature differentiation of the CD34⁺ cells we found no markers for advanced erythropoietic or megakaryocytic differentiation at the transcriptional level. Furthermore, protein expression for initial erythropoietic and megakaryocytic differentiation was approximately equal in the different patient groups. Because BM-derived CD34⁺ progenitors are known to belong to a more variously shaped, differentiated cell compartment an increased recruitment of BM stem and progenitor cells could be assumed. Two arguments, however, are not in keeping with this theory: i) the frequency of CD34⁺ progenitors not only in the PB but also in the BM of PV patients in the early proliferative state is not elevated (28), indicating a normal distribution of these cells in both compartments and ii) the BM-derived CD34⁺ cells normally express c-Kit at higher density than the PB progenitors under study (29). An activation or increased release of BM CD34⁺ progenitor cells as a reactive phenomenon accompanying erythrocytosis could further be ruled out by analyzing the SP patients samples. The pleomorphy therefore indicates the exaggerated activation of this cell population and might be a hallmark for the PB-derived CD34⁺ cells in PV.

In the second approach of our study we performed 96 h cocultures of CD34⁺ progenitors and BM-derived fibroblasts. In this context we chose the above mentioned culture system because it is known to sustain long-term hematopoiesis. Performing these investigations we found that after cultivation in PV the overall expression of CD34 antigen by LCA⁺ hematopoietic cells was higher compared to the controls. Further, in the CD34⁺ cell group a significantly higher rate of coexpression for IL-3R α and c-Kit was evident and also the GypC coexpression decreased compared to the healthy donor

group. According to this experimental design, there was an increased proliferation contrasting an equal apoptosis rate in PV cells. These findings indicate that differentiation of the CD34⁺ cells is slowed while self-renewal is simultaneously promoted. They are in line with other studies demonstrating that retarded differentiation and therefore accumulation of early progenitors could be an initial event in the pathogenesis of PV (10,11).

Increased self-renewal with expansion of the pool of candidate cells susceptible to second-hit mutations is a known phenomenon for various myeloid neoplasms with a constitutive activation of a (translocated) tyrosine phosphatase (30,31). In PV the molecular pathogenesis behind these observations is still unclear.

Acknowledgements

This work was supported by Sonderforschungsbereich 502 of the Deutsche Forschungsgemeinschaft and a grant from the Köln Fortune Foundation.

References

1. Dickstein JJ and Vardiman JW: Issues in the pathology and diagnosis of the chronic myeloproliferative disorders and the myelodysplastic syndromes. *Am J Clin Pathol* 99: 513-525, 1993.
2. Georgii A, Buesche G and Kreft A: The histopathology of chronic myeloproliferative diseases. *Baillieres Clin Haematol* 11: 721-749, 1998.
3. Dai CH, Krantz SB, Means RT, Horn ST and Gilbert HS: Polycythemia vera blood burst-forming units erythroid are hypersensitive to IL-3. *J Clin Invest* 87: 391-396, 1991.
4. Dai CH, Krantz SB and Dessypris EN: Polycythemia vera. II. Hypersensitivity of bone marrow erythroid, granulocyte-macrophage, and megakaryocyte progenitor cells to IL-3 and GM-CSF. *Blood* 80: 891-899, 1992.
5. Dai CH, Krantz SB, Green WF and Gilbert HS: Polycythemia vera. III. Burst-forming units-erythroid (BFU-E) response to stem cell factor and c-kit receptor expression. *Br J Haematol* 86: 12-21, 1994.
6. Moliterno AR, Hankins WD and Spivak JL: Impaired expression of the thrombopoietin receptor by platelets from patients with polycythemia vera. *N Engl J Med* 338: 572-581, 1998.
7. Silva M, Richard C, Benito A, Sanz C, Olalla I and Fernandez-Luna JL: Expression of bcl-x in erythroid precursors from patients with polycythemia vera. *N Engl J Med* 338: 565-571, 1998.
8. Le Blanc K, Berg A, Palmblad J and Samuelsson J: Stimulus-specific defect in platelet aggregation in polycythemia vera. *Eur J Haematol* 53: 145-149, 1994.
9. Samuelsson J, Forslid J, Hed J and Palmblad J: Studies of neutrophil and monocyte oxidative responses in polycythemia vera and related myeloproliferative disorders. *Br J Haematol* 87: 464-470, 1994.
10. Nunez C, Bashein AM, Brunet CL, Hoyland JA, Freemont AJ, Buckle A-M, Murphy C, Cross MA, Lucas G, Bostock VJ and Brady G: Expression of the imprinted tumor-suppressor gene H19 is tightly regulated during normal hematopoiesis and is reduced in hematopoietic precursors of patients with the myeloproliferative disease polycythemia vera. *J Pathol* 190: 61-68, 2000.
11. Temerinac S, Klippel S, Strunck E, Röder S, Lübbert M, Lange W, Azemar M, Meinhardt G, Schaefer H-E and Pahl HL: Cloning of PRV-1, a novel member of the uPAR receptor superfamily, which is overexpressed in polycythemia rubra vera. *Blood* 95: 2569-2576, 2000.
12. Stroneck D: Neutrophil alloantigens. *Transfus Med Rev* 16: 67-75, 2002.
13. Thiele J, Wickenhauser C, Baldus SE, Kümmel T, Zirbes TK, Drebber U, Wirtz R, Thiel A, Hansmann M-L and Fischer R: Characterization of CD34⁺ human hemopoietic progenitor cells from the peripheral blood: enzyme-, carbohydrate- and immunocytochemistry, morphometry, and ultrastructure. *Leukemia Lymphoma* 16: 483-491, 1995.

14. Kuemmel TA, Thiele J, Blaeser AH, Wickenhauser C, Baldus SE and Fischer R: Lectin binding sites on CD34⁺ human haematopoietic stem cells and lymphocytes from peripheral blood: an ultrastructural post-embedding study. *Histochem J* 29: 695-705, 1997.
15. Thiele J, Zirbes TK, Lorenzen J, Kvasnicka HM, Dresbach S, Manich B, Leder LD, Niederle N, Diehl V and Fischer R: Apoptosis and proliferation (PCNA labeling) in CML: a comparative immunohistological study on bone marrow biopsies following interferon and busulfan therapy. *J Pathol* 181: 316-322, 1997.
16. Wickenhauser C, Lorenzen J, Thiele J, Hillienhof A, Jungheim K, Schmitz B, Hansmann M-L and Fischer R: Secretion of cytokines (IL-1a - 3 and -6 and GM-CSF) by normal human bone marrow megakaryocytes. *Blood* 85: 685-691, 1995.
17. Wickenhauser C, Thiele J, Lorenzen J, Schmitz B, Frimpong S, Schramm K, Neumann I, Zankovich R and Fischer R: Polycythemia vera megakaryocytes but not megakaryocytes from normal controls and patients with smokers polyglobuly spontaneously express IL-6 and IL-6R and secrete IL-6. *Leukemia* 13: 327-334, 1999.
18. Thoma SJ, Lamping CP and Ziegler BL: Phenotype analysis of hematopoietic CD34⁺ cell populations derived from human umbilical cord blood using flow cytometry and cDNA polymerase chain reaction. *Blood* 83: 2103-2114, 1994.
19. Yarden Y, Kuang WY, Ynag-Feng T, Cousseus L, Mivemitsu S, Bull TJ, Cheul E, Schlessinger J, Franke U and Ullrich A: Human proto-oncogene c-kit: a new cell surface receptor tyrosine kinase for an unidentified ligand. *EMBO J* 6: 3341-3351, 1987.
20. Kitamura T, Sato N, Arai KI and Miyamjima A: Expression cloning of the human IL-3 receptor cDNA reveals a shared β subunit for the human IL-3 and GM-CSF receptors. *Cell* 66: 1165-1174, 1991.
21. DuPont BR, Grant SG, Oto SH, Bigbee WL, Jensen RH and Langlois RG: Molecular characterization of glycophorin A transcripts in human erythroid cells using RT-PCR, allele specific restriction, and sequencing. *Vox Sang* 68: 121-129, 1996.
22. Schmitz B, Thiele J, Witte O, Kaufmann R, Wickenhauser C and Fischer R: Influence of cytokines (IL-1a, IL-3, IL-11, GM-CSF) on megakaryocyte-fibroblast interactions in normal human bone marrow. *Eur J Haematol* 55: 24-32, 1995.
23. Daniels G and Greem C: Expression of red cell surface antigens during erythropoiesis. *Vox Sang* 78 (Suppl. 2): 149-153, 2000.
24. Prchal JF and Prchal JT: Molecular basis for polycythemia. *Curr Opin Haematol* 6: 100-109, 1999.
25. Pahl HL: Towards a molecular understanding of polycythemia rubra vera. *Eur J Biochem* 267: 3395-3401, 2000.
26. Andreasson B, Swolin B and Kutti J: Increase of CD34⁺ cells in polycythaemia vera. *Eur J Haematol* 59: 171-176, 1997.
27. Lambertenghi A, Deliliers G, Caneva L, Fumiatti R, Servida F, Rebulla P, Lecci L, De Harven E and Soligo D: Ultrastructural features of CD34⁺ hematopoietic progenitor cells from bone marrow, peripheral blood and umbilical cord blood. *Leukemia Lymphoma* 42: 699-708, 2001.
28. Thiele J and Kvasnicka HM: CD34⁺ stem cells in chronic myeloproliferative disorders. *Histol Histopathol* 17: 507-521, 2002.
29. De Bruyn C, Delforge A, Lagneaux L and Bron D: Characterization of CD34⁺ subsets derived from bone marrow, umbilical cord blood and mobilized peripheral blood after stem cell factor and interleukin 3 stimulation. *Bone Marrow Transpl* 25: 377-383, 2000.
30. Kelly LM, Liu Q, Kutok JL, Williams IR, Boulton CL and Gilliland DG: FLT3 internal tandem duplication mutations associated with human acute myeloid leukemias induce myeloproliferative disease in a murine bone marrow transplant model. *Blood* 99: 310-318, 2002.
31. Yamamoto Y, Kiyoi H, Nakano Y, Suzuki R, Kadera Y, Miyawaki S, Asou N, Kuriyama K, Yagasaki F, Shimazaki C, Akiyama H, Saito K, Nishimura M, Motoji T, Shinagawa K, Takeshita A, Saito H, Ueda R, Ohno R and Naoe T: Activating mutation of D835 within the activation loop of FLT3 in human hematologic malignancies. *Blood* 97: 2434-2439, 2001.

Udo Siebolts · Murat Ates · Rüdiger Spitz ·
Jürgen Thiele · Claudia Wickenhauser

Quantification of clonal hematopoiesis in polycythemia vera

Received: 23 June 2005 / Accepted: 3 July 2005
© Springer-Verlag 2005

Abstract Polycythemia vera (PV) is believed to represent a clonal trilineage myeloaccumulative hematopoietic disorder. This study was undertaken to estimate for the first time the proportion not only of the neoplastic clone but also of clonal and residual nonneoplastic CD34⁺ progenitor cells. Chromosomal abnormalities, including trisomy 8 or 9, are phenomena associated in about 20% of PV patients. Therefore, we screened peripheral blood (PB) mononuclear cells of PV patients in the chronic phase of the disease and looked for chromosomal abnormalities performing comparative genomic hybridization. Two of the ten patients revealed cytogenetic changes, including trisomy 8 or 9. To quantify the proportion of cytogenetic abnormal cells in these patients, we applied fluorescence in situ hybridization (FISH) technique on immunomagnetically enriched cell fractions. Ninety percent of the mononuclear cells and up to 79% of PB-derived CD34⁺ progenitor cells presented three signals for chromosome 8 or 9. The diagnostic value of FISH to detect trisomies in trephine biopsies was then tested in all patients under study. Although the probability to detect FISH signals in a certain section plane is reduced, constantly 10–15% of the cells revealed three signals. Concerning the CD34⁺ progenitor cell pool, a distinct nonclonal population exists in these patients. Our data underline the stem cell character of PV and additionally quantify the proportion of clonal CD34⁺ progenitor cells for the first time. The finding of a distinct, not aberrant, CD34⁺ progenitor cell population in chronic phase PV may

offer perspectives in treatment of the disease. Finally, FISH analysis of bone marrow biopsies can be helpful to consolidate diagnosis of early PV.

Keywords Polycythemia vera · Chromosomal aberrations · CD34⁺ · FISH · CGH

Introduction

Polycythemia vera (PV) is believed to be a clonal disorder arising in a multipotent hematopoietic progenitor cell that causes the accumulation of morphologically normal red cells, white cells, platelets, and their precursors in the absence of a definable stimulus [26]. However, the molecular basis of PV remains elusive. The hallmark of the disease is trilineage hematopoietic proliferation (panmyelosis) dominated by erythropoiesis [26]. Therefore, most investigations on the pathogenesis of PV have focused on the red cell lineage. Indeed, a peculiarity of PV patients is the reduced serum erythropoietin (Epo) level [6]. The results concerning functional aspects of the erythropoiesis in PV, however, are contradictory. PV erythroid progenitor cells are able to proliferate in vitro in the absence of Epo, but this does not define the limits of the abnormal clone since not all PV erythroid progenitor cells exhibit Epo independence [7]. The existence of several hematologic subpopulations in PV may therefore be speculated, and a quiescent significant proportion of nonneoplastic cells in blood and bone marrow of PV patients cannot be excluded. In several recently published studies, the hypersensitivity of PV progenitors to several growth factors was explained by a point mutation of Janus kinase 2 gene (JAK2), leading to a constitutive activation of this downstream transducer of growth-factor-induced signaling [2, 14, 21]. This point mutation, however, was also seen in other chronic myeloproliferative disorders and, therefore, is not specific for PV.

Although there is no pathognomonic chromosomal abnormality defining PV, consistent, acquired cytogenetic changes, including del(20q), del(13q), trisomies 8 and 9 as well as duplication of 1q, have been observed at diagnosis

U. Siebolts · M. Ates · J. Thiele · C. Wickenhauser (✉)
Institute of Pathology, University of Cologne,
Joseph-Stelzmannstr. 9,
50924 Cologne, Germany
e-mail: c.wickenhauser@uni-koeln.de
Tel.: +49-221-4786368
Fax: +49-221-4786360

R. Spitz
Children's Hospital, Pediatric Oncology,
University of Cologne,
Cologne, Germany

[1, 5, 24, 29]. Analysis of genomic abnormalities in individual cells of PV hematopoiesis, therefore, might elucidate the proportion of the neoplastic clone in this disease. In addition, fluorescence in situ hybridization (FISH) analysis on bone marrow trephine biopsies can be helpful for the diagnosis of early PV.

Materials and methods

Patients

Following informed consent, bone marrow trephine biopsies and peripheral blood (PB) derived samples from ten patients with histopathologically determined chronic phase PV (seven males and three females) were gained for diagnostic or therapeutical purpose (phlebotomy). The age of the patients ranged from 42 to 86 years (mean 64). According to the relevant clinical records, the duration of the disease ranged from 0.5 to 10 months. No additional myelosuppressive regimens were administered. The diagnosis of PV was ascertained according to the criteria of the WHO classification. At initial diagnosis, all patients presented hemoglobin values of >18.5 g/dl (in men) and >16.5 g/dl (in women), a thrombocytosis of $>400 \times 10^9/l$, and low Epo levels. Ten trephine biopsies from patients with lymphoproliferative disorders (without bone marrow involvement) and ten healthy blood donors served as controls.

Blood cell preparation

For FISH analysis, blood samples underwent centrifugation over Ficoll-Paque (Pharmacia, Uppsala, Sweden) to obtain a mononuclear cell concentrate. Selection of CD34⁺ progenitor cells was performed by immunofluorescence selection, employing an immunomagnetic separation kit (Miltenyi Biotec, Bergisch Gladbach, Germany) as described before [30]. The purified cells were washed three times in phosphate-buffered saline (PBS), swollen in 75 mmol/l KCl at 37°C for 45 min, and then resuspended in ice-cold acetic methanol (1:3) fixative. The nuclei were then washed twice and stored in fixative at -20°C before FISH analysis.

Fixed nuclei were dried onto glass slides and sequentially incubated in solutions of ribonuclease A (Sigma, Dreisenhofen, Germany) at 37°C for 60 min, saline sodium citrate (SSC) for 5 min, pepsin (100 µg/ml, pH 2.0, 37°C; Sigma) for 10 min, PBS (room temperature) for 10 min, and 2× SSC (37°C) for 30 min. The slides were then dehydrated through ethanol solutions (70, 90, and 100%) and dried before denaturing in formamide (70% in 2× SSC and sodium phosphate buffer, 50 mmol/l, pH 7.0; Fluka) under coverslips on a hot plate at 73°C for 1 min. The slides were washed in 2× SSC, dehydrated through the ethanol solutions, and dried.

Preparation of the bone marrow biopsies

Bone marrow biopsies were transferred in buffered fixative (pH 7.4) containing 0.5% glutaraldehyde and decalcified overnight in ethylenediaminetetraacetic acid (EDTA; 10% w/v in Tris pH 7.4). For phenotypic evaluation, 4-µm paraffin-embedded sections of trephine biopsies were dewaxed through xylene, air-dried, microwave-heated in appropriate buffer (100 mM Tris/50 mM EDTA, pH 7.0) for 12 min, cooled, and rinsed twice in Tris-HCl/0.05% Tween 20 buffer (pH 7.6) at 4°C. Subsequently, immunostaining with CD34 (QBEND10, Dako, Hamburg, Germany) or glycophorin C (Dako) monoclonal antibodies was performed by the alkaline phosphatase-antialkaline phosphatase method. Bromochloroindolylphosphate and nitro blue tetrazolium (Sigma) were used as chromogenic substances. Following preparation for FISH was performed as described before [31]. Briefly, samples were dehydrated through graded ethanol solutions, air-dried, and permeabilized by microwave treatment, followed by enzymatic digestion (proteinase K, Sigma). After this procedure, slides were quickly dehydrated and air-dried.

Fluorescence in situ hybridization

Fluorophore-labeled alpha-satellite DNA probes specific for the centromere of chromosomes 8 or 9 (Abbott-Vysis, Bergisch Gladbach, Germany) from all patients under study as well as the controls were placed on the coverslips. In case of the trephine biopsies, slides were incubated at 94°C for 3 min on a hot plate. After denaturation, the slides were quickly brought to 37°C, sealed with rubber cement, and then placed in a humidified box for 16 h at 42°C. Coverslips were removed, and slides were placed in 0.4× SSC at 73°C for 2 min, immersed in 2× SSC/0.01% NP40 at room temperature for 1 min, and then air-dried before mounting in 0.125 µg of 4'-6'-diamidino-2-phenylindole dihydrochloride (DAPI)/ml antifade (DAPI II, Vysis). Slides were evaluated with an Aristoplan microscope (Leitz, Wetzlar, Germany), equipped with an optimized triple-bandpass filter, and imaged by digital camera (Photometrics, SenSys, Tucson, AZ, USA) and appropriate software (IPLab Spectrum P, Vienna, VA, USA).

Specimens were evaluated using fluorescence microscopy by two observers independently of each other. The percentage of nuclei bearing one, two, or three signals for each probe was determined from counts of 200 nuclei concerning the mononuclear cells and the immunomagnetic enriched CD34⁺ progenitor cells and all cells bearing signals concerning the bone marrow slides.

Comparative genomic hybridization

DNA of mononuclear cells was extracted by standard methods. Samples of DNA were subsequently labeled using

digoxigenin-11-dUTP (normal DNA) or biotin-16-dUTP (test DNA) by nick-translation, according to the supplier's protocol (Roche, Mannheim, Germany). Comparative genomic hybridization (CGH) probes were prepared by coprecipitating gender-matched digoxigenin-1-dUTP normal DNA (1 µg), biotin-16-dUTP test DNA (1 µg), cot-1-DNA (100 µg, Gibco Life Technologies, Paisley, Scotland, UK), and salmon sperm DNA (11 µg, Roche) using 0.1- and 2.5-fold volumes, respectively, of sodium acetate and ethanol at -80°C followed by centrifugation at 4°C. The DNA pellets were dried, dissolved in 10 µl of hybridization buffer (50% v/v formamide, Fluka; 10% w/v dextran sulfate, Sigma, in 4× SSC), denatured at 73°C for 5 min, and preannealed at 37°C for 60 to 120 min. CGH target metaphase slides, prepared using acetic acid methanol (1:3) fixed phytohemagglutinin-stimulated normal male lymphocytes, were denatured in formamide (70% v/v in 2× SSC) at 75°C. The CGH probe was applied to the CGH target slide, sealed under a coverslip and the slide incubated at 37°C for 72 h. Posthybridization washes consisted of 0.3% v/v NP40 (Merck) in 0.4× SSC at 74°C for 2 min followed by 0.1% v/v NP40 in 2× SSC at room temperature for 1 min. For the signal detection, probes were incubated with 30 µl fluorescein isothiocyanate (FITC) conjugated avidin and TRIC-conjugated anti-digoxigenin for 30 min and 37°C (both from Oncor, Gaithersburg, MD, USA). The slides were then mounted under a DAPI-containing medium (Vector Laboratories) and subsequently analyzed using a Power Macintosh G3 and the Quips Genetics Workstation (IPLab Spectrum Imaging Software). Fluorescence and DAPI images were captured from as many as 19 meta-

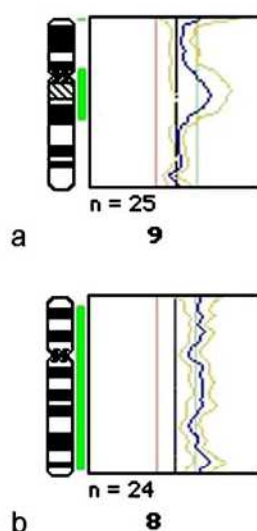


Fig. 1 CGH data of two PV cases: The vertical black line represents the mean green/red fluorescence ratio (1.0) of 24 (a) and 25 (b) captured chromosomes hybridized with CGH probes containing FITC-labeled DNA from the PV patient. The magenta line represents the 0.8, and the green line represents the 1.2 green/red fluorescence ratio. **a** CGH data from a patient (case 1) with gain of material from chromosome 9. **b** CGH data from a patient (case 2) with gain in material from the whole of chromosome 8 pointing at a trisomy of this chromosome

Table 1 Selected data from FISH assays with probes for centromere of chromosome 8 and 9

Case no.	Probe	PB mononuclear cells			PB CD34 ⁺ cells			BM hematopoiesis			BM erythropoiesis			BM CD34 ⁺ cells		
		One	Two	Three	One	Two	Three	One	Two	Three	One	Two	Three	One	Two	Three
		signal (%)	signals (%)	signals (%)	signal (%)	signals (%)	signals (%)	signal (%)	signals (%)	signals (%)	signal (%)	signals (%)	signals (%)	signal (%)	signals (%)	signals (%)
1	Centromere 9	0	9	91	4	17	79	35	54	12	41	49	10	49	43	8
9	Centromere 9	5	95	0	7	93	0	60	40	0	55	45	0	57	43	0
2	Centromere 8	2	12	86	2	36	62	30	52	18	47	45	8	54	40	6
6	Centromere 8	10	90	0	7	93	0	51	49	0	65	35	0	61	39	0

Cases 6 and 9 represent normal karyotype according to CGH data. Two hundred cells with at least one signal were counted concerning the PB-derived cell fractions; concerning the bone marrow slides, all cells with at least one signal were counted (18 to 210 cells) BM Bone marrow

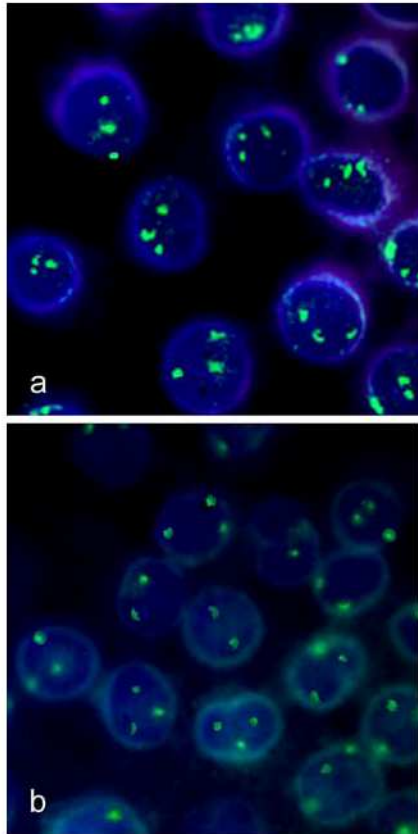


Fig. 2 FISH assays for centromeres 9 (a) and 8 (b). Alpha-satellite DNA probes for centromeres 8 and 9 were hybridized to fixed PB mononuclear cells (case 1) (a) and immunomagnetically enriched PB CD34⁺ progenitor cells (case 2) (b)

phases per slide for the generation of composite CGH profiles. Chromosome classification was validated by two authors. Deletions and amplifications were suspected when the slide average green/red fluorescence ratio for a given chromosomal region lay outside the range 0.7 to 1.2. Telomere regions, X and Y chromosomes, were excluded from analysis.

Results

Comparative genomic hybridization analysis of peripheral blood mononuclear cells

PB mononuclear cells from ten PV patients and the controls were tested for chromosomal aberrations. Evaluation of 15 to 19 metaphases per slide for fluorescence and DAPI images and generation of composite CGH profiles revealed abnormal pictures in CGH analysis in two of ten patients (cases 1 and 2) and in none of the controls. Both cases presented complex chromosomal aberrations, including gain of material from the centromere region and the q arm of chromosome 9 (Fig. 1a; case 1) or gain of material from the whole of chromosome 8 (Fig. 1b; case 2). Concerning the other eight patients, no chromosomal aberrations were

observable. The CGH data were then compared with FISH analysis for centromere region of chromosomes 8 and 9.

Fluorescence in situ hybridization analysis of peripheral blood mononuclear cells

FISH analysis from the PB mononuclear cells from the same ten patients and the controls were undertaken to prove CGH results. As summarized in Table 1, PB mononuclear cells of both CGH-positive cases revealed 91% (case 1) and 86% (case 2) triple FISH signals for centromeres 9 and 8, respectively (Fig. 2a). Concerning the CGH-negative patients and the healthy controls, no triple but 90 to 95% double signals were observed. These findings underline the excellent specificity and good sensitivity of the tests. When analyzing the CD34⁺ progenitor cells of the above-mentioned cases, the fraction of triple FISH signals was diminished with 79% (case 1) and 62% (case 2), compared to the findings in mononuclear cells (Fig 2b). The CGH-

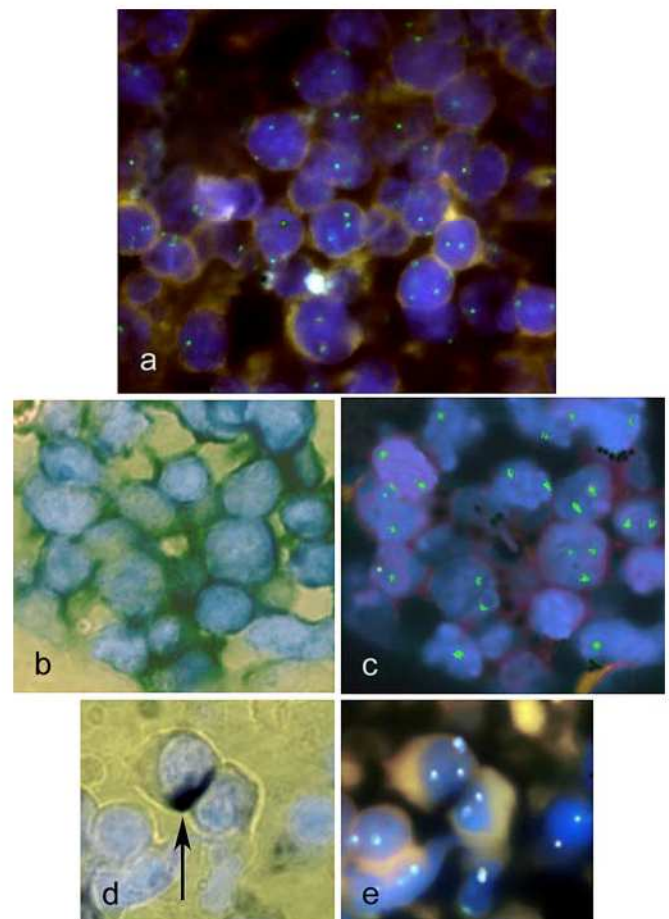


Fig. 3 Representative areas from bone marrow trephine biopsies. a and e FISH assays for centromere 8 (case 2). d Same area of case 2 with one CD34⁺ progenitor cell (arrow), CD34 immunostaining. c FISH assay for centromere 9 (case 1) of a selected erythron. b Same area of case 1 with strong glycophorin C immunostaining of the erythropoietic precursor cells

negative cases presented the same distribution of FISH signals for CD34⁺ progenitor cells as for mononuclear cells.

Fluorescence in situ hybridization analysis of bone marrow trephine biopsies

Of the above-mentioned ten patients and the controls, FISH analysis from 4- μ m-thick bone marrow slides were performed to test the probability for triple signals in individual hematopoietic cells. Corresponding to the results of the mononuclear cell fractions, none of the CGH-negative cases presented FISH data indicating trisomy 8 or 9. However, in cases 1 and 2, a small but distinct cellular subgroup (12 and 18%; Fig. 3a) bared three signals for chromosome 9 or 8, respectively. In addition, the proportion of two signals per cell was higher in this group, compared with the CGH-negative fraction.

In a second approach, immunohistochemistry was followed by FISH analysis (Fig. 3b–e). Assisted by photographic documentation of the same area of the biopsy in different types of light, phenotype and genotype of individual cells were ascertained. In this experiment, three signals in glycophorin-C-positive erythropoietic cells as well as in CD34⁺ progenitor cells could be demonstrated. Again, in the CGH-positive cases, CD34⁺ progenitor cells presented lower levels of triple signaling (6–8%), compared to the overall hematopoiesis (12–18%), and, concerning the erythropoiesis as well, slightly reduced levels of triple signaling were found (Table 1).

Discussion

When clinical features are suggestive for PV, assays for Epo and erythroid colony-forming cells, bone marrow trephine biopsies, and clonality assays can strongly support the diagnosis [9, 18, 26]. Analysis of X chromosome inactivation patterns, however, is reserved to female patients and may lead to false positive results because some normal elderly women present X chromosome inactivation patterns indistinguishable from those seen in patients with clonal myeloproliferative disorders [8, 10, 11]. Acquired karyotypic abnormalities, being direct markers of clonally transformed cells, are potentially more reliable for diagnostic purposes, but only 34% of PV patients have an abnormal karyotype revealed by conventional cytogenetic techniques [3, 13]. Among them, trisomies 8 and 9 or deletion of chromosome 20 represent the most frequent aberrations [5, 24, 29]. Although not specific for PV, cytogenetic conversion in one case treated with interferon alpha and clinical remission of the disease [23] indicates that the neoplastic cell fraction comprises the karyotypic abnormal cell clone. In this situation, analysis of frequent chromosomal aberrations might help to quantify the neoplastic clone proportion in PV hematopoiesis, even if above-mentioned aberrations in PV are characterized as secondary genetic changes [20].

CGH technique is a cytogenetic screening method with moderate sensitivity and excellent specificity (25% abnormal cells are necessary for correct diagnosis); it requires interphase cells and, therefore, can be applied on viable cells as well as fixed material [17, 22]. The diagnostic utility of this method applied to PV blood granulocytes has already been tested [28]. FISH analysis requires preknowledge of the abnormality to select the appropriate probes. Combined with immunohistochemical analysis, FISH technology allows the identification of single neoplastic cells and, therefore, the proper affiliation to a certain cell fraction. Altogether, this methodological approach is able to answer the question whether and to which extent clonal hematopoiesis in PV dominates residual reactive hematopoiesis and whether there are differences between the certain cell lineages.

The two cases presenting gain of material in CGH concerning chromosome 8 or 9 offered three signals in most PB mononuclear cells performing FISH. This finding as well as the result of 90–95% cells baring two signals in the CGH-negative patients indicates the high sensitivity of FISH. Further, the lack of triple signals in the CGH-negative cases demonstrates the high specificity of this method.

In detail, our data demonstrate a proportion of 86–91% clonal PB-derived mononuclear cells in contrast to 62–79% PB-derived CD34⁺ cells. In this context, it is necessary to mention that the possibility that CD34⁺ endothelial cells were taken into account, despite the different morphology of both cell types, cannot be ruled out. However, this difference might also be due to the fact that nonneoplastic primitive CD34⁺ progenitor cells survive by being quiescent and not proliferating. Probably depending on an ill-defined effect already described in chronic myelogenous leukemia (CML) [4], the microenvironment in the bone marrow seems to support neoplastic hematopoiesis, thus leading to a dominance of the clonally transformed cell fraction in the more differentiated hematopoietic cell pool of PV. Our data for the first time prove considerable contribution of CD34⁺ progenitor cells in the neoplastic cell clone in PV. In view of the fact that until now many investigations on PV were undertaken on granulocytes [25, 27], these results indicate that further investigations on molecular pathogenesis of this disease should focus on this CD34⁺ progenitor cell fraction. The detailed quantification of the CD34⁺ progenitor cell fraction might further offer important data for potential further therapy strategies in PV.

To analyze the value of FISH technique for diagnosis of early PV examination of bone marrow, biopsies from CGH-tested patients was undertaken to find out whether chromosomal aberrations, especially gain of chromosomal material in the centromere region 8 or 9, could be detected. In this context, it is noteworthy to emphasize that the probability to identify three signals per cell is much lower in the 4- μ m-thick sections than in cell smears. The excellent specificity of the test and the finding of 10% genotypic aberrant cells in all CGH-positive cases demonstrate that FISH indeed may facilitate PV diagnosis in chromosomal aberrant cases. Our results further indicate

the affiliation of the erythropoiesis and the CD34⁺ progenitor cell pool to the neoplastic cell fraction.

A point mutation of JAK2 leading to a constitutive activation was recently described for a certain proportion of PV patients as well as for other Philadelphia chromosome negative chronic myeloproliferative disorders [2, 14, 15, 19, 21]. However, according to the most recently published results, the incidence of JAK2 mutations reveals a significant range of about 65 to 97% in PV. Taking this genomic aberration into account, more detailed information about the distribution of the neoplastic cell clone as well as the dynamics following cytoreductive therapy will now be available and will give more insights in the biology of PV and further provides a means for molecularly targeted therapeutic strategies [12, 16].

Acknowledgements Supported by the Cologne Fortune Foundation and by the Center for Molecular Medicine, University of Cologne (CMMC).

Declaration: all experiments comply with the laws of the Federal Republic of Germany and the European Union.

References

- Amiel A, Gaber E, Manor Y, Fejgin M, Joseph-Lerner N, Ravid M, Lishner M (1995) Fluorescence in situ hybridization for the detection of trisomies 8 and 9 in polycythemia vera. *Cancer Genet Cytogenet* 79:153–156
- Baxter EJ, Scott LM, Campbell PJ, East C, Fourouclas N, Swanton S, Vassiliou GS, Bench AJ, Boyd EM, Curtin N, Scott MA, Erber WN, Green AR (2005) Acquired mutation of the tyrosine kinase JAK2 in human myeloproliferative disorders. *Lancet* 365:1054–1061
- Bench AJ, Nacheva EP, Champion KM, Green AR (1998) Molecular genetics and cytogenetics of myeloproliferative disorders. *Bailliere's Clin Haematol* 11:819–848
- Bhatia R, McGlave PB, Dewald GW, Blazar BR, Verfaillie CM (1995) Abnormal function of the bone marrow microenvironment in chronic myelogenous leukemia: role of malignant stromal macrophages. *Blood* 85:3636–3645
- Bussan M, Romana S, Khac FN, Bernard O, Berger R (2004) Cryptic translocations involving chromosome 20 in polycythemia vera. *Ann Genet* 47:365–371
- Carneskog J, Kutti J, Wadenvik H, Lundberg PA, Lindstedt G (1998) Plasma erythropoietin by high-detectability immunoradiometric assay in untreated and treated patients with polycythemia vera and essential thrombocythemia. *Eur J Haematol* 60:278–282
- Cashman J, Henkelman D, Humphries K, Eaves C, Eaves A (1983) Individual BFU-E in polycythemia vera produce both erythropoietin dependent and independent progeny. *Blood* 61:876–884
- Champion KM, Gilbert JG, Asimakopoulos FA, Hinshelwood S, Green AR (1997) Clonal haemopoiesis in normal elderly women: implications for the myeloproliferative disorders and myelodysplastic syndromes. *Br J Haematol* 97:920–926
- Florensa L, Besses C, Zamora L, Bellosillo B, Espinet B, Serrano S, Woessner S, Sole F (2004) Endogenous erythroid and megakaryocytic circulating progenitors, HUMARA clonality assay, and PRV-1 expression are useful tools for diagnosis of polycythemia vera and essential thrombocythemia. *Blood* 103:2427–2428
- Gale RE, Fielding AK, Harrison CN, Linch DC (1997) Acquired skewing of X-chromosome inactivation patterns in myeloid cells of the elderly suggests stochastic clonal loss with age. *Br J Haematol* 98:512–519
- Gilbert HL, Acharya J, Pearson TC (1998) Implications for the use of X-chromosome inactivation patterns and their relevance to the myeloproliferative disorders. *Eur J Haematol* 61:282–283
- Goldman JM (2005) A unifying mutation in chronic myeloproliferative disorders. *N Engl J Med* 352:1744–1746
- Herishanu Y, Lishner M, Bomstein Y, Kitay-Cohen Y, Fejgin MD, Gaber E, Amiel A (2001) Comparative genomic hybridization in polycythemia vera and essential thrombocythosis patients. *Cancer Genet Cytogenet* 128:154–157
- James C, Ugo V, Le Couedic JP, Staerk J, Delhommeau F, Lacout C, Garcon L, Raslova H, Berger R, Bennaceur-Griscelli A, Villeval JL, Constantinescu SN, Casadevall N, Vainchenker W (2005) A unique clonal JAK2 mutation leading to constitutive signalling causes polycythaemia vera. *Nature* 434:1144–1148
- Jones AV, Kreil S, Zoi K, Waghorn K, Curtis C, Zhang L, Score D, Seear R, Chase AJ, Grand FH, White H, Zoi C, Loukopoulos D, Terpos E, Vervessou EC, Schultheis B, Emig M, Ernst T, Lengfelder E, Hehlmann R, Hochhaus A, Oscier D, Silver RT, Reiter A, Cross NC (2005) Widespread occurrence of the JAK2 V617F mutation in chronic myeloproliferative disorders. *Blood* [Epub ahead of print]
- Kaushansky K (2005) On the molecular origins of the chronic myeloproliferative disorders: it all makes sense. *Blood* 105:4187–4190
- Knuutila S, Armengol G, Bjorkqvist AM, el-Rifai W, Larramendy ML, Monni O, Szymanska J (1998) Comparative genomic hybridization study on pooled DNAs from tumors of one clinical pathological entity. *Cancer Genet Cytogenet* 100:25–30
- Kralovics R, Buser AS, Teo SS, Coers J, Tichelli A, van der Maas AP, Skoda RC (2003) Comparison of molecular markers in a cohort of patients with chronic myeloproliferative disorders. *Blood* 102:1869–1871
- Kralovics R, Passamonti F, Buser AS, Teo SS, Tiedt R, Passweg JR, Tichelli A, Cazzola M, Skoda RC (2005) A gain-of-function mutation of JAK2 in myeloproliferative disorders. *N Engl J Med* 352:1779–1790
- Kralovics R, Stockton DW, Pichal JT (2003) Clonal hematopoiesis in familial polycythemia vera suggests the involvement of multiple mutational events in the early pathogenesis of the disease. *Blood* 102:3793–3796
- Levine RL, Wadleigh M, Cools J, Ebert BL, Wernig G, Huntly BJ, Boggon TJ, Wlodarska I, Clark JJ, Moore S, Adelsperger J, Koo S, Lee JC, Gabriel S, Mercher T, D'Andrea A, Frohling S, Dohner K, Marynen P, Vandenberghe P, Mesa RA, Tefferi A, Griffin JD, Eck MJ, Sellers WR, Meyerson M, Golub TR, Lee SJ, Gilliland DG (2005) Activating mutation in the tyrosine kinase JAK2 in polycythemia vera, essential thrombocythemia, and myeloid metaplasia with myelofibrosis. *Cancer Cell* 7:387–397
- Lichter P, Joos S, Bentz M, Lampel S (2000) Comparative genomic hybridization: uses and limitations. *Semin Hematol* 37:348–357
- Messora C, Bensi L, Vecchi A, Longo R, Giacobbi F, Temperani P, Bevisi M, Emilia G, Sacchi S (1994) Cytogenetic conversion in a case of polycythemia vera treated with interferon-alpha. *Br J Haematol* 86:402–404
- Najfeld V, Montella L, Scalise A, Fruchtman S (2002) Exploring polycythemia vera with fluorescence in situ hybridization: additional cryptic 9p is the most frequent abnormality detected. *Br J Haematol* 119:558–566
- Pellagatti A, Vetrie D, Langford CF, Gama S, Eagleton H, Wainscoat JS, Boulwood J (2003) Gene expression profiling in polycythemia vera using cDNA microarray technology. *Cancer Res* 63:3940–3944
- Spivak JL (2002) Polycythemia vera: myths, mechanisms, and management. *Blood* 100:4272–4290

27. Temerinac S, Klippel S, Strunck E, Roder S, Lubbert M, Lange W, Azemar M, Meinhardt G, Schaefer HE, Pahl HL (2000) Cloning of PRV-1, a novel member of the uPAR receptor superfamily, which is overexpressed in polycythemia rubra vera. *Blood* 95:2569-2576
28. Westwood NB, Gruszka-Westwood AM, Atkinson S, Pearson TC (2001) Polycythemia vera: analysis of DNA from blood granulocytes using comparative genomic hybridization. *Haematologica* 86:464-469
29. Westwood NB, Gruszka-Westwood AM, Pearson CE, Delord CF, Green AR, Huntly BJ, Lakhani A, McMullin MF, Pearson TC (2000) The incidences of trisomy 8, trisomy 9 and D20S108 deletion in polycythaemia vera: an analysis of blood granulocytes using interphase fluorescence in situ hybridization. *Br J Haematol* 110:839-846
30. Wickenhauser C, Perez F, Siebolts U, Lorenzen J, Varus E, Frimpong S, Thiele J (2003) Structural, antigenetic and transcriptional characteristics in peripheral blood CD34+ progenitor cells from polycythemia vera patients: evidence for delayed determination. *Int J Oncol* 23:437-443
31. Wickenhauser C, Thiele J, Perez F, Varus E, Stoffel MS, Kvasnicka HM, Beelen DW, Schaefer UW (2002) Mixed chimerism of the resident macrophage population after allogeneic bone marrow transplantation for chronic myeloid leukemia. *Transplantation* 73:104-111

Dualism of mixed chimerism between hematopoiesis and stroma in chronic idiopathic myelofibrosis after allogeneic stem cell transplantation

J. Thiele¹, E. Varus¹, U. Siebolts¹, H.M. Kvasnicka¹,
C. Wickenhauser¹, K.A. Metz², D.W. Beelen³, M. Ditschkowski³, A. Zander⁴ and N. Kröger⁴

Institutes of Pathology, Universities of ¹Cologne, Cologne and ²Essen, Essen and Departments of Bone Marrow Transplantation,

³University of Essen, Essen and ⁴University Hospital Hamburg, Germany

Summary. Scant knowledge exists concerning lineage-restricted mixed chimerism (mCh) after allogeneic peripheral blood stem cell transplantation (PSCT) in patients with chronic idiopathic myelofibrosis (CIMF). Following a sex-mismatched PSCT, a combined immunopheno- and genotyping by fluorescence in-situ hybridization (FISH) was performed on sequential bone marrow (BM) biopsies at standardized intervals. Results were compared with PCR analysis of corresponding peripheral blood samples in five patients. According to FISH, pretransplant specimens revealed a gender congruence of more than 99%, while in the first three months the total BM exhibited a persistent fraction of host cells (30% to 40%) with a tendency to decline after about one year. It is noteworthy that the majority of endothelial cells maintained a recipient origin, whereas CD34+ progenitors and especially CD61+ megakaryocytes exhibited only very few host-derived cells. In keeping with the prevalence of donor cells in the hematopoietic compartment, PCR analysis of peripheral blood cells displayed a non-significant degree of mCh.

In conclusion, according to FISH and PCR analysis, successful PSCT in CIMF results in an almost complete chimeric (donor-derived) state of the hematopoietic cell population. The non-transplantable stromal compartment includes the vascular endothelium with a predominance of recipient cells. The minimal mCh of this population implies probably a donor-derived origin (endothelial progenitor cells).

Key words: Mixed chimerism, CD34+ progenitors, Megakaryocytes, Endothelial cells, Peripheral stem cell transplantation, Chronic idiopathic myelofibrosis, Bone marrow biopsies

Introduction

In chronic idiopathic myelofibrosis (CIMF) relatively little information exists regarding mixed chimerism (mCh) following allogeneic bone marrow (BM) or stem cell transplantation (Deeg et al., 2003; Rondelli et al., 2005). A characteristic feature of histopathology in this disorder is the fibrous matrix of the BM that usually includes prominent vessels (Thiele et al., 2001). On the other hand, as has been repeatedly demonstrated, fibroblasts are no part of the leukemogenic (clonally transformed) process underlying the myeloproliferative disorders (Greenberg et al., 1978; Golde et al., 1980; O'Brien et al., 1988). However, controversy continues about the donor or host (recipient) origin of stroma constituents following myeloablative therapy and subsequent transplantation (Simmons et al., 1987; Athanasou et al., 1990; Agematsu and Nakahori, 1991; Santucci et al., 1992). It has been argued that engraftment of BM stroma cell precursors does not occur and that host stromal cells survive the various conditioning regimens applied before transplantation procedures (Athanasou et al., 1990). In this context, angiogenesis in CIMF is of special interest not only for its relationship with the progression of myelofibrosis (Reilly et al., 1985; Thiele et al., 1992; Kvasnicka and Thiele, 2004), but for its crucial role concerning restitution and maintenance of hematopoiesis (Davis et al., 1995; Rafii et al., 1995; Shalaby et al., 1995). A wealth of data has been accumulated concerning the functional properties of vascular structures, in particular the endothelial cells that serve as gatekeepers by controlling the trafficking and homing of progenitors (Simmons et al., 1992; Mohle et al., 1999). For this reason, a study was performed on gender-related mCh involving patients with CIMF in the early and late posttransplant period. Analysis included peripheral blood cells determined by the polymerase chain reaction (PCR) technique in comparison with the lineage

Offprint requests to: Juergen Thiele, M.D., Institute of Pathology, University of Cologne, Joseph-Stelzmannstr. 9, D-50924 Cologne, Germany. e-mail: j.thiele@uni-koeln.de

restricted chimeric state of CD34+ endothelial and progenitor cells as well as megakaryocytes by using the fluorescence in-situ hybridization (FISH) method.

Material and methods

Patients

A total of five patients (four men, one woman; age 45 years) with CIMF and a sex-mismatched transplantation constellation were enrolled into this study. All patients had a history of various therapeutic regimens including hydroxyurea, busulfan as well as radiation or a combination of these. Following dose-reduced myeloablative therapy that has been described in detail in previous studies (Kröger et al., 2005; van Besien and Deeg, 2005), patients received a peripheral blood stem cell transplantation (PSCT) with a median number of transplanted CD34+ progenitors of 8×10^6 per kg body weight (range 0.9–15.6) derived either from HLA-identical siblings or matched unrelated donors. Further information of this cohort which was derived from a larger prospective and clinically controlled trial have already been reported (Kröger et al., 2005). Explicit approval of this study was obtained from the Institutional Review Board on Medical Ethics at Essen University Hospital.

Bone marrow biopsies

Representative BM trephine biopsies (mean size $17.5 \pm 1.8 \text{ mm}^2$) were performed at standardized intervals from the posterior iliac crest. The fixation of samples was carried out in a low-concentrated phosphate-buffered formalin solution for 12–48 hours. Further processing included decalcification for 3–4 days in 10% buffered ethylene-diamine tetra-acetic acid (EDTA), pH 7.2, paraffin wax embedding, and employment of several staining techniques, involving Giemsa, PAS (periodic acid Schiff reagent), naphthol-AS-D-chloroacetate esterase, Perls' reaction for iron and a silver impregnation method (Gomori's technique).

Simultaneous immunostaining and dual color FISH

For a simultaneous immunophenotypic and genotypic evaluation, 4 μm paraffin-embedded sections were dewaxed through xylene, air-dried, microwave-heated in an appropriate buffer (100mM Tris/50mM EDTA, pH 7.0) for 4 min, cooled down and rinsed twice in Tris (HCl/0.05% Tween 20 buffer, pH 7.6) at 4°C. Subsequently, to detect progenitor cells and endothelial cells immunostaining with CD34+ (Soligo et al., 1991) was performed and to identify megakaryopoiesis CD61+ (Gatter et al., 1988) monoclonal antibodies were applied by using the APAAP method (Cordell et al., 1984). 5-Bromo-4-chloro-3-indolyl-phosphatase (BCIP) and nitroblue tetrazolium (NBT; Sigma, Deisenhofen, Germany) were used as chromogenic substances. Tissue

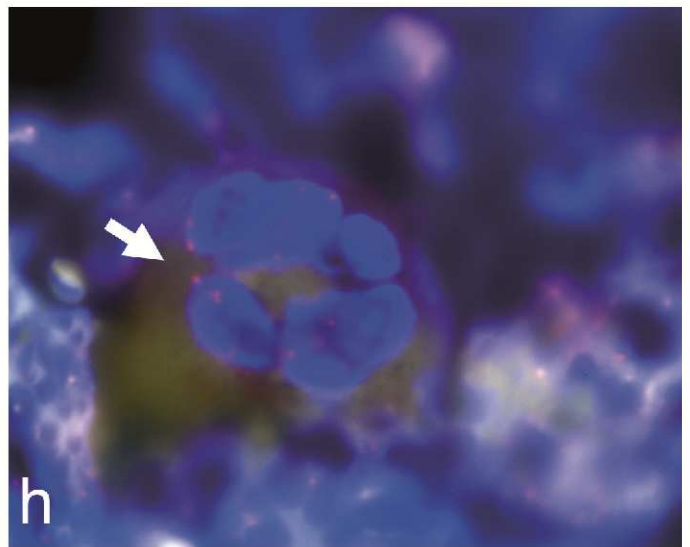
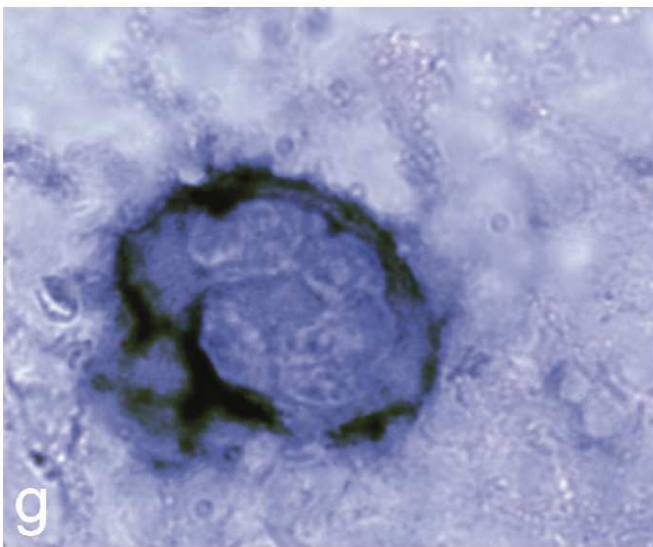
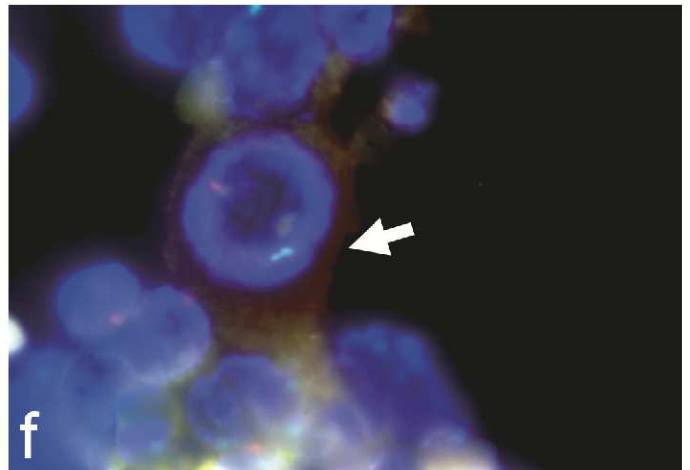
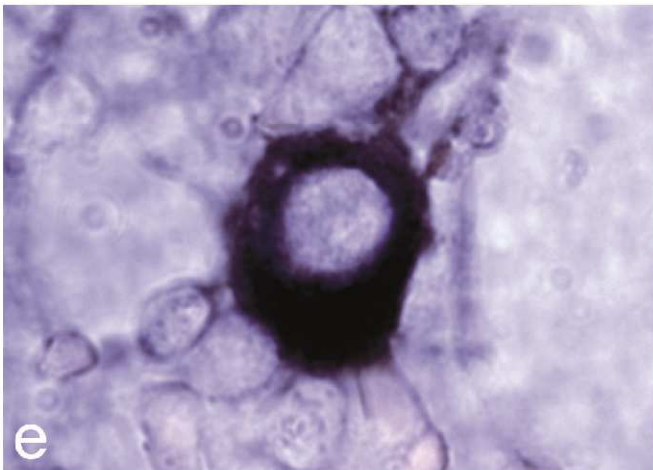
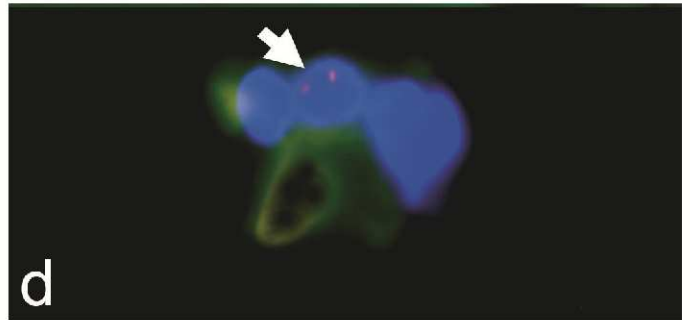
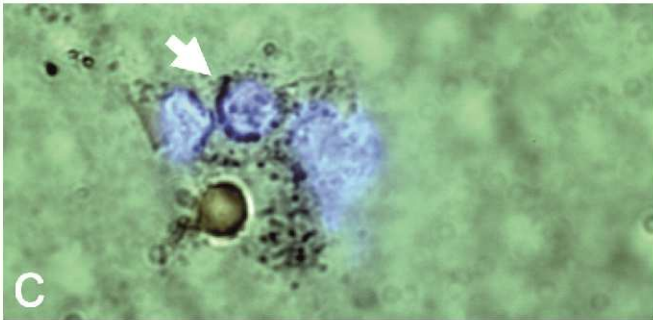
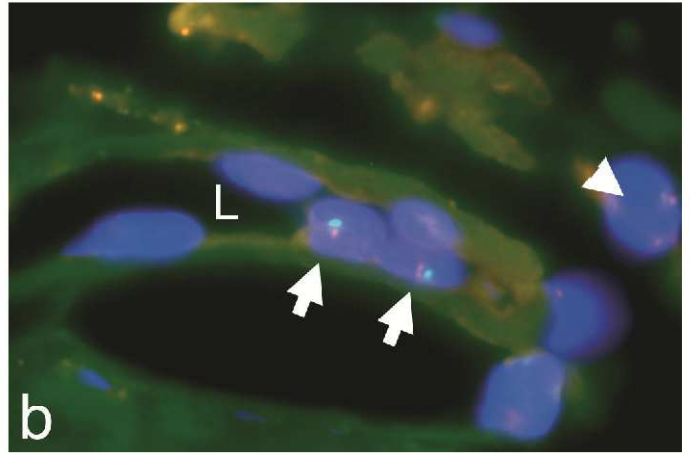
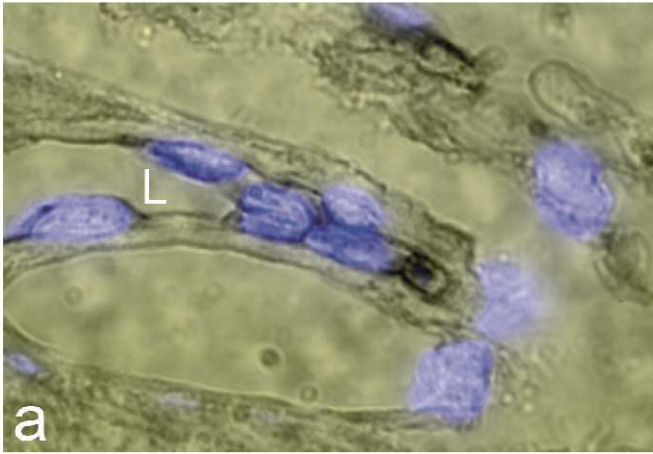
sections were dehydrated through graded ethanol solutions (70%, 90% and 100%), air-dried and permeabilized by microwave treatment, followed by 0.25 mg/ml proteinase K digestion (Sigma) for 3 min at 37°C before hybridization (Bull and Harnden, 1999). After this procedure, the slides were quickly transferred to 70% ethanol at 4°C, dehydrated in 100% ethanol and then air-dried. A 10- μl aliquot of a directly conjugated satellite probe mix for chromosomes x and y (CEP X Spectrum Orange/CEP Y Spectrum Green DNA Probe Kit or CEP X Spectrum Green/CEP Y Spectrum Orange DNA Probe Kit, respectively; Vysis, Bergisch Gladbach, Germany) was placed on a coverslip, picked up onto the slide and incubated at 73°C for 5 min on a hot plate. Because green fluorescence is more conspicuous than a red signal, following a pilot study (Table 1), correspondingly mismatched probes for the x- and y-chromosomes (green versus red signals) were also applied. After denaturation, the slides were quickly brought to 37°C, sealed with rubber cement, and then placed in a humidified box for 16 h at 42°C. Coverslips were removed, and slides were placed in wash buffer (0.4xSSC) at 73°C for 2 min, immersed in 2xSSC/0.01% NP 40 at room temperature for 1 min and then air-dried, before mounting in 0.125Fg DAPI/ml Antifade (DAPI II; Vysis). The slides were evaluated with an Aristoplan® microscope (Leitz, Wetzlar, Germany) equipped with an optimized triple bandpass filter and imaged with a digital camera (Photometrics SenSys; Tucson, Ari., USA) and appropriate software (IPLab Spectrum P, Vienna, Va., USA). Accordingly, positive (red: x-chromosome and green: y-chromosome signals) signals were differentiated following DNA hybridization (sex typing) at the various endpoint intervals of pre- and posttransplant examinations (sequential biopsies) by counting explicitly only those cells containing two marked signals.

PCR analysis

Real-time quantitative PCR for the detection of the y-chromosome was performed on peripheral blood cells by following methods that were formerly described (Fehse et al., 2001). According to this technique, sensitivity was very high to identify male cells present in very low proportions (i.e. 1 male in 10^6 female cells) (Fehse et al., 2001).

Results

Immunophenotyping of CD34+ endothelial cells, progenitors and CD61+ megakaryocytes revealed a distinctive staining pattern which was a basic mean for further FISH analysis. Thus, dual color FISH with a simultaneous demonstration of proper signals visualizing the x- and y-chromosomes was easily accomplished (Fig. 1a–h). A pilot study in a female patient with CIMF that received an allogeneic PSCT from a male donor showed a strikingly variable extent of mCh in the



different cell populations and also during the posttransplant period (Table 1). A total congruence with the female gender of this patient was shown in the 120 cells evaluated in the pretransplant specimen. On the other hand, in the early posttransplant period (up to about three months), about one third of all evaluated BM cells still displayed a host-derived sextyping that significantly declined in quantity after one year. A very different constellation was found in the vascular endothelium, where less than 10% of cells exhibited a donor origin. In contrast to the stroma cell compartment and the total cell count hematopoiesis, i.e. CD34+ progenitors and CD61+ megakaryocytes that include also precursors, showed an only minor fraction (less than 10%) of residual host-derived cells.

On the other hand, PCR analysis of peripheral blood cells exhibited a percentage of recipient cells ranging between 0% and 1% at the corresponding checkpoints of the early and late posttransplant period, corresponding with an almost complete chimeric state.

Following this preliminary investigation which clearly demonstrated a strikingly expressed discrepancy of mCh, we analyzed a significantly larger number of cells in four male patients with CIMF and a gender-mismatched graft constellation after PSCT (Table 2). Here, first of all, the sensitivity of our FISH method according to gender congruence was established to exceed 99%. The total cell count, including hematopoietic as well as stroma cells, revealed a persistent host origin ranging between 30% to 40% with a tendency to decrease after about one year (Table 2). Again, the vast majority of endothelial cells maintained a recipient type with only very few samples apparently generated from the donor (Fig. 1a,b). This incidence differed significantly when studying CD34+ progenitor cells (Fig. 1c,d) and megakaryopoiesis including precursors, i.e. CD61+ immature micromegakaryocytes (Fig. 1e,f) as well as mature megakaryocytes (Fig. 1g,h). In the hematopoietic cell compartment the situation was reversed, with less than 10% of host-derived cells in the

Table 1. Female patient with a sex-mismatched (donor male) graft constellation following allogeneic peripheral blood stem cell transplantation (PSCT) for chronic idiopathic myelofibrosis - pilot study with relative incidence (%) of sextyping based on the evaluation of at least 100 (up to 600) bone marrow (BM) cells in each category.

Endpoint (day)		All BM cells		CD34+ progenitor cells		CD61+ megakaryocytes		Endothelial cells	
		xy	xx	xy	xx	xy	xx	xy	xx
Before PSCT	190	0	100	0	100	0	100	0	100
After PSCT	20	74	26	100	0	100	0	7	93
	81	69	31	92	8	100	0	5	95
	290	83	17	91	9	100	0	7	93
	376	88	12	94	6	97	3	10	90

Table 2. Relative incidence (%) of mixed chimerism and evaluated number (No.) of cells at each checkpoint in the bone marrow (BM) following sex-mismatched allogeneic peripheral stem cell transplantation (PSCT) in four men with chronic idiopathic myelofibrosis (gender-graft constellation: host male - donor female).

Endpoint (ranges, days)		All BM cells			CD34+ progenitor cells			CD61+ megakaryocytes			Endothelial cells		
		No.	xx	xy	No.	xx	xy	No.	xx	xy	No.	xx	xy
Before PSCT	6-40	601	3	997	92	0	100	174	0	100	129	0	100
After PSCT	20-50	363	60	40	61	95	5	118	100	0	93	5	95
	80-200	380	64	36	77	95	5	94	98	2	99	6	94
	300-400	507	67	33	58	90	10	82	99	1	66	2	98

Fig. 1. Sex-genotyping of endothelial cells and hematopoiesis in the bone marrow after PSCT in patients with CIMF. Immunophenotyping of the different cells is shown in the left panel and FISH analysis (right panel) reveals either red signals (x-chromosomes) or green signals (y-chromosomes) indicating mCh. **a.** CD34+ Endothelial lining of a vascular lumen (L) is surrounded by hematopoietic cells in a female host. A donor origin (**b**) is displayed in two endothelial cells (arrows) and a maintained recipient genotype in a hematopoietic cell (arrow head). **c.** CD34+ progenitor cell in a female host (arrow) revealing a still persistent recipient genotype (arrow) after transplantation. **d.** Immature CD61+ megakaryocyte precursor in a male patient (**e**) demonstrates (arrow) a host origin (**f**), in contrast to a large hyperlobulated mature megakaryocyte (**g**) showing (arrow) a female donor genotype (**h**). a-d, x 870; e-h, x 1,500

primitive precursor cell population and only single recipient cells in the more differentiated megakaryopoietic lineage (Table 2). Relating this very low frequency to the corresponding data of the evaluable total cell count, it is reasonable to assume that the majority of maintained host cells in the posttransplant period belong to the stromal compartment.

In keeping with the prevalence of complete donor chimerisms in the hematopoietic cell population (progenitors, megakaryocytes) PCR analysis performed exactly at the same checkpoints revealed an incidence of mCh ranging between 0% to 6%.

Discussion

Following a gender-mismatched transplantation, concurrent characterization of genotype and cell lineage provides a suitable means for the identification of chimeric states and thus, the host/donor origin of a certain cell population (Thiede et al., 2004). Although a number of techniques are currently available to document definitely donor cell engraftment and residual host cells, PCR and FISH are the most popular methods. It is well known that PCR analysis yields results readily and in a short time, and is certainly the more sensitive technique, because it allows the detection of one abnormal cell in 10^6 cells (Fehse et al., 2001; Alizadeh et al., 2002; Thiede et al., 2004). However, a significant disadvantage is that in CIMF related to BM fibrosis (dry tap) this method is usually applied on peripheral blood cells and that no characterization of lineage-restricted mCh is possible. This shortcoming precludes, among others, the labeling of endothelial cells and the recognition of their chimeric state indicating their CD34+ progenitor cell origin (Gehling et al., 2000). In contrast, FISH allows the identification of mCh in single immunophenotyped cells (Kvasnicka et al., 2003). On the other hand, this technique may lead to false-positive and false-negative results ranging between 0.2% and up to 4.0% based on results gained from smears or diluted cell preparations (Koegler et al., 1995; Rondon et al., 1997). Moreover, the results of FISH analysis (Rondon et al., 1997; Smith et al., 1999; Tamura et al., 2000) have to be discussed very critically (Kvasnicka et al., 2003), especially in cases where the investigators restrict their evaluations only on the identification of the Y-chromosome (Mackinnon et al., 1994). We would like to pinpoint that our applied dual-colored sextyping analysis failed to reveal any relevant discrepancies (false positive signals 0.3%) between gender and positive labeling in the pretransplant specimens (Tables 1, 2). Finally, it has to be emphasized that the methodology of transplantation exerts a significant impact on the extent of mCh (Elmaagacli et al., 2001), and therefore only results derived from series with corresponding therapeutic strategies, especially including conditioning regimens, are comparable.

The labeling of peripheral blood cells and genotyping by FISH has been repeatedly performed to

monitor mCh in CML patients (Smith et al., 1999; Tamura et al., 2000) and posttransplantation donor-recipient constellations were assessed by means of DNA microsatellite analysis (Thiede et al., 1999) in CIMF (Deeg et al., 2003; Rondelli et al., 2005). In CML the presence of a small amount of host-derived (clonally transformed) CD34+ progenitors that significantly exceeded the more differentiated cell lineages like the megakaryopoiesis, stimulated a discussion about so-called tumor dormancy even in patients after successful transplantations (Uhr et al., 1997; Holyoake et al., 1999). Some data indicate that in CML patients with a complete cytogenetic remission, a minority of bcr/abl+ cells were maintained (Chomel et al., 2000; Kitzis et al., 2001). It is tempting to speculate that these clonally transformed progenitor cells may possibly be the source of a later relapse and presumably may also differentiate into endothelial cells. This complex, until now ill-defined, pathomechanism determining the oncogenic potential of hematopoietic progenitors is probably governed by a variety of mediators, such as specific immune response (Oka et al., 1998). When compared with the relevant data on the CD34+ progenitor cell compartment (Table 2) results gained from this study were consistent with a significantly lower incidence of persistent host-derived megakaryocytes that nearly reached the methodological limit (White and Sweeney, 1993; Koegler et al., 1995; Rondon et al., 1997). This striking quantitative difference points towards a minor degree or almost complete mCh in the more differentiated hematopoietic cell lineages, while a very small amount of the primitive cell population still harbors a clonally transformed (leukemogenic) fraction as a possible source of relapse.

By using long-term cell culture techniques and genotyping with x- and y-specific probes, a host (recipient) origin of BM fibroblasts has been reported after allogeneic BM transplantation (Simmons et al., 1987; Athanasou et al., 1990; Agematsu and Nakahori, 1991; Santucci et al., 1992). These findings supported the argument of a non-transplantability of stroma cells even in patients with a maintained hematopoietic reconstitution (Agematsu and Nakahori, 1991; Santucci et al., 1992). In CIMF with a prevalent fibrous matrix, the discrepancy between the extent of mCh concerning the quantity of analyzed cells derived from the peripheral blood (PCR analysis) versus all BM cells that definitely included a significant proportion of stroma cells (FISH analysis), are generally in keeping with this finding. It is reasonable to assume that a leukemic relapse will initiate in the BM and therefore the very first stages of transformation are hardly detectable by performing PCR on peripheral blood cells, at least in CIMF.

Regarding the stroma compartment, the vascular structures have to be discriminated. With the exception of the sinusoids, these are usually composed of at least two components of different origin, i.e. the endothelium and the cells of the larger vessel walls (i.e. myofibroblasts, adventitial cells of the capillaries and

arterioles). Following BM transplantation in CML, only a fraction of endothelial cells was demonstrated to be host-derived (bcr/abl⁺) and maintained, even after more than one year (Kvasnicka et al., 2003). Regarding this point, a conflict of opinion exists, because another group applying also the FISH method identified this cell population as being totally of host origin (Athanasou et al., 1990). In contrast, the results of several authors on the CD34⁺ progenitor origin of endothelial cells provided persuasive evidence that this peculiar cell compartment is not only the source of hematopoiesis, but plays a pivotal role in angiogenesis (Asahara et al., 1997; Choi et al., 1998; Gehling et al., 2000; Gunsilius et al., 2000). For this reason, as shown in this study, a minor degree of mCh has to be expected following transplantation procedures. All these results are in keeping with the finding of a certain, although small, quantity of donor-derived endothelial cells in the BM after transplantation (Gehling et al., 2000; Gunsilius et al., 2000; Kvasnicka et al., 2003) contrasting with the host origin of the myofibroblasts of the larger vessel walls (Kvasnicka et al., 2003). Moreover, convincing data have been recently accumulated supporting this concept that even in adult life so-called hemangioblasts or endothelial precursor cells of the peripheral blood are present, and contribute to the formation of new blood vessels (Shi et al., 1998; Hristov and Weber, 2004; Iwami et al., 2004; Schatteman, 2004; Murasawa and Asahara, 2005). Therefore, it is reasonable to assume that the minor mCh of the endothelial layer may probably derive from transplanted donor endothelial progenitor cells.

In conclusion, contrasting PCR on peripheral blood cells, FISH analysis of the BM reveals a striking quantity of mCh in the stroma compartment that survives conditioning. In this context, only a small amount of donor-derived endothelial cells is recognizable, while the chimeric state of the engrafted hematopoietic cell population is almost complete (less than 10%).

Acknowledgements. Supported by a grant from the Dr. Mildred Scheel Foundation for Cancer Research (#106324).

References

- Agematsu K. and Nakahori Y. (1991). Recipient origin of bone marrow-derived fibroblastic stromal cells during all periods following bone marrow transplantation in humans. *Br. J. Haematol.* 79, 359-365.
- Alizadeh M., Bernard M., Danic B., Dauriac C., Birebent B., Lapart C., Lamy T., Le Prise P.Y., Beauplet A., Bories D., Semana G. and Quelvennec E. (2002). Quantitative assessment of hematopoietic chimerism after bone marrow transplantation by real-time quantitative polymerase chain reaction. *Blood* 99, 4618-4625.
- Asahara T., Murohara T., Sullivan A., Silver M., van der Zee R., Li T., Witenbichler B., Schatteman G. and Isner J.M. (1997). Isolation of putative progenitor endothelial cells for angiogenesis. *Science* 275, 964-967.
- Athanasou N.A., Quinn J., Brenner M.K., Prentice H.G., Graham A., Taylor S., Flannery D. and McGee J.O. (1990). Origin of marrow stromal cells and haemopoietic chimaerism following bone marrow transplantation determined by in situ hybridisation. *Br. J. Cancer* 61, 385-389.
- Bull J.H. and Harnden P. (1999). Efficient nuclear FISH on paraffin-embedded tissue sections using microwave pretreatment. *Biotechniques* 26, 416-418, 422.
- Choi K., Kennedy M., Kazarov A., Papadimitriou J.C. and Keller G. (1998). A common precursor for hematopoietic and endothelial cells. *Development* 125, 725-732.
- Chomel J.C., Brizard F., Veinstein A., Rivet J., Sadoun A., Kitzis A., Guilhot F. and Brizard A. (2000). Persistence of BCR-ABL genomic rearrangement in chronic myeloid leukemia patients in complete and sustained cytogenetic remission after interferon-alpha therapy or allogeneic bone marrow transplantation. *Blood* 95, 404-408.
- Cordell J.L., Falini B., Erber W.N., Ghosh A.K., Abdulaziz Z., MacDonald S., Pulford K.A., Stein H. and Mason D.Y. (1984). Immunoenzymatic labeling of monoclonal antibodies using immune complexes of alkaline phosphatase and monoclonal anti-alkaline phosphatase (APAAP complexes). *J. Histochem. Cytochem.* 32, 219-229.
- Davis T.A., Robinson D.H., Lee K.P. and Kessler S.W. (1995). Porcine brain microvascular endothelial cells support the in vitro expansion of human primitive hematopoietic bone marrow progenitor cells with a high replating potential: requirement for cell-to-cell interactions and colony-stimulating factors. *Blood* 85, 1751-1761.
- Deeg H.J., Gooley T.A., Flowers M.E., Sale G.E., Slattery J.T., Anasetti C., Chauncey T.R., Doney K., Georges G.E., Kiem H.P., Martin P.J., Petersdorf E.W., Radich J., Sanders J.E., Sandmaier B.M., Warren E.H., Witherspoon R.P., Storb R. and Appelbaum F.R. (2003). Allogeneic hematopoietic stem cell transplantation for myelofibrosis. *Blood* 102, 3912-3918.
- Elmaagacli A.H., Runkel K., Steckel N., Opalka B., Trenscheil R., Seeber S., Schaefer U.W. and Beelen D.W. (2001). A comparison of chimerism and minimal residual disease between four different allogeneic transplantation methods in patients with chronic myelogenous leukemia in first chronic phase. *Bone Marrow Transplant.* 27, 809-815.
- Fehse B., Chukhlovina A., Kuhlcke K., Marinetz O., Vorwig O., Renges H., Kruger W., Zabelina T., Dudina O., Finckenstein F.G., Kroger N., Kabisch H., Hochhaus A. and Zander A.R. (2001). Real-time quantitative Y chromosome-specific PCR (QYCS-PCR) for monitoring hematopoietic chimerism after sex-mismatched allogeneic stem cell transplantation. *J. Hematother. Stem. Cell Res.* 10, 419-425.
- Gatter K.C., Cordell J.L., Turley H., Heryet A., Kieffer N., Anstee D.J. and Mason D.Y. (1988). The immunohistological detection of platelets, megakaryocytes and thrombi in routinely processed specimens. *Histopathology* 13, 257-267.
- Gehling U.M., Ergun S., Schumacher U., Wagener C., Pantel K., Otte M., Schuch G., Schafhausen P., Mende T., Kilic N., Kluge K., Schafer B., Hossfeld D.K. and Fiedler W. (2000). In vitro differentiation of endothelial cells from AC133-positive progenitor cells. *Blood* 95, 3106-3112.
- Golde D.W., Hocking W.G., Quan S.G., Sparkes R.S. and Gale R.P. (1980). Origin of human bone marrow fibroblasts. *Br. J. Haematol.* 44, 183-187.
- Greenberg B.R., Wilson F.D., Woo L. and Jenks H.M. (1978). Cytogenetics of fibroblastic colonies in Ph1-positive chronic

- myelogenous leukemia. *Blood* 51, 1039-1044.
- Gunsilius E., Duba H.C., Petzer A.L., Kahler C.M., Grunewald K., Stockhammer G., Gabl C., Dirnhofer S., Clausen J. and Gastl G. (2000). Evidence from a leukaemia model for maintenance of vascular endothelium by bone-marrow-derived endothelial cells. *Lancet* 355, 1688-1691.
- Holyoake T., Jiang X., Eaves C. and Eaves A. (1999). Isolation of a highly quiescent subpopulation of primitive leukemic cells in chronic myeloid leukemia. *Blood* 94, 2056-2064.
- Hristov M. and Weber C. (2004). Endothelial progenitor cells: characterization, pathophysiology, and possible clinical relevance. *J. Cell. Mol. Med.* 8, 498-508.
- Iwami Y., Masuda H. and Asahara T. (2004). Endothelial progenitor cells: past, state of the art, and future. *J. Cell. Mol. Med.* 8, 488-497.
- Kitzis A., Brizard F., Dascalescu C., Chomel J.C., Guilhot F. and Brizard A. (2001). Persistence of transcriptionally silent BCR-ABL rearrangements in chronic myeloid leukemia patients in sustained complete cytogenetic remission. *Leuk. Lymphoma* 42, 933-944.
- Koegler G., Wolf H.H., Heyll A., Arkesteijn G. and Wernet P. (1995). Detection of mixed chimerism and leukemic relapse after allogeneic bone marrow transplantation in subpopulations of leucocytes by fluorescent in situ hybridization in combination with the simultaneous immunophenotypic analysis of interphase cells. *Bone Marrow Transplant.* 15, 41-48.
- Kröger N., Zabelina T., Schieder H., Panse J., Ayuk F., Stute N., Fehse N., Waschke O., Fehse B., Kvasnicka H.M., Thiele J. and Zander A. (2005). Pilot study of reduced-intensity conditioning followed by allogeneic stem cell transplantation from related and unrelated donors in patients with myelofibrosis. *Br. J. Haematol.* 128, 690-697.
- Kvasnicka H.M. and Thiele J. (2004). Bone marrow angiogenesis: methods of quantification and changes evolving in chronic myeloproliferative disorders. *Histol. Histopathol.* 19, 1245-1260.
- Kvasnicka H.M., Wickenhauser C., Thiele J., Varus E., Hamm K., Beelen D.W. and Schaefer U.W. (2003). Mixed chimerism of bone marrow vessels (endothelial cells, myofibroblasts) following allogeneic transplantation for chronic myelogenous leukemia. *Leuk. Lymphoma* 44, 321-328.
- Mackinnon S., Barnett L., Heller G. and O'Reilly R.J. (1994). Minimal residual disease is more common in patients who have mixed T-cell chimerism after bone marrow transplantation for chronic myelogenous leukemia. *Blood* 83, 3409-3416.
- Mohle R., Bautz F., Rafii S., Moore M.A., Brugger W. and Kanz L. (1999). Regulation of transendothelial migration of hematopoietic progenitor cells. *Ann. NY Acad. Sci.* 872, 176-186.
- Murasawa S. and Asahara T. (2005). Endothelial progenitor cells for vasculogenesis. *Physiology (Bethesda)* 20, 36-42.
- O'Brien S., Kantarjian H., Shtalrid M., Blick M., Beran M. and Talpaz M. (1988). Lack of breakpoint cluster region rearrangement in marrow fibroblasts of patients with Philadelphia chromosome-positive chronic myelogenous leukemia. *Hematol. Pathol.* 2, 25-29.
- Oka T., Sastry K.J., Nehete P., Schapiro S.J., Guo J.Q., Talpaz M. and Arlinghaus R.B. (1998). Evidence for specific immune response against P210 BCR-ABL in long-term remission CML patients treated with interferon. *Leukemia* 12, 155-163.
- Rafii S., Shapiro F., Pettengell R., Ferris B., Nachman R.L., Moore M.A. and Asch A.S. (1995). Human bone marrow microvascular endothelial cells support long-term proliferation and differentiation of myeloid and megakaryocytic progenitors. *Blood* 86, 3353-3363.
- Reilly J.T., Nash J.R., Mackie M.J. and McVerry B.A. (1985). Endothelial cell proliferation in myelofibrosis. *Br. J. Haematol.* 60, 625-630.
- Rondelli D., Barosi G., Bacigalupo A., Prchal J.T., Popat U., Alessandrino E.P., Spivak J.L., Smith B.D., Klingemann H.G., Fruchtmann S. and Hoffman R. (2005). Allogeneic hematopoietic stem-cell transplantation with reduced-intensity conditioning in intermediate- or high-risk patients with myelofibrosis with myeloid metaplasia. *Blood* 105, 4115-4119.
- Rondon G., Giral S., Pereira M., Van Besien K., Mehra R., Champlin R. and Andreeff M. (1997). Analysis of chimerism following allogeneic bone marrow transplantation by fluorescent-in-situ hybridization. *Leuk. Lymphoma* 25, 463-467.
- Santucci M.A., Trabetti E., Martinelli G., Buzzi M., Zaccaria A., Pileri S., Farabegoli P., Sabatini E., Tura S. and Pignatti P.F. (1992). Host origin of bone marrow fibroblasts following allogeneic bone marrow transplantation for chronic myeloid leukemia. *Bone Marrow Transplant.* 10, 255-259.
- Schatteman G.C. (2004). Adult bone marrow-derived hemangioblasts, endothelial cell progenitors, and EPCs. *Curr. Top. Dev. Biol.* 64, 141-180.
- Shalaby F., Rossant J., Yamaguchi T.P., Gertsenstein M., Wu X.F., Breitman M.L. and Schuh A.C. (1995). Failure of blood-island formation and vasculogenesis in Flk-1-deficient mice. *Nature* 376, 62-66.
- Shi Q., Rafii S., Wu M.H., Wijelath E.S., Yu C., Ishida A., Fujita Y., Kothari S., Mohle R., Sauvage L.R., Moore M.A., Storb R.F. and Hammond W.P. (1998). Evidence for circulating bone marrow-derived endothelial cells. *Blood* 92, 362-367.
- Simmons P.J., Przepiorka D., Thomas E.D. and Torok-Storb B. (1987). Host origin of marrow stromal cells following allogeneic bone marrow transplantation. *Nature* 328, 429-432.
- Simmons P.J., Masinovsky B., Longenecker B.M., Berenson R., Torok-Storb B. and Gallatin W.M. (1992). Vascular cell adhesion molecule-1 expressed by bone marrow stromal cells mediates the binding of hematopoietic progenitor cells. *Blood* 80, 388-395.
- Smith A., Robson L.G., Sharma P. and Shaw P.J. (1999). Application of interphase FISH on direct bone marrow smears for evidence of chimerism in pediatric sex mismatched bone marrow transplantation. *Pathology* 31, 25-28.
- Soligo D., Delia D., Oriani A., Cattoretti G., Orazi A., Bertolli V., Quirici N. and Deliliers G.L. (1991). Identification of CD34+ cells in normal and pathological bone marrow biopsies by QBEND10 monoclonal antibody. *Leukemia* 5, 1026-1030.
- Tamura S., Saheki K., Takatsuka H., Wada H., Fujimori Y., Okamoto T., Takemoto Y., Hashimoto-Tamaoki T., Furuyama J. and Kakishita E. (2000). Early detection of relapse and evaluation of treatment for mixed chimerism using fluorescence in situ hybridization following allogeneic hematopoietic cell transplant for hematological malignancies. *Ann. Hematol.* 79, 622-626.
- Thiede C., Florek M., Bornhauser M., Ritter M., Mohr B., Brendel C., Ehninger G. and Neubauer A. (1999). Rapid quantification of mixed chimerism using multiplex amplification of short tandem repeat markers and fluorescence detection. *Bone Marrow Transplant.* 23, 1055-1060.
- Thiede C., Bornhauser M. and Ehninger G. (2004). Strategies and clinical implications of chimerism diagnostics after allogeneic hematopoietic stem cell transplantation. *Acta Haematol.* 112, 16-23.
- Thiele J., Rompcik V., Wagner S. and Fischer R. (1992). Vascular architecture and collagen type IV in primary myelofibrosis and

- polycythaemia vera: an immunomorphometric study on trephine biopsies of the bone marrow. *Br. J. Haematol.* 80, 227-234.
- Thiele J., Imbert M., Pierre R., Vardiman J.W., Brunning R.D. and Flandrin G. (2001). Chronic idiopathic myelofibrosis. In *WHO Classification of Tumours: Tumours of Haematopoietic and Lymphoid Tissues*. Jaffe E.S., Harris N.L., Stein H. and Vardiman J.W. (eds) IARC Press. Lyon. pp. 35-38.
- Uhr J.W., Scheuermann R.H., Street N.E. and Vitetta E.S. (1997). Cancer dormancy: opportunities for new therapeutic approaches. *Nat. Med.* 3, 505-509.
- van Besien K. and Deeg H.J. (2005). Hematopoietic Stem Cell Transplantation for Myelofibrosis. *Semin. Oncol.* 32, 414-421.
- White A.D. and Sweeney M.C. (1993). Detection of male cells in mixtures containing varying proportions of male and female cells by fluorescence in situ hybridization and G-banding. *Cytometry* 14, 9-15.

Accepted October 9, 2006

Differences in proportion and dynamics of recipient hematopoiesis following hematopoietic cell transplantation in CML and IMF

UDO SIEBOLTS^{1,5}, JÜRGEN THIELE¹, THOMAS ZANDER⁴, MARKUS DITSCHKOWSKI³,
DIETRICH W. BEELEN³, NICOLAUS KRÖGER², BORIS FEHSE² and CLAUDIA WICKENHAUSER¹

¹Institute of Pathology, University of Cologne, Kerpener Str. 62, D-50924 Cologne; ²Department of Bone Marrow Transplantation, University Hospital Hamburg, D-20246 Hamburg; ³Department of Bone Marrow Transplantation, University Hospital of Essen, Hufeland Str. 55, D-45122 Essen; ⁴Molecular Tumor Biology and Tumor Immunology, Clinic I for Internal Medicine, University of Cologne; ⁵Center for Molecular Medicine, University of Cologne (CMMC), Kerpener Str. 62, D-50924 Cologne, Germany

Received August 16, 2007; Accepted September 26, 2007

Abstract. Since decades myeloablation followed by allogeneic stem cell transplantation offered the only opportunity to cure leukemia patients and only recently the development of STI571 created a further alternative in chronic myeloid leukemia (CML). While among all leukemias this transplantation regimen had the best outcome in CML, trials with reduced intensity conditioning regimens (RIC) were rather humbling and recurrence of the neoplastic clone occurred frequently. However, the same therapy in patients with idiopathic myelofibrosis (IMF) resulted in a more favorable outcome. Therefore, long-term mixed chimerism (mCh) was determined on bone marrow (BM) biopsies derived from five IMF patients and from eight CML patients of the pre STI era following sex-mismatched transplantation. All patients presented lasting hematologic remission and were matched concerning age, sex and appearance of GvHD. Analysis of late transplant period (day +100) revealed a concentration of host cells within the CD34⁺ precursor cell compartment in both diseases. However, in IMF BM biopsies only up to 8% recipient CD34⁺ precursors but in CML biopsies up to 26% recipient CD34⁺ precursors were detected. Taken into account that in CML up to 10% of the host BM CD34⁺ precursors bear the BCR-ABL translocation our data suggest that the neoplastic CD34⁺ progenitor cell population might dispose of better strategies to escape immune surveillance in CML than in IMF.

Introduction

Allogeneic bone marrow and hematopoietic stem cell transplantation (allo-BMT/HSCT) has arguably been applied successful in the treatment of chronic myeloid leukemia (CML) and still remains the most effective strategy for inducing durable molecular remission in STI571 (imatinib mesylate, Gleevec) refractory patients (1,2). The application of conventional myeloablative allo-HSCT has, amongst others, been limited by the age of the recipient. Therefore, the use of reduced intensity conditioning (RIC) regimen was studied in a limited number of patients. However, even if some published data remain contradictory most studies reported an elevated risk for recurrence of the disease and an adverse outcome (1,3,4). Idiopathic myelofibrosis (IMF), a less common chronic myeloproliferative disease (CMPD) with an onset in the elderly, carries a prognosis with a median survival of four years (5,6). Initial studies on a small number of patients demonstrated that conventional myeloablative therapy lead to high transplant-related mortality (7-10). However, the use of RIC resulted in a better outcome in IMF patients (11). In general, the elimination of tumor cells is mostly due to a strong graft-versus-leukemia (GVL) effect of the donor alloimmune effector lymphocytes (12-14). When leukemia relapses after allogeneic hematopoietic cell transplantation (HCT), donor lymphocyte transfusions can induce sustained remissions in some patients (15). The different response of IMF and CML patients on above-mentioned therapy regimen could suggest that neoplastic hematopoiesis in CML might dispose of better escape strategies than hematopoiesis in IMF.

Patients and methods

Patients (IMF). A total of five patients (four men, one woman; mean age 45 years, fifteen sequential post-transplant trephine biopsies) with IMF in the chronic phase of the disease received PBSC grafts from sex-mismatched HLA identical family

Correspondence to: Dr Claudia Wickenhauser, Institute of Pathology, University of Cologne, Kerpener Str. 62, D-50924 Cologne, Germany
E-mail: c.wickenhauser@uni-koeln.de

Key words: chronic myeloproliferative disease, chronic myeloid leukemia, reduced intensity conditioning, graft-versus-leukemia, mixed chimerism, FISH, CD34⁺ progenitors

donors at the University Hospital Hamburg, Germany. All patients had a history of various therapeutic regimens including hydroxyurea, busulfan as well as radiation or a combination of these. All patients received standardized RIC with busulphan (10 mg/kg), fludarabine (180 mg/m²) and anti-thymocyte globulin followed by allo-HSCT with a median number of transplanted CD34⁺ progenitors of 8x10⁶ per kg body weight (range 0.9-15.6). No primary graft failure occurred. The median time until leukocyte (>1.0x10⁹/l) and platelet (>20x10⁹/l) engraftment was 16 (range, 11-26) and 23 days (range, 9-139) respectively. Acute graft-versus-host disease (GvHD) grade II-III occurred in three patients and two patients had limited chronic GvHD. Standard GvHD prophylaxis was performed (MTX + Cyclosporin A). Hematological response and complete histopathological remission without signs of relapse was seen in all five patients during the period under consideration. The patients were enrolled in a prospective pilot study of RIC. Explicit approval of this study was obtained from the local ethics committee and all patients gave written informed consent (see also refs. 11 and 16).

Patients (CML). Sixteen archived pre- and post-transplant BM biopsies (1985-1996) of eight patients from the pre-STI era (five men and three women, median age 37 years) with chronic phase CML were enrolled in the study. Patients had received BM grafts (median size 2.3x10⁸/kg nucleated cells) from sex-mismatched HLA identical family donors at the University Hospital of Essen, Germany, following standard procedures that included conditioning regimens (Cy 60 mg/kg/day x 2; dose of total body irradiation (TBI) 4 x 2.5 Gy cobalt-60 and GvHD prophylaxis (MTX + Cyclosporin A). A successful engraftment according to standard criteria was established at day 24±5 in all patients (17,18). Acute GvHD grade II-III developed in five patients and limited chronic GvHD was diagnosed in three patients. All patients presented complete hematologic remission for the period under study. Blood analysis revealed cytogenetic remission in the whole period under study (19).

BM biopsies. BM trephine biopsies were performed from the posterior iliac crest. The fixation of samples was carried out in a low-concentrated phosphate-buffered formalin solution for 12-48 h. Further processing included decalcification for 3-4 days in 10% buffered ethylene-diamine tetra-acetic acid (EDTA), pH 7.2, paraffin wax embedding, and employment of several staining techniques, involving Giemsa, PAS (periodic acid Schiff reagent), naphthol-AS-D-chloroacetate esterase, Perls' reaction for iron and a silver impregnation method (Gomori's technique).

Sequential immunostaining and dual color fluorescence in situ hybridization (FISH). For a simultaneous immunophenotypic and genotypic evaluation, 4 µm paraffin-embedded sections were immunostained with CD34⁺ (QBEND10, IgG1κ, Dako, Hamburg, Germany), or CD61⁺ (Y2/51, IgG1κ, Dako). Subsequently, the slides were incubated with a satellite probe mix for chromosomes x and y (CEP X Spectrum Orange/CEP Y Spectrum Green DNA Probe Kit; Vysis, Bergisch Gladbach, Germany) as described previously (20).

The slides were evaluated with an Aristoplan microscope (Leitz, Wetzlar, Germany) equipped with an optimized triple bandpass filter and imaged with a digital camera (Photometrics SenSys; Tucson, AZ, USA) and appropriate software (IPLab Spectrum P, Vienna, VA, USA). Only those cells containing exactly two marked signals were evaluated.

Polymerase chain reaction (PCR) analysis. Quantitative Y chromosome-specific PCR assay (QYCS-PCR) based on the DFFRY gene for the determination of hematopoietic donor chimerism was performed on peripheral blood cells of four male IMF patients as formerly described (11,16). This method can be used to detect remaining male cells after sex-mismatched allogeneic blood stem cell transplantation (HSCT) involving a male patient and female donor (16). For PCR, primers FP-Y (aactcactccaacacatactccac) and RP-Y (ttcatgatgaaatctgcttttgggtt) were synthesized according to the published sequence of the DFFRY gene (21). A FAM-labeled TaqMan probe (P-Y, cagccaccagaattatctccaagctctctga) was designed using Primer Express software to allow real-time quantitative PCR in an ABI PRISM 7700 Sequence Detection System (Applied Biosystems, Weiterstadt, Germany). To standardize DNA content, a second PCR reaction detecting the human hematopoietic cell kinase gene HCK was carried out in the same tube (multiplex) (22,23).

Male (Y chromosome-positive) cell content was quantified based on ct (threshold cycle) values obtained after real-time PCR. Statistical data evaluation was performed with Microsoft Excel software (16).

Results

Validation of polymerase chain reaction and fluorescence in situ hybridization. Serial dilutions of male mononuclear cells in female cells confirmed that the detection of <1 male in 100,000 female cells (<0.001%), was possible. Concerning the female patient in this collective, the Y chromosome-specific PCR was negative.

In all patients dual color FISH was performed on pre-treatment trephine biopsies to validate the method. Concerning the male patients, in 0.3% cells the genotype was spuriously suggested to be female while a total congruence with the female gender was found in all cells under investigation.

Distribution of donor and host hematopoiesis in BM and PB. Concerning the four male IMF patients mCh was verified to be a phenomenon affecting both, the BM and the PB compartment. In detail, QYCS-PCR data demonstrated a proportion of PB recipient cells ranging between 0 and 1% in the early as well as late post-transplant period. Concerning analysis of corresponding sequential BM biopsies and FISH examination 0 and 1% host megakaryocytes were seen in the early post-transplant period and also at day +100, respectively. In contrast, BM CD34⁺ progenitors displayed a host cell proportion of 5 and 8% by examination of the early transplant period and day +100, respectively. The variation in host cell distribution concerning early and late post-transplant period, however, was not statistically significant (t-test; unpaired).

Evidence of constitutive BM host hematopoiesis in CML patients with lasting cytogenetic remission in PB. MCh of

Table I. Portion of Graft and Host hematopoiesis of early and late transplant phase.

	Day ≤ 100 after HCT		Day ≥ 101 after HCT	
	Host (%)	Graft (%)	Host (%)	Graft (%)
IMF				
Progenitor cells (CD34)	6 (5)	109 (95)	11 (8)	135 (92)
Megakaryocytes (CD61)	0 (0)	182 (100)	3 (1)	222 (99)
CML				
Progenitor cells (CD34)	19 (18)	89 (82)	30 (26)	84 (74)
Megakaryocytes (CD61)	8 (11)	65 (89)	10 (13)	70 (87)

Portion of graft and host hematopoiesis of early and late transplant phase. Pooled data of five IMF patients and eight CML patients following FISH analysis and immunohistochemistry for CD34 of CD61 are demonstrated. Counted cells and parenthesized percentage for graft and host hematopoiesis of early and late transplant phase are presented. (Total no. of counted cells: 1043).

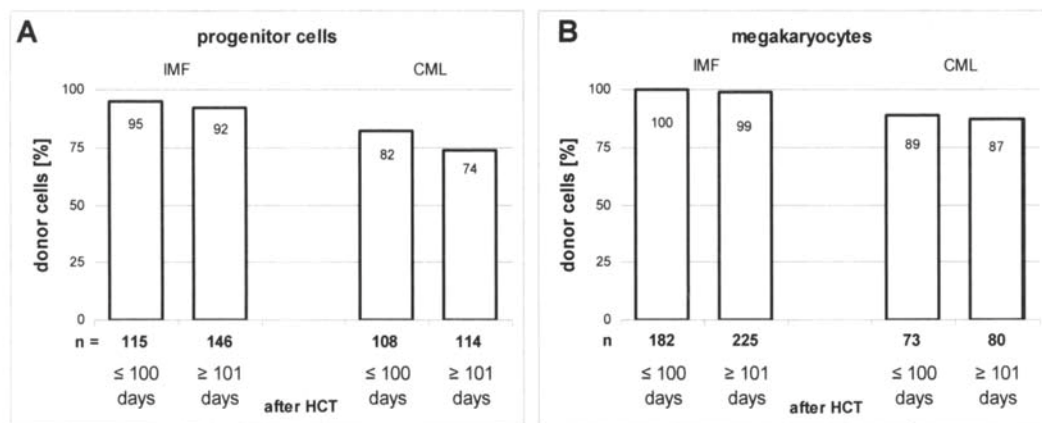


Figure 1. MCh in IMF and CML following HCT. Rate of donor cells for the time-points of early (≤ 100 days) and late (≥ 101 days) post-transplant period (n, number of counted cells). CD34⁺ progenitors (A) and megakaryopoiesis (B).

post-transplant BM biopsies exclusively derived from patients with lasting cytogenetic remission was analysed. In all cases under study a distinct proportion of host derived hematopoietic cells was seen. Detailed FISH analysis of megakaryocytes as an element of mature hematopoiesis revealed mCh of 11% in the early post-transplant period and of 13% at day +100. Concerning the CD34⁺ progenitors 18 and 26% were of host origin when examining BM biopsies of the early post-transplant period and day +100, respectively. These data indicate the presence of a lasting BCR-ABL negative host cell hematopoiesis in disease-free post-transplant CML patients. Observed variations of host cell distribution in early and late post-transplant period were not statistically significant for the megakaryocyte or for the CD34⁺ progenitor cell compartment.

MCh is particularly a phenomenon of the immature hematopoiesis. To compare mCh in mature and the immature hematopoiesis 29 BM biopsies of 5 IMF and 8 CML patients were analysed. In both diseases a higher proportion of host derived CD34⁺ progenitors was seen when compared to megakaryocytes. In detail, concerning the early post-transplant

period, 5% of the CD34⁺ progenitors but no megakaryocytes were of host origin in IMF patients while 18% of the CD34⁺ progenitors and 11% of the megakaryocytes were of host origin in CML. Concerning day +100, 8% host CD34⁺ progenitor cells but only 1% host megakaryocytes were seen in IMF and in CML mCh represented 26% of the CD34⁺ progenitors and 13% of the megakaryopoiesis. The prominent role of CD34⁺ progenitors in mCh was seen in all patients. Concerning the IMF patients this finding was statistically significant by unpaired t-test for both time periods. Concerning the CML patients results were marginally not significant but disclosed the same trend.

Superior bone marrow mCh in CML compared to IMF. FISH analysis of 1043 hematologic cells derived from BM biopsies of IMF and CML patients in hematological remission revealed a constant higher proportion of host derived megakaryopoiesis and CD34⁺ progenitors in CML patients. This phenomenon was observed in early as well as in late post-transplant period. As summarized in Table I in IMF patients complete chimerism of the CD61⁺ megakaryopoietic lineage was obtained within the first 100 days. At all later time-

points the fraction of recipient cells in this cell lineage was below 2%. In the group of CML patients 11% of the megakaryocytes were of host origin in the early post-transplant period while mCh was 13% at day +100 (Table I; Fig. 1).

When data for the CD34⁺ cell population of CML patients were compared to those of the IMF patients the contingent of recipient cells was significantly elevated in the CML group in the early as well as the late post-transplant period ($p < 0.05$; t-test; unpaired) (Table I; Fig. 1).

Discussion

QYCS-PCR is a rapid and sensitive technique to detect male cells and therefore enables analysis and quantification of PB mCh in sex mismatched HCT (16,24,25). A disadvantage of this method is the constriction on male patients. In the analysis of BM biopsies, recipient stromal cells cannot be differentiated from host hematopoiesis and therefore the changing relation between hematopoiesis and stromal cells during the engraftment and post-transplant period falsifies the results. In the evaluation of BM biopsies the FISH technique therefore outmatches the QYCS-PCR technique. In combination with immunohistochemical analysis this assay allows the genotyping of single phenotyped cells. Assuming that in CMPD the source of relapse probably is the undifferentiated hematopoietic progenitor cell FISH analysis also is an important tool in monitoring hematopoietic engraftment in the BM after transplantation (26).

Following a gender-mismatched transplantation, the concurrent characterization of genotype and cell lineage provides suitable means for the identification of chimeric states and thus the host/donor origin of a certain cell population (24). However, it has to be considered that the number of host cells does not necessarily reflect the number of neoplastic hematopoiesis (17,18,20) and the relevance of host cell number on HCT outcome remains controversial (27-30). Analyzing the same BM biopsies, we reported a BCR/ABL positive population within the CD34⁺ cell compartment ranging from 5 to 10% (18) indicating that 30-50% of the host CD34⁺ cells bear the translocation. These data indicate that an increase in mCh indeed is a powerful indicator of initial relapse and therefore an important tool to initialize accurate treatment as soon as possible (31). In IMF our data also indicate that measurement of mCh is a useful and true instrument in the monitoring of clonal diseases when a defined chromosomal aberration is unknown (7,8,32,33).

In this study the FISH technique was applied to compare and monitor IMF and CML patients transplanted with sex-mismatched donors. Combination of FISH technique with IHC allowed subdivision of maturing and immature hematopoiesis. In this context CD61⁺ megakaryopoiesis lineage was selected because, based on previous data, the probability to detect single recipient cells in these lineage is higher when compared with those of the erythro- and granulopoiesis presumably by virtue of the polyploid state of these cells (17). The immature, potentially dormant hematopoiesis was detected by CD34 IHC. Morphological control of the stained cells within the BM allowed a clear discrimination from CD34 endothelial cells because BM vessels were omitted in the evaluation (18).

With CML and IMF two CMPD were selected which are both hematopoietic stem cell diseases. Although a specific chromosomal aberration is only described in CML this disease shares a lot of clinical and morphological similarities with IMF. A maximum similarity in both groups was achieved as follows: i) patients were matched concerning age, phase of their disease and risk of GvHD; ii) only patients in lasting complete hematologic remission were elected; and iii) patients achieved grafts from sex-mismatched HLA identical family donors. In addition, only CML patients in complete cytogenetic remission were elected. Differences in the management of both diseases included i) the manner of hematopoietic eradication (myeloablation in the CML group versus myeloreduction via RIC in the IMF group) and ii) the manner of transplantation (allo-BMT in the CML group versus allo-HSCT in the IMF group) and resulted from the adverse outcome of the therapy concerning the setting vice versa (1,3,7-11). Concerning the time-points day +100 post-transplant, however, effects of initial therapy (allo-BMT and allo-HSCT) are blurred because at that time-point the interplay between immune reactivity of the graft and immunogenicity of the tumor cells is regarded to be essential for the course of the individual disease (19,34). In addition, individual ranges of the relative proportion of T-cells are indeed broad but are reported not to differ between BM and peripheral blood stem cell allografts (35).

In both diseases under study mCh was concentrated within the population of CD34⁺ progenitors. Assuming that the majority of neoplastic cells are comprised in this compartment our data are in line with the findings that early leukemia relapse is indicated by sequential monitoring of mCh in PB CD34⁺ cells (36). Concerning CML, the prominent role of BM CD34⁺ cells is further highlighted by the finding of constant persistence of malignant hematopoietic progenitors in patients in complete PB cytogenetic remission (18). Although a direct comparison was not conducted it is likely that these findings affect CD34⁺ progenitors from both sources, PB and BM, respectively.

The most prominent difference between IMF and CML BM findings was the significantly elevated rate of mCh in CML hematopoiesis. These data indicate that host CD34⁺ cells and therefore also primary neoplastic stem cells in CML seem not to be as sensitive to myeloreductive drugs and, even more important, to graft versus leukemia reactions than their counterparts in IMF. In other words, the presented data indicate that the interplay between reduction of the host cell mass and efficiency of the unedited donor immune system in eradication of host and tumor cells has to be linked to each disease and disease stage. An excess of tumor mass over each individual threshold therefore leads to uncontrolled proliferation of the neoplastic progenitors, an observation that can be underlined by previously published FISH data on sequential trephine biopsies of relapsing CML patients (17,18). The finding that myeloablative regime may not be sufficient to cure CML at least in advanced disease, points to the same direction (3,37,38).

In this context, allowing the assumption that immunological responses against tumor cells are likely to be most effective against the most immunogenic of the tumor cell population and least effective against the escape mutants that

have evolved various means of camouflage or resistance for immune mediated toxicity (37). Our present data indicate that CML CD34⁺ progenitors are more resistant and harder to eradicate than their IMF counterparts. This, in part, could depend on the low translation of immunogenic BCR-ABL protein by CML CD34⁺ progenitor cells (34). However, the concomitant higher fraction of recipient megakaryopoiesis in CML patients bearing large amount of BCR-ABL protein indicates that this might not be a major reason for the less complete eradication. Altogether, our findings support the conclusion that neoplastic hematopoiesis in IMF patients might be more vulnerable to immunological responses than the neoplastic CD34⁺ progenitor cell population in CML patients perhaps due to better strategies in escaping immune surveillance of the latter. Further studies will have to clarify which GVL target antigens could be responsible for the more effective strategies of CML CD34⁺ progenitors to escape immune surveillance.

Acknowledgements

Supported by a grant from the Dr. Mildred Scheel Foundation for Cancer Research (No. 106324).

References

- Crawley C, Szydlo R, Lallancette M, Bacigalupo A, Lange A, Brune M, Juliusson G, Nagler A, Gratwohl A, Passweg J, Komarnicki M, Vitek A, Mayer J, Zander A, Sierra J, Rambaldi A, Ringden O, Niederwieser D and Apperley JF: Outcomes of reduced-intensity transplantation for chronic myeloid leukemia: an analysis of prognostic factors from the Chronic Leukemia Working Party of the EBMT. *Blood* 106: 2969-2976, 2005.
- Goldman JM and Druker BJ: Chronic myeloid leukemia: current treatment options. *Blood* 98: 2039-2042, 2001.
- Sloand E, Childs RW, Solomon S, Greene A, Young NS and Barrett AJ: The graft-versus-leukemia effect of non-meloablative stem cell allografts may not be sufficient to cure chronic myelogenous leukemia. *Bone Marrow Transplant* 32: 897-901, 2003.
- Or R, Shapira MY, Resnick I, Amar A, Ackerstein A, Samuel S, Aker M, Naparstek E, Nagler A and Slavin S: Non-meloablative allogeneic stem cell transplantation for the treatment of chronic myeloid leukemia in first chronic phase. *Blood* 101: 441-445, 2003.
- Barosi G and Hoffman R: Idiopathic myelofibrosis. *Semin Hematol* 42: 248-258, 2005.
- Reilly JT: Idiopathic myelofibrosis: pathogenesis to treatment. *Hematol Oncol* 24: 56-63, 2006.
- Rondelli D, Barosi G, Bacigalupo A, Prchal JT, Popat U, Alessandrino EP, Spivak JL, Smith BD, Klingemann HG, Fruchtman S and Hoffman R: Allogeneic hematopoietic stem-cell transplantation with reduced-intensity conditioning in intermediate- or high-risk patients with myelofibrosis with myeloid metaplasia. *Blood* 105: 4115-4119, 2005.
- Deeg HJ, Gooley TA, Flowers ME, Sale GE, Slattery JT, Anasetti C, Chauncey TR, Doney K, Georges GE, Kiem HP, Martin PJ, Petersdorf EW, Radich J, Sanders JE, Sandmaier BM, Warren EH, Witherspoon RP, Storb R and Appelbaum FR: Allogeneic hematopoietic stem cell transplantation for myelofibrosis. *Blood* 102: 3912-3918, 2003.
- Guardiola P, Anderson JE, Bandini G, Cervantes F, Runde V, Arcese W, Bacigalupo A, Przypiora D, O'Donnell MR, Polchi P, Buzyn A, Sutton L, Cazals-Hatem D, Sale G, De Witte T, Deeg HJ and Gluckman E: Allogeneic stem cell transplantation for agnogenic myeloid metaplasia: a European Group for Blood and Marrow Transplantation, Societe Francaise de Greffe de Moelle, Gruppo Italiano per il Trapianto del Midollo Osseo, and Fred Hutchinson Cancer Research Center Collaborative Study. *Blood* 93: 2831-2838, 1999.
- Ditschkowski M, Beelen DW, Trensche R, Koldehoff M and Elmaagacli AH: Outcome of allogeneic stem cell transplantation in patients with myelofibrosis. *Bone Marrow Transplant* 34: 807-813, 2004.
- Kroger N, Zabelina T, Schieder H, Panse J, Ayuk F, Stute N, Fehse N, Waschke O, Fehse B, Kvasnicka HM, Thiele J and Zander A: Pilot study of reduced-intensity conditioning followed by allogeneic stem cell transplantation from related and unrelated donors in patients with myelofibrosis. *Br J Haematol* 128: 690-697, 2005.
- Horowitz MM, Gale RP, Sondel PM, *et al*: Graft-versus-leukemia reactions after bone marrow transplantation. *Blood* 75: 555-562, 1990.
- Mathe G, Amiel JL, Schwarzenberg L, Cattani A, Schneider M, Devries MJ, Tubiana M, Lallancette C, Binet JL, Papiernik M, Seman G, Matsukura M, Mery AM, Schwarzmann V and Flaisler A: Successful allogeneic bone marrow transplantation in man: chimerism, induced specific tolerance and possible anti-leukemic effects. *Blood* 25: 179-196, 1965.
- Kolb HJ, Schmid C, Barrett AJ and Schendel DJ: Graft-versus-leukemia reactions in allogeneic chimeras. *Blood* 103: 767-776, 2004.
- Kobayashi T, Hashimoto K, Matsumoto K, Yoshizaki K and Yoshikawa K: Analysis of the interleukin 6 receptor on normal human keratinocytes by digital imaging fluorescence microscopy. *J Dermatol* 20: 585-587, 1993.
- Fehse B, Chukhlovina A, Kuhlcke K, Marinetz O, Vorwig O, Renges H, Kruger W, Zabelina T, Dudina O, Finckenstein FG, Kroger N, Kabisch H, Hochhaus A and Zander AR: Real-time quantitative Y chromosome-specific PCR (QYCS-PCR) for monitoring hematopoietic chimerism after sex-mismatched allogeneic stem cell transplantation. *J Hematother Stem Cell Res* 10: 419-425, 2001.
- Thiele J, Wickenhauser C, Kvasnicka HM, Varus E, Schneider C, Muller H and Beelen DW: Mixed chimerism of erythro- and megakaryopoiesis following allogeneic bone marrow transplantation. *Acta Haematol* 109: 176-183, 2003.
- Thiele J, Wickenhauser C, Kvasnicka HM, Varus E, Kleppe S, Beelen DW and Schaefer UW: Mixed chimerism of bone marrow CD34⁺ progenitor cells (genotyping, bcr/abl analysis) after allogeneic transplantation for chronic myelogenous leukemia. *Transplantation* 74: 982-986, 2002.
- Elmaagacli AH, Peceny R, Steckel N, Trensche R, Ottinger H, Grosse-Wilde H, Schaefer UW and Beelen DW: Outcome of transplantation of highly purified peripheral blood CD34⁺ cells with T-cell add-back compared with unmanipulated bone marrow or peripheral blood stem cells from HLA-identical sibling donors in patients with first chronic phase chronic myeloid leukemia. *Blood* 101: 446-453, 2003.
- Wickenhauser C, Thiele J, Perez F, Varus E, Stoffel MS, Kvasnicka HM, Beelen DW and Schaefer UW: Mixed chimerism of the resident macrophage population after allogeneic bone marrow transplantation for chronic myeloid leukemia. *Transplantation* 73: 104-111, 2002.
- Brown GM, Furlong RA, Sargent CA, Erickson RP, Longepied G, Mitchell M, Jones MH, Hargreave TB, Cooke HJ and Affara NA: Characterisation of the coding sequence and fine mapping of the human DFFRY gene and comparative expression analysis and mapping to the Sxrb interval of the mouse Y chromosome of the Dffry gene. *Hum Mol Genet* 7: 97-107, 1998.
- Schiedlmeier B, Kuhlcke K, Eckert HG, Baum C, Zeller WJ and Kruehauf S: Quantitative assessment of retroviral transfer of the human multidrug resistance 1 gene to human mobilized peripheral blood progenitor cells engrafted in non-obese diabetic/severe combined immunodeficient mice. *Blood* 95: 1237-1248, 2000.
- Klein D, Bugl B, Gunzburg WH and Salmons B: Accurate estimation of transduction efficiency necessitates a multiplex real-time PCR. *Gene Ther* 7: 458-463, 2000.
- Thiede C, Bornhauser M and Ehniger G: Strategies and clinical implications of chimerism diagnostics after allogeneic hematopoietic stem cell transplantation. *Acta Haematol* 112: 16-23, 2004.
- Alizadeh M, Bernard M, Danic B, Dauriac C, Birebent B, Lapart C, Lamy T, Le Prise PY, Beauplet A, Bories D, Semana G and Quelvennec E: Quantitative assessment of hematopoietic chimerism after bone marrow transplantation by real-time quantitative polymerase chain reaction. *Blood* 99: 4618-4625, 2002.

26. Kvasnicka HM, Wickenhauser C, Thiele J, Varus E, Hamm K, Beelen DW and Schaefer UW: Mixed chimerism of bone marrow vessels (endothelial cells, myofibroblasts) following allogeneic transplantation for chronic myelogenous leukemia. *Leuk Lymphoma* 44: 321-328, 2003.
27. Huss R, Deeg HJ, Gooley T, Bryant E, Leisenring W, Clift R, Buckner CD, Martin P, Storb R and Appelbaum FR: Effect of mixed chimerism on graft-versus-host disease, disease recurrence and survival after HLA-identical marrow transplantation for aplastic anemia or chronic myelogenous leukemia. *Bone Marrow Transplant* 18: 767-776, 1996.
28. Branch DR, Gallagher MT, Forman SJ, Winkler KJ, Petz LD and Blume KG: Endogenous stem cell repopulation resulting in mixed hematopoietic chimerism following total body irradiation and marrow transplantation for acute leukemia. *Transplantation* 34: 226-228, 1982.
29. Bertheas MF, Lafage M, Levy P, Blaise D, Stoppa AM, Viens P, Mannoni P and Maraninchi D: Influence of mixed chimerism on the results of allogeneic bone marrow transplantation for leukemia. *Blood* 78: 3103-3106, 1991.
30. Baron F and Sandmaier BM: Chimerism and outcomes after allogeneic hematopoietic cell transplantation following non-myeloablative conditioning. *Leukemia* 20: 1690-1700, 2006.
31. Serrano J, Roman J, Sanchez J, Jimenez A, Castillejo JA, Herrera C, Gonzalez MG, Reina L, Rodriguez MC, Alvarez MA, Maldonado J and Torres A: Molecular analysis of lineage-specific chimerism and minimal residual disease by RT-PCR of p210(BCR-ABL) and p190(BCR-ABL) after allogeneic bone marrow transplantation for chronic myeloid leukemia: increasing mixed myeloid chimerism and p190(BCR-ABL) detection precede cytogenetic relapse. *Blood* 95: 2659-2665, 2000.
32. Smith A, Robson LG, Sharma P and Shaw PJ: Application of interphase FISH on direct bone marrow smears for evidence of chimerism in pediatric sex mismatched bone marrow transplantation. *Pathology* 31: 25-28, 1999.
33. Tamura S, Saheki K, Takatsuka H, Wada H, Fujimori Y, Okamoto T, Takemoto Y, Hashimoto-Tamaoki T, Furuyama J and Kakishita E: Early detection of relapse and evaluation of treatment for mixed chimerism using fluorescence *in situ* hybridization following allogeneic hematopoietic cell transplant for hematological malignancies. *Ann Hematol* 79: 622-626, 2000.
34. Clark RE, Dodi IA, Hill SC, Lill JR, Aubert G, Macintyre AR, Rojas J, Bourdon A, Bonner PL, Wang L, Christmas SE, Travers PJ, Creaser CS, Rees RC and Madrigal JA: Direct evidence that leukemic cells present HLA-associated immunogenic peptides derived from the BCR-ABL b3a2 fusion protein. *Blood* 98: 2887-2893, 2001.
35. Yakoub-Agha I, Saule P, Depil S, Micol JB, Grutzmacher C, Boulanger-Villard F, Bauters F, Jouet JP, Dessaint JP and Labalette M: A high proportion of donor CD4(+) T cells expressing the lymph node-homing chemokine receptor CCR7 increases incidence and severity of acute graft-versus-host disease in patients undergoing allogeneic stem cell transplantation for hematological malignancy. *Leukemia* 20: 1557-1565, 2006.
36. Thiede C, Lutterbeck K, Oelschlagel U, Kiehl M, Steudel C, Platzbecker U, Brendel C, Fauser AA, Neubauer A, Ehninger G and Bornhauser M: Detection of relapse by sequential monitoring of chimerism in circulating CD34⁺ cells. *Ann Hematol* 81 (Suppl. 2): S27-S28, 2002.
37. Chan L, Hardwick NR, Guinn BA, Darling D, Gaken J, Galea-Lauri J, Ho AY, Mufti GJ and Farzaneh F: An immune edited tumour versus a tumour edited immune system: prospects for immune therapy of acute myeloid leukaemia. *Cancer Immunol Immunother* 55: 1017-1024, 2006.
38. Slavin S, Nagler A, Naparstek E, Kapelushnik Y, Aker M, Cividalli G, Varadi G, Kirschbaum M, Ackerstein A, Samuel S, Amar A, Brautbar C, Ben-Tal O, Eldor A and Or R: Non-myeloablative stem cell transplantation and cell therapy as an alternative to conventional bone marrow transplantation with lethal cytoreduction for the treatment of malignant and non-malignant hematologic diseases. *Blood* 91: 756-763, 1998.

Imbalance of DNA-dependent protein kinase subunits in polycythemia vera peripheral blood stem cells

Udo Siebolts^{1,2,3*}, Kai Breuhahn⁴, Andrea Hennecke¹, Joachim L. Schultze^{2,5} and Claudia Wickenhauser^{1,3}

¹Institute of Pathology, University of Cologne, Cologne, Germany

²Center for Molecular Medicine, University of Cologne (CMC), Cologne, Germany

³Institute of Pathology, University Hospital of Leipzig, Leipzig, Germany

⁴Institute of Pathology, University Hospital Heidelberg, Molecular Hepatopathology, Im Neuenheimer Feld, Heidelberg, Germany

⁵Molecular Tumor Biology and Tumor Immunology, Center for Internal Medicine, University of Cologne, Cologne, Germany

Polycythemia vera (PV) is a clonal hematopoietic stem cell disease characterized by a trilinear accumulation of blood cells that has been recently associated with a *JAK2*^{V617F} point mutation. However, this molecular defect represents a rather late event in the disease progression, is not specific for this disease, and is not ascertained in all patients indicating that additional factors contribute to the specific phenotype of PV. Therefore, cDNA microarray analyses were performed on CD34⁺ peripheral blood stem cells (PBSC) with subsequent evaluation on mRNA and protein level of a larger cohort of PV patients. Microarray analyses revealed a significant dysregulation of 11 genes. *KU86*, a gene coding for a subunit of the DNA-dependent protein kinase (DNA-PK), displayed the strongest upregulation in all patients under study. This peculiarity was accompanied by downregulation of the catalytic DNA-PK subunit *DNA-PKcs*. Also *Ku86* protein was upregulated and expressed in the vast majority of CD34⁺ PBSC nuclei while a weak nuclear expression was detected in only one blood donor. Differential expression of several genes, imbalance of the distinct subunits of DNA-PK, and particularly the strong upregulation of *Ku86* protein, are new findings in PV CD34⁺ PBSC. These factors may contribute to the accumulation of chromosomal aberrations, accumulation of hematopoietic cells (especially of erythropoiesis), and prolongation of CD34⁺ PBSC life span observed in PV.

© 2008 Wiley-Liss, Inc.

Key words: polycythemia vera; CD34⁺; gene signature; DNA-PK; *KU86*

Chronic myeloproliferative disorders are characterized by abnormal accumulation of more than one hematopoietic lineage associated with relatively normal maturation.¹ Amongst these polycythemia vera (PV) is an acquired clonal myeloaccumulative disease (panmyelosis) with increased red cell production independent of mechanisms that normally regulate erythropoiesis.² An acquired and activating *JAK2*^{V617F} point mutation was previously described occurring in most patients suffering from this disease.^{3–7} However, it has to be taken into account that this point mutation is not specific for PV and that 3–36% of PV patients are *JAK2*^{V617F} negative.^{3,6} In addition, Kralovics *et al.* were able to demonstrate that *JAK2*^{V617F} represents a rather late event in disease progression.^{8,9} Therefore, other molecular defects within the stem cell compartment have to be responsible for the specific phenotype of PV.

On this account, we analyzed gene regulation of CD34⁺ peripheral blood stem cells (PBSC) from PV patients and healthy blood donors. The most prominent elevated gene was *KU86*, a subunit of the DNA-dependent protein kinase (DNA-PK). As a multifunctional protein *Ku86* has been implicated in the regulation of many pivotal nuclear processes such as DNA double-strand break repair by non-homologous end joining (NHEJ).^{10–12} Furthermore, in acute and chronic myeloid leukemias an aberrant activity of DNA-PK subunits *Ku70/Ku86* has been shown to be a candidate mechanism for chromosomal instability.^{13,14} Therefore, taken into account that DNA-PK subunits not only acting as a precise adjusted entity but also each exhibiting their own distinct func-

tions an imbalance may cause severe disorder to cell metabolism.¹⁵ Consequently, we further analyzed gene expression of the 3 DNA-PK subunits and *Ku86* protein expression in PV CD34⁺ PBSC. Furthermore, in PV bone marrow biopsies cellular distribution and abundance of *Ku86* protein in hematopoiesis was scrutinized.

Material and methods

Study design

After informed consent, bone marrow trephine biopsies and peripheral blood (PB) samples from 9 patients with histopathologically determined chronic phase PV were obtained for diagnostic or therapeutic purpose (phlebotomy). No additional myelosuppressive regimens were administered. The diagnosis of PV was ascertained according to the criteria of the WHO classification of 2001 and all patients also meet the criteria of the new WHO classification of 2008.^{16–18}

At initial diagnosis, all patients presented hemoglobin values of >18.5 g/dl (in men) and >16.5 g/dl (in women), a thrombocytosis of >400 × 10⁹/l, and low Epo levels. Beside biopsies from 5 PV patients in the chronic phase of their disease 5 archived trephine biopsies conducted to evaluate dissemination of the disease were taken from patients with nodal lymphoma (without bone marrow involvement) and 26 blood samples from healthy individuals served as controls. All patients under study carried the *JAK2*^{V617F} point mutation as evaluated by PCR.

Additionally, to verify the influence of the allelic burden of the *JAK2*^{V617F} point mutation due to the RNA expression levels of the 6 genes examined by RT-PCR we used allele specific PCR and PCR product sequencing to answer this question. All patients under study revealed heterozygosity in their CD34⁺ PBSC compartment (Supporting Figure 1).

Selection and isolation of CD34⁺ and CD14⁺ cells

Phlebotomy samples of 500 ml peripheral blood underwent centrifugation over Ficoll-Paque (Pharmacia, Uppsala, Sweden) to obtain a mononuclear cell concentrate. Mononuclear cells were labeled with either anti-CD34 micro beads or anti-CD14 micro beads (both Miltenyi Biotec, Bergisch-Gladbach, Germany) and selected by an immunomagnetic separation system according to the manufacturer's instruction (mini-MACS, Miltenyi Biotec). To increase purity of the eluted cells two further passes through

Additional Supporting Information may be found in the online version of this article.

Grant sponsors: The Cologne Fortune Foundation, Center for Molecular Medicine, University of Cologne (CMC).

*Correspondence to: Institute of Pathology, University Hospital of Leipzig, 04103 Leipzig, Germany. Fax: +49 341-97-15009.

E-mail: udo.siebolts@uniklinik-leipzig.de

Received 9 January 2008; Accepted after revision 4 August 2008

DOI 10.1002/ijc.23985

Published online 9 September 2008 in Wiley InterScience (www.interscience.wiley.com).

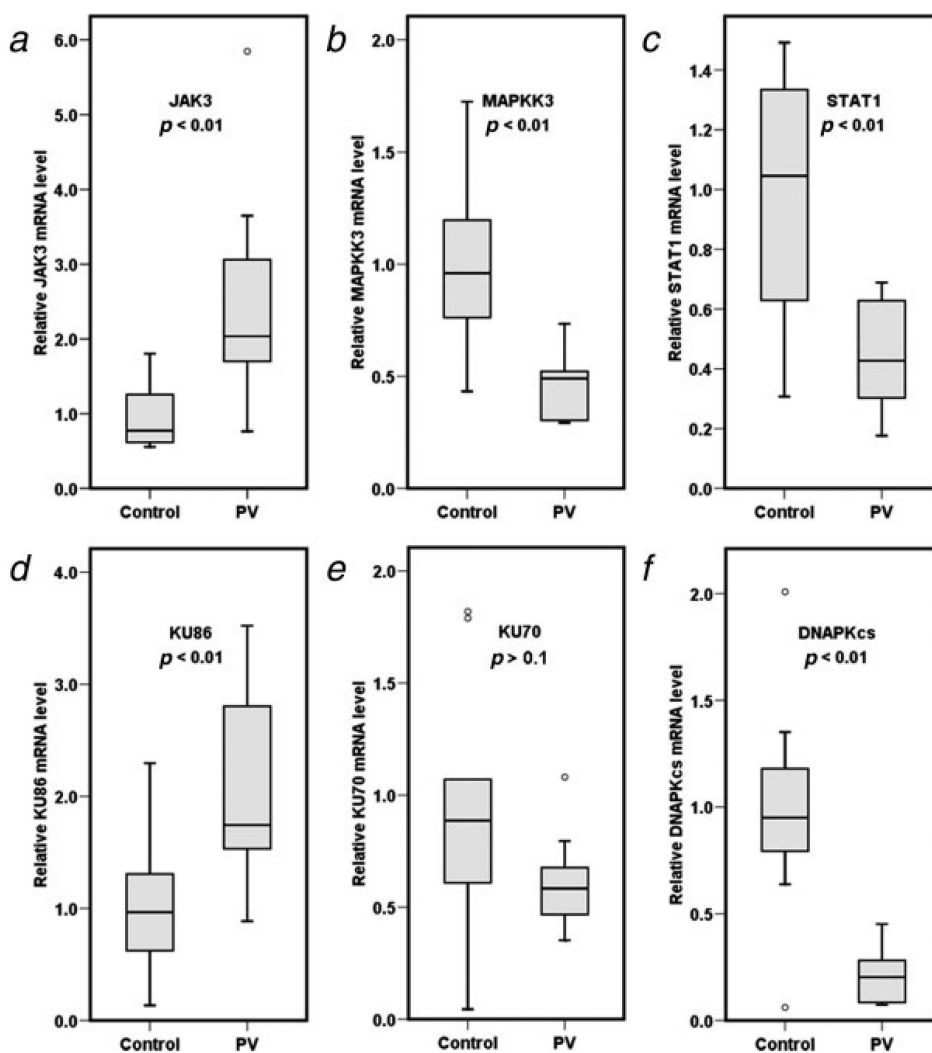


FIGURE 1 – mRNA expression of *JAK3*, *MAPKK3*, *STAT1*, DNA-PK subunits *KU86*, *KU70*, and *DNA-PKcs* in $CD34^+$ peripheral blood stem cells. mRNA expression of *JAK3* (a), *MAPKK3* (b), *STAT1* (c), DNA-PK subunits *KU86* (d), *KU70* (e), and *DNA-PKcs* (f) in $CD34^+$ peripheral blood stem cells of 9 polycythemia vera patients compared with mRNA expression of 9 healthy blood donors (control) employing semiquantitative RT-PCR technique. Vertical axis represents factor of relative mRNA expression. Graph indicating 25th and 75th percentiles as box margins, 10th and 90th percentiles as error bars and the median as a line in the box. Outlying points are displayed as dots. The *p* value is given for each graph.

separation columns were performed. Purity was ascertained by FACS flow cytometry (Becton Dickinson, San Jose, CA). Cells were washed, immediately frozen in liquid nitrogen, and stored at -80°C .

DNA and RNA extraction

Isolation of genomic DNA and total RNA from 1×10^5 to 5×10^5 $CD34^+$ PBSC was performed with the DNeasy or the RNeasy Micro Kit including DNase treatment, respectively (Qiagen AG, Hilden, Germany) according to the manufacturer's instructions. DNA and RNA yield, purity and quality were measured photometrically and validated by gel electrophoresis.

cDNA microarray

Atlas Human 1.2 I array (BD Biosciences Clontech, Heidelberg, Germany) containing 1185 gene specific cDNA was used for hybridization experiments. Total RNA was reversely transcribed and radioactively labeled with [alpha- ^{32}P] dATP (Amersham Biosciences, Buckinghamshire, UK). The very low RNA content of the samples required the selection of the omniscrypt reverse transcriptase (Qiagen AG, Hilden, Germany) according to a modified protocol of the manufacturer's instructions. With this modification samples of minimum 500 ng RNA could be analyzed. Hybridization was performed according to the producer's instructions. For

signal detection Phosphor Imager screens (Amersham) were exposed for up to 1 week and scanned with the Storm Imaging System (Amersham). Data were quantified using the ArrayVision V4.0 software (Imaging Research, Ontario, Canada) and normalized against 6 housekeeping genes included on the microarray (glyceraldehyde-3-phosphate dehydrogenase; alpha tubulin; major histocompatibility complex, class I; beta actin; ribosomal protein L13a; ribosomal protein S9).

Allele-specific QPCR and PCR product sequencing

AS-QPCR was performed on an MX3000p (Stratagene, Amsterdam, Netherlands) detection system with typical reactions of a final volume of 20 μl , containing primers (300 nM) and probes (200 nM) of a *JAK2*^{V617F} specific SNP assay (Applied Biosystems, Foster City, CA) mixed with the appropriate volume of Eppendorf RealMasterMix (Eppendorf AG, Hamburg, Germany) and 2 μl genomic DNA.

Briefly, the results of PCR were validated using sequence specific primers labeled with the IRD 800 fluorescence dye (Metabion, Planegg-Martinsried, Germany). Sequence analysis was carried out on a LI-COR DNA analyzer (Gene Reader 4200; MWG-Biotech). The sequences products were compared with the published data of the NCBI database by BLAST analyses to exclude amplification of a false amplicon.

TABLE I – PRIMERS AND PROBES FOR REAL-TIME RT-PCR ASSAYS

Protein	Gene		Primers/probes 5' → 3'	Amplicon length
Ku86	XRCC5	F	CAA AGA GGA AGC CTC TGG AA	116bp
		R	CCA CAT CAC CAC CTT CTT CA	
		P	FAM—TTC TGT CAC AGC TGA GGA AGC CAA A—BHQ1	
Ku70	XRCC6	F	GAC ATT GCC CAA GGT TGA AG	185bp
		R	TGT GGG TCT TCA GCT CCT CT	
		P	FAM—AGA CTG GGC TCC TTG GTG GAT GAG—BHQ1	
DNA-PKcs	PRKDC	F	GCG AAT ACT TCC AGG CTT TG	155bp
		R	TTG TTT CGC AAC CAG TTC AC	
		P	FAM—AAA GAA GTG TAT GCC GCT GCA GCA—BHQ1	
Jak3	JAK3	F	TAT CCT TGA CCT GCC AGT CC	119bp
		R	ACT CAC CCT GCT CCT TGA GA	
		P	FAM—AGC ACC GCA GTG ACC TGG TGA GT—BHQ1	
MAPKK3	MAP2K3	F	GGA GCT CAT GGA CAC ATC CT	105bp
		R	CGC ACG ATA GAC ACA GCA AT	
		P	FAM—ACA AGT TCT ACC GGA AGG TGC TGG A—BHQ1	
STAT1	STAT1	F	CAA GTT CGG CAG CAG CTT A	144bp
		R	CAC CAC AAA CGA GCT CTG AA	
		P	FAM—TGT TAT GGG ACC GCA CCT TCA GTC—BHQ1	
GAPDH	GAPDH	F	CTC TGC TCC TCC TGT TCG AC	112bp
		R	ACG ACC AAA TCC GTT GAC TC	
		P	FAM—AGC CAC ATC GCT CAG ACA CCA TG—BHQ1	

F, indicates forward primer; R, reverse primer; P, TaqMan probe.

Real-time RT-PCR

Total RNA was reversely transcribed using random hexamer primers (Invitrogen, Karlsruhe, Germany) and Sensiscript RT Kit (Qiagen AG, Hilden, Germany) in case of CD34⁺ PBSC and Omniscript RT Kit (Qiagen AG, Hilden, Germany) in case of CD14⁺ cells. Primers and probes were designed using open source Primer3-web software (http://frodo.wi.mit.edu/cgi-bin/primer3/primer3_www.cgi) and were evaluated by Blast searches at NCBI (<http://www.ncbi.nlm.nih.gov/blast/>) (Table I). All primers and probes were synthesized by Metabion (Planegg-Martinsried, Germany). For detection and quantification of the PCR assays the MX3000p (Stratagene, Amsterdam, Netherlands) was employed. The real-time PCR amplification was performed in a final reaction volume of 20 µl containing primers (300 nM) and probe (200 nM) mixed with the appropriate volume of Eppendorf RealMasterMix (Eppendorf AG, Hamburg, Germany) and 4 µl cDNA. The reaction mixture was preheated at 95°C for 2 minutes, followed by 45 cycles at 95°C for 20 seconds and 60°C for 1 minute. All experiments were evaluated by performing an identical second run. To avoid quantification bias a standard curve of every assay on every single run has been carried out to ascertain the specific amplification efficiency. Briefly, the relative expression mRNA level was determined setting the cycle threshold against the standard curve in each case. Normalization against the internal control Glyceraldehyde-3-phosphate dehydrogenase (*GAPDH*) was followed by calculating the case specific calibrated gene expression. The mean value of normalized gene expression of all healthy controls in one assay served as calibrator.

Western blot analysis

Extracted CD34⁺ PBSC were immediately removed from buffer solutions and frozen in liquid nitrogen. For western blot analysis, cells were homogenized in 200 µl lyses buffer consisting of RIPA-buffer, 10 µl Protease Inhibitor Cocktail (Sigma-Aldrich, Munich, Germany), and 5 µl PMSF (100 mM) by multiple aspirations through a 24-gauge needle. Protein concentrations were measured employing BCA-Protein Assay (Pierce Biotechnology, Bonn, Germany). Equal amounts of protein (10 ng) were separated on a NuPAGE 4–12% Bis-Tris Gel (Invitrogen, Paisley, UK) and transferred to a 0.2 µm pore size nitrocellulose membrane. Western blotting was performed with antibodies against Ku86 (B-1) (Santa Cruz Biotechnology, Heidelberg, Germany). Filters were reprobed with anti-actin (Sigma-Aldrich, St. Louis, MO) mouse

IgG2a monoclonal antibody (clone AC-40), to normalize the protein levels. After incubation with the respective secondary antibodies specific bands were observed *via* enhanced chemiluminescence analysis employing the ECL Plus Western Blotting Detection Kit (GE Healthcare, Munich, Germany). Measurement of the relative optical density (OD) was performed using the Scion Image software release alpha 4.0.3.2 (Scion Corporation; Frederick, MD). For every case the obtained relative OD of Ku86 was normalized by the relative OD of actin.

Immunocytochemistry

Enriched CD34⁺ PBSC were immediately removed from buffer solutions and mixed with sheep erythrocytes not only to obtain a visible pellet but also to avoid cell clustering. After formalin fixation and paraffin embedding 4 µm sections were dewaxed through xylene, rinsed with descending alcohol concentrations, heated in appropriate buffer (100 mM Tris/50 mM EDTA, pH 8.0, 120°C, 5 min), cooled, and rinsed twice in Tris-HCl/0.05% Tween 20 buffer (pH 7.6). Subsequently, immunostaining with Ku86 (B-1) (Santa Cruz Biotechnology, Heidelberg, Germany) was performed by EnVision HRP labeled System (Dako, Hamburg, Germany). AEC Substrate Chromogen (Dako, Hamburg, Germany) was used as chromogenic substance.

Immunohistochemistry on bone marrow biopsies

Four micrometer paraffin-embedded sections from archived bone marrow trephine biopsies (5 PV patients, 5 controls; mean size 17.5 ± 1.8 mm²) were dewaxed through xylene, air-dried, microwave-heated in appropriate buffer (100 mM Tris/50 mM EDTA, pH 8.0) for 12 min, cooled, and rinsed twice in Tris-HCl/0.05% Tween 20 buffer (pH 7.6) at 4°C. Subsequently, immunostaining with CD34 (QBEND10, Dako, Hamburg, Germany) or Ku86 (B-1) (Santa Cruz Biotechnology, Heidelberg, Germany) was performed by EnVision HRP labeled System (Dako, Hamburg, Germany). AEC substrate (Dako, Hamburg, Germany) was used as chromogenic substance. In case of immunophenotypic double staining incubation with CD34 antibody (120 min, 37°C) was followed by addition of a biotinylated secondary antibody (polyclonal rabbit anti-mouse; Dako, Hamburg, Germany) and detection with streptavidin alkaline phosphatase (Lab Vision; Fremont, CA). Fast Red substrate system was used as chromogenic substance. Subsequently, immunodetection with Ku86 antibody (over night, 4°C) was performed by EnVision HRP labeled Sys-

TABLE II – GENE EXPRESSION DATA FROM cDNA ARRAYS

Classification	Genes	UniGene	PV patients		
			A	B	C
Cell cycle	MAP kinase kinase 3 (MKK3)	Hs.514012	-2.89	-2.91	-4.05
	DNA replication licensing factor MCM7 (MCM7)	Hs.438720	3.01	3.46	3.11
Intracellular transducers/ effectors/modulators	Activated CDC42 kinase 1 (TNK2)	Hs.518513	-3.48	-7.17	-8.51
	Janus kinase 3 (JAK3)	Hs.515247	3.32	4.1	3.84
	Non-receptor tyrosine-protein kinase TNK1 (TNK1)	Hs.203420	3.17	3.5	3.75
	STAT1	Hs.642990	-3.28	-2.5	-3.26
DNA-synthesis, recombination, repair	Replication factor C subunit 2 (RFC2)	Hs.647062	-3.76	-4.95	-8.06
	KU86 (XRCC5)	Hs.388739	6.27	5.89	4.97
Transcription	C/EBP alpha (CEBPA)	Hs.76171	-2.72	-4.51	-11.11
Heat shock proteins	Heat-shock protein beta-1 (HSPB1)	Hs.520973	-3.55	-4.32	-7.58
Cell signaling	Interleukin 13 (IL13)	Hs.845	3.34	2.64	9.72

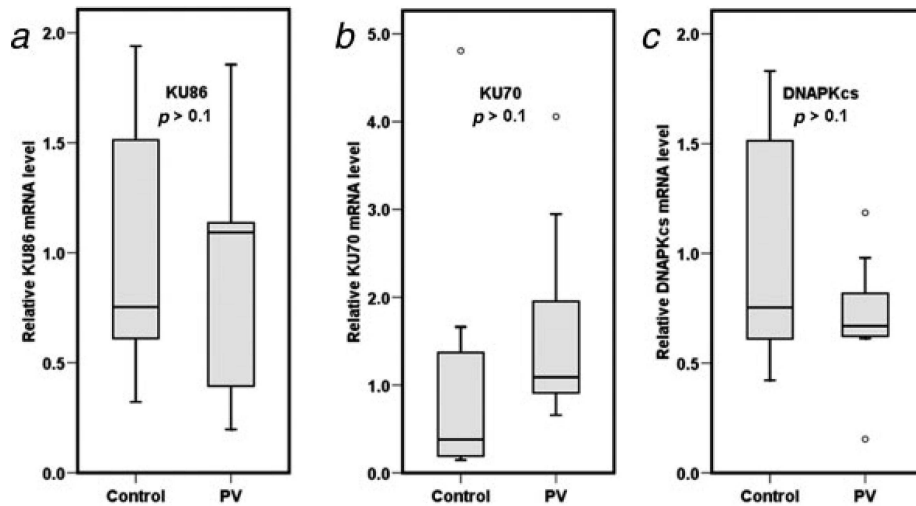


FIGURE 2 – mRNA expression of DNAPK subunits *KU86*, *KU70*, and *DNA-PKcs* in $CD14^+$ monocytes. mRNA expression of DNAPK subunits *KU86* (a), *KU70* (b), and *DNA-PKcs* (c) in $CD14^+$ monocytes of 9 polycythemia vera (PV) patients compared with mRNA expression of 9 healthy blood donors (control) employing semiquantitative RT-PCR technique. Vertical axis represents factor of relative expression. Graph indicating 25th and 75th percentiles as box margins, 10th and 90th percentiles as error bars, and the median as a line in the box. Outlying points are displayed as dots. The p value is given for each graph. In all assays a congeneric expression was seen in PV patients and healthy blood donors.

tem (Dako, Hamburg, Germany) with following diaminobenzidine (DAB)-nickel (Vectorlabs, Burlingame, CA) staining.

Photographic documentation

All pictures were performed on a Zeiss Axiophot microscope (Zeiss, Oberkochen, Germany) with the objective lenses 40X/0.70 NA PL Fluotar or 100X/1.32 oil NA PL Fluotar, respectively. Digital photography was employed with a JVC KY-F75 U (JVC Germany, Friedberg, Germany) using the acquisition software Diskus Version 4.60.342 (Diskus, Koenigswinter, Germany). No further image processing was performed.

Statistical analysis

The Student's t -test was performed for statistical analysis of the data achieved by semiquantitative real-time PCR after testing the normal distribution with one-sample Kolmogoroff-Smirnov-Test. p values ≤ 0.05 were considered as statistically significant and values ≤ 0.01 are shown indicating a higher level of significance. Statistical analysis was achieved using SPSS 14.0.1 software (SPSS, Chicago, IL).

Results

KU86 is the most significantly upregulated gene in PV $CD34^+$ peripheral blood stem cells

To assess potential differences in gene expression between $CD34^+$ cells derived from PV patients and healthy individuals an

initial screen interrogating 1185 genes was performed (Atlas Human 1.21 array). $CD34^+$ PBSC of 3 PV patients and 12 healthy individuals were immunomagnetically enriched (purity $> 95\%$) before analysis. For this initial screen samples from healthy individuals were pooled while the samples from the 3 PV patients were analyzed individually. The experiments revealed that 5 out of 1185 genes were significantly upregulated and 6 out of 1185 genes were downregulated by a more than twofold difference in either PV patient (Table II). The most prominent upregulated gene was the *KU86* subunit of DNA-PK which was significantly elevated 4.97 to 6.27 fold in PV $CD34^+$ PBSC. In contrast, no significant difference in *KU70* mRNA expression between PV patients and healthy controls could be revealed. The cDNA of the catalytic subunit of the holoenzyme *DNA-PKcs* was not spotted on the array.

Among the other dysregulated genes 3 candidates have been described to be involved in the JAK-STAT signaling pathway.^{19–21} Representing the class of cell cycle promoting genes the expression level of mitogen-activated protein kinase 3 (*MAPKK3*) was significantly reduced in the PV $CD34^+$ PBSC as assessed by examination of 138 genes involved in cell cycle regulation. Also the signal transducer and activator of transcription 1 gene (*STAT1*) was downregulated whereas expression of Janus kinase 3 (*JAK3*) revealed significantly increased expression. Altered expression of the JAK-STAT signaling pathway associated genes determined by cDNA array was verified by RT-PCR employing $CD34^+$ PBSC from further 9 PV patients and 9 healthy individuals. All 3 genes revealed analogous dysregulation (Figs. 1a–1c).

As comprised in Table II further upregulated genes were seen in the group of cell cycle regulating genes (*i.e.*, DNA replication licensing factor *MCM7*), intracellular transducers (*i.e.*, non-receptor tyrosine-protein kinase *TNK1*), and cell signaling genes (*i.e.*, interleukin 13 *IL13*). A significant downregulation was seen in the group of intracellular transducers (*i.e.*, activated CDC42 kinase 1 *TNK2*), DNA synthesis associated genes (*i.e.*, replication factor C subunit 2 *RFC2*), transcriptional activators (*i.e.*, C/EBP alpha *CEBPA*), and heat shock proteins (*i.e.*, heat shock protein β -1 *HSPB1*).

Dysregulation of DNA-PK subunits in PV blood cells is restricted to CD34⁺ cells

As the DNA-PK complex has been implicated in DNA replication, regulation of transcription, and DNA double-strand break repair, regulation of gene expression of the *KU86*, *KU70*, and *DNA-PKcs* subunits of the holoenzyme was analyzed performing RT-PCR. In keeping with the cDNA array results again *KU86* was significantly higher expressed in PV CD34⁺ PBSC compared with the controls. Concerning *KU70*, a congeneric expression in PV CD34⁺ PBSC and CD34⁺ PBSC of healthy individuals was seen. In contrast, in PV CD34⁺ PBSC a significant decrease of *DNA-PKcs* compared with the controls could be highlighted (Figs. 1d–1f).

To determine whether the dysregulation of the 3 DNA-PK subunits is restricted to CD34⁺ PBSC or still relevant in mature blood cells we assessed expression of DNA-PK subunits in CD14⁺ monocytes. CD14⁺ cells were isolated from peripheral blood and mRNA was analyzed by RT-PCR. In contrast to CD34⁺ cells of the same individuals, expression of the 3 DNA-PK subunits was not significantly altered between healthy individuals and PV patients (Fig. 2).

Nuclear overexpression of Ku86 protein in PV CD34⁺ peripheral blood stem cells

To assess whether the increased mRNA expression of *KU86* resulted in even increased protein level, immunoblotting on protein lysates of CD34⁺ PBSC was performed. As demonstrated in Figure 3 the Ku86 protein (83kDa) was detected in CD34⁺ PBSC of all PV patients under study while only in 1 of 9 healthy volunteers a faint band was observed.

When examining the subcellular localization of Ku86 in CD34⁺ PBSC by immunocytochemistry a strong and strictly nuclear Ku86 expression in the vast majority of cells was seen in all PV samples while an absent or at most weak staining was detected in CD34⁺ PBSC of healthy individuals. As an internal control the few contaminating leukocytes amidst the enriched PV CD34⁺ PBSC all remained unstained (Fig. 4).

Nuclear overexpression of Ku86 protein in PV bone marrow biopsies

Considering the constant overexpression of Ku86 protein in CD34⁺ PBSC we asked whether this phenomenon could also been revealed in bone marrow CD34⁺ cells. We therefore analyzed paraffin embedded bone marrow biopsies of 5 PV patients and tumor-free staging bone marrow biopsies of 5 patients with nodal ascertained lymphoma as control. Immunohistochemical analysis described Ku86 expression as a rather rare and again strictly nuclear restricted event in the bone marrow biopsies (Fig. 5). However, affecting less than 1% of hematopoietic cells in the control group and up to 10% of the cells in PV it was clearly more frequently seen in the PV biopsies. Thereby, Ku86 was stained in cells of the erythroid and megakaryocytic lineage. In addition, as already presumed in these assays, double immunostaining against Ku86 and CD34 could further clarify that in PV but not in the control biopsies a major subpopulation of CD34⁺ cells expressed Ku86 (Fig. 5).

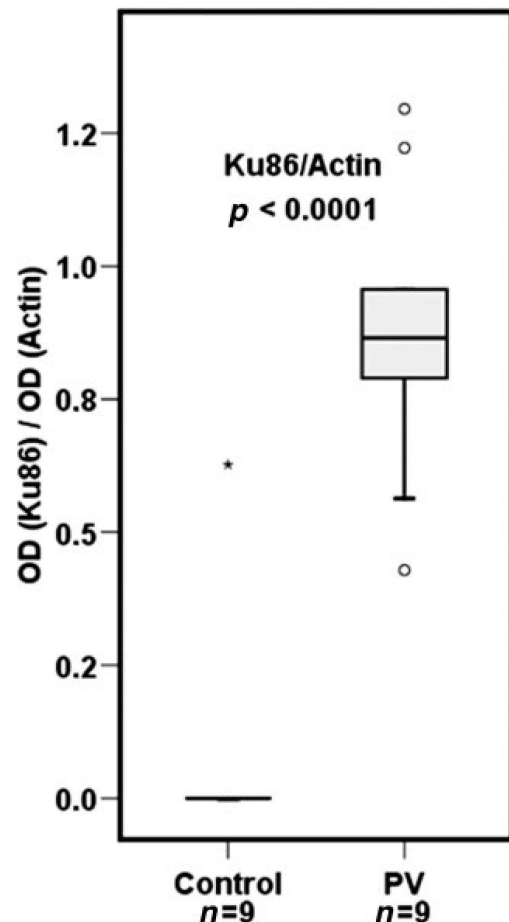


FIGURE 3 – Western blot analysis of Ku86 protein expression in CD34⁺ peripheral blood stem cells. Western blot analysis of Ku86 protein expression in CD34⁺ PBSC of 9 polycythemia vera (PV) patients compared with 9 healthy blood donors. Relative protein expression was determined by setting the optical density (OD) of Ku86 bands against actin OD. Concerning the healthy blood donors (control) a Ku86 expression was seen only in 1 individual (extreme outlying point displayed as an asterisk). In PV patients Ku86 was seen in all individuals. Graph indicating 25th and 75th percentiles as box margins, 10th and 90th percentiles as error bars and the median as a line in the box. Outlying points are displayed as dots.

Discussion

In 2005, 5 groups independently published a point mutation of *JAK2*^{V617F} resulting in an activated kinase activity without the need of ligand binding to hematopoietic receptors, and also effecting cytokine receptor expression and modulating epigenetic cell profile.^{3–7,22} This mutation was described to occur in up to 97% of PV patients. However, the mutation is not specific for PV and is also seen in other Ph⁻ chronic myeloproliferative disorders (CMPD). In addition, individual cases of *JAK2*^{V617F} mutations in other patients and even in healthy volunteers have been described.^{23–26} Finally, data published by others indicate that *JAK2*^{V617F} represents a rather late event in disease progression.^{8,9} Altogether, although detection of the *JAK2*^{V617F} mutation is a milestone in the understanding of PV, this activating point mutation alone cannot explain the specific picture of this disease and other yet unknown mechanisms must account for the pathogenesis restricted in the stem cell compartment.² In this context it has to be underscored that circulating CD34⁺ PBSC as a potential source for stem and progenitor cells can be easily achieved and consist of a higher number of stem and progenitor cells with a lower cell cy-

FIGURE 4 – Ku86 immunocytochemistry of CD34⁺ peripheral blood stem cell clots. Ku86 immunocytochemistry of CD34⁺ peripheral blood stem cells (PBSC) cell clots of 5 polycythemia vera patients compared with 5 healthy blood donors. Ku86 is expressed in a strictly nuclear pattern. Only few cells present a weak expression in CD34⁺ of healthy blood donors (*a*, *b*) while in the PV patients almost all PBSC are intensively stained (*c*, *d*). Note the Ku86 negative mature leukocytes (arrows). Original magnification $\times 1000$ for all panels. [Color figure can be viewed in the online issue, which is available at www.interscience.wiley.com.]

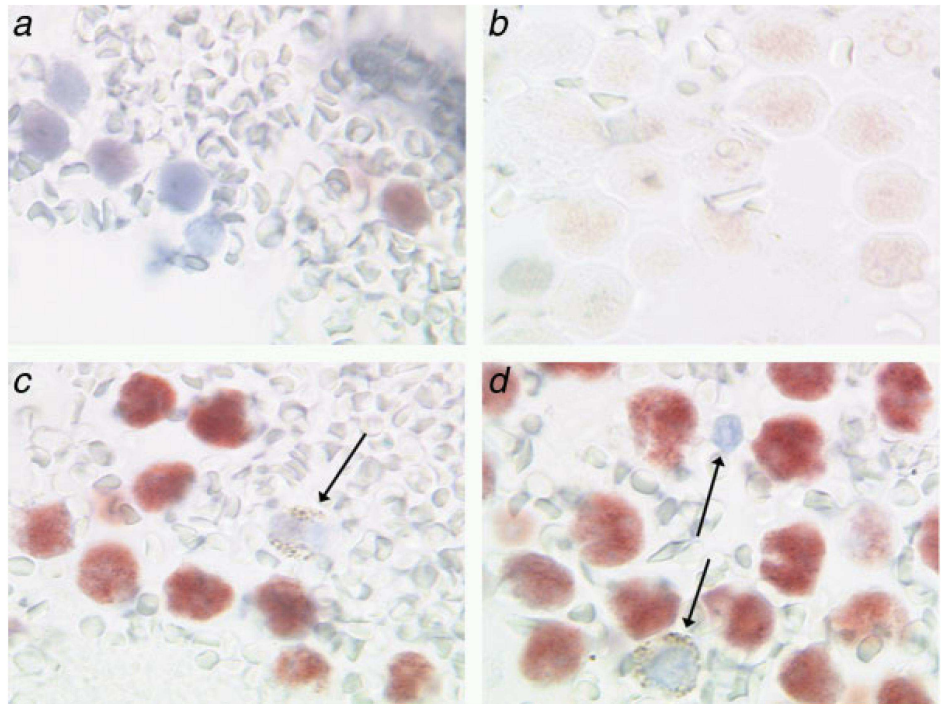
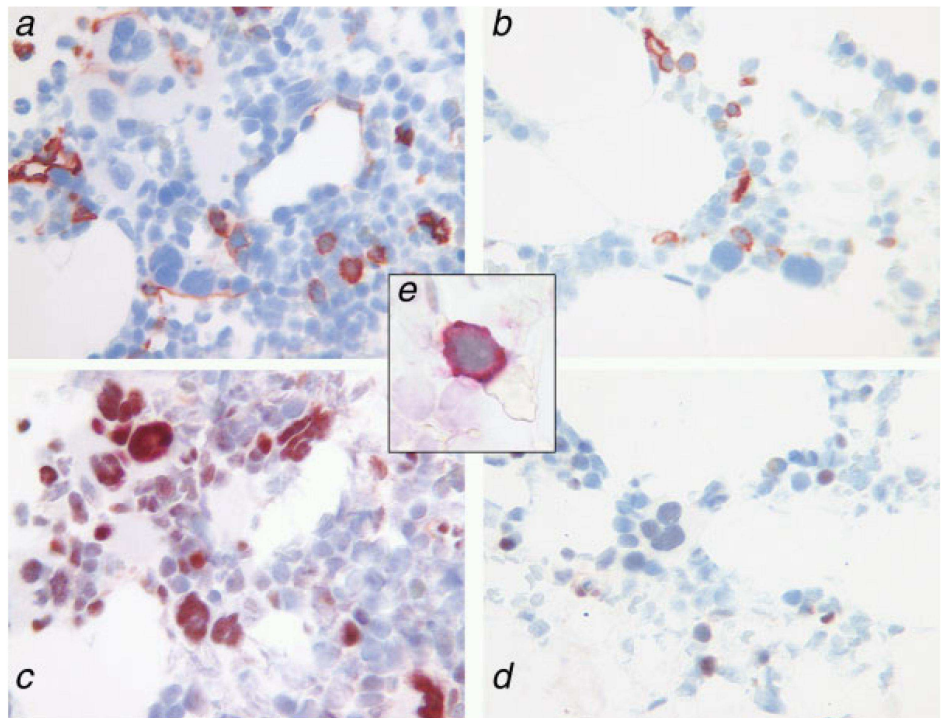


FIGURE 5 – Ku86 and CD34 immunohistochemistry of archived paraffin embedded bone marrow biopsies. Ku86 and CD34 immunohistochemistry of archived paraffin embedded bone marrow biopsies from 5 polycythemia vera (PV) patients (*a*, *c*) and 5 controls (*b*, *d*). CD34 immunohistochemistry is demonstrated in A and B, Ku86 immunohistochemistry representing the identical area in C and D. The overall expression of Ku86 in PV patients clearly exaggerates Ku86 expression in the controls. In direct comparison with each other a coexpression of Ku86 and CD34 in PV patients seems likely. Immuno-doublestaining (CD34 and Ku86) substantiates strong membranous CD34 (red) and nuclear Ku86 (dark-gray) staining (*e*). Original magnifications $\times 400$ (*a-d*) and $\times 1000$ (*e*). [Color figure can be viewed in the online issue, which is available at www.interscience.wiley.com.]



clinging activity compared to CD34⁺ bone marrow stem cells.^{27,28} Therefore, comparative gene signatures of CD34⁺ PBSC, compared with bone marrow CD34⁺ stem cells, offers easy access by phlebotomy and reflects cells which are highly representative for examination of this hematological stem cell disease.

Employing this setting, we show for the first time distinct dysregulation of several genes in PV CD34⁺ PBSC important for regulation of apoptosis, cell cycle and DNA repair. Most notably, the

upregulation of *KU86* on mRNA and protein level together with downregulation of *DNA-PKcs* is an exciting finding and leads to further speculation of mechanisms in the pathophysiology of PV.

Performing cDNA microarray analyses we found gene expression of *MAPKK3*, an activator of p38 mitogen-activated protein kinase modulated apoptosis,^{29,30} and *STAT1*, an activator of Fas and Caspase cascade dependent apoptosis,³¹ significantly downregulated. Furthermore, altered gene expression of additional factors

involved in the fine tune regulation of apoptosis were detected (*i.e.*, *IL13* and *JAK3*).^{32–35} Apoptosis is affected by many signaling pathways and due to its importance fine adjustment is an essential prerequisite to cell fate. Imbalance of even a few or just one factor can lead to severe disorder. In this regard these experimental findings may explain longer live span of PV CD34⁺ PBSC.^{36–38}

Downregulation of 6 pro apoptotic genes and upregulation of 1 anti apoptotic gene was already described in PV CD34⁺ bone marrow stem cells when compared with their healthy counterparts.³⁹ Comparing these data with our results revealed that 2 genes (*HSPB1* and *IL13*) were congruently dysregulated in both compartments (*i.e.*, peripheral blood and bone marrow) and 4 genes (*COMT*, *NUCB1*, *HSPA1A*, and *NTF3*) exhibited a similar tendency but failed to exceed the twofold threshold in our study. However, there also are clear constitutional varieties of gene expression in both compartments.²⁸ In this context, the finding of a prominent Ku86 protein expression by nearly all CD34⁺ PBSC but only by a subpopulation of bone marrow CD34⁺ cells therefore remains unsurprising.

Within the blood cells a significant upregulation of *KU86* together with a downregulation of *DNA-PKcs* and a prominent upregulation of Ku86 protein was restricted to the PV CD34⁺ PBSC. In PV monocytes this complex was not regulated, although these cells are known to be clonal as well.^{4,6,40} However, in PV bone marrow biopsies a strong upregulation of Ku86 protein was also seen in maturing cells of the erythropoiesis and the megakaryopoiesis. As these cell lineages form the specific phenotype of the disease it is tempting to speculate that ongoing dysregulation of DNA-PK in maturing erythropoiesis and megakaryopoiesis might be responsible for their accumulation or at least reflects a today unknown phenomenon in PV.

Ku86 together with Ku70 builds a heterodimer which represents the regulatory subunit of the DNA-dependent protein kinase. This holoenzyme and also its unbound subunits are known to play a pivotal role within the cell and an imbalance of the subunits leads to several interferences in cell metabolism.¹⁰ Beside other functions Ku86 has been implicated to be involved in many nuclear processes such as DNA replication, transcription regulation, and DNA double-strand break repair by NHEJ in a directly or indirectly manner.^{10,11} This repair mechanism rejoins free DNA ends within minutes of their occurrence, but this error-prone process may involve the loss or alteration of nucleotides.⁴¹ Therefore activated Ku86 is able to induce genetic abnormalities like deletions

and end to end ligations in several hematological disorders.^{13,14} Hence, the well-known elevated frequency of chromosomal aberrations including the *JAK2*^{V617F} point mutation observed in chronic phase PV may be a primary effect of increased Ku86 action—even if this phenomenon could also be reactive and caused by previous DNA damage due to unknown effects.^{13,42} Indeed, the relation between increased Ku86 activity and the *JAK2*^{V617F} point mutation must be embedded in a multifactor event due to the specificity of this activating mutation in CMPD.

Beside its mutagenic potential, DNA-PK is known to play a pivotal role in stabilization of p53 protein resulting in G₁ phase block and induction of apoptosis.⁴³ Therefore, downregulation of *DNA-PKcs* together with the above mentioned dysregulation of several apoptosis related genes may be involved in the well-known prolonged cell survival in PV.^{36–38}

Finally, Ku86 protein has been shown to directly affect telomerase activity by telomere capping and recruitment of telomerase.^{10,11} An increase in telomerase activity protects cells and prevents apoptosis. In this context a direct involvement of telomerase activity in the hematopoietic progenitor cell fraction and in erythroid differentiation has already been demonstrated.^{44–46} Both compartments are typically altered and mark impressive hallmarks in PV leading to the assumption that the overexpression of Ku86 contributes to this specific phenotype.

Even it is not clear today whether the above mentioned changes in gene and protein expression are primary or reactive events in the pathophysiology of PV, these results may give new impetus in research of this field. Comprehensively, the differential expression of several genes, imbalance of the distinct subunits of DNA-PK in PV CD34⁺ PBSC, and particularly the upregulation of Ku86 protein are new findings in PV CD34⁺ PBSC. These factors may contribute to accumulation of chromosomal aberrations, accumulation of hematopoietic cells (especially of erythropoiesis) and prolonged CD34⁺ PBSC life span in PV. Our observations of dysregulation in important pathways such as apoptosis, hematopoiesis, cell cycle or DNA repair at the stem cell level open new avenues of research into unknown aspects of PV pathogenesis.

Acknowledgements

This work was accomplished in the Institute of Pathology, University of Cologne.

References

- Dickstein JI, Vardiman JW. Issues in the pathology and diagnosis of the chronic myeloproliferative disorders and the myelodysplastic syndromes. *Am J Clin Pathol* 1993;99:513–25.
- Spivak JL. Polycythemia vera: myths, mechanisms, and management. *Blood* 2002;100:4272–90.
- Baxter EJ, Scott LM, Campbell PJ, East C, Fourouclas N, Swanton S, Vassiliou GS, Bench AJ, Boyd EM, Curtin N, Scott MA, Erber WN, et al. Acquired mutation of the tyrosine kinase *JAK2* in human myeloproliferative disorders. *Lancet* 2005;365:1054–61.
- Levine RL, Wadleigh M, Cools J, Ebert BL, Wernig G, Huntly BJ, Boggon TJ, Wlodarska I, Clark JJ, Moore S, Adelsperger J, Koo S, et al. Activating mutation in the tyrosine kinase *JAK2* in polycythemia vera, essential thrombocythemia, and myeloid metaplasia with myelofibrosis. *Cancer Cell* 2005;7:387–97.
- James C, Ugo V, Le Couedic JP, Staerk J, Delhommeau F, Lacout C, Garcon L, Raslova H, Berger R, Bennaceur-Griscelli A, Villeval JL, Constantinescu SN, et al. A unique clonal *JAK2* mutation leading to constitutive signalling causes polycythaemia vera. *Nature* 2005;434:1144–8.
- Kralovics R, Passamonti F, Buser AS, Teo SS, Tiedt R, Passweg JR, Tichelli A, Cazzola M, Skoda RC. A gain-of-function mutation of *JAK2* in myeloproliferative disorders. *N Engl J Med* 2005;352:1779–90.
- Zhao R, Xing S, Li Z, Fu X, Li Q, Krantz SB, Zhao ZJ. Identification of an acquired *JAK2* mutation in polycythemia vera. *J Biol Chem* 2005;280:22788–92.
- Kralovics R, Teo SS, Li S, Theocharides A, Buser AS, Tichelli A, Skoda RC. Acquisition of the V617F mutation of *JAK2* is a late genetic event in a subset of patients with myeloproliferative disorders. *Blood* 2006;108:1377–80.
- Nussenzweig RH, Swierczek SI, Jelinek J, Gaikwad A, Liu E, Verstovsek S, Prchal JF, Prchal JT. Polycythemia vera is not initiated by *JAK2*^{V617F} mutation. *Exp Hematol* 2007;35:32–8.
- Dip R, Naegeli H. More than just strand breaks: the recognition of structural DNA discontinuities by DNA-dependent protein kinase catalytic subunit. *Faseb J* 2005;19:704–15.
- Gullo C, Au M, Feng G, Teoh G. The biology of Ku and its potential oncogenic role in cancer. *Biochim Biophys Acta* 2006;1765:223–34.
- Downs JA, Jackson SP. A means to a DNA end: the many roles of Ku. *Nat Rev Mol Cell Biol* 2004;5:367–78.
- Brady N, Gaymes TJ, Cheung M, Mufti GJ, Rassool FV. Increased error-prone NHEJ activity in myeloid leukemias is associated with DNA damage at sites that recruit key nonhomologous end-joining proteins. *Cancer Res* 2003;63:1798–805.
- Gaymes TJ, Mufti GJ, Rassool FV. Myeloid leukemias have increased activity of the nonhomologous end-joining pathway and concomitant DNA misrepair that is dependent on the Ku70/86 heterodimer. *Cancer Res* 2002;62:2791–7.
- Collis SJ, DeWeese TL, Jeggo PA, Parker AR. The life and death of DNA-PK. *Oncogene* 2005;24:949–61.
- Jaffe ES, Harris NL, Stein H, Vardiman JWE. World Health Organization classification of tumours: pathology and genetics of

Tissues from routine pathology archives are suitable for microRNA analyses by quantitative PCR

U Siebolts,^{1,2} H Varnholt,¹ U Drebber,¹ H-P Dienes,¹ C Wickenhauser,¹ M Odenthal¹

¹ Institute of Pathology, University Hospital of Cologne, Cologne, Germany; ² Center for Molecular Medicine, University of Cologne, Cologne, Germany

Correspondence to: Margarete Odenthal, Institute of Pathology, University Hospital Cologne, Kerperer Straße 62, 50924 Cologne, Germany; m.odenthal@uni-koeln.de

US and HV contributed equally to this work.

Accepted 12 August 2008
Published Online First
28 August 2008

ABSTRACT

Background: MicroRNAs have recently taken centre stage as short non-coding RNAs that regulate mRNA expression.

Aim/Methods: To assess the feasibility of using microRNA techniques on routinely processed tissues, the accessibility of two representative microRNAs was examined by real-time quantitative PCR in 86 human formalin-fixed paraffin-embedded (FFPE) samples from liver, breast, bone marrow, lymphatic tissues and colon. Murine liver was used to analyse the influence of fixation time and different fixatives.

Results: High-quality microRNA was successfully extracted from routinely processed formalin-fixed tissues, resembling PCR amplification results from snap-frozen material analysed in parallel. While fixation time did not affect microRNA accessibility, non-buffered formalin or fixative supplements such as glutaraldehyde influenced PCR results. Storage of human tissues for up to 7 years did not cause a significant deterioration of microRNA. However, microRNA quality in human archival material following routine processing 10–20 years ago was decreased. Oxidation by ambient air during storage and fixation in non-buffered formalin is a possible reason for loss of microRNA quality.

Conclusion: The assessment of microRNAs in readily obtained formalin-fixed paraffin-embedded samples is a highly promising tool in molecular pathology when similarly treated samples are analysed. Therefore, microRNA analyses will gain wider acceptance as an adjunct to morphological tissue assessment in routine pathology and retrospective studies.

Extraordinary progress in molecular pathology has been made during the last 10 years, and molecular pathology techniques are moving rapidly from the research bench to routine utilisation in diagnostic pathology. Many molecular RNA-based techniques suffer from challenges when routinely processed tissues, which have passed through fixation and embedding steps, are utilised.^{1–8} Commonly used formaldehyde-containing fixatives cause cross-linkage between nucleic acids and proteins, making subsequent extraction and quantification of RNA challenging.^{4–6} One advantage of PCR technologies is that they do not require high amounts of target molecules.⁷ However, a major obstacle to RNA expression fingerprinting of formalin-fixed paraffin-embedded (FFPE) tissues has been the uncertainty about whether gene expression analyses from routinely archived tissues accurately reflect the expression before fixation⁸ because of poor quality due to high fragmentation by tissue processing.⁹ Since fragmentation does not cause further loss of quality when naturally occurring

small RNAs are targeted, microRNA (miRNA) might be ideal to be analysed by PCR in molecular pathology applications. The recently discovered miRNAs are non-coding RNAs that are not longer than 22 bases in mature size and play a crucial regulatory role in organ development, tumorigenesis and chronic disease.^{10–16} miRNA expression profiling of human tumours has already identified signatures associated with diagnosis, progression, prognosis and response to treatment,^{11–16} but most of these studies have used cell culture material or snap-frozen tissue from rodents or humans.^{17–19} Although a number of authors have shown that routinely processed FFPE tissue is suitable for real-time quantitative PCR studies as long as the amplicon sizes are shorter than 200 nucleotides and normalisation to one or several housekeeping genes is accomplished,^{5–8–9–20–21} there are only a few detailed studies about the feasibility of PCR assays from FFPE tissues for non-coding short RNAs.^{22–24} FFPE tissue samples have been collected throughout decades of routine histopathological examination and are thus the most widely available material in tissue archives around the world.^{4–9} Thus, if miRNAs could be analysed in FFPE material, miRNAs could gain wider acceptance as molecular markers in retrospective studies of large tissue cohorts and as general diagnostic and scientific tools. To our knowledge, no study has systematically assessed the effects of formalin fixation from 12 h onward, the effects of tissue storage for more than 25 years, or the effects of miRNA expression in a variety of human tissues across the spectrum from highly adipose breast parenchyma to cellular liver parenchyma and decalcified bone marrow specimens.

The aims of this study are twofold: to demonstrate the effects of fixatives and prolonged storage in paraffin blocks on accessibility of two representative miRNAs and to show the suitability of routine FFPE tissue for comprehensive miRNA expression analyses using real-time PCR.

MATERIAL AND METHODS

Human snap-frozen and FFPE specimens

All specimens were obtained from the tumour bank or from the archive of paraffin-embedded diagnostic tissues of the Institute for Pathology at the University Hospital of Cologne, Germany, 1980–2007, and were used in accordance with the policies of the institutional review board of the hospital.

Eighty-eight FFPE samples from different organs, patients and diagnoses as well as matched snap-frozen tissue from liver (n = 4) and colon (n = 3) were selected (table 1).



This paper is freely available online under the BMJ Journals unlocked scheme, see <http://jcp.bmj.com/info/unlocked.dtl>

Table 1 Human tissue sample origins and diagnoses

miR-16 expression analysis	Description of tissue sample				
Human FFPE tissue from different organs (see fig 2)	Normal lymphoid tissue (n = 8)	Intestine (n = 11): tubular adenoma (3), tubulo-villous adenoma (1), tubular adenoma high-grade dysplasia (1), ulcerative colitis (3), Crohn disease (1), collagenous colitis (1)	Bone marrow (n = 9): chronic idiopathic myelofibrosis (3), polycythaemia vera (3), essential thrombocythaemia (3)	Liver (n = 15): normal transplant organ (2), breast carcinoma metastasis (1), colon carcinoma met (4), small cell lung carcinoma metastasis (1), HCV+cirrhosis (1), HCV+mild fibrosis (1), HBV+moderate fibrosis (2), steatohepatitis (3)	Breast (n = 15): fibroadenoma (4), fibrocystic tissue (5), normal with calcifications (1), invasive ductal carcinoma (4), DCIS (1)
FFPE versus snap-frozen tissues (see fig 1C)	FFPE human liver tissue (n = 4)	FFPE human colon tissue (n = 3)	Snap-frozen human liver tissue (n = 4)	Snap-frozen human colon tissue (n = 3)	
Length of archival tissue storage (see fig 4)	7 years: human lymph nodes, FFPE (n = 7)	17 years: human lymph nodes, FFPE (n = 7)	27 years: human lymph nodes, FFPE (n = 7)	Present day: human lymph nodes, FFPE (n = 11)	

DCIS, ductal carcinoma in-situ; FFPE, formalin-fixed paraffin-embedded; HBV, hepatitis B virus; HCV, hepatitis C virus; miR-16, miR-16 microRNA.

Mouse liver tissues

After killing FVB mice, liver samples were punched from one liver segment using a 5 mm dermatological skin punch biopsy instrument (Stiefel Laboratories, Coral Gables, Florida, USA) and either immediately snap-frozen in liquid nitrogen or fixed in 10% neutral buffered formalin for 12, 24 and 72 h and embedded in paraffin. In addition, 10% non-buffered formalin (pH 3) and Schaefer solution²⁵ were used to fix and decalcify the sample for 24 h.

RNA isolation from snap-frozen and FFPE tissues

For total RNA isolation, N₂-frozen tissues (<100 mg) were homogenised in 500 µl Trizol reagent using a Precellys 24 tissue homogeniser (Carlsbad, California, USA). Then, total RNA was isolated by Trizol reagent extraction after homogenization, following the instructions of the supplier (Invitrogen, California, USA). The FFPE samples were deparaffinised in xylene by incubation at 65°C for a total of 20 min, substituting xylene twice. After two washes with 100% ethanol, samples were lysed in 200 µl proteinase K buffer (500 µg/ml proteinase K (Invitrogen), 50 mM Tris-HCl pH 7.4, and 5 mM EDTA pH 8) overnight. Total RNA was extracted twice by phenol/chloroform and precipitated with 200 mM sodium acetate and isopropanol.

Reverse transcription and real-time PCR

Extracts of total RNA were resuspended in 20 µl H₂O, measured with the ND-1000 NanoDrop spectrophotometer (NanoDrop, Wilmington, Delaware, USA) and then treated with 30 U DNase and 10 U RNase inhibitor, both from Roche Diagnostics (Mannheim, Germany), for 30 min at 37°C in the presence of 1.5 mM MgCl₂. A 35 ng quantity of human and mouse total RNA was reverse transcribed in a 10 µl volume using the TaqMan MicroRNA reverse transcriptase kit (Applied Biosystems, Foster City, California, USA) according to the manufacturer's recommendations. A 3 µl volume of the reverse transcription reaction was used in each of the real-time PCR assays by means with the TaqMan MicroRNA assay kit (Applied Biosystems) following the manufacturer's instructions.

Data normalisation and statistical evaluation

A standard curve of every assay in each run was generated to ascertain the specific amplification efficiency in order to avoid quantification bias. To determine the amount of miR-16 microRNA, a dilution series of total RNA in five steps was performed. Fixation kinetics of mouse livers and experiments with different fixatives were normalised using miR-16 as a reference, and this was followed by calculating the specific calibrated mirR-122a microRNA expression of each mouse liver sample. The mean values of normalised miR-122a levels of

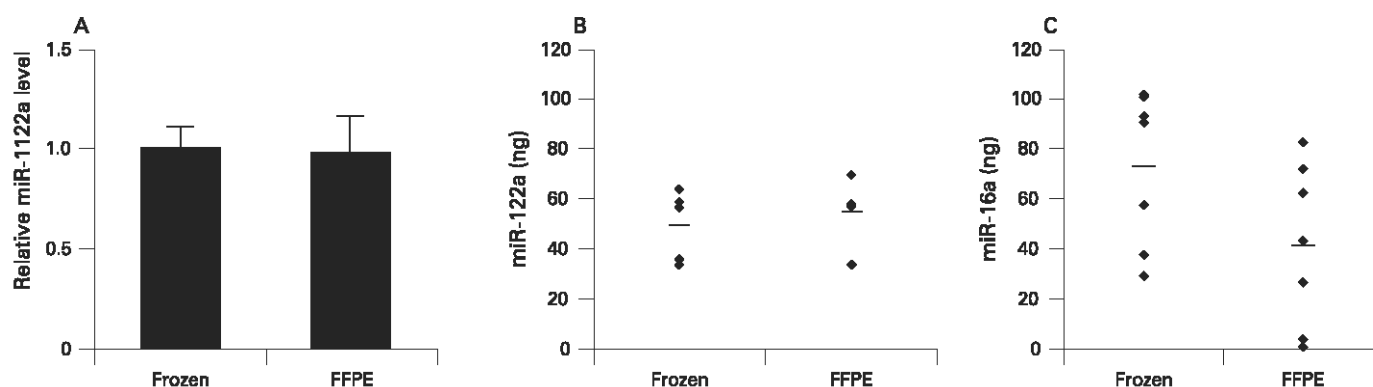


Figure 1 Formalin-fixed paraffin-embedded (FFPE) versus snap-frozen samples of liver tissue. (A) Level of miR-122a microRNA normalised against miR-16 microRNA in snap-frozen (n = 5) and in FFPE mouse liver tissues (n = 5). The mean value of the snap-frozen samples served as calibrator. Error bars indicate SD. (B) miR-122a detection in snap-frozen and FFPE mouse liver tissues, and (C) miR-16 in matched samples of human snap-frozen and FFPE tissues of liver and colon (see also table 1)

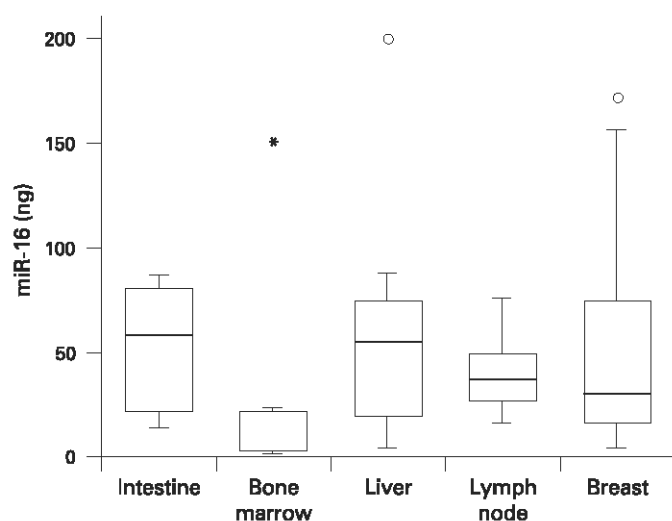


Figure 2 Level of miR-16 microRNA in different formalin-fixed paraffin-embedded tissues. Median of miR-16 level in different organs determined by real-time PCR of 10 ng RNA for each sample. Outlying points are displayed as circles and an extreme outlying point is displayed as an asterisk.

snap-frozen liver tissues or after 12 h formalin fixation served as calibrators, respectively.

A Student t test was performed for statistical analysis of the data achieved by real time PCR after testing the normal distribution with one-sample Kolmogoroff–Smirnov test. A p value ≤ 0.05 was considered to be statistically significant. Statistical analysis was performed using SPSS 14.0.1 software (SPSS, Chicago, Illinois, USA).

RESULTS

Archival formalin-fixed specimens can be used reliably for microRNA expression studies

In our study, we selected two miRNAs: one that is organ-specific and highly expressed in liver and another one that

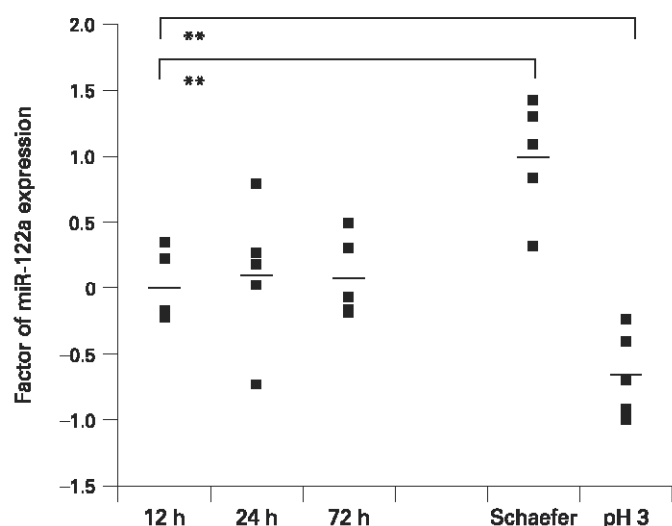


Figure 3 Quantitative real-time PCR expression of miR-122a microRNA in correlation to different length of formalin fixation and different fixatives. Quantitative real-time PCR analysis of miR-122a. The mean values of normalised miR-122a levels of the 24 h snap-frozen samples served as calibrator. Two asterisks indicate a high level of statistical significance ($p < 0.01$).

shows ubiquitous, but just moderate expression. We compared the levels of these representative miRNAs in snap-frozen material with FFPE tissues of mouse and human by real-time PCR. Four snap-frozen murine liver biopsies were compared with four FFPE liver samples from the same FVB mouse, and their miR-122a and miR-16 levels were determined (fig 1).

Similarly, the amount of miR-16 in human matched samples from a total of seven patients was assessed (fig 1C, table 1). miR-122a was chosen as a liver-specific miRNA, while miR-16, known to be ubiquitously expressed, was considered as a representative miRNA of all other organs and tissues. The expression of archival FFPE tissue for both miRNAs closely mimicked that of snap-frozen tissue. Thus, miRNA expression studies can be reliably performed with routinely obtained pathological materials and the results are similar to the yield from snap-frozen tissues.

High quality microRNA can be obtained from FFPE tissues of different origin and pathological diversity

Tissues from different organs in the human body vary to large degrees in their cellularity, infiltration by inflammatory cells, epithelial/mesenchymal ratios, vascularity, fat and extracellular matrix content etc. In order to demonstrate miRNA accessibility in a wide range of tissues, we studied the ubiquitously expressed miRNA-16 in 58 routinely obtained and processed tissues from a variety of organs, consisting of benign and malignant tissues (table 1). PCR analysis revealed some variation in miRNA-16 level; this was expected because of the unique nature of each sample and the wide morphological differences. However, tissues that are traditionally challenging to examine with regards to their nucleic acid contents (ie, bone marrow) showed an acceptable miRNA yield (fig 2). As a consequence, FFPE archival human tissues from many organs and disease processes, including inflammatory and neoplastic, are suitable for miRNA expression profiling.

Effects of different fixatives on microRNA accessibility

Although buffered formalin is currently the most widely used tissue fixative worldwide, some tissues require additional processing steps, such as decalcification of osseous specimens. Since length of tissue fixation in formalin may range from a few hours to multiple days due to departmental work-flow variations, we also compared fixation times of 12, 24 and 72 h in formalin. We showed that fixation in buffered formalin for different time periods does not significantly alter the levels of miRNA expression in the PCR assays (fig 3). Fixation in non-buffered formalin or Schaefer solution resulted in different miRNA yields, but was similar for each fixative and causes only slight but significant variations in relative expression levels compared to buffered formalin fixation (fig 3). Therefore, samples should only be compared with others after treatment with the same fixative.

Effects of length of FFPE tissue storage on microRNA accessibility

Tissue blocks after formalin-fixation and paraffin-embedding are stored in most hospitals worldwide at room temperature with the cut surface of the tissue exposed to ambient air. A loss of miRNA quality during this time is possible. We compared miR-16 accessibility in recently processed human tissues samples with that in tissues that had been routinely processed and stored 7, 17 and 27 years ago (fig 4). We found a decrease of miR-16 accessibility by PCR assays with samples that had been in long-term storage for several decades. However, overall,

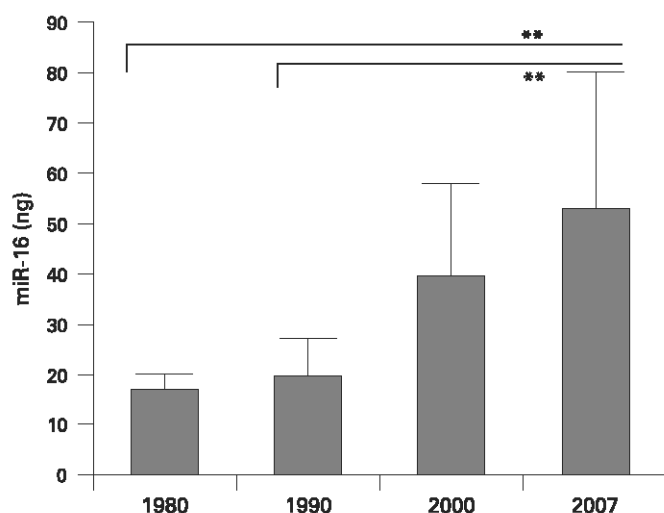


Figure 4 Level of miR-16 microRNA in archived formalin-fixed paraffin-embedded samples from three decades. miR-16 levels were determined in formalin-fixed paraffin-embedded human lymph nodes by real-time PCR. A 10 ng quantity of total RNA for each sample was used and miR-16 levels were taken from a standard curve. Error bars indicate standard deviation and asterisks indicate a significant decrease of miR-16 level after 17 and 27 years of storage ($p < 0.01$).

miRNA levels were in the satisfactory range for all tissues, even after prolonged tissue storage.

DISCUSSION

Molecular techniques are rapidly gaining importance as adjuncts to histological tissue assessment. Since disease-related molecules harbouring genetic as well as morphological disease characteristics are locked away in the vast collection of formalin-fixed paraffin-embedded FFPE tissues stored by the world's pathologists,^{4,9} it is crucial to evaluate the applicability of new molecular tools for routinely stored human FFPE tissues.^{4,26}

In the study presented herein, we demonstrate that miRNA accessibility is not affected by prolonged formalin fixation during routinely performed tissue processing, confirming the results of previous studies.^{23,24} Our data reveal that the accessibility of miRNA from FFPE tissue is comparable to snap-frozen material for human and murine samples. These findings confirm and expand the results of studies of other authors, who used fixed cell culture material²² or mouse tissues.²⁹ The length of fixation time in formalin varies in most pathology departments due to normal fluctuations of workflow depending on the time of the day or the day of the week that any given specimen reaches the pathology laboratory. Here, we demonstrate that the time of formalin fixation up to 3 days did not significantly alter miRNA detection by real-time PCR, thus allowing miRNA analyses in routinely processed tissues. Fixation in different solutions with or without buffering led to different miRNA yields and slight but significant variations of relative miRNA levels by real-time PCR; these variations should prompt pathologists to compare only those tissues that have been treated with the same fixative. In contrast to total RNA, whose fragmentation has been shown to continue to occur after dehydration and paraffin embedding of the formalin-fixed specimens,²⁷ miRNA levels of FFPE mice tissues are not affected by a storage time of up to several months. Even routinely processed human FFPE tissues showed only a moderate but not significant loss of miRNA accessibility within

Take-home messages

- ▶ Accurate and sensitive microRNA (miRNA) expression profiling can be accomplished from a variety of routinely processed and stored human formalin-fixed paraffin-embedded (FFPE) tissues regardless of tissue cellularity, length of fixation time, or length of archival storage. This technical prerequisite allows expression profiling of FFPE archived specimens and offers new opportunities of diagnostic and research in the field of molecular pathology.
- ▶ In order to obtain satisfactory results for miRNA expression assays, it is particularly important to compare like with like (ie, tissues that have been stored for a similar length of time and have been fixed by the same fixatives).

5–7 years. However, stored tissues processed more than 10 or 20 years ago showed nearly a 50% decrease in miRNA accessibility by PCR. Although tissue exposure to ambient air during prolonged storage might be one of the reasons for a loss in miRNA quality, the utilisation of non-buffered formalin at that time might have also contributed to low miRNA yield.

An additional major conclusion of our study is that miRNAs can be assessed reliably by real-time PCR in tissues from various organs and with different diagnoses (normal, neoplastic, inflammatory) regardless of their cellularity, fat content, inflammatory cell infiltrates and degree of stromal fibrosis. Li *et al* have suggested in the past that further work may be necessary to determine the precise effects of formalin fixation and paraffin embedding on miRNA expression profiles across different tissue samples.²² Thus, in the future, miRNA expression profiles of different benign and malignant diseased tissues will be of crucial value to understand disease mechanisms. Reliable miRNA accessibility in tissues of different origin is also of special interest, because a detailed analysis of 345 miRNAs in 40 normal human tissues revealed a number of miRNAs that are specific markers of certain tissue origins.²⁸ Therefore, miRNA accessibility in a wide spectrum of different FFPE tissues will allow these organ-specific miRNA members to serve as markers of the primary tumour site when metastases of unknown origin are encountered by a pathologist.

Acknowledgements: We thank Ali Manav, Elisabeth Konze, and Silke Kummer for their excellent technical support.

Funding: This work was partly supported by the Koeln Fortune Program/Faculty of Medicine, University of Cologne (to HV), and by the program for Research and Education of the Medical Faculty of the University Cologne.

Competing interests: None.

Ethics approval: Ethics approval was obtained.

REFERENCES

1. Rupp GM, Locker J. Purification and analysis of RNA from paraffin-embedded tissues. *Biotechniques* 1988;**6**:56–60.
2. Korbler T, Giskovic M, Dominis M, *et al*. A simple method for RNA isolation from formalin-fixed and paraffin-embedded lymphatic tissues. *Exp Mol Pathol* 2003;**74**:336–40.
3. Haque T, Faury D, Albrecht S, *et al*. Gene expression profiling from formalin-fixed paraffin-embedded tumors of pediatric glioblastoma. *Clin Cancer Res* 2007;**13**:6284–92.
4. Srinivasan M, Sedmak D, Jewell S. Effect of fixatives and tissue processing on the content and integrity of nucleic acids. *Am J Pathol* 2002;**161**:1961–71.
5. Masuda N, Ohnishi T, Kawamoto S, *et al*. Analysis of chemical modification of RNA from formalin-fixed samples and optimization of molecular biology applications for such samples. *Nucleic Acids Res* 1999;**27**:4436–43.
6. Antonov J, Goldstein DR, Oberli A, *et al*. Reliable gene expression measurements from degraded RNA by quantitative real-time PCR depend on short amplicons and a proper normalization. *Lab Invest* 2005;**85**:1040–50.

7. **von Weizsacker F**, Labeit S, Koch HK, *et al*. A simple and rapid method for the detection of RNA in formalin-fixed, paraffin-embedded tissues by PCR amplification. *Biochem Biophys Res Commun* 1991;**174**:176–80.
8. **Godfrey TE**, Kim SH, Chavira M, *et al*. Quantitative mRNA expression analysis from formalin-fixed, paraffin-embedded tissues using 5' nuclease quantitative reverse transcription-polymerase chain reaction. *J Mol Diagn* 2000;**2**:84–91.
9. **Specht K**, Richter T, Muller U, *et al*. Quantitative gene expression analysis in microdissected archival formalin-fixed and paraffin-embedded tumor tissue. *Am J Pathol* 2001;**158**:419–29.
10. **Ro S**, Park C, Jin J, *et al*. A PCR-based method for detection and quantification of small RNAs. *Biochem Biophys Res Commun* 2006;**351**:756–63.
11. **Sassen S**, Miska EA, Caldas C. MicroRNA-implications for cancer. *Virchows Arch* 2008;**452**:1–10.
12. **Yang N**, Coukos G, Zhang L. MicroRNA epigenetic alterations in human cancer: one step forward in diagnosis and treatment. *Int J Cancer* 2008;**122**:963–8.
13. **Barbarotto E**, Schmittgen TD, Calin GA. MicroRNAs and cancer: profile, profile, profile. *Int J Cancer* 2008;**122**:969–77.
14. **Calin GA**, Croce CM. MicroRNA signatures in human cancers. *Nat Rev Cancer* 2006;**6**:857–66.
15. **Cowland JB**, Hother C, Gronbaek K. MicroRNAs and cancer. *APMIS* 2007;**115**:1090–106.
16. **Negrini M**, Ferracin M, Sabbioni S, *et al*. MicroRNAs in human cancer: from research to therapy. *J Cell Sci* 2007;**120**:1833–40.
17. **Gillis A**, Stoop H, Hersmus R, *et al*. High-throughput microRNAome analysis in human germ cell tumours. *J Pathol* 2007;**213**:319–28.
18. **Gramantieri L**, Ferracin M, Fornari F, *et al*. Cyclin G1 is a target of miR-122a, a microRNA frequently down-regulated in human hepatocellular carcinoma. *Cancer Res* 2007;**67**:6092–9.
19. **Lanza G**, Ferracin M, Gafa R, *et al*. mRNA/microRNA gene expression profile in microsatellite unstable colorectal cancer. *Mol Cancer* 2007;**6**:54.
20. **Koch I**, Slotta-Huspenina J, Hollweck R, *et al*. Real-time quantitative RT-PCR shows variable, assay-dependent sensitivity to formalin fixation: implications for direct comparison of transcript levels in paraffin-embedded tissues. *Diagn Mol Pathol* 2006;**15**:149–56.
21. **Roehrl MH**, Becker KF, Becker I, *et al*. Efficiency of single-cell polymerase chain reaction from stained histologic slides and integrity of DNA in archival tissue. *Diagn Mol Pathol* 1997;**6**:292–7.
22. **Li J**, Smyth P, Flavin R, *et al*. Comparison of miRNA expression patterns using total RNA extracted from matched samples of formalin-fixed paraffin-embedded (FFPE) cells and snap frozen cells. *BMC Biotechnol* 2007;**7**:36.
23. **Xi Y**, Nakajima G, Gavin E, *et al*. Systematic analysis of microRNA expression of RNA extracted from fresh frozen and formalin-fixed paraffin-embedded samples. *Rna* 2007;**13**:1668–74.
24. **Hoefig KP**, Thoms C, Roehle A, *et al*. Unlocking pathology archives for microRNA-profiling. *Anticancer Res* 2008;**28**:119–23.
25. **Schaefer HE**. [Histological processing of iliac crest biopsies based on decalcification and paraffin embedding with reference to osteolytic and hematologic diagnosis]. *Pathologe* 1995;**16**:11–27.
26. **Abrahamsen HN**, Steiniche T, Nexø E, *et al*. Towards quantitative mRNA analysis in paraffin-embedded tissues using real-time reverse transcriptase-polymerase chain reaction: a methodological study on lymph nodes from melanoma patients. *J Mol Diagn* 2003;**5**:34–41.
27. **Cronin M**, Pho M, Dutta D, *et al*. Measurement of gene expression in archival paraffin-embedded tissues: development and performance of a 92-gene reverse transcriptase-polymerase chain reaction assay. *Am J Pathol* 2004;**164**:35–42.
28. **Liang Y**, Ridzon D, Wong L, *et al*. Characterization of microRNA expression profiles in normal human tissues. *BMC Genomics* 2007;**8**:166.

Access a vast information database with Toll-Free linking

“Toll-free” linking gives you immediate access to the full text of many of the cited articles in a paper’s reference list—FOR FREE. With the support of HighWire’s vast journal catalogue, a huge reference library is now open to you. If HighWire hosts the journal, you can view the full text of the referenced article, completely free of charge by following the Free Full Text links in the references.

Allele-specific wild-type blocker quantitative PCR for highly sensitive detection of rare JAK2 p.V617F point mutation in primary myelofibrosis as an appropriate tool for the monitoring of molecular remission following therapy

Udo Siebolts,^{1,2} Thoralf Lange,³ Dietger Niederwieser,³ Claudia Wickenhauser¹

► Additional data are published online only at <http://jcp.bmj.com/content/vol63/issue4>

¹Institute of Pathology, University of Leipzig, Leipzig, Germany

²Centre for Molecular Medicine, University of Cologne (CMMC), Cologne, Germany

³Department of Haematology/Oncology, University of Leipzig, Leipzig, Germany

Correspondence to

Udo Siebolts, Institute of Pathology, University of Leipzig, Liebigstrasse 26, Leipzig 04103, Germany; udo.siebolts@uniklinik-leipzig.de

Accepted 16 November 2009

ABSTRACT

Screening of JAK2 V617F point mutation becomes more and more important in monitoring of JAK2 positive MPN following stem cell transplantation. In an attempt to achieve the required high sensitivity (1:10⁵), specificity and robustness we created an approach applicable on bone marrow biopsies where we adapted the principle of wild-type blocker PCR with allele-specific Q-PCR. The significance of the assay was demonstrated on a retrospective series of sequential bone marrow biopsies as diagnosis of molecular relapse now preceded the diagnosis of clinical relapse by far. This method offers the urgently needed tool for a systematic molecular analysis of sequential biopsies in the course of stem cell transplantation to develop guidelines for the management of these patients.

The myeloproliferative neoplasms (MPNs) comprise diverse entities of haematopoietic stem cell disorders.^{1 2} A collective finding of some subgroups is an activating point mutation within JAK2 exon 14, JAK2 p.V617F.³ In this context verification of JAK2 p.V617F mutation is an important tool for the initial diagnosis of polycythaemia vera, essential thrombocythaemia and primary myelofibrosis (PMF) or of advanced disease with predominant osteomyelofibrosis and only low tumour cell density. p.V617F mutation has been further discussed to have a prognostic impact because the mutational status is related to a more favourable outcome in patients with PMF and a more adverse outcome in patients with essential thrombocythaemia.^{1 4} Verification of the mutation also enables patients to be monitored following stem cell transplantation, and it enables selection of patients who would potentially benefit from tyrosine kinase inhibitory therapy.⁵ As retrieval of neoplastic cells may be hampered by bone marrow fibrosis, molecular pathological examination of trephine biopsy samples can offer advantages in test sensitivity.

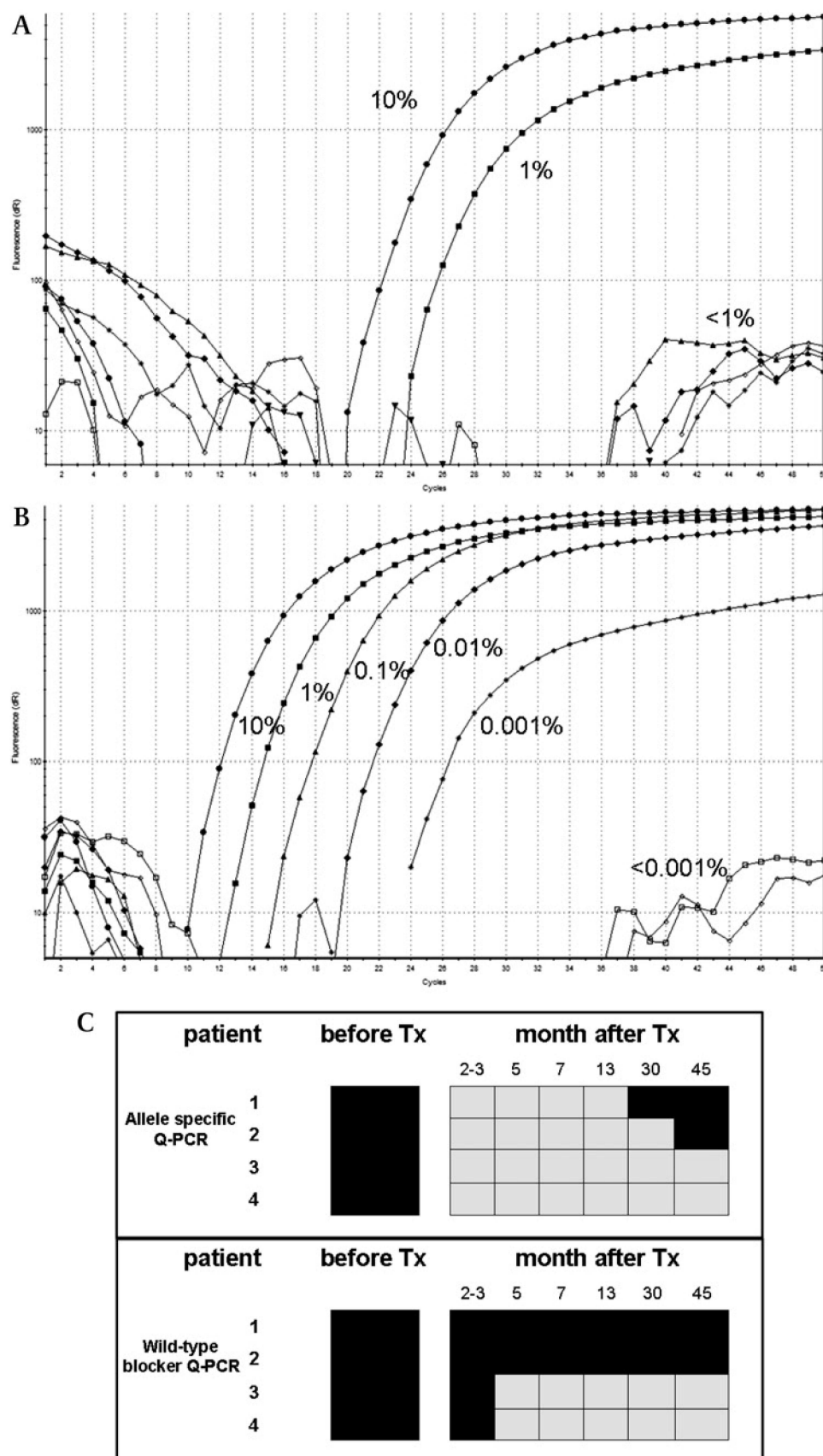
In principle, a number of approaches exist to permit the detection of point mutations in bone marrow biopsy samples, but each amplification procedure has to deal with an excess of wild-type DNA. PCR amplification and subsequent Sanger sequencing requires the mutated allele to be present at a frequency of at least 20%.² The restriction fragment length polymorphism (RFLP)-PCR

method is highly sensitive, but it is limited by the need for a restriction enzyme site at the position that the base pair substitution is to be detected. In contrast, the amplification refractory mutation system PCR is able to discriminate between templates that differ in a single nucleotide, by using specific 3' primer modification; however, due to non-specific hybridisation of these long oligonucleotides, this method is difficult to perform and false-positive results place great demands on laboratory staff. Finally, multiplex assays with two specific taqman probes labelled with minor groove binder (MGB), resulting in very specific hybridisation, allow detection of wild-type DNA and the mutated region. Therefore, this approach is very practicable, but it is strongly limited by competitive inhibition of the more abundant template.

In an attempt to combine high sensitivity and robustness we created an approach where we adapted the principle of wild-type blocking (WTB)-PCR employing locked nucleotide acid (LNA)-substituted oligonucleotides and the Taq polymerase Stoffel fragment with allele-specific (AS) quantitative real-time PCR (QPCR) applying a two-step procedure. The procedure is described in detail in the supplementary material. The LNA-substituted oligonucleotides demonstrate a strong affinity for complementary sequences, resulting in high melting points, and allowing a LNA oligonucleotide to discriminate a 1 bp difference between templates.^{6 7} In order to allow LNA-substituted oligonucleotides to block amplification of wild-type DNA, it was necessary to apply a mutated form of Taq polymerase (Stoffel fragment) that lacks intrinsic 5'–3' exonuclease activity.

Employing the Stoffel fragment, the LNA oligonucleotides and an appropriate primer, we performed PCR (amplicon of 232 nt) and stopped the reaction after 15 rounds to remain in the exponential phase of amplification. Henceforward, the wild-type:JAK2 p.V617F ratio had turned in favour of the mutated region. The amplified PCR product then was adopted in a nested duplex QPCR assay employing AmpliTaq DNA polymerase and fluorescent-labelled TaqMan minor groove binder probes for the JAK2 wild-type and the region harbouring the specific point mutation (table 1). After 40 rounds of PCR, amplification of the wild-type and/or the point mutation was visualised on a MX3000p

Figure 1 (A, B) Sensitivity of quantitative real-time PCR (QPCR) and allele-specific wild-type blocker QPCR (AS-WTB-QPCR) (semi-logarithmic plots). (A) In conventional allele-specific QPCR, amplicates of the JAK2 p.V617F region are seen in a 10% and 1% mixture with wild-type DNA, while higher dilutions of mutated cells were not detected in this assay. (B) When performing AS-WTB-QPCR, mixtures up to 0.001% were easily detected at C_q 27. (C) Schematic presentation of JAK2 p.V617F monitoring by using AS-WTB-QPCR on sequential bone marrow biopsies preceding and following stem-cell transplantation. The colour of the box indicates the JAK p.V617F status of the corresponding bone marrow biopsy (black, JAK p.V617F positive; grey, JAK p.V617F negative). Two of four patients^{1,2} developed clinical relapse of their disease, while two patients^{3,4} remained clinically disease free. Top panel: results obtained using allele-specific QPCR; bottom panel: results obtained using AS-WTB-QPCR. When comparing the two graphs, a striking persistence of single neoplastic cells following stem cell transplantation, only visible when performing the more sensitive test, is seen at very early time points. Even more important is that it was shown, when using the more sensitive assay, that the relapsing patients did not achieve a complete molecular remission during the period of study. Therefore the diagnostic impact can be clearly enlarged performing the more sensitive test.



(Stratagene, Amsterdam, The Netherlands) and a StepOne Plus (Applied Biosystems, Foster City, California, USA). This second AS-QPCR assay, when used alone, exhibited a sensitivity of 1% only (figure 1A). The efficiency of the drafted combined proce-

cedure in reduction of wild-type DNA was therefore demonstrated by the detection of one mutated allele in 10 000 wild-type alleles, and this clearly illustrated that the wild-type allele burden was now highly reduced (dependent on the initial ratio).

Short report

Table 1 Sequences of oligonucleotides

Oligonucleotide name	Amplicon size (bp)	Sequence (5' → 3')
JAK2 1.forw	232	atggacaacagtgtaacaacaa
JAK2 1.rev	232	cactgacacctagctgtgatcc
JAK2 2.forw	101	agcaagctttctcacaagca
JAK2 2.rev	101	gctctgagaaggcattagaaa
JAK2 WTB LNA	Probe	ATGTGTCTGTGGA
JAK2-MGB-FAM	Probe	FAM-ccacagacacatact-MGB
JAK2-MGB-VIC	Probe	VIC-tccacagaacatac-MGB

Locked nucleotide acid (LNA) modified nucleotides are shown in upper case letters.
WTB, wild-type blocking.

AS-QPCR efficiency was then determined by measuring serial dilutions of 100% mutated JAK2 PCR products in triplicate. Only C_q (cycle of quantification) values between 18 and 35 were used for the calculation, and the assay displayed low interassay variation (three independent runs performed on three consecutive days) and an amplification efficiency of 94–99%.

To establish sensitivity and specificity of the AS-WTB-QPCR, serial dilutions of the human erythroleukaemic cell line HEL (DSMZ, Braunschweig, Germany), which is biallelic for the JAK2 p.V617F mutation, and the Hodgkin cell line L1236 (DSMZ), were performed. First, employing the cell line L1236, the ability of the blocking LNA oligonucleotides to prevent primer extension by AmpliTaq DNA polymerase was excluded. A 5 log reduction of wild-type amplification was achieved when the AmpliTaq DNA polymerase was replaced by the Stoffel fragment. This blocking was selective for the wild-type region. Serial dilutions of the blocking oligonucleotides revealed that a minimum of 200 nM blocker was necessary to prevent a PCR amplificate up to C_q 30.

We then spiked wild-type genomic DNA with genomic DNA carrying the point mutation. Here, $1:10^5$ (0.001%) mutant cells were detected when performing the AS-WTB-QPCR, but not when performing conventional AS-QPCR (figure 1A,B). False-positive amplification of the JAK2 p.V617F region was not seen in any of the control experiments before C_q 40, indicating that the assay had excellent specificity. Nevertheless, we evaluated only those amplicates appearing before C_q 35.

To determine the utility of our technique in monitoring JAK2 p.V617F-positive MPN following allogeneic stem cell transplantation, we performed AS-WTB-QPCR on genomic DNA extracted from 24 blinded follow-up formalin-fixed EDTA decalcified paraffin-embedded sequence biopsies from four patients with JAK2 p.V617F-positive PMF at diagnosis and following transplantation. All patients gave written informed consent in accordance with the Declaration of Helsinki, and the study was approved by the local ethics committee and the national health authorities. The study was registered at <http://www.clinicaltrials.gov> (NCT 00599547). Two of the patients remained in lasting clinical remission, whereas two patients presented a clinical relapse at the end of the observation period. When performing conventional AS-QPCR, all patients were shown to have achieved temporary molecular remission. Not surprisingly, at the same time point when the two patients went into clinical relapse, a molecular relapse was detected (figure 1C).

Take-home messages

- Verification of JAK2 p.V617F mutation is an important tool for the diagnosis of a subset of myeloproliferative neoplasms, and it also enables monitoring of patients following stem cell transplantation.
- The monitoring of minimal residual disease demands molecular techniques with a sensitivity of at least $1:10^5$. Also, analysis of formalin-fixed and decalcified bone marrow biopsies with degradation of DNA fragments requires a robust assay.
- The allele-specific wild-type blocking quantitative real-time PCR presented here combines high sensitivity and specificity with robustness in a simple and fast to perform two-step procedure that detects minimal residual disease after stem cell transplantation.

In contrast, data derived from AS-WTB-QPCR provided much more precise monitoring, and in fact it was shown that a total molecular remission was not achieved in the group of the clinically relapsed patients. On the other hand, the two patients with lasting clinical remission were shown to have achieved molecular remission, indicating the high specificity of the test. Taking into account that the outcome for patients with MPN who had had allogeneic stem cell transplantation strongly depends on the early identification of relapse, these data suggest that monitoring of JAK2 p.V617F⁺ MPN demands molecular techniques with a sensitivity of at least $1:10^5$.

In combination with AS-QPCR, the assay presented here is highly reliable and reproducible, simple and fast to perform (3 h), easy to interpret, and should be equally applicable to other single-base mutations. Taking into account that molecular detection of tiny bone marrow infiltrates is becoming more and more important in other contexts (eg, systemic mastocytosis), it is imperative that the method should quickly find its way into the methodological spectrum of molecular haematopathology.

Competing interests None.

Ethics approval Ethics approval was obtained.

Provenance and peer review Not commissioned; externally peer reviewed.

REFERENCES

1. Beer PA, Campbell PJ, Scott LM, *et al.* MPL mutations in myeloproliferative disorders: analysis of the PT-1 cohort. *Blood* 2008;**112**:141–9.
2. Adamson JW, Fialkow PJ, Murphy S, *et al.* Polycythemia vera: stem-cell and probable clonal origin of the disease. *N Engl J Med* 1976;**295**:913–6.
3. Baxter EJ, Scott LM, Campbell PJ, *et al.* Acquired mutation of the tyrosine kinase JAK2 in human myeloproliferative disorders. *Lancet* 2005;**365**:1054–61.
4. Campbell PJ, Scott LM, Buck G, *et al.* Definition of subtypes of essential thrombocythaemia and relation to polycythaemia vera based on JAK2 V617F mutation status: a prospective study. *Lancet* 2005;**366**:1945–53.
5. Manshouri T, Quintas-Cardama A, Nussenzweig RH, *et al.* The JAK kinase inhibitor CP-690,550 suppresses the growth of human polycythemia vera cells carrying the JAK2V617F mutation. *Cancer Sci* 2008;**99**:1265–73.
6. Dominguez PL, Kolodney MS. Wild-type blocking polymerase chain reaction for detection of single nucleotide minority mutations from clinical specimens. *Oncogene* 2005;**24**:6830–4.
7. Latorra D, Arar K, Hurley JM. Design considerations and effects of LNA in PCR primers. *Mol Cell Probes* 2003;**17**:253–9.

Antioxidants Relieve Phosphatase Inhibition and Reduce PDGF Signaling in Cultured VSMCs and in Restenosis

Kai Kappert, Jan Sparwel, Åsa Sandin, Alexander Seiler, Udo Siebolts, Olli Leppänen, Stephan Rosenkranz, Arne Östman

Objective—Growth factor- and reactive oxygen species (ROS)-induced activation of VSMCs is involved in vascular disease. This study investigates whether inhibitory oxidation of protein tyrosine phosphatases (PTPs) contributes to signaling in VSMCs in vitro and in vivo, and analyzes whether ROS- and growth factor-dependent vascular smooth muscle cell (VSMC) signaling is blunted by antioxidants that are able to activate oxidized PTPs.

Methods and Results—Signaling induced by H₂O₂ and platelet-derived growth factor (PDGF) was analyzed in VSMCs with or without the antioxidants N-acetyl-cysteine (NAC) and tempol. Effects of antioxidants on PDGF-stimulated chemotaxis and proliferation were determined. In vivo effects of antioxidants were analyzed in the rat carotid balloon-injury model, by analyzing neointima formation, cell proliferation, PDGF β -receptor status, and PTP expression and activity. NAC treatment prevented H₂O₂-induced PTP inhibition, and reduced H₂O₂- and ligand-induced PDGF β -receptor phosphorylation, PDGF-induced proliferation, and chemotaxis of VSMCs. Antioxidants inhibited neointima formation and reduced PDGF receptor phosphorylation in the neointima and also increased PTP activity.

Conclusion—PTP-inhibition was identified as an intrinsic component of H₂O₂- and PDGF-induced signaling in cultured VSMCs. The reduction in PDGF β -receptor phosphorylation in vivo, and the increase in PTP activity, by antioxidants indicate activation of oxidized PTPs as a previously unrecognized mechanism for the antirestenotic effects of antioxidants. The findings thus suggest, in general terms, reactivation of oxidized PTPs as a novel antirestenotic strategy. (*Arterioscler Thromb Vasc Biol.* 2006;26:2644-2651.)

Key Words: restenosis ■ VSMC ■ protein tyrosine phosphatase ■ platelet-derived growth factor ■ neointima formation

Vascular injury induces oxidative stress and elevated production of reactive oxygen species (ROS) in the vessel wall.^{1,2} Moreover, ROS are produced and act as second messengers as part of the signaling of receptor tyrosine kinases (RTKs) (reviewed in references^{3,4}), which are activated after vascular injury. The most important ROS for pathological conditions are superoxide (O₂⁻) and hydrogen peroxide (H₂O₂). Inhibition of ROS reduce vessel remodeling and restenosis.⁵ The underlying mechanisms remain incompletely understood.

PDGF β -receptor activation contributes significantly to vascular smooth muscle cell (VSMC) proliferation and migration, which is a hallmark of vascular diseases such as atherosclerosis and restenosis. PDGF ligands and receptors are significantly upregulated in atherosclerotic plaques. Moreover, PDGF β -receptor antagonists inhibit atherogenesis and restenosis in various models.⁶

PDGF β -receptors and other tyrosine kinases involved in VSMC proliferation and migration are regulated by protein tyrosine phosphatases (PTPs).⁷ PTPs which have

been identified as negative regulators of PDGF β -receptors include the receptor-like PTP DEP-1, and the cytosolic phosphatases TC-PTP and PTP-1B (reviewed in reference⁸). However, there are also indications that some PTPs, such as SHP-2, act as positive mediators of PDGF β -receptor signaling. The expression pattern of PTPs in VSMCs remains incompletely characterized. However, expression of PDGF receptor-antagonizing PTPs such as DEP-1, TC-PTP, and PTP-1B has been confirmed in previous studies.⁹

PTPs themselves are subject to multiple regulatory mechanisms. Reversible oxidation of the active site cysteine residue has been described as a general mechanism for negative regulation of PTPs.^{3,4,10} Oxidation of PTPs is therefore a candidate mechanism for ROS-mediated effects on VSMC proliferation and migration in vitro and in vivo.

This study investigates whether PTP-inactivation contributes to ROS signaling in VSMCs, and explores the possibility of antioxidant-mediated prevention of PTP-inhibition as a novel strategy for interference with restenosis.

Original received January 22, 2006; final version accepted August 23, 2006.

From the Department of Oncology-Pathology (K.K., J.S., Å.S., A.Ö.), Karolinska Institutet, Stockholm, Sweden; Clinic for Internal Medicine III (J.S., S.R.), University of Cologne, Germany; Institute of Clinical Molecular Biology and Tumor Genetics (A.S.), GSF-Research Centre for Environment and Health, Munich, Germany; Institute for Pathology (U.S.), University of Cologne, Germany; Division of Vascular Surgery (O.L.), Uppsala University Hospital, Uppsala, Sweden; and the Center for Molecular Medicine Cologne (CMMC) (S.R.), University of Cologne, Germany.

Correspondence to Arne Östman, Department of Oncology-Pathology, Karolinska Institutet, 17176 Stockholm, Sweden. E-mail arne.ostman@ki.se
© 2006 American Heart Association, Inc.

Arterioscler Thromb Vasc Biol. is available at <http://www.atvbaha.org>

DOI: 10.1161/01.ATV.0000246777.30819.85

Downloaded from atvb.ahajournals.org at 254/ETS SUBS SERV on December 18, 2008

Materials and Methods

Detailed Materials and Methods are available as online supplement (please see <http://atvb.ahajournals.org>).

Primary Antibodies

Polyclonal rabbit antiserum against the PDGF β receptor was in-house derived, raised against a fusion protein composed of the C-terminal of the PDGF β -receptor and GST (CT β). The other antibodies were derived from commercial sources (see online supplement).

Animals, Surgical Procedures, and Drug Treatment Protocol

Adult male Sprague-Dawley rats weighing 291 to 351 g (Møllegaard Breeding Center, Ry, Denmark) were used. Animal housing followed standard procedure. The experimental protocol was approved by the local Ethics Committee according to the European Union guidelines.

During inhalative Isoflurane-anesthesia balloon injury of the left common carotid artery was performed using a 2F atherectomy (V-Tech AB) catheter.¹¹

The animals received no drug treatment (control), treatment with N-acetyl-cysteine (NAC, Sigma-Aldrich Sweden AB, Stockholm, Sweden), or 4-hydroxy-2,2,6,6-tetramethylpiperidine-N-oxyl (tempol, Fluka Chemie GmbH, Buchs, Switzerland) (control $n=6$, NAC $n=8$, tempol $n=9$). NAC (150 mg/kg bodyweight per day) was dissolved into the drinking water. Fresh solutions were prepared once daily. Tempol (30 mg/kg bodyweight per day dissolved in 1 mL NaCl 0.9%) was administered via gavage once per day, and was kept protected from light until gavage. All animals not treated with tempol received 1 mL NaCl 0.9% via gavage. Drug treatment was started at the day of surgery and continued for 14 days until sacrifice of the animals.

Tissue Preparation

Fourteen days after angioplasty, the common carotid arteries were excised bilaterally and were divided into four parts. One part was OCT-embedded and snap-frozen in liquid nitrogen (LN₂), the other three parts were fixed and paraffin-embedded.¹¹

Histomorphometric Measurement

Six- μ m sections of paraffin-embedded tissue were stained with hematoxylin-eosin. Three parts of the carotid vessel heights (proximal, middle, and distal parts) were sectioned and two sections per animals were quantified morphometrically for each height. Morphometric analysis of digital pictures was performed using NIH Image-J 1.41 software. For each arterial cross section the luminal, neointimal and medial area, and the intima-media ratio were calculated.

Immunohistochemistry

Antibody-staining and detection was performed as described.¹² Primary antibodies (CT β and ab16868) were incubated overnight at 4°C.

Staining intensity of ab16868 was quantified on an arbitrary scale between 1 to 10 by two investigators blinded to the treatment protocol. The quantifications of the two investigators of each individual section never varied more than 1 on the arbitrary scale. Additionally, sections were analyzed on a score according to following scheme: 0% cells stained=0, 1% to 25%=1, 26% to 50%=2, 51% to 75%=3, and 76% to 100%=4. The staining intensity was quantified on an arbitrary scale between 0 to 4. For quantification the two scores were multiplied. For both quantification methods, one section per animal was used for statistical analyses.

Quantitative RT-PCR

Fifty μ m of injured arteries were sectioned separately from frozen tissue (control $n=6$, NAC $n=8$, tempol $n=9$) and pooled according to the treatment-groups. qRT-PCR was performed using standard

procedures (see online supplement). Expression of analyzed genes was normalized to the expression of the house-keeping gene HPRT. Primer sequences are specified in supplemental Table I.

Cell Culture, Immunoprecipitation, and Immunoblotting

Rat vascular smooth muscle cells (VSMCs) were prepared from aortic arteries and used between passage 3 and 13.¹³

VSMCs were grown in DMEM supplemented with 10% FCS to subconfluence, synchronized by serum-deprivation (0.1% serum), and left resting or stimulated with PDGF-BB, H₂O₂ or with sodium vanadate (Sigma-Aldrich Sweden AB). Antioxidants were given to VSMCs for 60 minutes (NAC) or 30 minutes (tempol) before PDGF or H₂O₂ stimulation.

After rinsing twice in ice-cold PBS, cell lysis immunoblotting, visualization, and densitometric quantification was performed as described previously.¹⁴

Analysis of Proliferation, Chemotaxis, and Cell Viability

Analyses of DNA synthesis, chemotaxis, and cell viability was performed with commercial kits as detailed in online supplement. Calculations were performed according to the manufacturer's instructions. Cell viability for NAC was assessed by trypan blue staining because of interference of NAC with the LDH-assay kit. The assay was performed twice in duplicates and counted by at least two individuals, blinded to the treatment protocol.

Phosphatase Assay

VSMCs were synchronized by serum deprivation and were stimulated with 0.1 mmol/L H₂O₂ for 5 minutes. In assays with antioxidants, these were given to cells 60 minutes (NAC, 10 mmol/L) or 30 minutes (tempol, 3 mmol/L) before H₂O₂-treatment. Cells were lysed in buffer supplemented with 5 mmol/L NAC, but without Na₃VO₄. Thereafter, total cell lysate representing approximately 5000 cells were diluted in assay buffer. For analyses of phosphatase activity in tissue, sections of injured carotid arteries derived from control-treated animals (300 μ m/animal) and NAC- and Tempol-treated animals (200 μ m/animal) were pooled in lysis buffer without Na₃VO₄ according to treatment-groups. After adjustment for protein concentration, tissue lysates were subjected to phosphatase activity measurement. Assays were performed in duplicate, and phosphatase activity was expressed as the amount of ³²P-labeled radioactivity released from the peptide after 7 minutes of incubation at 30°C.¹⁵

Determination of Intracellular Peroxides

Intracellular peroxides were detected by flow cytometry. VSMCs (1 \times 10⁶ cells) were starved in serum-free medium for 6 hours and then loaded with CM-H₂DCFDA (5-[and-6]-chloromethyl-2',7'-dichlorodihydrofluorescein diacetate, acetyl ester [Molecular Probes, C6827], 1 μ mol/L, 15 minutes at 37°C). After treatment with or without N-acetylcysteine (10 mmol/L, 60 minutes) and tempol (3 mmol/L, 30 minutes), cells were stimulated with H₂O₂ (0.1 mmol/L, 5 minutes). Cells were washed with ice cold PBS and detached from plates using trypsin. Cells were harvested by centrifugation (600g, 5 minutes) and washed again in PBS. Cells were excited with 488 nm UV line argon ion laser in a flow cytometer (BD FACSCalibur), and the DCF emission was recorded at 530 nm. Data were collected from at least 20 000 cells.

Statistics

Analysis of variance (ANOVA), and paired or unpaired *t* test were performed for statistical analysis, as appropriate. A probability value less than 0.05 was considered to be statistically significant. For morphometric analyses the mean of each animal at three different vessel heights were quantified and an unpaired *t* test was performed for statistical analysis. Data were expressed as mean \pm SEM or mean \pm SD, as indicated.

Results

H₂O₂ Induces Ligand-Independent and Antioxidant-Sensitive PDGF Signaling in VSMCs

Increased production of reactive oxygen species, such as H₂O₂, occurs under pathological circumstances in the vessel wall after eg, vascular injury by balloon-treatment.¹⁶ H₂O₂ has been shown to induce ligand-independent activation of RTKs. We therefore analyzed whether H₂O₂ was capable to induce ligand-independent activation of PDGF β -receptors and downstream signaling molecules in VSMCs.

VSMCs were subjected to H₂O₂ treatment. The concentration range was selected based on previous studies in which ROS-mediated PDGF receptor activation had been demonstrated.¹⁷ Phosphorylation of PDGF β -receptor, Akt, and MAPK p42/44 was induced by H₂O₂ treatment, and this could be blocked by NAC (supplemental Figure I). Antioxidants also decreased ligand-induced receptor phosphorylation (supplemental Figure II), suggesting that PDGF receptor phosphorylation in VSMCs is subject to negative control by PTPs subjected to oxidative regulation. The presence of PDGF receptor-antagonizing PTPs in VSMCs was also demonstrated by a strongly induced receptor phosphorylation following treatment with the general PTP inhibitor sodium-vandate (supplemental Figure I).

H₂O₂ Leads to PTP Inactivation in VSMCs, Which Can Be Restored by NAC

A large series of studies suggest that H₂O₂-mediated RTK activation involves inactivation of PTPs (reviewed in reference 3). We therefore analyzed whether H₂O₂ exposure of VSMCs was associated with a reduction in PTP activity.

Cells were exposed to 0.1 mmol/L H₂O₂ for 5 minutes. This concentration was selected based on previous studies on oxidation-induced PTP inactivation in fibroblasts which indicated partial PTP oxidation at this concentration.¹⁰ After H₂O₂ treatment, cells were lysed and total PTP activity was determined. This analysis revealed a significant reduction of PTP activity after H₂O₂ treatment, which could be prevented by pretreatment with NAC, but not tempol (Figure 1A). The ability of NAC to reduce cellular ROS levels, after H₂O₂-treatment was directly demonstrated by fluorescence measurements (Figure 1B). The same type of analyses also indicated a partial effect of tempol in H₂O₂-treated cells, although this effect was less prominent than that induced by NAC.

We thus conclude that H₂O₂-induced ligand-independent receptor phosphorylation is caused by inactivation of PDGF-receptor-targeting PTPs.

NAC and Tempol Reduce PDGF-Induced Receptor Phosphorylation, Proliferation, and Migration

Transient production of ROS, leading to PTP inactivation, has been described as an intrinsic part of RTK signaling (reviewed in 3). To explore whether this mechanism also operates in VSMCs, we analyzed the effects of antioxidants on PDGF stimulation of VSMCs.

PDGF stimulation induced robust proliferative and migratory responses in VSMCs. Interestingly, cotreatment with

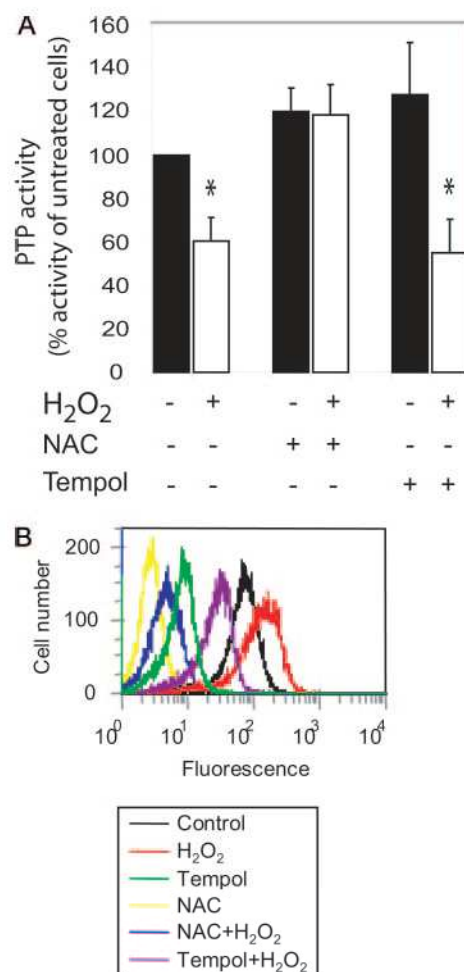


Figure 1. N-acetyl-cysteine, but not tempol, prevents hydrogen peroxide-induced reduction in PTP activity in VSMCs. **A**, Synchronized VSMCs were untreated (–) or pretreated with NAC (10 mmol/L, 60 minutes) or tempol (3 mmol/L, 30 minutes). Cells were stimulated with H₂O₂ (0.1 mmol/L) for 5 minutes, followed by cell lysis. Cell lysate from approximately 5000 cells were used for quantification. Phosphatase activity was determined and is expressed as fraction of activity of untreated cells. Each assay was performed in duplicate, and the data are given as mean \pm SE of the mean from at least 6 separate experiments. * $P < 0.05$ vs control-treated cells. **B**, ROS levels in cells subjected to the treatments of panel A were analyzed by fluorescence measurements.

antioxidants significantly reduced these responses in a dose-dependent manner (Figure 2A and 2B). Cell viability was also analyzed with or without antioxidants and demonstrated clearly that antioxidants, at these concentrations, did not affect cell viability (Figure 2C).

Expression of DEP-1, PTP-1B, SHP-2, and TC-PTP was monitored by qRT-PCR analyses of control cells and cells cultured with NAC or tempol. After 5 hours of treatment, a time point relevant for the migration assay, all PTPs were expressed at similar or lower levels, as compared with control cells (data not shown). However, after 24 hour treatment an increase in PTP-1B and TC-PTP expression was observed in NAC-treated cells (data not shown), which indicates that modulation of PTP expression levels by antioxidants might contribute to the antiproliferative effect in vitro.

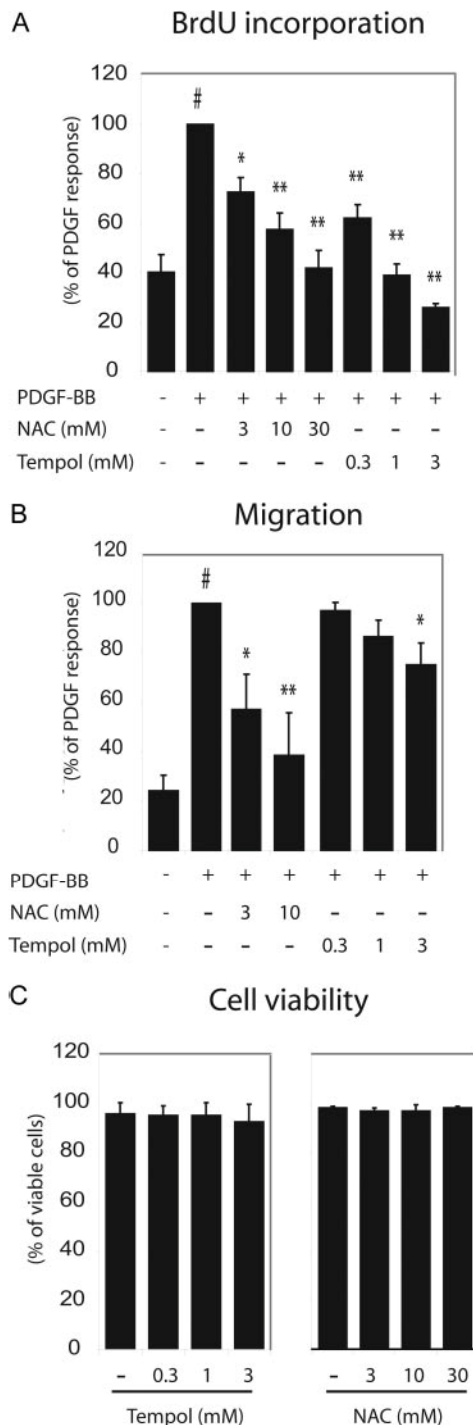


Figure 2. N-acetyl-cysteine and tempol inhibit PDGF-induced cellular responses, without reducing cell viability. **A**, Proliferation was measured by BrdU incorporation. DNA synthesis rates are expressed as percentage of PDGF response. Shown are the means \pm SE of the means from five independent experiments performed in quadruplicates. **B**, Chemotaxis was evaluated utilizing modified Boyden chambers. Data are expressed as percentage of PDGF response. Shown are means \pm SE of the means from three to six independent experiments. Each experiment was performed in sextuplicate per condition. **C**, Cell viability was analyzed by lactate dehydrogenase (LDH) release from cells (tempol, left) or by trypan blue staining (NAC, right). Data are expressed as percentage of viable cells calculated as described in materials and methods and represent means \pm SE of the means from $n=3$ (tempol) or $n=2$ (NAC) experiments. # $P<0.01$ vs control, * $P<0.05$ vs PDGF, ** $P<0.01$ vs PDGF.

We thus conclude that inactivation of PTPs, through transient production of ROS, is a functionally significant aspect of PDGF β -receptor signaling in VSMCs, and that interference with this process, through treatment with antioxidants, represents a strategy for reducing PDGF-induced cell responses.

NAC and Tempol Inhibit Neointima Formation After Balloon Injury

Our in vitro experiments revealed that antioxidants potently inhibited H_2O_2 - and PDGF-signaling, as well as migratory and proliferative responses in VSMCs through a mechanism involving reactivation of oxidized PTPs. This prompted analyses of the effects of antioxidants on restenosis and PDGF β -receptor phosphorylation in vivo, because both ROS and PDGF stimulation of VSMCs have been implied in this pathologic process.

NAC (150 mg/kg per day) and tempol (30 mg/kg per day) were administered on the day of balloon injury of the common carotid artery and daily for the following 14 days after injury. The neointimal area and intima-media-(I/M) ratio were significantly reduced in NAC- and tempol-treated animals compared with control rats (Figure 3A and 3B). In contrast, the medial area did not change in treated rats compared with the control group. Furthermore, in rats treated with NAC the levels of the proliferation-dependent transcript Ki67 were significantly lower compared with vehicle-treated animals (Figure 3C).

Together, these results clearly demonstrate that NAC and tempol inhibit neointima formation, through a mechanism that includes reduced proliferation of VSMCs.

NAC and Tempol Reduce PDGF β -Receptor Activation, but not Expression, In Vivo

The animal study was performed with the rationale that antioxidants might reactivate oxidized PTPs and thereby blunt ROS- and PDGF-induced VSMC proliferation and migration. To experimentally validate this hypothesis, restenotic lesions were analyzed to determine PDGF β -receptor status, ligand production, and PTP expression.

IHC revealed no altered expression of the PDGF β -receptor in vessel lesions after NAC- or tempol-treatment compared with vehicle-treated animals (Figure 4A, left). Transcript levels for the PDGF β -receptor were equal among the groups (Figure 4A, right). Furthermore, IHC and qRT-PCR analyses indicated similar levels of PDGF α -receptor expression in control- and NAC-treated animals, and a moderate reduction in the tempol-treated group (data not shown).

No significant differences in PDGF-B expression, or significant upregulations in the expression of PDGF receptor targeting PTPs, were observed as determined by qRT-PCR (Figure 4B).

Phosphorylation of the PDGF β -receptor in vivo was analyzed by IHC using an antibody recognizing pY1021 of the PDGF β -receptor (Figure 4C). Interestingly, a significant reduction of staining in both NAC- and tempol-treated animals was observed in the intima (Figure 4C). Two different methods for quantification of pY1021 staining were used.

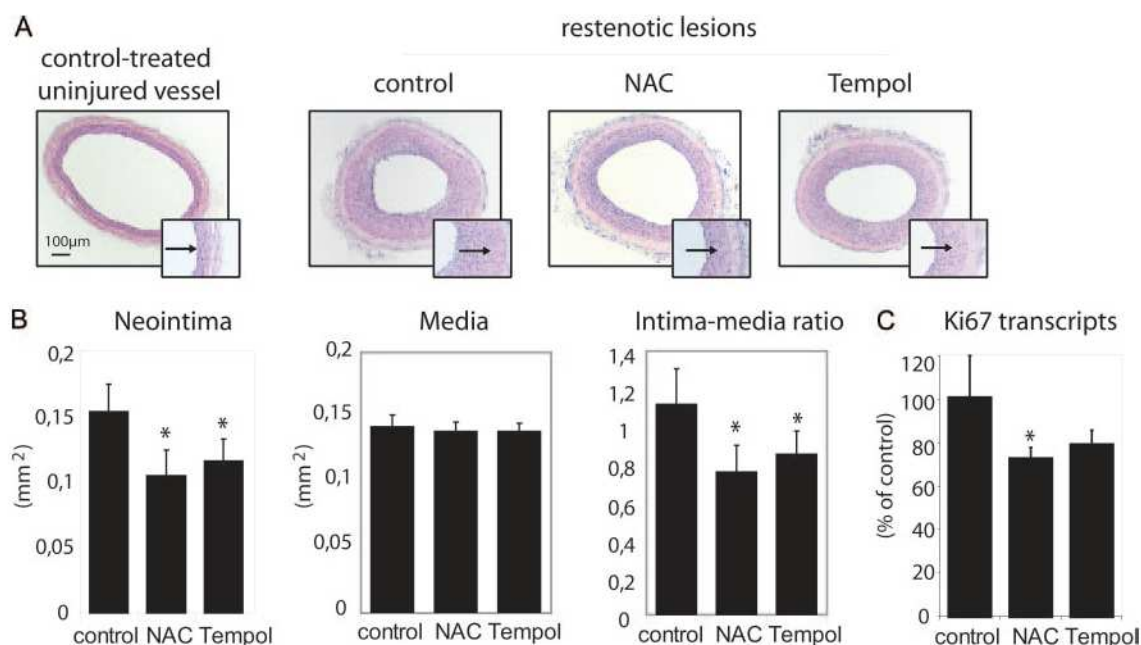


Figure 3. N-acetyl-cysteine and tempol inhibit neointima formation at two weeks after balloon-injury. **A**, Representative photomicrographs of hematoxylin-eosin-stained sections of uninjured and balloon-injured rat carotid arteries. The arrows indicate the internal elastic lamina (inserts). Original magnification $\times 40$ and $\times 200$ (inserts). **B**, Morphometric analysis of the neointimal area (left), medial area (middle), and the intima-media ratio (right). **C**, Analysis of the proliferation-associated transcript levels of Ki67 in total vessel tissues by quantitative real-time PCR. The expression of Ki67 was normalized to the expression of the house-keeping gene HPRT. * $P < 0.05$ vs control-treated animals.

As shown in Figure 4D, both methods revealed a significant reduction in the pY1021 staining in the intima, whereas no significant differences were observed in the adventitial and medial vessel layers. Decreased phosphorylation of PDGF β -receptor in antioxidant-treated animals was also indicated by an ELISA-based assay of PDGF β -receptor phosphorylation (data not shown).

Together, these analyses strongly suggest that activation of oxidized PDGF β -receptor-targeting PTPs contributes to the antirestenotic effects of NAC and tempol.

NAC and Tempol Increase PTP Activity in Vessels
To directly investigate whether treatment with antioxidants was associated with activation of oxidized PTPs, measurements of total PTP activity in vessel extracts was performed.

As shown in Figure 5, extracts from sections derived from antioxidant-treated animals displayed a significantly higher tyrosine phosphatase activity, as determined in an assay of *in vitro* dephosphorylation of ³²P-labeled phospho-tyrosine peptides.

This experiment thus provides independent support for the notion that the reduction in PDGF β -receptor phosphorylation observed after treatment with NAC or tempol is caused by increased PTP activity.

Discussion

We demonstrate in this study that the antioxidant NAC reduces H₂O₂-induced phosphorylation of PDGF β -receptors in VSMCs, and directly demonstrate the ability of NAC to prevent H₂O₂-mediated PTP inhibition in VSMCs (online supplement and Figure 1). The effects of H₂O₂ on PDGF receptor activation and on PTP activity occurred at similar

concentrations of H₂O₂ (0.1 to 1 mmol/L). Furthermore, the antioxidants NAC and tempol, reduced PDGF-induced receptor phosphorylation, as well as migration and proliferation of VSMCs *in vitro* (online supplement and Figure 2). This implies that PTP inhibition is an intrinsic part of the PDGF-induced proliferative and migratory signaling. Finally, both antioxidants significantly reduced neointima formation (Figure 3). Importantly, the reduced neointima formation was paralleled by a reduction in receptor phosphorylation (Figure 4) and an increase in vessel PTP activity (Figure 5). These changes occurred in the absence of changes in expression levels of PDGF β -receptor, PDGF-B, and without upregulation of transcript levels of PDGF β -receptor targeting PTPs. This indicates that neointima reduction caused by antioxidants involved increased activity of PDGF β -receptor-antagonizing PTPs.

The findings of the present study thus provides experimental support for the two concepts that PTPs are endogenous antagonists of PDGF β -receptor signaling in VSMCs, and that this negative regulation of PDGF β -receptor signaling by PTPs is partially kept in check by inhibitory oxidation of receptor-antagonizing PTPs.

The strongest evidence for an involvement of PTPs in control of PDGF β -receptor signaling are derived from knockout studies, which have demonstrated enhanced PDGF β -receptor signaling in PTP1B and TC-PTP^{-/-} fibroblasts.^{14,18} In the case of TC-PTP depletion, a site-specific hyperphosphorylation of PDGF β -receptors was demonstrated, suggesting pathway-specific effects of individual PDGF β -receptor-targeting PTPs. In addition to these PTPs, SHP-1 and DEP-1 have also been implicated as negative regulators of PDGF β -receptor signaling.^{19,20} Although the

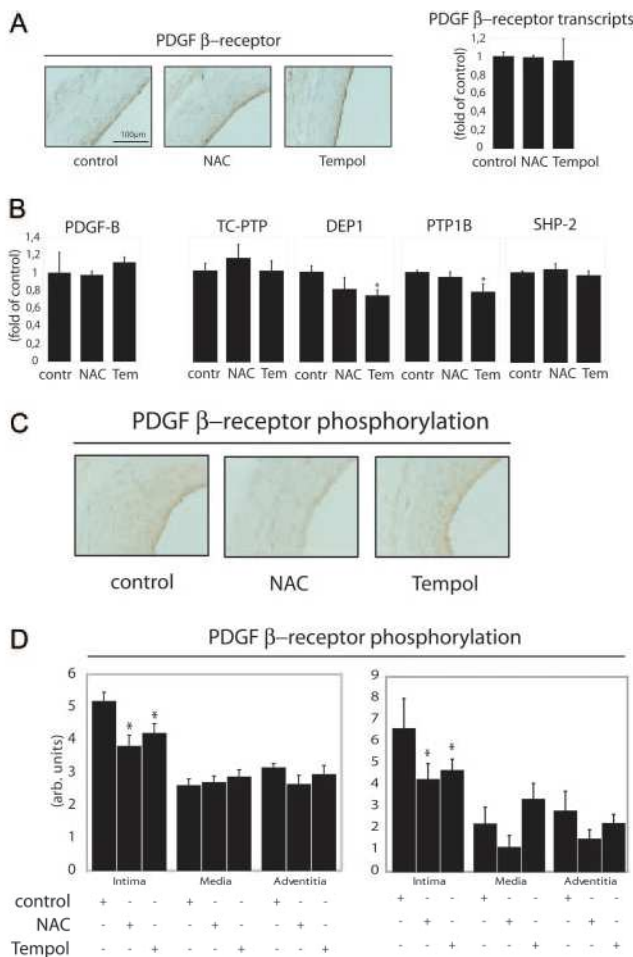


Figure 4. Antioxidants reduce PDGF β -receptor phosphorylation, but not expression, in vivo. **A**, Sections of paraffin-embedded vessels were subjected to PDGF β -receptor immunohistochemistry (left). Total vessel tissue was subjected to quantitative real-time PCR for analysis of the expression of the PDGF β -receptor (right). Expression was normalized to the expression of the house-keeping gene HPRT. **B**, Quantitative real-time PCR of the amount of PDGF-B transcripts and PTPs was carried out as described under **A**. contr indicates control; Tem, tempol. **C** and **D**, Paraffin-embedded vessels were subjected to phospho-PDGF β -receptor immunohistochemistry (PDGF β -receptor phosphorylation). Staining was quantified using two different approaches as detailed in Material and Methods ($P < 0.05$ vs control-treated animals).

pattern on PTP expression in VSMCs is incompletely characterized, it is noteworthy that expression of all four of these PTPs in VSMCs has been reported (reviewed in reference⁸). Furthermore, downregulation of DEP-1 with siRNA enhances ligand-induced PDGF receptor phosphorylation and Erk activation, thus implying this particular PTP as one of the relevant PTPs in VSMCs.^{20a} The notion of an antagonistic effect of PTPs on PDGF-dependent restenosis was recently also supported by demonstration of an increase in neointima formation following adenoviral transfer of a dominant-negative version of PTP-1B.²¹

Concerning the importance of oxidative inhibition of PTPs for PDGF β -receptor signaling, it was shown already in 1995 that H_2O_2 production was a critical aspect of PDGF β -receptor signaling, although PTPs were not identified as the

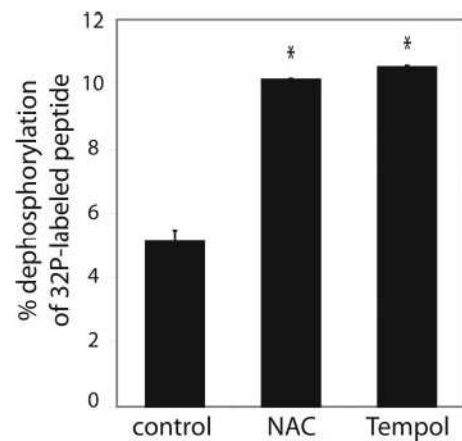


Figure 5. Antioxidants increase vessel PTP activity. Tissue extracts were isolated from sections of snap-frozen vessels, and extracts were analyzed for tyrosine phosphatase activity in an assay monitoring dephosphorylation of a ^{32}P -labeled phosphotyrosine peptide.

key targets at that time.¹⁷ More recently, demonstration of PTP oxidation on PDGF stimulation has been demonstrated in mouse and rat fibroblasts.^{10,22} These studies also demonstrated that PDGF β -receptor-induced PTP inhibition is PI3-kinase dependent and that PTP oxidation is restricted to PTPs in physical vicinity of PDGF β -receptors. The physiological significance of these events was recently supported by the demonstration that depletion of ROS-scavenging peroxiredoxin II enhances PDGF-receptor-induced proliferation, and concomitantly increases PDGF β -receptor phosphorylation and reduces PTP activity.²³

These findings, and the observations of the present study, suggest a series of topics for continued studies. Highly prioritized is the identification of PTPs, which are the most important targets for PDGF β -receptor-induced ROS production, and investigations of the effects of antioxidants on different PDGF-receptor responses. It is also predicted that future studies on the details of ROS production and scavenging in VSMCs will reveal important insights.

NAC and tempol are both antioxidants, but belong to different antioxidant subgroups. NAC is the N-acetyl derivative of the protein amino acid L-cysteine and reacts with ROS such as H_2O_2 .²⁴ NAC serves also as a major precursor to the antioxidant glutathione. It is thought that NAC, in its role as a precursor to L-cysteine and glutathione, protects cell membranes against lipid peroxidation and protein oxidation.²⁵ Tempol, in contrast, predominantly acts as a superoxide dismutase mimic and therefore acts upstream of H_2O_2 production.²⁶ These described mechanisms of action are in general agreement with the present study which showed that tempol failed to affect phosphorylation induced by exogenous H_2O_2 , but was almost equally potent as NAC in decreasing PDGF-induced responses.

Key findings of the present study are the novel demonstration that treatment with antioxidants reduces PDGF β -receptor phosphorylation and increases PTP activity in neointima lesions. These findings merit special highlighting. Firstly, they suggest in general terms PTP reactivation as a previously unrecognized mechanism underlying the benefi-

cial effect of antioxidants on neointima formation. Our study, focusing on PDGF receptors, are also compatible with inhibitory effects of antioxidants on other prorestenotic receptor tyrosine kinases, eg, the FGF receptor which recently was shown to be negatively regulated by PTP-1B.²¹ Secondly, it provides evidence that PTP oxidation is a physiologically relevant mechanism for control of PDGF β -receptor signaling in vivo, particularly in restenosis. This notion has earlier only received experimental support from the demonstration of enhanced PDGF-dependent restenosis on depletion of peroxiredoxin II.²³ Finally, and potentially most important, it suggests reactivation of oxidized PDGF β -receptor-targeting PTPs as a novel strategy for pharmacological interference with restenosis. Future studies will reveal whether this latter possibility will best be achieved through agents acting on oxidized PTPs, or with drugs modulating ROS levels.

Inhibitory effects of antioxidants or catalase on smooth muscle cell signaling and restenosis have been described earlier,^{26–30} and some suggestions on the underlying mechanism has been presented. These include demonstration of effects on apoptotic pathways as indicated by increased Bax expression and a reduced NF- κ B activity,^{26,29} as well as reduced c-src activation.³⁰ These changes could be secondary to reduced tyrosine kinase receptor activation. However, it is also possible that other mechanisms than PTP activation and concomitantly reduced tyrosine kinase activation contribute to antioxidant-mediated reduction in restenosis.

In summary, this study presents cell culture and in vivo experiments that demonstrate the possibility to interfere with PDGF β -receptor signaling in VSMCs by antioxidants that prevent PTP oxidation. It thereby suggests a novel molecular mechanism for the protective effect of antioxidants on neointima formation. In more general terms the study suggests activation of oxidized PTPs as a previously not recognized strategy for reducing vascular diseases associated with oxidative stress and/or dysregulated RTK-signaling. It is finally also predicted that future studies on the details of ROS production and scavenging in VSMCs will reveal yet unexplored options for novel treatments.

Sources of Funding

This study was supported by the "NRW-Sweden-Initiative" from the Ministry of Science and Research of the Federal Government of the State of North-Rhine-Westphalia, Germany, to K.K. A.Ö. receives funding from the Swedish Research Council, Swedish Cancer Society and Karolinska Institutet, Stockholm, Sweden. K.K. is supported by the Deutsche Forschungsgemeinschaft (KA 1820/1-1). S.R. receives funding from the Center of Molecular Medicine Cologne (CMMC), Germany.

Disclosures

None.

References

- Sorescu D, Szocs K, Griendling KK. NAD(P)H oxidases and their relevance to atherosclerosis. *Trends Cardiovasc Med*. 2001;11:124–131.
- Cai H. NAD(P)H oxidase-dependent self-propagation of hydrogen peroxide and vascular disease. *Circ Res*. 2005;96:818–822.
- Rhee SG, Kang SW, Jeong W, Chang TS, Yang KS, Woo HA. Intracellular messenger function of hydrogen peroxide and its regulation by peroxiredoxins. *Curr Opin Cell Biol*. 2005;17:183–189.
- Salmeen A, Barford D. Functions and mechanisms of redox regulation of cysteine-based phosphatases. *Antioxid Redox Signal*. 2005;7:560–577.
- Khatri JJ, Johnson C, Magid R, Lessner SM, Laude KM, Dikalov SI, Harrison DG, Sung HJ, Rong Y, Galis ZS. Vascular oxidant stress enhances progression and angiogenesis of experimental atheroma. *Circulation*. 2004;109:520–525.
- Raines EW. PDGF and cardiovascular disease. *Cytokine Growth Factor Rev*. 2004;15:237–254.
- Ostman A, Bohmer FD. Regulation of receptor tyrosine kinase signaling by protein tyrosine phosphatases. *Trends Cell Biol*. 2001;11:258–266.
- Kappert K, Peters KG, Bohmer FD, Ostman A. Tyrosine phosphatases in vessel wall signaling. *Cardiovasc Res*. 2005;65:587–598.
- Wright MB, Seifert RA, Bowen-Pope DF. Protein-tyrosine phosphatases in the vessel wall: differential expression after acute arterial injury. *Arterioscler Thromb Vasc Biol*. 2000;20:1189–1198.
- Meng TC, Fukada T, Tonks NK. Reversible oxidation and inactivation of protein tyrosine phosphatases in vivo. *Mol Cell*. 2002;9:387–399.
- Leppanen O, Janjic N, Carlsson A, Pietras K, Levin M, Vargeese C, Green LS, Bergqvist D, Ostman A, Heldin CH. Intimal hyperplasia recurs after removal of PDGF-AB and -BB inhibition in the rat carotid artery injury model. *Arterioscler Thromb Vasc Biol*. 2000;20:e89–e95.
- Furuhashi M, Sjoblom T, Abramsson A, Ellingsen J, Micke P, Li H, Bergsten-Folestad E, Eriksson U, Heuchel R, Betsholtz C, Heldin CH, Ostman A. Platelet-derived growth factor production by B16 melanoma cells leads to increased pericyte abundance in tumors and an associated increase in tumor growth rate. *Cancer Res*. 2004;64:2725–2733.
- Kappert K, Blaschke F, Meehan WP, Kawano H, Grill M, Fleck E, Hsueh WA, Law RE, Graf K. Integrins α v β 3 and α v β 5 mediate VSMC migration and are elevated during neointima formation in the rat aorta. *Basic Res Cardiol*. 2001;96:42–49.
- Persson C, Savenhed C, Bourdeau A, Tremblay ML, Markova B, Bohmer FD, Haj FG, Neel BG, Elson A, Heldin CH, Ronnstrand L, Ostman A, Hellberg C. Site-selective regulation of platelet-derived growth factor beta receptor tyrosine phosphorylation by T-cell protein tyrosine phosphatase. *Mol Cell Biol*. 2004;24:2190–2201.
- Sorby M, Sandstrom J, Ostman A. An extracellular ligand increases the specific activity of the receptor-like protein tyrosine phosphatase DEP-1. *Oncogene*. 2001;20:5219–5224.
- Szocs K, Lassegue B, Sorescu D, Hilenski LL, Valppu L, Couse TL, Wilcox JN, Quinn MT, Lambeth JD, Griendling KK. Upregulation of Nox-based NAD(P)H oxidases in restenosis after carotid injury. *Arterioscler Thromb Vasc Biol*. 2002;22:21–27.
- Sundaresan M, Yu ZX, Ferrans VJ, Irani K, Finkel T. Requirement for generation of H₂O₂ for platelet-derived growth factor signal transduction. *Science*. 1995;270:296–299.
- Haj FG, Markova B, Klamann LD, Bohmer FD, Neel BG. Regulation of receptor tyrosine kinase signaling by protein tyrosine phosphatase-1B. *J Biol Chem*. 2003;278:739–744.
- Kovalenko M, Denner K, Sandstrom J, Persson C, Gross S, Jandt E, Vilella R, Bohmer F, Ostman A. Site-selective dephosphorylation of the platelet-derived growth factor beta-receptor by the receptor-like protein-tyrosine phosphatase DEP-1. *J Biol Chem*. 2000;275:16219–16226.
- Yu Z, Su L, Hoglinger O, Jaramillo ML, Banville D, Shen SH. SHP-1 associates with both platelet-derived growth factor receptor and the p85 subunit of phosphatidylinositol 3-kinase. *J Biol Chem*. 1998;273:3687–3694.
- Kappert K, Paulsson J, Sparwell J, Leppanen O, Hellberg C, Ostman A, Micke P. Dynamic changes in the expression of DEP-1 and other PDGF receptor-antagonizing PTPs during and on termination of neointima formation. *FASEB J*. In press.
- Chang Y, Ceacareanu B, Zhuang D, Zhang C, Pu Q, Ceacareanu AC, Hassid A. Counter-regulatory function of protein tyrosine phosphatase 1B in platelet-derived growth factor- or fibroblast growth factor-induced motility and proliferation of cultured smooth muscle cells and in neointima formation. *Arterioscler Thromb Vasc Biol*. 2006;26:501–507.
- Persson C, Sjoblom T, Groen A, Kappert K, Engstrom U, Hellman U, Heldin CH, den Hertog J, Ostman A. Preferential oxidation of the second phosphatase domain of receptor-like PTP-alpha revealed by an antibody against oxidized protein tyrosine phosphatases. *Proc Natl Acad Sci U S A*. 2004;101:1886–1891.
- Choi MH, Lee IK, Kim GW, Kim BU, Han YH, Yu DY, Park HS, Kim KY, Lee JS, Choi C, Bae YS, Lee BI, Rhee SG, Kang SW. Regulation of PDGF signalling and vascular remodelling by peroxiredoxin II. *Nature*. 2005;435:347–353.

24. Aruoma OI, Halliwell B, Hoey BM, Butler J. The antioxidant action of N-acetylcysteine: its reaction with hydrogen peroxide, hydroxyl radical, superoxide, and hypochlorous acid. *Free Radic Biol Med*. 1989;6: 593–597.
25. Marthaler MT, Keresztes PA. Evidence-based practice for the use of N-acetylcysteine. *Dimens Crit Care Nurs*. 2004;23:270–273.
26. Jagadeesha DK, Lindley TE, Deleon J, Sharma RV, Miller F, Bhalla RC. Tempol therapy attenuates medial smooth muscle cell apoptosis and neointima formation after balloon catheter injury in carotid artery of diabetic rats. *Am J Physiol Heart Circ Physiol*. 2005;289:H1047–H1053.
27. Miyauchi K, Aikawa M, Tani T, Nakahara K, Kawai S, Nagai R, Okada R, Yamaguchi H. Effect of probucol on smooth muscle cell proliferation and dedifferentiation after vascular injury in rabbits: possible role of PDGF. *Cardiovasc Drugs Ther*. 1998;12:251–260.
28. Ghigliotti G, Mereto E, Eisenberg PR, Martelli A, Orsi P, Sini D, Spallarossa P, Olivotti L, Brunelli C. N-acetyl-cysteine reduces neointimal thickening and procoagulant activity after balloon-induced injury in abdominal aortae of New Zealand white rabbits. *Thromb Haemost*. 2001; 85:724–729.
29. Hayashi K, Takahata H, Kitagawa N, Kitange G, Kaminogo M, Shibata S. N-acetylcysteine inhibited nuclear factor-kappaB expression and the intimal hyperplasia in rat carotid arterial injury. *Neurol Res*. 2001;23: 731–738.
30. Sato H, Sato M, Kanai H, Uchiyama T, Iso T, Ohyama Y, Sakamoto H, Tamura J, Nagai R, Kurabayashi M. Mitochondrial reactive oxygen species and c-Src play a critical role in hypoxic response in vascular smooth muscle cells. *Cardiovasc Res*. 2005;67:714–722.



Morphometric analysis of murine skin wound healing: Standardization of experimental procedures and impact of an advanced multitissue array technique

Michael Gerharz, MD¹; Anke Baranowsky, PhD²; Udo Siebolts, MD¹; Sabine Eming, MD²; Roswitha Nischt, PhD²; Thomas Krieg, PhD²; Claudia Wickenhauser, MD¹

1. Institute of Pathology and

2. Department of Dermatology, University of Cologne, Cologne, Germany

Reprint requests:

Claudia Wickenhauser, MD, Institute for Pathology, University of Cologne, Kerperner Strasse 62 50924 Cologne, Germany.
Tel: +49 221 478 6368;
Fax: +49 221 478 6360;
Email: C.Wickenhauser@uni-koeln.de

Manuscript received: February 4, 2006

Accepted in final form: October 20, 2006

DOI:10.1111/j.1524-475X.2006.00191.x

ABSTRACT

Morphometric data based on skin wounding offer important information for the characterization of the phenotype of transgenic mouse models. The goal of this study was the comparison of technical procedures concerning wounding, processing, and evaluation of samples in different mouse strains. The multitissue array technique was used to estimate its adaptability for standardized analysis in wound healing. Skin wounds between days 1 and 14 after wounding were analyzed. The influence of mouse strain (C57Bl/6 vs. FVB/N mice), sex, size of the punch biopsies, and preparation of the tissue sections was investigated on 94 mice. The parameters distance between the migration tongues (δ MT) and surface not covered by epithelium were evaluated to describe the reepithelialization, and the distance between the adnexa was chosen to measure wound contraction. In addition, the techniques to measure the area of granulation tissue (GT) were evaluated. The data illustrate the requirement of standardized conditions for skin wound-healing experiments and demonstrate that histological preparation in serial sections is mandatory to detect slight differences in wound contraction. For the analysis of cellular composition in GT, multitissue arrays are useful tools in wound-healing studies.

Tissue repair processes following wounding depend on several factors including the age of the individual, metabolic diseases, vascular factors, e.g., micro-/macro-angiopathia and diseases of the venous system as well as exogenic factors like local and systemic medical treatment. Chronic nonhealing wounds of the skin are poorly accessible to effective therapy management. Therefore, improvements in the understanding of the wound-healing process and effective treatment will directly enhance not only the life quality of the patients but will also decrease costs of the health care system.

To evaluate the impact and dynamics of the diverse factors involved in wound healing, animal models are helpful devices. One of the advantages of animal models is that wounding can be performed in a standardized manner. In addition, the wound-healing process is accelerated in mice and rats, which enables to study the course within days and not over weeks as required in humans.¹ Also, generation and analysis of knockout and transgenic mice are useful tools to estimate the influence of single factors in wound healing.² Comparing different studies, the location, and size of the wound as well as strain, sex, age range, and choice of anesthetic agents were identified as important factors.³ The literature review, however, revealed that considerable methodological variations especially concerning wound depth and dimensions as well as wound location have been described by different groups.³

The aim of this study was to investigate which techniques are required to describe different phases of murine wound healing and whether standardization of wound

healing experiments is pivotal. According to our data, the choice of mouse strains and technical procedures including assortment of round knives and orientation of the wounds indeed has a significant impact on data describing reepithelialization and contraction. Moreover, multitissue array technology⁴ can be a useful tool in wound-healing analysis.

METHODS

Animals

Eighty adult C57Bl/6 mice (45 females, 35 males) and 14 adult FVB/N mice (all female) were analyzed (age 8–12 weeks). In the C57Bl/6 group, 70 mice received 4 mm punch biopsies and 10 mice 6 mm punch biopsies. All FVB/N mice under study received 6 mm punch biopsies (see also Table 1).

Wounding

Wound samples were harvested from different groups engaged in wound healing over a period of 4 years. In all experiments, mice were anesthetized by an intraperitoneal injection of a ketamine (10 g/L)/xylazine (8 g/L) solution (10 μ L/g body weight). After shaving the dorsal hair and cleaning of the exposed skin, four full-thickness (including the *Panniculus carnosus*) excisional wounds were punched at two sites in the middle of the dorsum using sterile 4 and 6 mm biopsy needles. Wounds were left uncovered. All

Table 1. Number of wounds descending from C57Bl/6 or FVB/N mice, respectively

	Male	Female	4 mm	6 mm	Method 1	Method 2	Caudocranial	Mediolateral
C57Bl/6 total	35	45	70	10	20	60	60	20
C57Bl/6	0	10	0	10	0	10	10	0
C57Bl/6	0	20	20	0	20	0	20	0
C57Bl/6	35	0	35	0	0	35	20	15
C57Bl/6	0	15	15	0	0	15	10	5
FVB/N	0	14	0	14	0	14	14	0

Mice sex and size of the punch biopsies, preparation in serial sections (method 1), and bisectioning of the wounds (method 2) and direction of sectioning (caudocranial vs. mediolateral) are considered.

animal experimentation was performed in accordance with institutional guidelines.

Harvesting and preparation of wound samples

At indicated time points (days 1, 3, 5, 7, 10, 14), wounds and the underlying muscle with the adjacent 3–4 mm unwounded skin were harvested by excising an area of 9–12 mm diameter. A deep excision including the underlying muscle assured the complete withdrawal of the granulation tissue.

As illustrated in Table 1, 20 wounds with 4 mm diameter (female C57Bl/6 mice) were embedded in paraffin and then cut in 3 µm serial sections from the surrounding wound margin skin across the center of the wound toward the opposite surrounding wound margin skin in the caudocranial

direction (method 1, see also Figure 1A and C). The slide presenting the largest wound diameter was defined as the wound center. As a second practice approach, 50 wound samples of 4 mm diameter (all C57Bl/6) and 24 wound samples of 6 mm diameter (10 C57Bl/6 and 14 FVB/N) from days 1 to 7 were cut perpendicular to the skin surface by macroscopic estimation of the wound center (method 2, see also Figure 1D). The first complete section prepared from the estimated wound center was analyzed. Seventy-five wounds were cut in the caudocranial direction (Figure 1A), and 21 wounds in the mediolateral direction (all C57Bl/6, see also Figure 1B). Thirty-five male mice (all C57Bl/6) and 59 female mice (45 C57Bl/6 and 14 FVB/N mice) were studied. Seventy wounds of 4 mm diameter (all C57Bl/6) and 24 wound samples with 6 mm diameter (10 C57Bl/6 and 14 FVB/N) were analyzed. All sections were stained with hematoxylin and eosin (H&E) and evaluated with an Aristoplan microscope (Leitz Wetzlar, Germany).

Morphometry

Healing of skin wounds was analyzed by measuring the following parameters (1) distance between the migration tongues (δ MT) in micrometer, (2) the surface not covered by epithelium (SE) in micrometer (SE), (3) the distance between the surrounding wound margin skin (adnexa, δ A), in micrometer and (4) area of GT in square micrometer. Morphometry was performed applying the DISKUS software (Hilgers, Koenigswinter, Germany), a semiautomatic operator-dependent imaging system. Two morphologically experienced coworkers independently defined the measuring points (see also Figure 2A–D). The DISKUS software allows a specific calibration for each lens and directly calculates the distance or the area in the chosen unit.

Multitissue array and immunostaining

Instead of incubating and analyzing samples one slide at a time, multitissue array technology allows concomitant examination of multiple samples of one and the same slide. All histochemical and molecular detection techniques used with regular sections can also be used with this technology. Paraffin-embedded 6 mm murine wounds from different time points were used as donor tissue blocks for setting up a multitissue array. For this purpose, first the H&E-stained slices were screened and the relevant area was marked. Thereafter, 2 mm diameter pillars were punched out of the marked areas of the donor block and transferred

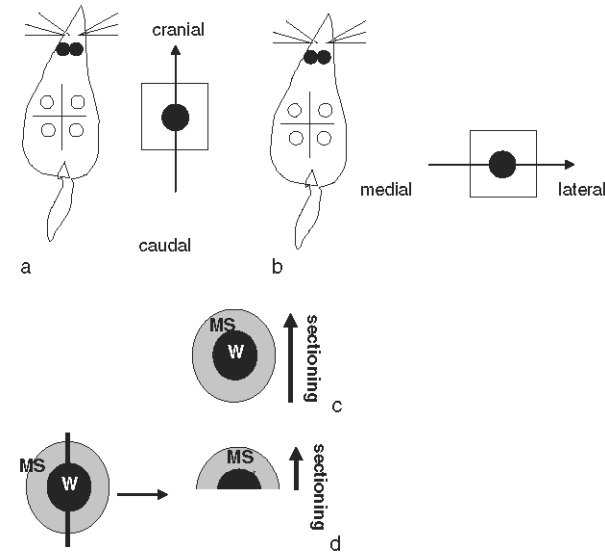


Figure 1. (A–D) Schematic illustration of the standardized processing of wound samples: wound tissues were either orientated in the caudocranial (A) or in the mediolateral direction (B). After paraffin embedding, samples of murine wounds (W) and the surrounding wound margin skin (MS) were either completely sectioned from the surrounding margin skin through the center to the opposite margin (C) or wound samples were cut into two halves (D) and sectioned from the center toward the wound margin.

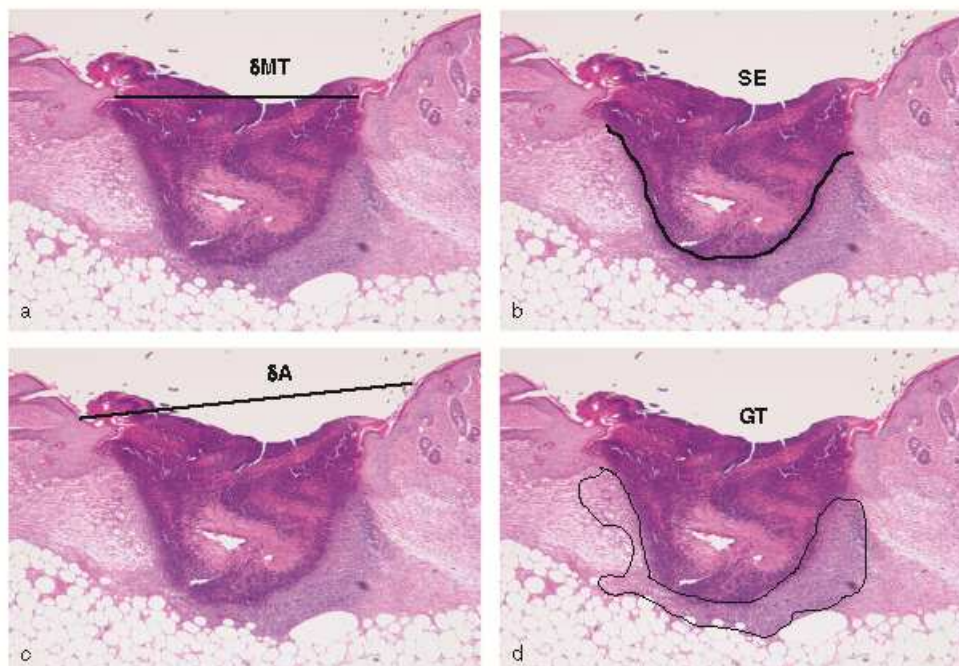


Figure 2. (A–D) Assessment of reepithelization and granulation tissue (GT) formation: skin wounds 5 days after wounding with a 4 mm punch needle (female C57Bl/6). Morphometrical analysis included the distance between the epithelial migration tongues (δ MT) (A), surface not covered by epithelium (SE) (B), determination of the distance between the hair follicles δ A (C), and the area of GT (D) (hematoxylin and eosin [H&E] staining, $\times 25$).

into the “master” (acceptor) block using the manual tissue arrayer from Beecher instruments (Sun Prairie, WI). The created “master” block was first trimmed until every pillar appeared on the surface. The samples captured by an adhesive tape were then sectioned and placed, section side down, onto an adhesive-coated slide (Instrumedics, Hackensack, NJ). The created slide was placed under an ultra-violet lamp for 30–60 seconds to polymerize the slide adhesive. After that, the slide was dipped into a solvent bath (tpc solvent, Instrumedics) and the adhesive tape was pulled away from the slide now ready for deparaffinization and staining. The generated tissue microarray contained murine dermal wound-healing samples from 4 FVB/N mice at days 1, 3, 5, 7, 10, and 14. Four samples per time point were chosen, and two samples of unwounded skin served as controls. Slides from the “master” block were stained with H&E. In addition, enzymatic staining with naphthol-AS-D-chloroacetate esterase was performed on the donor block sections as described before.⁵ For immunostaining, sections of the paraffin-embedded tissues (3 μ m thick) were cut and deparaffinized according to standard histological techniques. After pretreatment with citrate buffer (pH 6.0) and pressure cooking (121 $^{\circ}$ C, 5 minutes), endogenous peroxidase activity was blocked by 0.03% hydrogen peroxide-containing sodium acid (5 minutes). Sections were incubated with the proliferation marker TEC-3 (rat anti-mouse, DAKO, Hamburg, Germany) at 4 $^{\circ}$ C overnight. The secondary antibody (polyclonal rabbit anti-rat; DAKO, biotin labeled) was incubated for 30 minutes, followed by streptavidin-conjugated horseradish peroxidase (30 minutes) and AEC (DAKO) as chromogen (10 minutes). After rinsing in aqua dest, the nuclei were counterstained with hematoxylin, and the tissues were embedded in glycerol jelly.

Statistical analysis

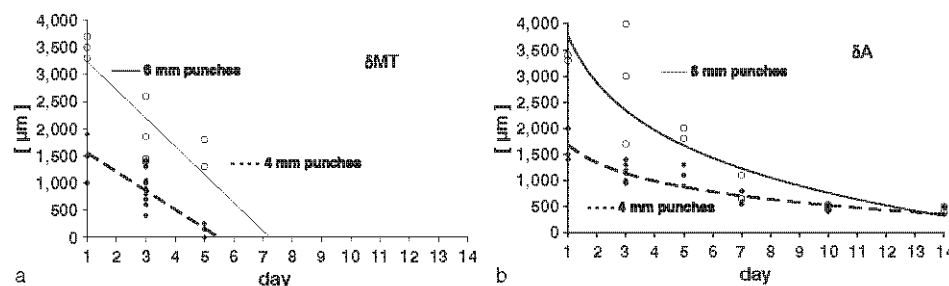
The following variables were included in the statistical analysis: size of the biopsies, preparation procedures of the wound tissue, mouse strains, and mouse sex. In univariate analysis, the influence of the different variables on wound-healing data was evaluated by the Student's *t* test. All calculations were performed using the SPSS statistical software package (SPSS for Windows release 10.0.7 de, SPSS Inc., Chicago, IL).

RESULTS

Influence of methodological procedures on reepithelization and wound contraction

Diameter of punch biopsies

Controversial data exist about the ideal size of the punch biopsies in skin wounding. We therefore compared reepithelization and wound contraction of female C57Bl/6 mice following 4 and 6 mm biopsies. Data were evaluated at day 1, 3, 5, 7, 10, and 14. Reepithelization was assessed by the distance between epidermal δ MT and the surface not covered by the SE as well. For each experiment, both parameters produced identical results so that only δ MT values are presented. One day after wounding, the standard deviation of both parameters was lower in the 6 mm group. Reepithelization proceeded faster in the larger wounds visible in the inclination of the straight lines ($p < 0.05$; see Figure 3A). Also, wound contraction was accelerated in the larger wounds ($p < 0.05$; see logarithmic curves in Figure 3B). After day 7, data converged in both groups.



distance between the hair follicles (δA). Reepithelization (visible in the inclination of the straight lines, a) and wound contraction (logarithmic curve, b) develops faster in the larger wounds ($p < 0.05$). Single values (circles for the 6 mm wounds, rhombi for the 4 mm wounds) are indicated.

Direction of the wound tissue sections

To evaluate the influence of the chosen direction of the sections, 11 female C57Bl/6 mice were examined on day 5 after wounding with 4 mm biopsies. Six wounds were cut in the caudocranial direction, and five wounds in the mediolateral direction (see also Figure 1A and B). As presented in Figure 4, parameters describing reepithelization (δMT) and wound contraction (δA) of the wounds were significantly different at that time point and the values after cutting in mediolateral direction surpassed the values after cutting in the caudocranial direction by far ($p < 0.01$).

Preparation of the wound tissue sections

Four millimeter wounds of 20 female C57Bl/6 mice between days 1 and 7 were cut into $3\mu m$ sections from the surrounding wound margin skin across the center of the wound toward the opposite surrounding wound margin skin in the caudocranial direction (method 1, see also Figure 1C). By comparing the slides, the wound center was ascertained by determining the largest wound diameter. These data were compared with the values obtained from 15 wounds (female C57Bl/6 mice) cleaved perpendicular to the skin surface by macroscopic estimation of the wound center (Figure 1D; method 2). Beyond day 7, the small scars were difficult to bisect and further preparation in serial sections was mandatory. As shown in Figure 5B wound

contraction data were significantly lower following method 2 ($p < 0.05$). Reepithelization data also were reduced following method 2 but due to high standard deviations the differences were not significant (Figure 5A).

Influence of selection of mice strains and sex

Sex of the mice

The influence of the sex on skin wound healing was evaluated in 28 C57Bl/6 mice (12 females, 16 males) at day 3 after wounding with 4 mm punches. At that time point, wound contraction was minimally more advanced in the female group. Concerning reepithelization, no differences could be seen between both groups, and high standard deviations were obvious (Figure 6).

Mice strains

To evaluate the influence of the genetic background in murine skin wound healing 10 female C57Bl/6 and 14 female FVB/N mice were analyzed after wounding with 6 mm punch biopsies. Data were evaluated on days 1, 3, 5, 7, 10, and 14. Concerning dynamics in reepithelization, skin wounds in FVB/N mice closed faster than wounds of the C57Bl/6 group ($p < 0.05$). These differences were the most significant between days 3 and 5. In both groups, reepithelization was complete at day 7 (Figure 7A). Concerning the wound contraction, however, the process was

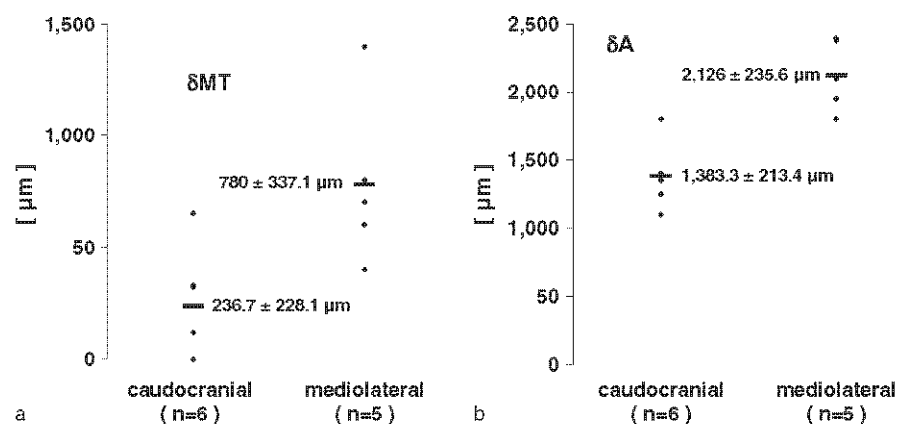
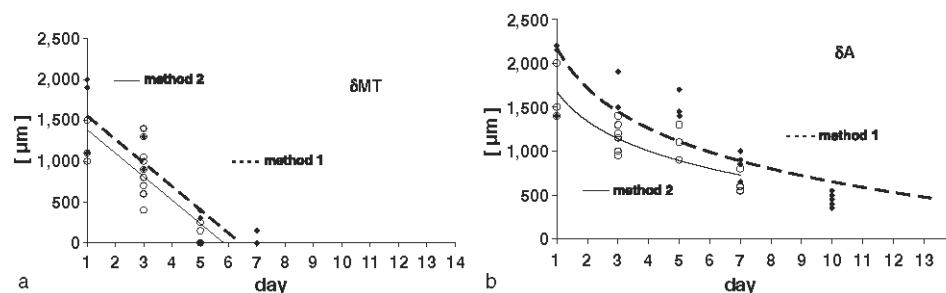


Figure 4. Reepithelization (A) and wound contraction data (B) assessed by morphometric analysis of 4 mm diameter murine wounds cut in the caudocranial or mediolateral direction (11 female C57Bl/6 mice). Day 5 after wounding. Dot plots with horizontal bars indicating mean value. Significant differences between both groups ($p < 0.01$).



indicated. Reepithelization data are demonstrated in linear presentation, and contraction data in logarithmic curves. Contraction data for bisected wounds are significantly lower than those for wounds prepared with method 1 ($p < 0.05$).

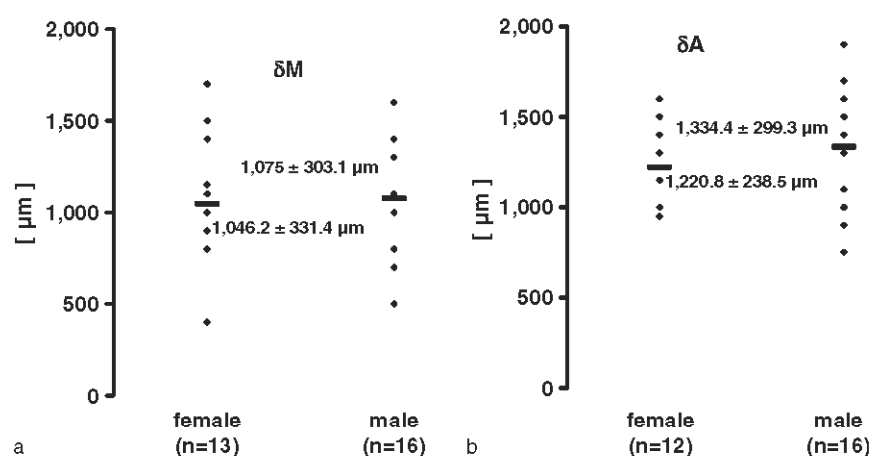


Figure 6. Reepithelization (A) and wound contraction data (B) assessed by morphometric analysis of 12 female and 16 male 4 mm diameter murine wounds (C57Bl/6). Day 3 after wounding. Dot plots with horizontal bars indicating mean value. No significant differences are seen between both groups.

more effective in the C57Bl/6 group ($p < 0.05$). The differences between both groups were most obvious between days 5 and 10. At day 14, in both groups, the wound contraction was concluded (see also Figure 7B).

method 1 (10 samples) and method 2 (10 samples). In all cases, GT formation was initiated at day 3 after wounding and peaked between days 5 and 7. Concerning the area of GT, standard deviation between single experiments was low. Data from all experiments are summarized in Figure 8.

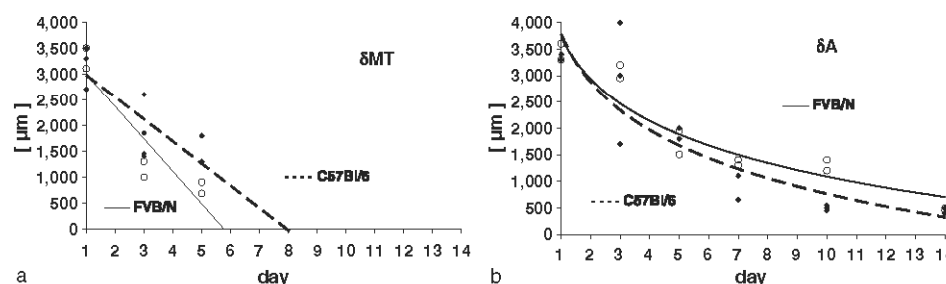
Influence of methodological procedures on GT analysis

Evaluation of morphometric data

GT formation was assessed in 20 female C57Bl/6 mice, among them 15 wounds after 4 mm punches and five wounds after 6 mm punches. Wounds were cut following

Significance of multitissue array technology

Multitissue array technology was used to estimate the value of this method for the analysis of the cellular composition of granulation tissue. As shown in Figure 9, 2 mm punched pillars taken from the donor block comprised all



ithelization data are demonstrated in linear presentation, and contraction data in logarithmic curves. Reepithelization of skin wounds in FVB/N mice proceeds faster than in wounds of the C57Bl/6 group ($p < 0.05$). These differences are most obvious between day 3 and day 5. In both groups, reepithelization is complete at day 7. Conversely, the wound contraction process is more effective in the C57Bl/6 group ($p < 0.05$). The differences between both groups are most obvious between days 5 and 10. At day 14 in both groups the wound contraction is concluded.

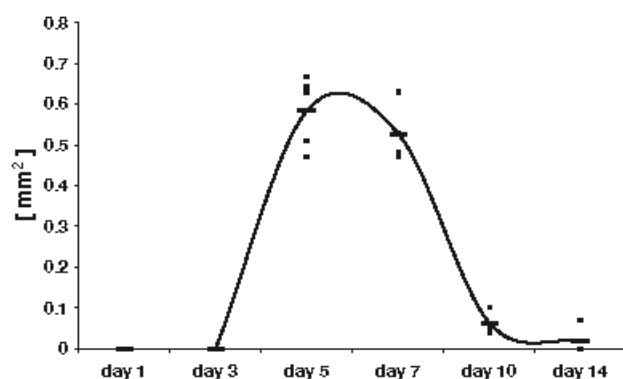


Figure 8. Granulation tissue (GT) formation assessed by morphometric analysis of 4 and 6 mm diameter murine wounds. Summarized data from 20 female C57Bl/6 mice (among them 15 wounds after 4 mm punches and five wounds after 6 mm punches, wound processing following method 1 (10 samples) and method 2 (10 samples)) are presented. Analysis of days 1 to 14 after wounding. Dot plots with maximal values for GT area between days 5 and 7 can be seen.

relevant areas of the wounds including wound margin skin, migration tongue, GT, and subcutaneous fat tissue (Figure 9A). When comparing the original slides with the slides obtained from the multitissue, block quality of histomorphology appeared to be equivalent (see also Figure 9B). As shown in Figure 9C and D, both enzymatic and immunohistochemical staining procedures could be applied to the tissue array.

DISCUSSION

This morphometric study was performed to provide systematic data on the assessment of skin wound healing.

Here, we analyzed the dynamics of wound closure, wound contraction and area of GT formation following standardized wounding, embedding, and tissue preparation in a murine full-thickness wound-healing model. To describe wound closure, the parameters distance between epidermal δ MT and surface not covered by SE were chosen. As these two parameters correlated well, we suggest that the distance between the δ MT is sufficient for the description of reepithelization. Several techniques were compared with standardize wounding and subsequent processing of wound samples in two different inbred mouse strains. To our surprise, the sex of mice had no significant impact on wound healing at day 3 according to our data. Others, however, described a significant influence of estrogen in murine wound healing.⁶ In this context it is important to mention that this group performed incision biopsies that might account for the differences observed in our studies. Besides the sex of the mice, all other parameters had a significant influence on wound-healing data. Thus, in our setting the selection of the mouse strain substantially affects reepithelization and wound contraction data, a phenomenon also described by others.⁷ In this context, the discordance between reepithelization and wound contraction was most striking, indicating that these parameters are not causally related. The data clearly underline the necessity to control a homogeneous genetic background in full-thickness wound models in mice.

In a parallel set of experiments, the impact of preparation procedures on the wound tissue was evaluated. Bisectioning of the wounds in the mediolateral direction led to highly elevated reepithelization and wound contraction data compared with samples that were cut in the caudo cranial direction as measured by morphometry. These discrepancies are presumably due to differences in local tension and traction that may result from anatomic features. Also, the influence of wound size was evaluated. Here, using 4 mm punch biopsies and C57Bl/6 mice compared with

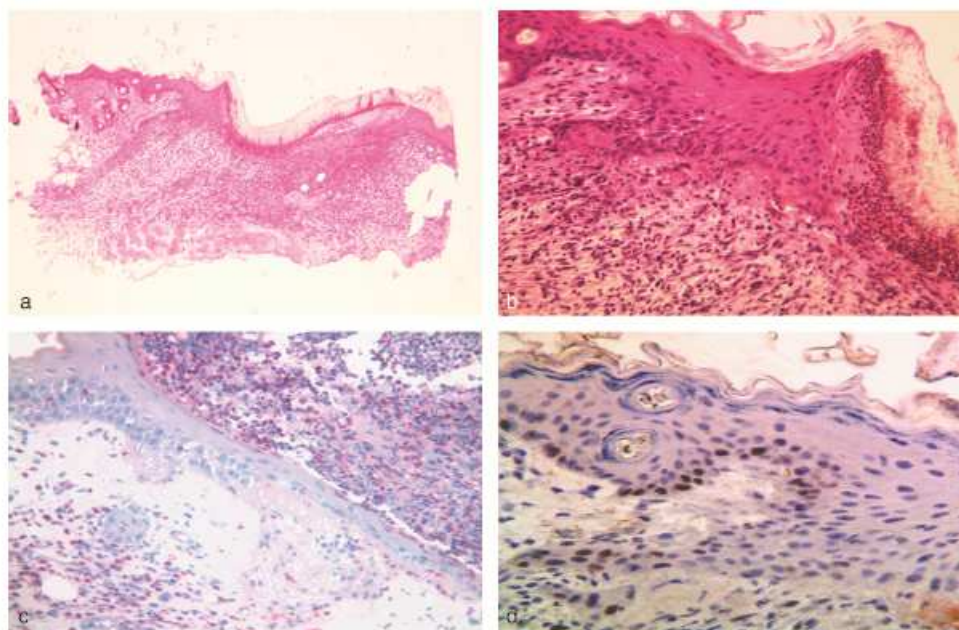


Figure 9. Representative pictures of a multitissue array: sections taken of one 2 mm diameter pillar from the donor block containing a total of 26 pillars (including two controls). (A) Skin wound 5 days after biopsy. All characteristic parts of the wound are visible (hematoxylin and eosin [H&E], $\times 25$). (B) Excellent cytomorphology of the tissue can be seen (H&E $\times 200$). (C) Naphthol-AS-D-chloroacetate esterase reaction with strongly marked neutrophil granules at the wound edge ($\times 400$). (D) Immunohistochemical staining for estimation of proliferative activity. Proliferating cells are concentrated at the basal layer of the epidermis (TEC-3 $\times 400$).

6 mm biopsies, we found considerable variability at day 1 after wounding with regard to wound closure, even if wounds were sectioned extensively in 3 μ m plates. These interindividual variations may indicate that 4 mm punch biopsies are difficult to standardize or wounds are too small to detect differences reliably. By contrast, using 6 mm biopsies, wound reepithelization, and contraction in the early phases of wound healing was more reliable. At later time points, we found that not only wound reepithelization but also wound contraction proceeded with more dynamics in the larger wounds after 6 mm punch biopsies. The choice of 6 mm biopsies therefore offers advantages in studies on wound healing between days 1 and 7. Biologically, the more effective wound contraction in larger wounds may be due to a still incomplete barrier of the newly reepithelized epidermis. In fact, protein and lipid synthesis and moisture of the environment influence the process, eventually leading to the normalization of the barrier function.^{8–10} In addition, it is possible that a larger full-thickness wound results in an enhanced recruitment of neutrophils and macrophages, which, by the release of growth factors such as TGF- β 1, substantially control the wound contraction process.¹¹ When morphometric analysis after wound tissue bisectioning was compared with wounds prepared in serial sections, we found that wound contraction data were significantly lower in the first group ($p < 0.05$). Concerning the reepithelization, the data presented the same tendency but were not significantly different due to high standard deviations. Therefore, a larger amount of samples is required to analyze this parameter.

Wound closure depends on several endogenous and exogenous factors including local infections or scratching effects, which are directly influence procedures pivotal in the early phase of wound healing response patterns such as the coagulation system,^{12–15} chemokines,^{16,17} and the moisture of the environment.¹⁸ Taking these disturbing factors into account and considering that wound healing in genetically manipulated mice often reveal only minor differences, it becomes obvious that besides a large amount of samples a laborious preparation in multiple 3 μ m sections is required—especially if early phases in wound contraction are of particular interest. Where reepithelization data are the subject of interest, the bisection of wounds might be justified. The macroscopic analysis of 2D photographs applied by others (10), however, represents a rather rough estimation to describe the parameters of wound healing in particular if only minor differences are expected.

As a morphometric parameter describing the activation of the system during the course of wound healing, we chose the area of granulation tissue.^{19–23} When the bisection method of 4 and 6 mm wounds and the preparation in serial slides were compared, GT formation was initiated at day 3 and peaked between days 5 and 7 with only moderate variation, which we found to be independent of the experimental design. Therefore, morphometric analysis of GT formation does not require labor-intensive serial sections. The quality of the cellular composition of the GT might offer more precise information on specific wound-healing dynamics than with mere morphometry. Therefore, we evaluated the significance of multitissue array technology in describing GT formation. For high throughput analysis of paraffin-embedded tissue, multitissue arrays have been

shown to be a simple and effective tool mainly for immunophenotyping of large numbers of tumor samples.⁴ Here, for the first time, a tissue microarray of murine wounds containing the entire migration tongue, the adjacent healthy wound margin skin, and GT was established. Plates obtained from the master block contained 24 wound samples and could be stained with enzymatic and immunohistochemical methods. We found an excellent preservation of histological and cytomorphological structures in many independent wound samples on one and the same slide. Also, we showed that immunohistochemical staining with distinct antibodies revealed clear results in this multitissue array approach. These data may help to reduce the variability of wounds normally individually cut and processed. Therefore, this technique appears to be highly suitable for evaluating the dynamics of GT formation and tissue repair.

ACKNOWLEDGMENT

This work was supported by a grant from the Deutsche Forschungsgemeinschaft through the SFB 589 at the University of Cologne.

REFERENCES

1. Cross SE, Naylor IL, Coleman RA, Teo TC. An experimental model to investigate the dynamics of wound contraction. *Br J Plast Surg* 1995; 48: 189–97.
2. Bedell MA, Largaespada DA, Jenkins NA, Copeland NG. Mouse models of human disease. Part II: recent progress and future directions. *Genes Dev* 1997; 11: 11–43.
3. Dorsett-Martin WA. Rat models of skin wound healing: a review. *Wound Repair Regen* 2004; 12: 591–9.
4. Bubendorf L, Kononen J, Koivisto P, Schraml P, Moch H, Gasser TC, Willi N, Mihatsch MJ, Sauter G, Kallioniemi OP. Survey of gene amplifications during prostate cancer progression by high-throughput fluorescence in situ hybridization on tissue microarrays. *Cancer Res* 1999; 59: 803–6.
5. Schaefer HE, Fischer R. [On the demonstration of tissue mast cells by means of naphthol-AS-D- chloroacetate esterase reaction in histiocytoma of the skin]. *Zentralbl Allg Pathol* 1966; 109: 397–401.
6. Ashcroft GS, Dodsworth J, van Boxtel E, Tarnuzzer RW, Horan MA, Schultz GS, Ferguson MW. Estrogen accelerates cutaneous wound healing associated with an increase in TGF- β 1 levels. *Nat Med* 1997; 3: 1209–15.
7. Colwell AS, Krummel TM, Kong W, Longaker MT, Lorenz HP. Skin wounds in the MRL/MPJ mouse heal with scar. *Wound Repair Regen* 2006; 14: 81–90.
8. Elias PM. Epidermal lipids, barrier function, and desquamation. *J Invest Dermatol* 1983; 80 (Suppl.): 44s–9s.
9. Ekanayake-Mudiyanselage S, Aschauer H, Schmook FP, Jensen JM, Meingassner JG, Proksch E. Expression of epidermal keratins and the cornified envelope protein involucrin is influenced by permeability barrier disruption. *J Invest Dermatol* 1998; 111: 517–23.
10. Schunck M, Neumann C, Proksch E. Artificial barrier repair in wounds by semi-occlusive foils reduced wound contraction

- and enhanced cell migration and reepithelialisation in mouse skin. *J Invest Dermatol* 2005; 125: 1063–71.
11. Peters T, Sindrilaru A, Hinz B, Hinrichs R, Menke A, Al-Azzeh EA, Holzwarth K, Oreshkova T, Wang H, Kess D, Walzog B, Sulyok S, Sunderkotter C, Friedrich W, Wlaschek M, Krieg T, Scharffetter-Kochanek K. Wound-healing defect of CD18(–/–) mice due to a decrease in TGF-beta1 and myofibroblast differentiation. *EMBO J* 2005; 24: 3400–10.
 12. Mahoney E, Reichner J, Bostom LR, Mastrofrancesco B, Henry W, Albina J. Bacterial colonization and the expression of inducible nitric oxide synthase in murine wounds. *Am J Pathol* 2002; 161: 2143–52.
 13. Matsuka YV, Pillai S, Gubba S, Musser JM, Olmsted SB. Fibrinogen cleavage by the *Streptococcus pyogenes* extracellular cysteine protease and generation of antibodies that inhibit enzyme proteolytic activity. *Infect Immun* 1999; 67: 4326–33.
 14. Musser JM, Stockbauer K, Kapur V, Rudgers GW. Substitution of cysteine 192 in a highly conserved *Streptococcus pyogenes* extracellular cysteine protease (interleukin 1beta convertase) alters proteolytic activity and ablates zymogen processing. *Infect Immun* 1996; 64: 1913–7.
 15. Kapur V, Topouzis S, Majesky MW, Li LL, Hamrick MR, Hamill RJ, Patti JM, Musser JM. A conserved *Streptococcus pyogenes* extracellular cysteine protease cleaves human fibronectin and degrades vitronectin. *Microb Pathogenesis* 1993; 15: 327–46.
 16. McGrory K, Flaitz CM, Klein JR. Chemokine changes during oral wound healing. *Biochem Biophys Res Commun* 2004; 324: 317–20.
 17. Gillitzer R, Goebeler M. Chemokines in cutaneous wound healing. *J Leukoc Biol* 2001; 69: 513–21.
 18. Kannon GA, Garrett AB. Moist wound healing with occlusive dressings: a clinical review. *Dermatol Surg* 1995; 21: 583–90.
 19. Lundberg C, Campbell D, Agerup B, Ulfendahl H. Quantification of the inflammatory reaction and collagen accumulation in an experimental model of open wounds in the rat. A methodology study. *Scand J Plast Reconstr Surg* 1982; 16: 123–31.
 20. Im MJ, Freshwater MF, Hoopes JE. Enzyme activities in granulation tissue: energy for collagen synthesis. *J Surg Res* 1976; 20: 121–5.
 21. Howdieshell TR, Callaway D, Webb WL, Gaines MD, Procter CD Jr, Sathyanarayana, Pollock JS, Brock TL, McNeil PL. Antibody neutralization of vascular endothelial growth factor inhibits wound granulation tissue formation. *J Surg Res* 2001; 96: 173–82.
 22. Galeano M, Altavilla D, Cucinotta D, Russo GT, Calo M, Bitto A, Marini H, Marini R, Adamo EB, Seminara P, Minutoli L, Torre V, Squadrito F. Recombinant human erythropoietin stimulates angiogenesis and wound healing in the genetically diabetic mouse. *Diabetes* 2004; 53: 2509–17.
 23. Tonnesen MG, Feng X, Clark. Angiogenesis in wound healing. *J Invest Dermatol Symp Proc* 2000; 5: 40–6.

Shedding of Collagen XXIII Is Mediated by Furin and Depends on the Plasma Membrane Microenvironment^{*S}

Received for publication, April 24, 2007, and in revised form, June 14, 2007. Published, JBC Papers in Press, July 11, 2007, DOI 10.1074/jbc.M703425200

Guido Veit[†], Elena P. Zimina[§], Claus-Werner Franzke[§], Stefanie Kutsch[†], Udo Siebolds[¶], Marion K. Gordon^{||}, Leena Bruckner-Tuderman[§], and Manuel Koch^{†,***††1}

From the [†]Center for Biochemistry, the ^{**}Department of Dermatology, and the ^{††}Center for Molecular Medicine, Medical Faculty, University of Cologne, 50931 Cologne, Germany, the [§]Department of Dermatology, University of Freiburg, 79104 Freiburg, Germany, the [¶]Institute of Pathology, University of Cologne, 50924 Cologne, Germany, and the ^{||}Department of Pharmacology and Toxicology, Ernest Mario School of Pharmacy, and the Environmental and Occupational Health Sciences Institute, Rutgers University, Piscataway, New Jersey 08854

Collagen XXIII belongs to the class of type II orientated transmembrane collagens. A common feature of these proteins is the presence of two forms of the molecule: a membrane-bound form and a shed form. Here we demonstrate that, in mouse lung, collagen XXIII is found predominantly as the full-length form, whereas in brain, it is present mostly as the shed form, suggesting that shedding is tissue-specific and tissue-regulated. To analyze the shedding process of collagen XXIII, a cell culture model was established. Mutations introduced into two putative proprotein convertase cleavage sites showed that altering the second cleavage site inactivated much of the shedding. This supports the idea that furin, a major physiological protease, is predominantly responsible for shedding. Furthermore, our studies indicate that collagen XXIII is localized in lipid rafts in the plasma membrane and that ectodomain shedding is altered by a cholesterol-dependent mechanism. Moreover, newly synthesized collagen XXIII either is cleaved inside the Golgi/trans-Golgi network or reaches the cell surface, where it becomes protected from processing by being localized in lipid rafts. These mechanisms allow the cell to regulate the amounts of cell surface-bound and secreted collagen XXIII.

The group of collagenous transmembrane proteins consists of type XIII, XVII, XXIII, and XXV collagens and several related proteins such as ectodysplasin A, the class A macrophage scavenger receptors, the MARCO1 receptor, and the group of colmedins. These are type II transmembrane proteins that contain at least one collagenous triple helical domain (summarized in Ref. 1). Collagens XIII, XXIII, and XXV are of unknown function and consist of three collagenous domains that are flanked and separated by non-collagenous domains. Whereas collagen XVII is more distantly

related, types XIII, XVII, XXIII, and XXV all exist in two forms: a transmembrane form and a shed ectodomain form. Whereas collagen XVII is shed from the surface by TACE (tumor necrosis factor- α -converting enzyme), a member of the ADAM (a disintegrin and metalloproteinase) family (2), mutation analysis of collagens XIII and XXV demonstrated that the protease furin produces the shed forms (3, 4). Initial cell culture studies suggested an involvement of furin either directly or indirectly in the cleavage of collagen XXIII as well (5). Furthermore, the co-existence in tissues of both the transmembrane and shed forms of collagen XXIII was suggested from immunoblot analyses (6).

The shedding of an ectodomain amplifies the possible functional role of a protein because different forms, *i.e.* full-length cell surface-bound or soluble, likely have different biological activity. The "shedase" furin is a member of a proprotein convertase family. Among other functions, furin participates in the maturation and activation of proteins at the cell surface, endowing the cell with the ability to change its functional behavior (7–9). Moreover, conversion by proteolytic cleavage can be tightly regulated (10, 11). Furin-dependent shedding has been implicated in the activation of growth factors, initiating protease cascades as well as affecting pathogen entry into cells. With regard to the latter, it is notable that the virulence of pathogens such as anthrax, Ebola virus, and influenza virus is influenced by the presence of furin cleavage sites in viral proteins (9). Furthermore, there is at least one instance demonstrating that pathology results if shedding does not occur. A mutation in the furin cleavage site of the transmembrane collagen-like molecule ectodysplasin A is responsible for 20% of the cases of X-linked hypohidrotic ectodermal dysplasia (12). The consensus sequence for furin cleavage is Arg-X-(Lys/Arg)-Arg (13), with the most critical position being Arg at position 1. Less conserved sequences such as Arg-X-X-Arg also serve as furin cleavage sites, but with 10-fold lower efficiency than the consensus sequence. Furin is activated by two autocatalytic cleavage processes in the trans-Golgi network (TGN)² (14). As a mature enzyme, furin cycles between the cell surface and the TGN in a well regulated clathrin-dependent fashion (8).

^{*} This work was supported by an award from the Alexander von Humboldt Foundation, the Federal Ministry of Education and Research in Germany, Deutsche Forschungsgemeinschaft Grants SFB 589 P1 and Br 1475/6-3, NIEHS Center Grant ES05022 and National Eye Institute Grant 09056 from the National Institutes of Health. The costs of publication of this article were defrayed in part by the payment of page charges. This article must therefore be hereby marked "advertisement" in accordance with 18 U.S.C. Section 1734 solely to indicate this fact.

[§] The on-line version of this article (available at <http://www.jbc.org>) contains supplemental Figs. S1 and S2 and Table S1.

¹ To whom correspondence should be addressed: Center for Biochemistry, Medical Faculty, University of Cologne, Joseph-Stelzmannstr. 52, 50931 Cologne, Germany. Tel.: 49-221-478-88736; Fax: 49-221-478-6977; E-mail: Manuel.Koch@uni-koeln.de.

² The abbreviations used are: TGN, trans-Golgi network; AEBF, 4-(2-aminoethyl)benzenesulfonyl fluoride hydrochloride; cmk, chloromethyl ketone; M β CD, methyl- β -cyclodextrin; RT, reverse transcription; HEK, human embryonic kidney; EBNA, Epstein-Barr virus nuclear antigen; DMEM, Dulbecco's modified Eagle's medium; PLAP, phosphatidylinositol-linked placental alkaline phosphatase; hTfR, human transferrin receptor; PBS, phosphate-buffered saline; PC, proprotein convertase; α_1 -PDX, α_1 -antitrypsin Portland.

To regulate which form of a transmembrane molecule is present in a cell's environment, control is exerted not only by activation of the sheddase, but also by accessibility of the sheddase enzyme to the cell-surface protein to be shed. In this context, the plasma membrane microenvironment has a crucial regulatory function for the shedding of a variety of transmembrane proteins such as Alzheimer amyloid precursor protein (15), CD30 (16), the interleukin-6 receptor (17), and collagen XVII (18). Lipid rafts are small, dispersed, cholesterol-rich, and sphingolipid-rich microdomains that are fluid, but tightly packed (19). The lipid raft and non-raft microdomains have different association capabilities and therefore accumulate and separate membrane proteins. Lipid rafts play an important role in signal transduction, cell-cell interaction, and endocytosis of certain proteins (20, 21).

Here we present evidence for processing of collagen XXIII directly by furin. We also show that ectodomain shedding is influenced by the plasma membrane microenvironment: lowering the cellular cholesterol level significantly increases the shedding of collagen XXIII. This, together with partial shedding already occurring in the secretory pathway, likely represents the mechanism used by cells to regulate the ratio of the membrane-bound to released ectodomain forms of collagen XXIII. In addition, shedding is also tissue-dependent: in brain, collagen XXIII is present predominantly as the shed form, and in other tissues such as skin and lung, the full-length molecule is the prevailing form.

EXPERIMENTAL PROCEDURES

Reagents—The following protease inhibitors were used: AEBSF (4-(2-aminoethyl)benzenesulfonyl fluoride hydrochloride; Merck); antipain, 1,10-*ortho*-phenanthroline, aprotinin, E-64 (*trans*-epoxysuccinyl-L-leucylamido-(4-guanidino)butane), pepstatin A, leupeptin, and chymostatin (Sigma); the furin inhibitor decanoyl-Arg-Val-Lys-Arg-chloromethyl ketone (cmk; Bachem); the hydroxamate inhibitor TAPI-0 (Calbiochem-Novabiochem GmbH); and the membrane-impermeable furin inhibitor α_1 -PDX (Calbiochem). Other chemicals used were methyl- β -cyclodextrin (M β CD) and filipin III from *Streptomyces filipiensis* (Sigma), brefeldin A (Epicentre Biotechnologies), and 3,3'-dithiobis(sulfosuccinimidyl propionate) (Pierce).

Cloning of Full-length $\alpha 1$ (XXIII) and Furin cDNAs and Site-directed Mutagenesis—Reverse transcription (RT)-PCR was used to clone the full-length mouse $\alpha 1$ (XXIII) and furin cDNAs. Primers were designed according to the mRNA sequences provided for GenBankTM accession numbers NM153393 ($\alpha 1$ (XXIII)) and NM011046 (furin). The full-length $\alpha 1$ (XXIII) cDNA was amplified from mouse embryonic day 15.5 cDNA using the primer pair K500/K501 (see the list of PCR primers in supplemental Table S1). The full-length construct was ligated into a modified pCEP-Pu vector carrying a 3'-His₆ tag. The full-length furin cDNA was amplified from mouse embryonic day 15.5 reverse-transcribed mRNA using the primer pair P185/P186. Additional furin cDNA was ligated into a modified pCEP-Pu vector carrying a 5'-SPARC/BM40 signal peptide and a 3'-FLAG tag. Site-directed mutagenesis was carried out using the QuikChange[®] II site-directed mutagenesis

kit (Stratagene) according to the manufacturer's instructions. Amino acids of the two potential furin cleavage sites within non-collagenous domain 1 of collagen XXIII were altered. The primer pair M515/M517 was used to introduce the mutation R86Q (termed A), and the primer pairs M506/M507 and M508/M509 were used to insert the mutations R96S (B1) and R99G (B2), respectively.

Semiquantitative RT-PCR—Total RNA was extracted from various tissues and primary cells of newborn and adult C57BL/6J mice using the RNeasy fibrous tissue midi kit (Qiagen Inc.). Aliquots (2 μ g) were transcribed into cDNA using random hexamer primers and the enzymes SuperScriptTM II and III (Invitrogen). The relative RT-PCRs were performed in the linear range of amplification. The mouse $\alpha 1$ (XXIII) primers M630 and K501 produced a 727-bp product, and the control primers for γ -actin (M542 and M543) produced a 569-bp product. Products were run on agarose gels containing ethidium bromide. On-line quantification of the bands was performed using a Diana III advanced imaging system (Raytest).

Real-time RT-PCR—Primers and probes were designed using open source Primer3 web software (frodo.wi.mit.edu/cgi-bin/primer3/primer3_www.cgi) and were evaluated by Blast searches at NCBI (www.ncbi.nlm.nih.gov/blast/). All primers and probes were synthesized by Metabion. For detection and quantification of the PCR assays, the Mx3000P real-time PCR system (Stratagene) was employed. For relative quantification, 18 S rRNA served as an internal control. All primer/probe combinations were designed intron-spanning. The primer/probe combinations RT1-RT2/RTprobe1 for collagen XXIII and RT3-RT4/RTprobe2 for 18 S RNA were used (see the list of PCR primers in supplemental Table S1). The real-time PCR amplification was performed in a final reaction volume of 20 μ l containing primers (300 nM) and probe (200 nM) mixed with the appropriate volume of Eppendorf RealMasterMix (Eppendorf AG) and 4 μ l of cDNA. The reaction mixture was preheated at 95 °C for 2 min, followed by 45 cycles at 95 °C for 20 s and 60 °C for 1 min. All experiments were evaluated by performing three identical runs. To avoid quantification bias, a standard curve of every assay on every single run was carried out to ascertain the specific amplification efficiency. Briefly, the relative mRNA expression level was determined setting the cycle threshold against the standard curve in each case. Normalization against the internal control 18 S RNA was followed by calculating the case-specific calibrated gene expression. The mean value of normalized gene expression of skin mRNA served as a calibrator.

Isolation and Cultivation of Cells and Cell Culture-based Assays—Keratinocytes were isolated from newborn mouse skin and placed in primary culture according to established procedures (22). They were either kept under low calcium conditions to sustain their proliferative potential or treated for 2 h with 2 mM CaCl₂-containing medium to induce the formation of cell-cell contacts. Full-length collagen XXIII cDNA (ligated into the pCEP-Pu vector) was used to transfect human embryonic kidney (HEK) 293 cells expressing Epstein-Barr virus nuclear antigen-1 (HEK 293-EBNA cells; Invitrogen) and HT1080 cells using FuGENE 6 reagent (Roche Applied Science) according to the manufacturer's instructions. The medium used was Dul-

becco's modified Eagle's medium (DMEM)/nutrient mixture F-12 with GlutaMAXTM (Invitrogen) containing 10% fetal calf serum (Biocrom AG). Supplements of 250 μ M L-ascorbic acid and 450 μ M L-ascorbic acid 2-phosphate (Sigma) were added every day. Stable transfectants were selected with puromycin (1.25 μ g/ml; Sigma). For shedding assays, the stably transfected cells were incubated in serum-free DMEM/nutrient mixture F-12 supplemented with 250 μ M ascorbate, followed by incubation with the indicated chemicals for specified periods. The media and cell lysates were prepared and processed as described below.

Protein Isolation from Cells and Tissue and Western Blot Analysis—Protein isolation from tissue and subsequent immunoprecipitation and detection of collagen XXIII by Western blot analysis were performed as described previously (6). For protein extractions from cultured cells, the media and cell layers were processed separately as described (23). The medium was collected on ice; protease inhibitors (1 mM AEBSF and 10 mM EDTA) were added immediately; and cell debris were removed by centrifugation. To the remaining cell layer was added chilled extraction buffer (Tris-buffered saline, 1% Nonidet P-40, 2 mM EDTA, and Complete proteinase inhibitor mixture (Roche Applied Science)), and the sample was incubated for 30 min at 4 °C. The material was then collected using cell scrapers, and insoluble material was removed by centrifugation. The supernatant was precipitated with acetone or methanol/chloroform, and normalized aliquots were run on gels for immunoblotting with the previously described guinea pig anti-collagen XXIII antibody (6). Normalization was accomplished 1) by working with same cell numbers, 2) by determination of the protein content of the cell lysates and application of specified protein amounts and comparable volumes of cell supernatant for analysis, and 3) by analyzing the Western blot signals of cell supernatants with respect to the signals of the corresponding cell lysates. For quantitation, densitometry of signals was done using the Gel-Pro Express program (Media Cybernetics) or by performing on-line signal quantification with a Diana III advanced imaging system.

Immunofluorescence Staining and Antibody-induced Patching—Antibody-induced patching was performed as described previously (18). Briefly, HEK 293-EBNA cells cultured on coverslips were cotransfected with full-length α 1(XXIII) or furin cDNA and phosphatidylinositol-linked placental alkaline phosphatase (PLAP) or human transferrin receptor (HTrR) cDNA, respectively. First, the clustering of proteins was induced by incubation of the cells with the respective combination of anti-HTrR (DakoCytomation) or anti-PLAP (Biomed) monoclonal antibodies with either the guinea pig polyclonal antibodies against the ectodomain of collagen XXIII or the anti-furin polyclonal antibody (Alexis Biochemicals) for 60 min at 12 °C. After washing with phosphate-buffered saline (PBS), rhodamine-labeled goat anti-mouse (Jackson ImmunoResearch Laboratories) and fluorescein isothiocyanate-labeled anti-rabbit (DakoCytomation) secondary antibodies were applied for 1 h at 12 °C. Subsequently, the cells were fixed with 2% paraformaldehyde in PBS for 15 min at room temperature and mounted in PBS (pH 7.0) containing 37% glycerol, 12.5% Mowiol (Calbiochem), and 0.65% *N*-propyl gallate (Sigma) as an anti-fade agent. Fluores-

cent images were taken on an Axiophot microscope equipped with a Zeiss AxioCam MRc digital camera. Quantitative analysis was performed by subtracting background fluorescence and transforming the fluorescence signals to binary values. Each individual membrane patch was classified into the categories co-localization, partial co-localization, and segregation. Typically 100–250 membrane patches were present per cell, and a total number of eight cells were evaluated for each collagen XXIII-marker protein double labeling. For each furin-marker protein double labeling, four cells were quantified. For immunofluorescence staining, cells cultured on Nunc glass chamber slides were either incubated with serum-free medium containing guinea pig anti-collagen XXIII antibody for 1 h, followed by fixation with ice-cold methanol for 2 min, or directly fixed and permeabilized with 0.1% Triton X-100, followed by incubation with guinea pig anti-collagen XXIII antibody and anti-GM130 monoclonal antibody (BD Biosciences). After washing with PBS, CyTM3-conjugated anti-guinea pig (DakoCytomation) and Alexa 488-conjugated anti-mouse (Molecular Probes) antibodies were applied, and the stained slides were analyzed with a Leica TCS SL confocal laser scanning microscope.

Cross-linking Experiments—HEK 293-EBNA cells were cotransfected with full-length α 1(XXIII) cDNA and PLAP or HTrR cDNA. 24 h after transfection, cells were washed with PBS and incubated with 0.25 mM 3,3'-dithiobis(sulfosuccinimidyl propionate) for 30 min at room temperature. Alternatively, cells were treated with 10 mM M β CD prior to cross-linking. The reaction was stopped with 50 mM Tris-HCl (pH 7.5). The cells were lysed (1% Nonidet P-40, 0.1 M NaCl, 25 mM Tris-HCl (pH 7.4), and inhibitor mixture set III (Calbiochem)) and immunoprecipitated with guinea pig anti-collagen XXIII polyclonal antibodies. The precipitated proteins were eluted from antibody-coupled beads, and the cross-linker was reduced by heating for 10 min at 95 °C in SDS sample buffer containing 50 mM dithiothreitol. Subsequently, the eluates were separated on a 10% SDS-polyacrylamide gel and immunoblotted with guinea pig anti-collagen XXIII polyclonal, anti-PLAP monoclonal (Sigma), and anti-HTrR monoclonal antibodies.

Cell-surface Biotinylation—Cell-surface biotinylation was carried out as described by Franzke *et al.* (2). Briefly, cell-surface proteins were biotinylated with 6.6 mM biotin-X-NHS (Calbiochem) for 5 min at room temperature. After washing five times with PBS, the cells were cultured in fresh medium supplemented with ascorbate. At the desired time points, the media were collected, and cell lysates were prepared as described above. Biotinylated proteins from both the medium and the cell layer extract were precipitated with streptavidin-agarose (Novagen) and immunoblotted for reaction with guinea pig anti-collagen XXIII antibody to detect biotinylated collagen XXIII.

Quantification of Cellular Cholesterol and Protein Content of Cell Lysates—To normalize cell lysates for Western blot analysis, the protein content was determined with a bicinchoninic acid assay kit (Uptima). Cellular cholesterol content was assayed spectrophotometrically using a cholesterol quantitation kit (BioVision, Inc.) following the manufacturer's instructions.

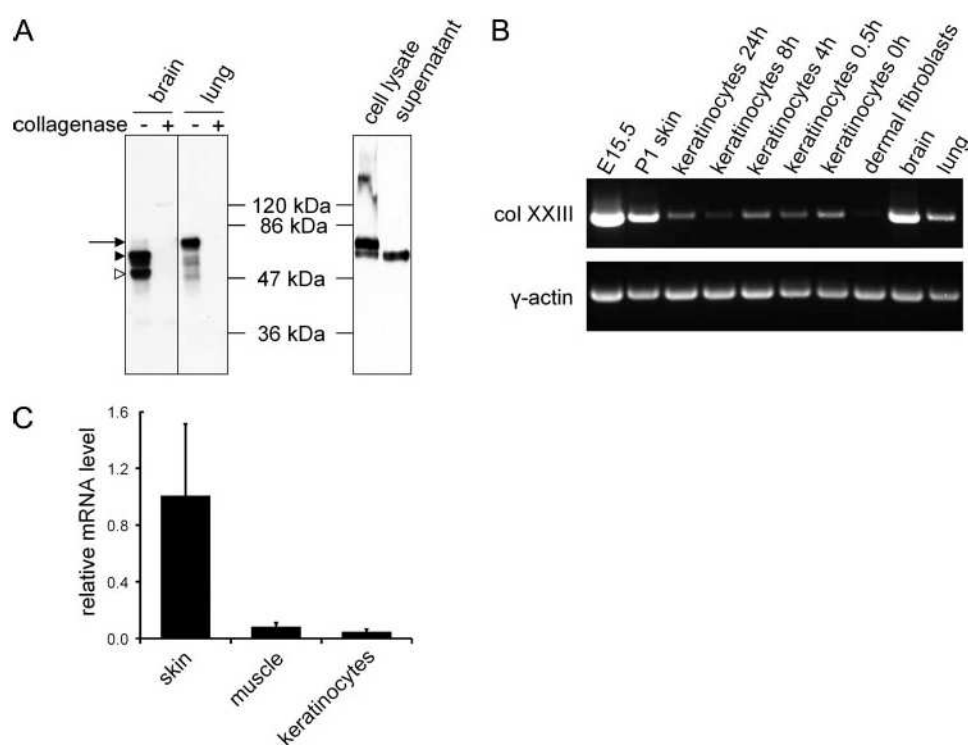


FIGURE 1. Tissue distribution of collagen XXIII protein and mRNA. *A*, detection of collagen XXIII in immunoprecipitation with subsequent Western blot analysis of mouse tissue extracts. Collagen XXIII was detectable in Nonidet P-40 tissue extracts of brain and lung after predigestion with guinea pig and detection with rabbit anti-collagen XXIII polyclonal antibodies. In the corresponding lanes loaded with collagenase-treated protein, the signal was absent. The arrow indicates the molecular mass of the full-length protein, and there were also signals at the molecular mass of the ectodomain (closed arrowhead) and at an even lower molecular mass (open arrowhead). For comparison, the lysate and conditioned medium of HT1080 cells stably transfected with $\alpha 1(\text{XXIII})$ cDNA are shown. *B*, semiquantitative tissue distribution of mouse $\alpha 1(\text{XXIII})$ mRNA. Fragments of mouse $\alpha 1(\text{XXIII})$ or γ -actin mRNA were amplified and detected after 31 cycles (in the linear range) for $\alpha 1(\text{XXIII})$ and after 27 cycles (in the linear range) for γ -actin. *col*, collagen; *E*, embryonic day. *C*, quantitative analysis of collagen XXIII mRNA levels by real-time PCR. The signals obtained were normalized against the internal control 18 S RNA, and the relative levels are displayed in comparison with signals in skin.

RESULTS

Shedding of Collagen XXIII Is Tissue-dependent—We demonstrated previously the tissue distribution of collagen XXIII in mouse skin, kidney, lung, and brain (6). Preliminary indications from immunoblots suggested that the protein is shed in some tissue and full-length in others. Using brain and lung as examples, immunoblot analysis of immunoprecipitated collagen XXIII revealed that the largest (full-length) form of collagen XXIII is predominant in lung, whereas in brain, three additional signals at lower mass were detected (Fig. 1*A*). The largest of these ran at the same molecular mass as the ectodomain from the conditioned medium of HT1080 cells stably transfected with full-length $\alpha 1(\text{XXIII})$ cDNA (see *supernatant* lane in Fig. 1*A*). The specificity of the antibody was confirmed by the products being specifically digested with highly purified bacterial collagenase. These data suggest that, if ectodomain shedding occurs, it is extensive in brain tissue, but minor in lung. Curiously, the two lower molecular mass immunoprecipitates from brain were not present in the lysates or medium of cells expressing recombinant collagen XXIII. This likely represents either a further degree of tissue-related processing that does not occur in recombinant HEK 293-EBNA and HT1080 cell cultures or cleavage by an enzyme present in brain, but not in the cell lines. To test this, we attempted to isolate this lowest molecular mass

form to perform microsequence analysis, but enough could not be obtained. Therefore, we validated it as a processed form of collagen XXIII by excluding the possibility that it arose from a splice variant of the mRNA: RT-PCR amplification of full-length collagen XXIII cDNA was performed with total RNA isolated from different tissues. The amplified product from brain, lung, skin, and total embryonic RNA was the same size (data not shown). The results are consistent with the lower molecular mass bands being processed forms of collagen XXIII.

To study the shedding process in a cell culture system, a collagen XXIII-containing tissue (*i.e.* skin) (6) with cells that could be easily separated and cultured was utilized for the next set of studies. To our surprise, semiquantitative PCR showed that primary keratinocytes cultured from mouse skin and stimulated for various periods with calcium contained sharply reduced amounts of $\alpha 1(\text{XXIII})$ mRNA, and cultured dermal fibroblasts gave an mRNA signal that was barely detectable compared with mRNA levels from tissues (Fig. 1*B*). The drastic down-regulation of $\alpha 1(\text{XXIII})$ mRNA expression in cul-

tured keratinocytes compared with skin was confirmed by real-time PCR (Fig. 1*C*). For comparison, real-time PCR was performed with RNA from muscle, a tissue containing only minimal amounts of collagen XXIII mRNA and protein (6). Therefore, to manipulate collagen XXIII in an *in vitro* culture system, we employed immortalized cell lines (HEK 293-EBNA and HT1080) that we stably transfected with full-length $\alpha 1(\text{XXIII})$ cDNA.

Subcellular localization of collagen XXIII in the transfected cell lines was analyzed by immunofluorescence staining in comparison with the low expression levels in primary mouse keratinocytes. In keratinocytes cultivated under low calcium conditions and kept at a low passage number, weak signals for collagen XXIII that co-localized with the Golgi marker protein GM130 could be detected (Fig. 2*A*). Similarly, co-localization was found in the transfected cell lines (Fig. 2, *B* and *C*). Also, cell-surface localization of collagen XXIII was detected in non-permeabilized primary keratinocytes that were stimulated with calcium to form cell-cell contacts and in non-permeabilized transfected cells, emphasizing detection of the molecule at the cell-cell boundaries (Fig. 2, *D* and *E*). Therefore, because the expression pattern of collagen XXIII in transfected cultures is similar to that in keratinocytes, we used transfected cell cultures to study shedding.

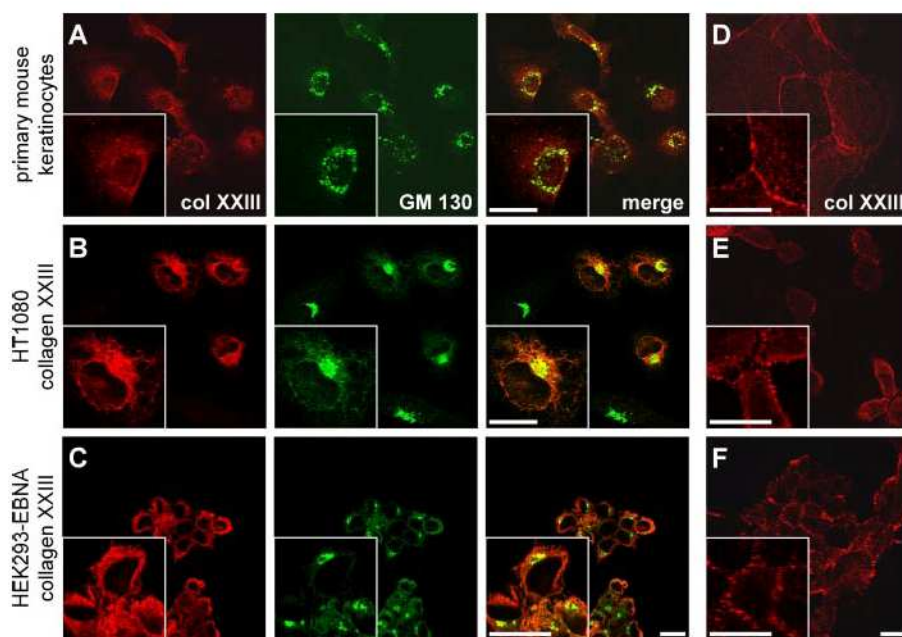


FIGURE 2. Subcellular localization of collagen XXIII in primary mouse keratinocytes and cell lines transfected with $\alpha 1$ (XXIII). Primary mouse keratinocytes (A and D), $\alpha 1$ (XXIII)-transfected HT1080 cells (B and E), and $\alpha 1$ (XXIII)-transfected HEK 293-EBNA cells (C and F) were stained with anti-collagen (col) XXIII polyclonal antibody (red) after (A–C) or prior (D–F) to fixation and solubilization of the cells. Counterstaining (A–C) was performed with antibody against the Golgi marker protein GM130 (green). Merging the images indicated intracellular co-localization (yellow) of collagen XXIII with the Golgi marker (A–C). Staining for collagen XXIII in non-permeabilized cells (D–F) identified its localization at the plasma membrane as well as its concentration at cell-cell boundaries. Scale bars = 20 μ m.

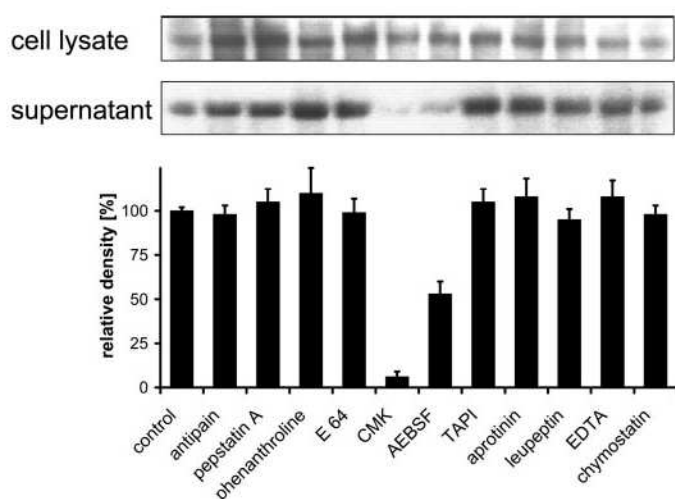


FIGURE 3. Effect of protease inhibitors on the release of the collagen XXIII ectodomain. Stably $\alpha 1$ (XXIII)-transfected HEK 293-EBNA cells were cultured in serum-free DMEM supplemented with protease inhibitors, including 50 μ M decanoyl-Arg-Val-Lys-Arg-cmk (CMK), 50 μ M antipain, 45 μ M TAPI-0, 100 μ M chymostatin, 10 μ M E-64, 10 μ M leupeptin, 10 μ M pepstatin A, 200 μ M 1,10-ortho-phenanthroline, 1 mM AEBSE, 200 μ M EDTA, and 10 μ M aprotinin. Shedding in the presence or absence of inhibitors was analyzed by immunoblotting the precipitated media, followed by semiquantitative densitometry of the signals. The histogram shows the release of the collagen XXIII ectodomain as percent \pm S.D. ($n = 3$) relative to the controls.

Furin/Proprotein Convertases Are the Major Class of Enzymes Responsible for Collagen XXIII Shedding—It has been suggested previously that furin likely plays a role in the processing of collagen XXIII (5). To further explore the enzymes involved in the shedding of collagen XXIII, stably transfected HEK 293-EBNA

cells were cultured in the presence of protease inhibitors, and the release of the ectodomain was analyzed by immunoblotting. As shown in Fig. 3, the ectodomain shedding was efficiently inhibited ($\sim 95\%$) only with the furin/proprotein convertase (PC)-specific agent decanoyl-Arg-Val-Lys-Arg-cmk. It was also partially inhibited ($\sim 45\%$) by the broad-range sulfonamide-type serine protease inhibitor AEBSE. Very minimal inhibition ($\sim 5\%$) was seen with antipain, leupeptin, and chymostatin, three primary serine protease/cysteine protease inhibitors, and with E-64, a cysteine protease inhibitor. No inhibition was observed with the aspartic protease-directed inhibitor pepstatin A, with the metalloprotease inhibitors 1,10-ortho-phenanthroline and EDTA, or with the hydroxamate-derived inhibitor TAPI-0. These last data excluded the potential involvement of matrix metalloproteinases or ADAM proteins in the ectodomain shedding of type

XXIII collagen in the cell culture model system.

For cleavage, most PCs require the consensus sequence RX(K/R)R. For processing by furin, the minimal amino acid sequence RXXR is sufficient (13, 24). The translated amino acid sequence of mouse collagen XXIII cDNA revealed two potential furin/PC cleavage sites in non-collagenous domain 1: 81 LERLLR 86 and 94 KIRTVR 99 (Fig. 4A). Edman degradation sequencing of the purified ectodomain revealed the major cleavage site to be after RTVR. No cleavage was observed in the recombinant protein after the predicted sequence RLLR. Interestingly, a very minor amount of recombinant shed protein commenced with sequence RGDPG, which follows a potential furin cleavage site (RGKPGR) in collagenous domain 1. Whether such a cleavage occurs *in vivo* could not be verified because of the lack of abundance of the shed product isolated from any tissue. Therefore, the cell culture system, being the only tool available to date to study the mechanism of shedding, was used to concentrate on furin cleavage of collagen XXIII. To analyze whether the more upstream furin site is cleaved less frequently or whether there is a cooperative interaction between the two sites that might result in a double cleavage, we altered the recognition sites by site-directed mutagenesis and assessed their influence on shedding. The mutation R86Q (termed A) was introduced into the first potential cleavage site, and the mutations R96S (B1) and R99G (B2) were introduced into the second potential cleavage site (Fig. 4A). The mutated cDNAs were transfected into HT1080 cells for expression. Mutant and wild-type proteins were extracted from the cells and shown to form disulfide-linked trimers by Western blotting of nonreduced SDS-polyacrylamide gels (supplemental Fig.

Collagen XXIII-Lipid Raft Localization and Shedding

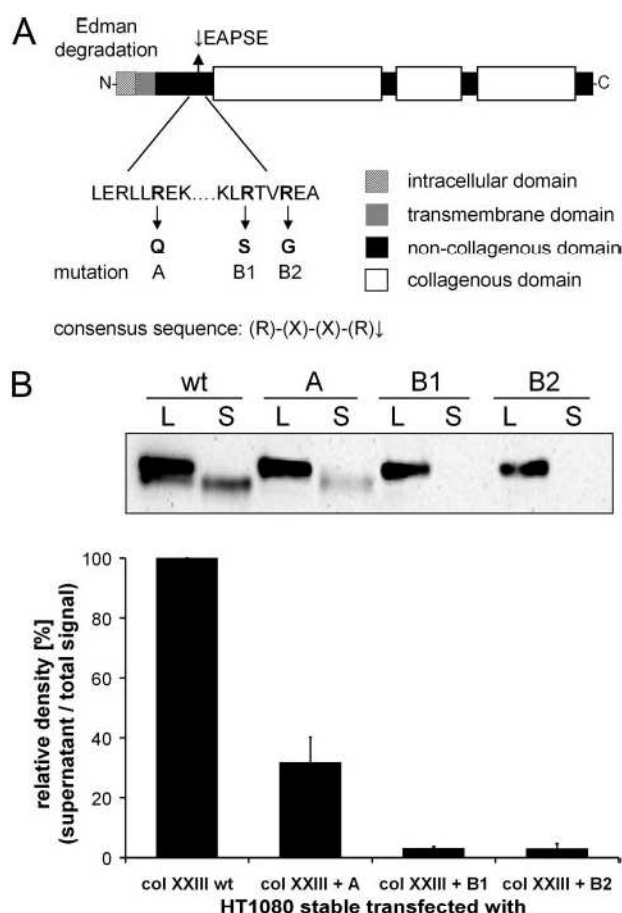


FIGURE 4. Mutation of potential furin/PC cleavage sites reduces ectodomain shedding. A, schematic depiction of the domain structure of mouse collagen XXIII highlighting the potential furin/PC cleavage sites and displaying the mutations introduced. B, effect of the mutations on the shedding of collagen XXIII. HT1080 cells stably expressing wild-type (wt) collagen (col) XXIII and mutant forms were cultured in serum-free DMEM/nutrient mixture F-12 supplemented with ascorbate. The collagen XXIII content of the cell lysate (L) and conditioned medium (S) was analyzed by Western blotting, followed by densitometric evaluation of the signals. The histogram shows the release of the collagen XXIII ectodomain as percent \pm S.D. ($n = 3$) relative to the signal from the corresponding cell lysates and wild-type controls.

SLA). To ensure that the mutations did not have any adverse impact on the triple-helix formation of collagen XXIII, stability was tested by resistance to trypsin digestion (supplemental Fig. S1B). The results indicated that all mutant proteins and the wild-type triple helical protein have comparable stability. We examined the relative level of the full-length form of collagen XXIII in cell lysates to the shed ectodomain form in cell medium. The B1 and B2 mutants were nearly completely retained on the cell surface as indicated by the strong signal in the cell lysates and the barely detectable signal in the conditioned medium (Fig. 4B). In addition, mutation of the first furin/PC cleavage site (RLLR to RLLQ; A2) led to a reduction in shedding and therefore less accumulation of the ectodomain in the conditioned medium (Fig. 4B), although not nearly to the extent caused by the B mutations in the RTVR recognition site.

To get an idea whether other PCs are able to compensate for furin activity, LoVo cells, which are known to lack furin but still contain active PACE4 and PC7 (4, 25, 26), were employed. Upon transfection with full-length $\alpha 1$ (XXIII) cDNA, they showed strongly reduced shedding of collagen XXIII compared

with other transfected cell lines (supplemental Fig. S2). These data, the enzyme inhibition assays, and the mutation analysis together indicate that collagen XXIII is predominantly but not exclusively processed by furin.

Localization of Collagen XXIII in the Membrane Microenvironment Regulates Shedding—Lipid rafts are small local regions of cholesterol- and sphingolipid-rich plasma membrane. These microdomains can be visualized with antibodies that laterally cross-link microdomain-specific marker proteins. This causes redistribution of the molecules, forming patches on the cell surface (15, 18, 27). Antibody-induced clustering was used to elucidate the membrane microdomain location of collagen XXIII and furin on the cell surface in our cell culture model system. PLAP is a component of lipid rafts, whereas HTrR is localized outside of rafts (15, 28). The cDNAs for these marker proteins (PLAP and HTrR) and $\alpha 1$ (XXIII) or furin were transiently cotransfected into HEK 293-EBNA cells, and patching was obtained by antibody cross-linking. Reactions with primary antibodies against 1) collagen XXIII and PLAP, 2) collagen XXIII and HTrR, 3) furin and PLAP, or 4) furin and HTrR, followed by incubation with appropriate secondary antibodies, were performed for 60 min at 12 °C to minimize the metabolic activity of the cells. The antibody-induced clustering showed that collagen XXIII co-localized in patches with PLAP, but segregated from HTrR (Fig. 5A), whereas furin co-localized predominantly in patches with HTrR, but segregated from PLAP (Fig. 5B). For quantitative analysis of the co-patching extent, the localization of individual membrane patches positive for collagen XXIII or furin in relation to PLAP- or HTrR-positive patches was assigned into three categories: co-localization (100% overlap), partial co-localization, and segregation (0% overlap). Because of the close localization of the individual patches in the membrane, a certain amount of partial co-localization was observed in all experiments, but comparison between the percentage of co-localization and the percentage of segregation clearly showed co-patching of collagen XXIII with PLAP and co-patching of furin with HTrR (Table 1). This indicates the localization of collagen XXIII mainly in lipid rafts and the localization of furin predominantly outside lipid rafts. To confirm these findings, a second method that avoids the clustering of lipid rafts prior to analysis was employed (29). Cell-surface proteins on HEK 293-EBNA cells transiently cotransfected with $\alpha 1$ (XXIII) and marker protein cDNAs were cross-linked with 250 μ M 3,3'-dithiobis(sulfosuccinimidyl propionate). This agent is a reducible, membrane-impermeable, and short-range (1.2 nm) cross-linker. Immunoprecipitation with guinea pig anti-collagen XXIII antibody, followed by immunoblotting with antibodies against the marker proteins, revealed that PLAP, but not HTrR, was in near association with the collagen (Fig. 5C). When the cells were treated with M β CD prior to cross-linking, the co-precipitated PLAP signal was consistently significantly reduced (Fig. 5C). For furin, this method is not applicable, as the necessary high expression levels of the protease seem to be cytotoxic for the cells.

The presence of collagen XXIII in lipid rafts and its main sheddase, furin, outside of rafts suggests that furin-mediated shedding is regulated by the plasma membrane microenvironment. To further understand the controlling mechanism,

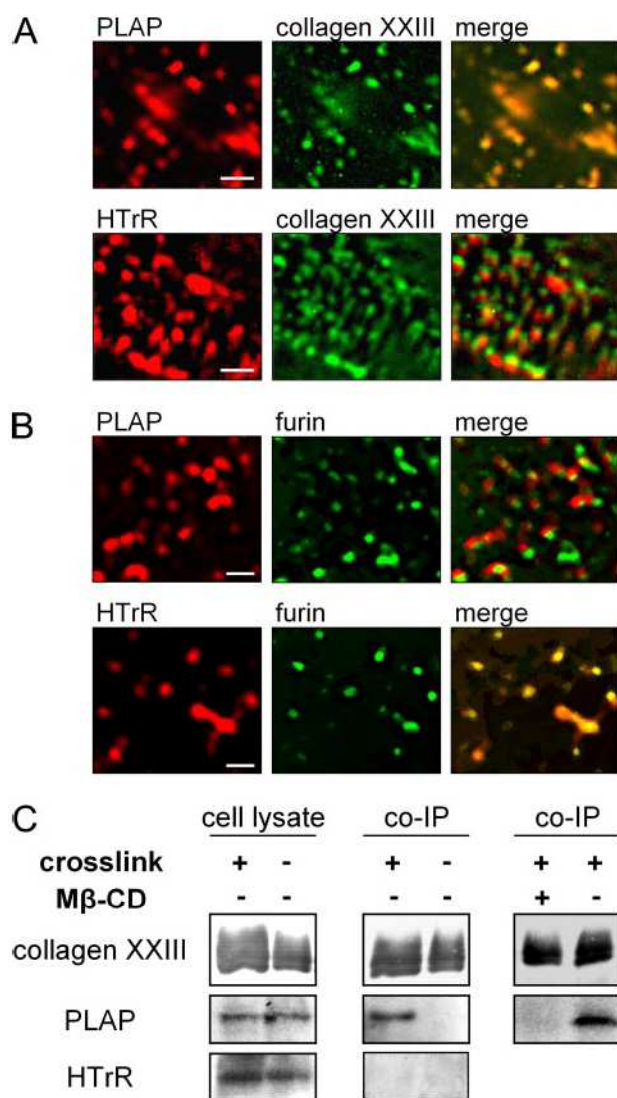


FIGURE 5. Plasma membrane microdomain localization of collagen XXIII and furin. *A*, collagen XXIII co-patching with the lipid raft marker protein PLAP and segregation from the non-raft marker HTrR after antibody cross-linking. *B*, furin co-patching with HTrR and segregation from PLAP after antibody cross-linking. The clustering of proteins was induced by incubation of the cells with the respective combination of anti-HTrR monoclonal antibodies or incubation of anti-PLAP monoclonal antibodies with guinea pig anti-collagen XXIII or anti-furin polyclonal antibodies. Scale bars = 0.5 μ m. *C*, co-immunoprecipitation (co-IP) of collagen XXIII with the lipid raft marker protein PLAP after cross-linking of the cell-surface proteins. Cross-linking of cell-surface proteins was performed with the reducible, membrane-impermeable, short-range (1.2 nm) cross-linker 3,3'-dithiobis(sulfosuccinimidyl propionate) (250 μ M) for 30 min at room temperature. Expression of the proteins was confirmed by immunoblotting without prior precipitation with anti-collagen XXIII polyclonal antibody. After cross-linking, the lipid raft marker protein PLAP, but not the non-raft marker HTrR, co-precipitated with collagen XXIII, indicating localization in the same membrane microdomain. Alternatively, cells were treated with 10 mM M β CD prior to cross-linking. This resulted in reduced co-precipitation of PLAP.

M β CD was used to deplete cholesterol from cells stably transfected with α 1(XXIII) cDNA. M β CD is not incorporated into the membrane, but contains a central non-polar cavity that binds cholesterol molecules, leading to disintegration of lipid rafts (30). Treatment of HT1080 or HEK 293-EBNA cells with increasing concentrations of M β CD (5–20 mM) for 60 min led to a concentration-dependent reduction in cellular cholesterol levels (Fig. 6A). The highest concentration reduced cholesterol

TABLE 1

Quantification of individual membrane patches positive for collagen XXIII or furin co-patching with the lipid raft marker PLAP or the non-lipid raft marker HTrR

	Double labeling	Co-localization	Partial co-localization	Segregation
		% \pm S.D.	% \pm S.D.	% \pm S.D.
Collagen XXIII-PLAP		57 \pm 12	24 \pm 8	19 \pm 12
Collagen XXIII-HTrR		5 \pm 4	51 \pm 9	44 \pm 10
Furin-PLAP		6 \pm 8	43 \pm 18	51 \pm 20
Furin-HTrR		37 \pm 5	49 \pm 9	14 \pm 7

levels by \sim 50%. The effect of this treatment on the shedding of collagen XXIII was assessed by Western blot analysis of full-length collagen XXIII in cell lysates and ectodomain released into the conditioned medium. M β CD treatment resulted in a dose-dependent enhancement of the release of the collagen XXIII ectodomain from stably transfected HEK 293-EBNA cells (Fig. 6B) as well as from stably transfected HT1080 cells (Fig. 6C). Shedding was increased by 4-fold in transfected HT1080 cells treated with 20 mM M β CD and by 5-fold in transfected HEK 293-EBNA cells treated with 10 mM M β CD. To validate the implication that shedding is mediated by furin, HT1080 cells stably transfected with the B1 mutation of α 1(XXIII) cDNA were subjected to M β CD cholesterol depletion (Fig. 6C, lower panel). The shedding of the mutant protein was minor and was seen to be only slightly increased in a dose-dependent manner by M β CD treatment. Further evidence that furin is the major sheddase came from treatment of the stably transfected HEK 293-EBNA cells with the furin-specific inhibitor decanoyl-Arg-Val-Lys-Arg-cmk (50 μ M), which lowered the shedding activity in untreated cells by \sim 60%. The increase in shedding with cholesterol depletion could be attenuated by \sim 65% in the presence of decanoyl-Arg-Val-Lys-Arg-cmk (Fig. 6D). In addition, the effects of another cholesterol-binding agent, filipin, which acts via a different mechanism, were tested. Filipin, a polyene macrolide antibiotic, is a sterol-binding agent that interacts with cholesterol in the plasma membrane, destabilizing lipid rafts by interfering with the cholesterol-sphingolipid interaction (31, 32). Stably transfected HT1080 cells expressing full-length α 1(XXIII) cDNA were treated with 10–30 μ g/ml filipin. This resulted in a concentration-dependent increase in collagen XXIII shedding of up to 3-fold (Fig. 6E). Taken together, these results indicate that lowering the cholesterol content of the membrane, thereby disrupting lipid rafts, significantly enhances the furin-mediated shedding of collagen XXIII.

Golgi-localized Furin Cleaves Collagen XXIII—Because collagen XXIII exists in a cell-surface membrane-bound form as well as a soluble shed form and because the cell-surface molecules are at least predominantly protected from furin shedding due to their localization in lipid rafts, we were interested in the dynamics and subcellular localization of the shedding event. To assess the kinetics of shedding from the cell surface, biotinylation of HEK 293-EBNA cells stably expressing full-length collagen XXIII was performed, and biotinylated collagen XXIII was followed in a pulse-chase experiment (Fig. 7). Western blot analysis revealed that the shedding of collagen XXIII from the cell surface occurred slowly. Even after 72 h, biotinylated molecules were detected on the cell surface as assessed by their

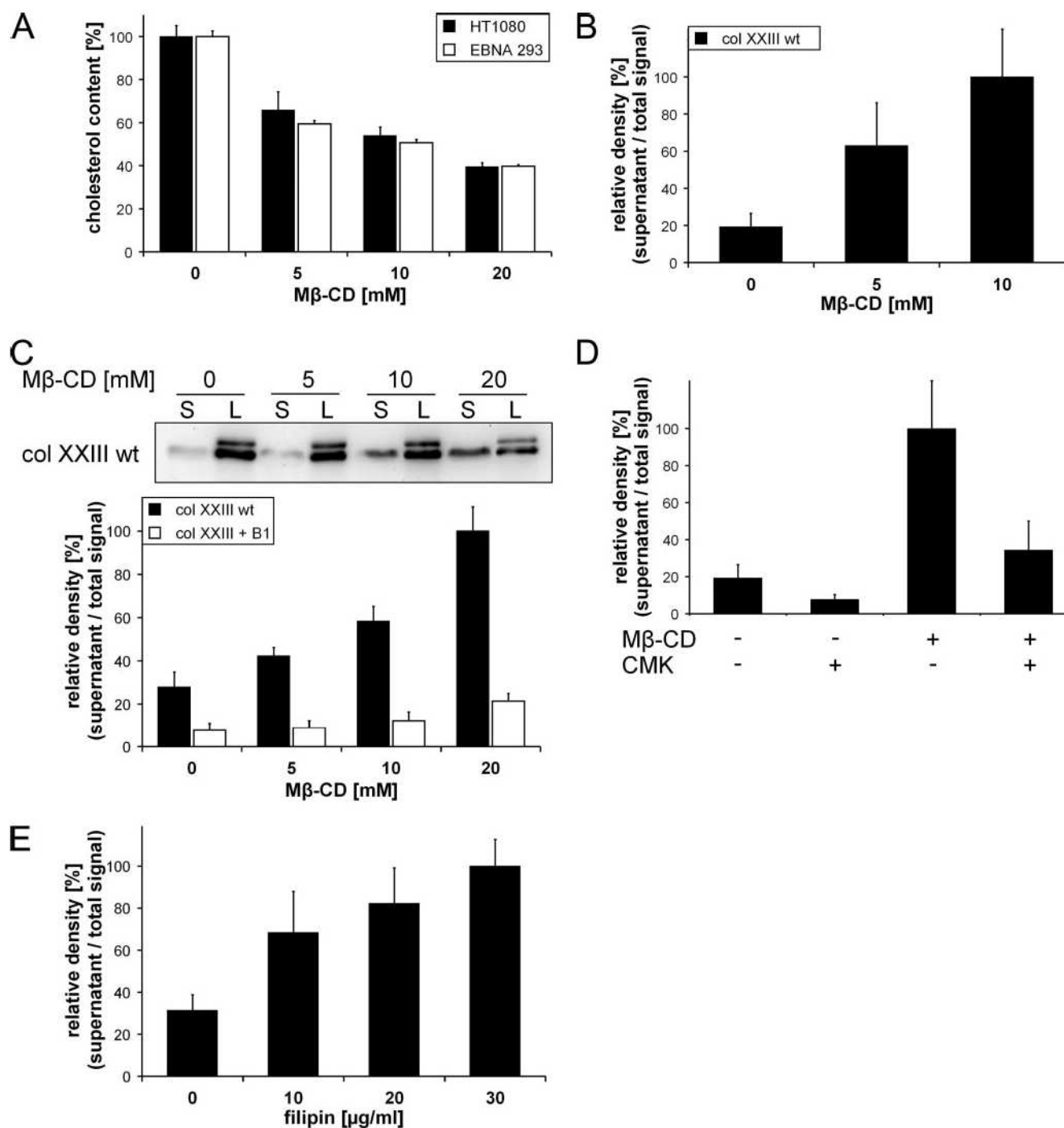


FIGURE 6. Cholesterol depletion of the plasma membrane induces the shedding of collagen XXIII. *A*, alterations in the concentration of HEK 293-EBNA and HT1080 cell plasma membrane cholesterol after 60 min of M β CD treatment. *B* and *C*, cholesterol depletion by 0–20 mM M β CD enhances the shedding of wild-type (wt) α 1(XXIII) stably transfected into HEK 293-EBNA and HT1080 cells, respectively. In addition, shedding is shown for α 1(XXIII) with the B1 mutation stably transfected into HT1080 cells (*C*). *col*, collagen; *L*, cell lysate; *S*, conditioned medium. *D*, inhibition of furin decreases collagen XXIII shedding in the presence of the lipid raft disruptor, M β CD. HEK 293-EBNA cells stably transfected with α 1(XXIII) cDNA were treated with 10 mM M β CD in combination with the furin-specific protease inhibitor decanoyl-Arg-Val-Lys-Arg-cmk (CMK; 50 μ M). *E*, stimulation of collagen XXIII shedding in stably transfected HT1080 cells by treatment with 0–30 μ g/ml filipin. Cells were incubated with M β CD or filipin for 60 min, and the soluble collagen XXIII ectodomain from the culture medium and cellular collagen XXIII were analyzed by immunoblotting with guinea pig anti-collagen XXIII polyclonal antibody. After densitometric evaluation of the signals, histograms show the release of the collagen XXIII ectodomain as percent \pm S.D. ($n = 3$) relative to the signal in corresponding cell lysates.

persistence in the cell lysate. The shed ectodomain of biotinylated collagen XXIII was detectable in the medium only after 24 h and increased in concentration at ensuing time points.

Interestingly, biotinylated collagen XXIII from cell lysates, which represents the surface-bound form, appeared as a double

band in Western blot analysis, with the lower band having the size of the ectodomain. The ectodomain-sized product at the early time points post-biotinylation is not likely to be the result of cell-surface collagen XXIII being recycling to the Golgi and being cleaved by furin. This form was very abundant at early

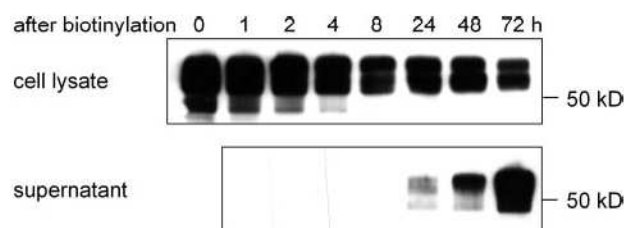


FIGURE 7. **Time dependence of collagen XXIII ectodomain shedding.** HEK 293-EBNA cells stably expressing full-length collagen XXIII were surface-biotinylated, chased with biotin-free medium, and cultured for 72 h. Aliquots of the culture medium and cell extract were precipitated with streptavidin-agarose and analyzed by Western blotting with guinea pig anti-collagen XXIII polyclonal antibody.

time points, and one would expect that not all of it could be captured at the cell surface; some would have to appear in the early supernatant time points. Although we expect that recycling does occur, the abundance of the ectodomain-sized product in the cell lysate suggests either that the shed form is derived from full-length collagen XXIII cleaved at the surface of the cell, sequestered at the cell surface by some other unidentified molecule, or that the sheddase is not compelled to clip all three chains of a trimeric collagen XXIII molecule at once. If the latter, just one of the three chains in the triple helical molecule, if not clipped by furin (thus retaining its transmembrane domain), would be sufficient to serve as a membrane anchor for the other two α -chains participating in the triple helix, holding them at the cell surface. Whichever the case, it is clear that clipped chains are retained. Taken together, these results indicate that transmembrane collagen XXIII resides on the cell surface with a half-life on the order of days.

To evaluate the extent of furin activity that takes place in the Golgi, HEK 293-EBNA cells stably transfected with $\alpha 1(\text{XXIII})$ cDNA were treated with brefeldin A, a macrocyclic lactone that inhibits vesicle transport from the endoplasmic reticulum to the Golgi and that leads to disassembly of Golgi stacks (33, 34). Western blot analysis after treatment of the cells for 5 h with brefeldin A revealed a sharp decrease in the collagen XXIII ectodomain in the supernatant compared with untreated cells, suggesting that much of collagen XXIII is normally cleaved in the Golgi. In HEK 293-EBNA cells, brefeldin A caused shedding to be reduced by $\sim 95\%$ and caused an increase in full-length collagen XXIII detected in the cell lysate (Fig. 8, A and B). In contrast, if only cell-surface collagen XXIII was assessed (using surface biotinylation), brefeldin A treatment had a less drastic effect, decreasing shedding by $\sim 50\%$ in HEK 293-EBNA cells (Fig. 8C). Comparable results were obtained with stably transfected HT1080 cells (data not shown). Thus, cleavage of collagen XXIII by furin occurs predominantly intracellularly. To evaluate the extracellular shedding of collagen XXIII after it is deposited into the plasma membrane, the membrane-impermeable furin inhibitor α_1 -PDX (a bioengineered variant of α_1 -antitrypsin) was employed (35, 36). Biotinylated proteins on HEK 293-EBNA cells were incubated for 6 h in presence of $8 \mu\text{M}$ α_1 -PDX and showed a 45% reduction in shedding. Additionally, an increase in biotinylated collagen XXIII molecules in the cell lysate was observed compared with untreated cells (Fig. 9).

In additional experiments, the effect of cholesterol depletion specifically on the cell-surface collagen XXIII molecules was

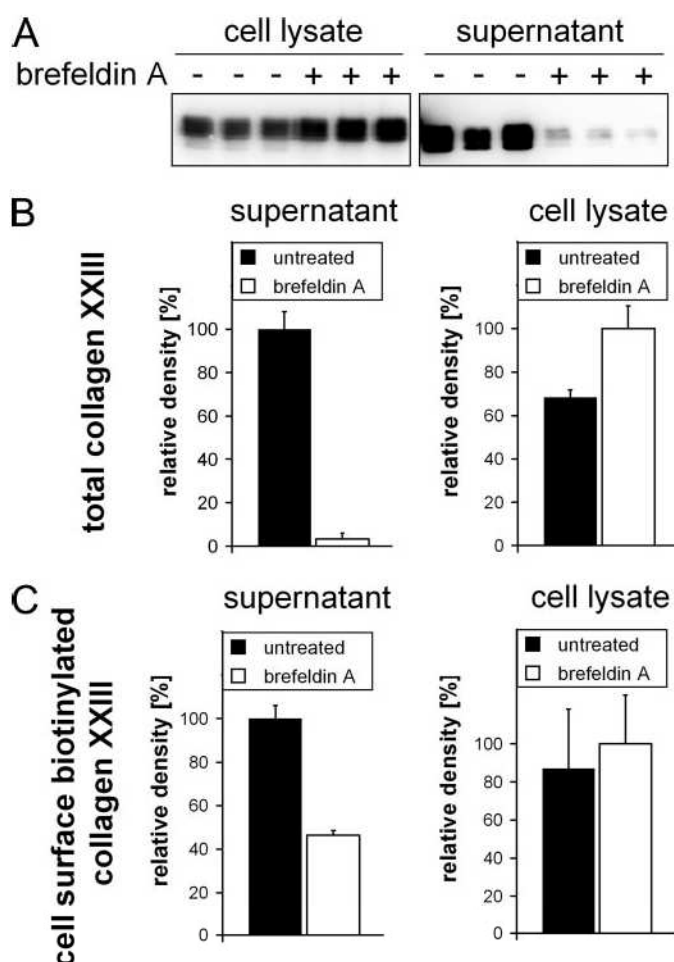


FIGURE 8. **Subcellular localization of the collagen XXIII shedding event.** Disassembly of the Golgi by brefeldin A treatment drastically reduced the shedding of collagen XXIII. A and B, HEK 293-EBNA stably transfected with $\alpha 1(\text{XXIII})$ cDNA were cultured in serum-free DMEM supplemented with 50 ng/ml brefeldin A for 5 h. The collagen XXIII content of the cell lysate and conditioned medium was analyzed by Western blotting, followed by densitometric evaluation of the signals. C, shown is the effect of Golgi disassembly on cell-surface collagen XXIII molecules. HEK 293-EBNA cells stably expressing full-length collagen XXIII were surface-biotinylated and incubated with biotin-free medium containing 50 ng/ml brefeldin A for 5 h. Aliquots of the culture medium and cell extract were precipitated with streptavidin-agarose and analyzed by Western blotting with guinea pig anti-collagen XXIII polyclonal antibody, followed by densitometry of bands. The brefeldin A effect was less drastic on biotinylated collagen XXIII compared with total collagen XXIII. The histograms show collagen XXIII signals as percent \pm S.D. ($n = 3$).

analyzed. Cell-surface biotinylation and cholesterol depletion could not be combined due to the fact that, after 1 h of treatment, insufficient biotinylated ectodomain for streptavidin-agarose precipitation was accumulated in the supernatant and because prolonged treatment with cholesterol-depleting agents adversely affected cell survival. Therefore, co-treatment with brefeldin A and the cholesterol-depleting agent M β CD was employed. As already described, single treatment of HEK 293-EBNA stably expressing collagen XXIII with brefeldin A for 1 h led to a strong decrease in the shedding of collagen XXIII. Likewise, single treatment of the cells with 5 mM M β CD led to an increase in shedding. Co-incubation of the brefeldin A-treated cells with 5 mM M β CD resulted in a strong increase in the shedding of collagen XXIII compared with the cells treated only with brefeldin A (Fig. 10). Similar results were obtained in

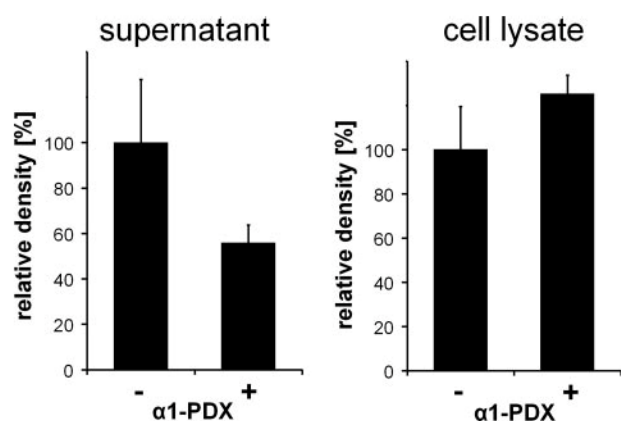


FIGURE 9. Partial inhibition of the shedding of cell surface-biotinylated collagen XXIII by the membrane-impermeable furin inhibitor α_1 -PDX. HEK 293-EBNA cells stably transfected with α_1 (XXIII) cDNA were surface-biotinylated and incubated for 6 h with biotin-free medium containing 8 μ M α_1 -PDX. Aliquots of the culture medium and cell lysate were precipitated with streptavidin-agarose and analyzed by Western blotting with guinea pig anti-collagen XXIII polyclonal antibody, followed by densitometry. The histograms show collagen XXIII signals as percent \pm S.D. ($n = 3$).

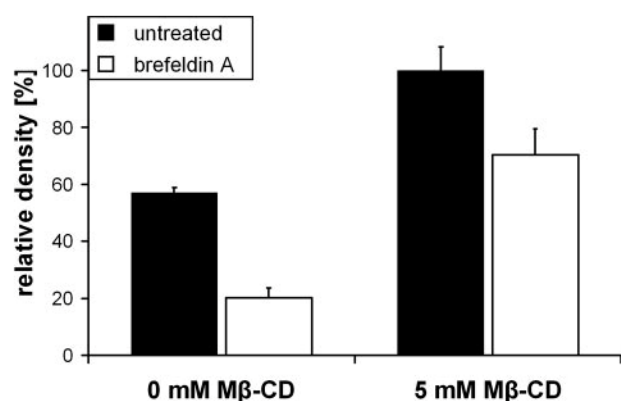


FIGURE 10. Cholesterol depletion of brefeldin A-treated cells increases the shedding of collagen XXIII. HEK 293-EBNA cells stably expressing collagen XXIII were treated with 1 μ g/ml brefeldin A, 5 mM M β CD, or a combination of both for 1 h. The soluble collagen XXIII ectodomain from the culture medium was analyzed by immunoblotting with guinea pig anti-collagen XXIII polyclonal antibody, followed by densitometry. Note that co-treatment resulted in a strong increase in shedding, indicating that cholesterol depletion increases cleavage predominantly at the cell surface. The histograms show collagen XXIII ectodomain release as percent \pm S.D. ($n = 3$).

α_1 (XXIII)-transfected HT1080 cells (data not shown). These findings indicate that, in particular, the shedding of collagen XXIII localized at the cell surface is altered by a cholesterol-dependent mechanism.

To conclude, the shedding of collagen XXIII predominantly occurs intracellularly. Collagen XXIII molecules that escape intracellular shedding are present at the cell surface. These molecules are proteolytically processed slowly because of their protection inside lipid rafts.

DISCUSSION

Release of an ectodomain by selective proteolysis has turned out to be a common feature of type II transmembrane collagens (3, 5, 23, 37). Previous work suggested that the shedding of collagen XXIII is not pervasive in skin and kidney (6), but is in prostate cancer cells (5). We have shown here that collagen XXIII is shed by cells in culture, by cells in brain tissue, and to a

minor degree by cells in lung. Every transmembrane collagen known to date contains potential furin convertase recognition sites, but only collagens XIII, XXIII, and XXV have been shown to be directly processed by furin (this work and Refs. 3 and 4). For collagen XVII, processing by TACE was demonstrated. However, furin is likely to play a role in a protease cascade leading to activation of the sheddase (2).

Collagen XXIII contains what we consider to be two biologically relevant furin/PC recognition sequences. A consensus site in collagenous domain 1 would participate in a triple helical structure and would likely not be available for furin cleavage. For furin cleavage, an arginine is required that defines position 1, and an arginine downstream is required in position 4. Additional basic residues in positions 2 and 6 considerably enhance cleavage by furin (13). In fact, furin is the only PC that is capable of recognizing basic residues at position 6 (24). Other PCs such as PC1 and PC2 require the basic residue at position 2. In collagen XXIII, the most N-terminal potential furin/PC cleavage site contains no additional basic residues, but the more downstream C-terminal cleavage site has a lysine at position 6. Edman degradation of the purified recombinantly expressed ectodomain revealed that the downstream site is the major location for processing of collagen XXIII. Inhibition studies revealed that primary serine proteases or cysteine protease are capable of producing 5% or less of the shed ectodomain. Aspartate proteases and metalloproteases (responsible for collagen XVII shedding) (2) are not involved in processing collagen XXIII. Effective inhibition of shedding is observed only with AEBSF, a broad-range sulfonyl fluoride-type serine proteinase inhibitor, and with decanoyl-Arg-Val-Lys-Arg-cmk, a PC-specific protease inhibitor (38). Even though furin itself is a serine protease, it is relatively insensitive to serine protease inhibitors (38), and thus, it is influenced only by AEBSF and not by primary serine protease inhibitors. Although Edman degradation indicated that the more C-terminal furin cleavage site was used, it could not reveal whether processing occurred in steps, such as a first cleavage at the most N-terminal site, followed by a cleavage at the downstream site. Mutation of one arginine in the more N-terminal site decreased shedding, but to a minor degree, suggesting there is not a specific temporal sequence to the processing event. Processing at the most N-terminal site is likely to be less efficient because of the lack of additional basic residues beyond the minimally required arginines. Mutation of the two arginines in the downstream furin cleavage site drastically reduced shedding. Any minor shedding activity observed in this mutant molecule most likely represents cleavage at the upstream, less used furin cleavage site or at a site cleaved infrequently by a primary serine protease or cysteine protease. Processing of collagen XXIII by PCs other than furin is suggested by studies with LoVo cells, which lack furin but still contain active PACE4 and PC7 (4, 24, 25). In these cells, processing of collagen XXIII is strongly reduced, but is not completely absent. In further support of the downstream furin cleavage site as being the major location for furin-mediated shedding, the cDNAs of all species analyzed to date show a strong conservation of the more C-terminal collagen XXIII furin cleavage site, whereas the more N-terminal site is not as conserved. Also, the reported furin cleavage sites in transmembrane collagens XIII and XXV (3, 37)

demonstrate strong homology to the downstream collagen XXIII furin site. Taken together, these data indicate that furin is the major protease to process collagen XXIII and that the processing occurs after the downstream recognition motif (⁹⁴KIRTVR⁹⁹), releasing the ectodomain.

The release of an ectodomain is influenced by the spatial organization of a transmembrane molecule and its particular sheddase within the plasma membrane lipid microenvironment. For example, the β -secretase localized in lipid rafts is able to process the Alzheimer β -amyloid precursor protein that is localized within lipid rafts, but not the precursor protein molecules outside of rafts (15). Transmembrane collagen XVII is localized inside lipid rafts and is therefore less accessible to its sheddase, TACE, which is outside the rafts (18). The activated form of furin is present in the Golgi and the TGN and on the cell surface (7, 39). The fact that processing by cell-surface furin increases the pathogenicity of anthrax toxin PA and *Clostridium* α -toxin highlights the biological relevance of this sheddase (8, 9). Here we used co-patching immunofluorescence analysis of non-permeabilized cells to reveal the plasma membrane microdomain localization of furin and collagen XXIII on the cell surface. Collagen XXIII co-localized with the lipid raft marker PLAP, whereas furin co-localized predominantly with the non-lipid raft marker HTRr. To confirm the lipid raft localization of collagen XXIII, we applied a cross-linking technique (29) and avoided using the previously widely used, but currently disputed method of cold Triton extraction for lipid raft preparation (40, 41). Cross-linking of collagen XXIII with the lipid raft marker protein PLAP in non-clustered rafts supported the immunofluorescence results.

The influence of the membrane microenvironment on shedding was demonstrated by disintegration of lipid rafts with M β CD and by hampering lipid raft formation. These cholesterol disturbances led to an increased release of the collagen XXIII ectodomain from the cell surface, presumably by facilitating contact between furin and collagen XXIII, thereby dysregulating natural controls. In agreement with the previous observations for other lipid raft-localized transmembrane proteins (16, 18), a small decrease in cell-surface cholesterol led to a significant enhancement of shedding. Both treatment with the furin inhibitor decanoyl-Arg-Val-Lys-Arg-cmk and mutations in the downstream furin cleavage site inhibited shedding in untreated as well as cholesterol-depleted cells. This indicates that collagen XXIII shedding induced by cholesterol reduction is due to furin action and not to secondary effects. Therefore, the data suggest a model in which cell-surface furin is localized primarily outside lipid rafts, whereas collagen XXIII is located mainly within lipid rafts, inaccessible to furin processing. Upon disruption of lipid rafts, collagen XXIII molecules become accessible to furin, and an increased release of collagen XXIII ectodomain is seen.

Despite the evidence that transmembrane collagen shedding is influenced by modulating membrane cholesterol levels (this work and Refs. 18 and 42), little is known about the dynamics and subcellular localization of the shedding event. Pulse-chase analyses suggested that the shedding of cell-surface collagen XXIII is a limited proteolysis occurring rather slowly, with the half-life of the full-length protein being in the range of days.

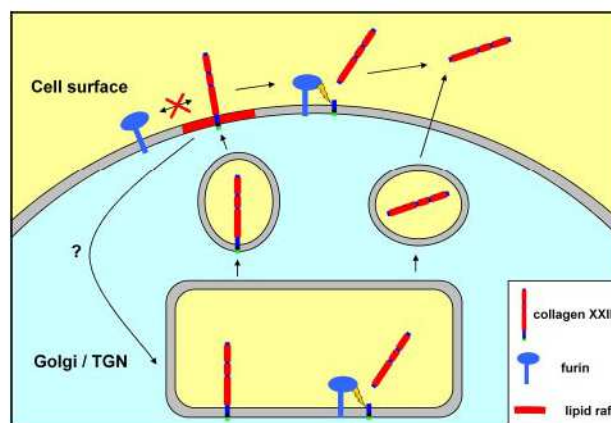


FIGURE 11. Schematic diagram of collagen XXIII shedding as it may occur in different cellular compartments. Newly synthesized collagen XXIII may be transported to the cell surface as a transmembrane protein; alternatively, the ectodomain may be secreted due to cleavage by furin in the Golgi/TGN. At the cell surface, collagen XXIII is protected from cleavage because it is localized predominantly in lipid rafts. A change in lipid raft dynamics or an artificial depletion of cellular cholesterol causes shedding to occur at the cell surface. Also, collagen XXIII may be recycled from the cell surface into the Golgi/TGN.

This implies that the full-length protein localized on the plasma membrane has a biological function. Moreover, disassembly of the Golgi suggested that a population of collagen XXIII molecules is shed while passing through the secretory pathway and that another population reaches the cell surface as full-length molecules (summarized in the scheme in Fig. 11). Experiments with the membrane-impermeable furin inhibitor α_1 -PDX confirmed our previous conclusion (6) that shedding at the cell surface does occur, but only at a low rate. Minor shedding is observed at the cell surface, perhaps because a small amount of collagen XXIII or furin molecules may be unrestricted in the plasma membrane subcompartments or because of the activity of the primary serine or cysteine proteases, which have a minimal effect on collagen XXIII. We favor the former idea because the raft/non-raft phase association of membrane proteins is a dynamic process and because lipid rafts themselves are dynamic entities within the cell membrane (43, 44). The effect of Golgi disassembly on cell surface-biotinylated collagen XXIII molecules hints at the possibility that cell-surface collagen XXIII molecules may be internalized to the Golgi/TGN compartment for processing or reinsertion into the cell membrane. This dynamic scenario is consistent with previous findings for other lipid raft-localized proteins (45). Discrimination between ectodomain shedding on the cell surface regulated by recycling to the Golgi/TGN *versus* that by only lipid raft manipulation is further supported by the fact that cholesterol depletion in the presence of brefeldin A strongly increased the shedding of collagen XXIII.

With the use of one transmembrane molecule, the cell may economically adjust its phenotype 1) by influencing the amount of collagen XXIII shedding in the secretory pathway and 2) either by modulating its lipid raft composition or by recycling to favor or disfavor the shedding of cell-surface collagen XXIII (Fig. 11). The importance of a highly regulated shedding process influencing the cellular phenotype is further highlighted by the observation that cell surface-localized collagen XXIII was concentrated at sites of cell-cell contact (Fig. 2D), where it can

interact with integrin $\alpha_7\beta_1$.³ Up-regulation of shedding would enable the cell to liberate any collagen XXIII-mediated cell-cell adhesion and could positively influence the migratory behavior of the cell. Such action could play an important role in effective wound healing. In addition, such action could, in turn, affect neighboring cells, as the soluble ectodomain could act as a competitor for integrin $\alpha_7\beta_1$ binding. Similar observations were made for regulated release of soluble E-cadherin, which, after shedding by ADAM10, decreases cell-cell adhesion and increases migration (46).

The importance of furin cleavage to the function of collagen XXIII is not yet known. However, furin-mediated shedding *in vivo* has been shown to be vital in at least one instance involving a collagen-like transmembrane molecule: mutations within the furin consensus sequence of transmembrane collagen-related ectodysplasin A impede shedding and cause the X-linked disorder hypohidrotic ectodermal dysplasia (12, 47). Like collagen XXIII, ectodysplasin A is present as both a full-length plasma membrane-localized form and a soluble ectodomain form in cell culture. Mutation of the furin consensus sequence results in abrogation of ectodysplasin A receptor-mediated signaling (48). Collagen XXIII is newly described, and thus, no human mutations have yet been associated with it. It is tempting, however, to speculate that alterations of the furin cleavage site will be found and that preventing the release of the ectodomain will have pathological consequences.

Acknowledgments—We thank M. Daamen for excellent technical assistance and Drs. J. Blume and M. Plomann for helpful suggestions with the brefeldin A experiments.

REFERENCES

1. Franzke, C.-W., Bruckner, P., and Bruckner-Tuderman, L. (2005) *J. Biol. Chem.* **280**, 4005–4008
2. Franzke, C.-W., Tasanen, K., Schacke, H., Zhou, Z., Tryggvason, K., Mauch, C., Zigrino, P., Sunnarborg, S., Lee, D. C., Fahrenholz, F., and Bruckner-Tuderman, L. (2002) *EMBO J.* **21**, 5026–5035
3. Hashimoto, T., Wakabayashi, T., Watanabe, A., Kowa, H., Hosoda, R., Nakamura, A., Kanazawa, I., Arai, T., Takio, K., Mann, D. M., and Iwatsubo, T. (2002) *EMBO J.* **21**, 1524–1534
4. Vaisanen, M. R., Vaisanen, T., and Pihlajaniemi, T. (2004) *Biochem. J.* **380**, 685–693
5. Banyard, J., Bao, L., and Zetter, B. R. (2003) *J. Biol. Chem.* **278**, 20989–20994
6. Koch, M., Veit, G., Stricker, S., Bhatt, P., Kutsch, S., Zhou, P., Reinders, E., Hahn, R. A., Song, R., Burgeson, R. E., Gerecke, D. R., Mundlos, S., and Gordon, M. K. (2006) *J. Biol. Chem.* **281**, 21546–21557
7. Mayer, G., Boileau, G., and Bendayan, M. (2004) *J. Histochem. Cytochem.* **52**, 567–579
8. Molloy, S. S., Anderson, E. D., Jean, F., and Thomas, G. (1999) *Trends Cell Biol.* **9**, 28–35
9. Thomas, G. (2002) *Nat. Rev. Mol. Cell Biol.* **3**, 753–766
10. Werb, Z. (1997) *Cell* **91**, 439–442
11. Werb, Z., and Yan, Y. (1998) *Science* **282**, 1279–1280
12. Chen, Y., Molloy, S. S., Thomas, L., Gambee, J., Bachinger, H. P., Ferguson, B., Zonana, J., Thomas, G., and Morris, N. P. (2001) *Proc. Natl. Acad. Sci. U. S. A.* **98**, 7218–7223
13. Nakayama, K. (1997) *Biochem. J.* **327**, 625–635
14. Anderson, E. D., Molloy, S. S., Jean, F., Fei, H., Shimamura, S., and Thomas, G. (2002) *J. Biol. Chem.* **277**, 12879–12890
15. Ehehalt, R., Keller, P., Haass, C., Thiele, C., and Simons, K. (2003) *J. Cell Biol.* **160**, 113–123
16. von Tresckow, B., Kallen, K. J., von Strandmann, E. P., Borchmann, P., Lange, H., Engert, A., and Hansen, H. P. (2004) *J. Immunol.* **172**, 4324–4331
17. Matthews, V., Schuster, B., Schutze, S., Bussmeyer, I., Ludwig, A., Hundhausen, C., Sadowski, T., Saftig, P., Hartmann, D., Kallen, K. J., and Rose-John, S. (2003) *J. Biol. Chem.* **278**, 38829–38839
18. Zimina, E. P., Bruckner-Tuderman, L., and Franzke, C.-W. (2005) *J. Biol. Chem.* **280**, 34019–34024
19. Simons, K., and Ikonen, E. (1997) *Nature* **387**, 569–572
20. Simons, K., and Toomre, D. (2000) *Nat. Rev. Mol. Cell Biol.* **1**, 31–39
21. Brown, D. A., and London, E. (2000) *J. Biol. Chem.* **275**, 17221–17224
22. Zhang, Z. G., Bothe, I., Hirche, F., Zweers, M., Gullberg, D., Pfitzer, G., Krieg, T., Eckes, B., and Aumailley, M. (2006) *J. Cell Sci.* **119**, 1886–1895
23. Schacke, H., Schumann, H., Hammami-Hausli, N., Raghunath, M., and Bruckner-Tuderman, L. (1998) *J. Biol. Chem.* **273**, 25937–25943
24. Rockwell, N. C., Krysan, D. J., Komiya, T., and Fuller, R. S. (2002) *Chem. Rev.* **102**, 4525–4548
25. Seidah, N. G., Chretien, M., and Day, R. (1994) *Biochimie (Paris)* **76**, 197–209
26. Seidah, N. G., Hamelin, J., Mamarbachi, M., Dong, W., Tardos, H., Mbikay, M., Chretien, M., and Day, R. (1996) *Proc. Natl. Acad. Sci. U. S. A.* **93**, 3388–3393
27. Harder, T., Scheiffele, P., Verkade, P., and Simons, K. (1998) *J. Cell Biol.* **141**, 929–942
28. Saslowsky, D. E., Lawrence, J., Ren, X., Brown, D. A., Henderson, R. M., and Edwardson, J. M. (2002) *J. Biol. Chem.* **277**, 26966–26970
29. Friedrichson, T., and Kurzchalia, T. V. (1998) *Nature* **394**, 802–805
30. Ilangumaran, S., and Hoessli, D. C. (1998) *Biochem. J.* **335**, 433–440
31. Kojro, E., Gimpl, G., Lammich, S., Marz, W., and Fahrenholz, F. (2001) *Proc. Natl. Acad. Sci. U. S. A.* **98**, 5815–5820
32. Smart, E. J., Ying, Y. S., Conrad, P. A., and Anderson, R. G. (1994) *J. Cell Biol.* **127**, 1185–1197
33. Klausner, R. D., Donaldson, J. G., and Lippincott-Schwartz, J. (1992) *J. Cell Biol.* **116**, 1071–1080
34. Hurtley, S. M. (1992) *Trends Biochem. Sci.* **17**, 325–327
35. Jean, F., Stella, K., Thomas, L., Liu, G., Xiang, Y., Reason, A. J., and Thomas, G. (1998) *Proc. Natl. Acad. Sci. U. S. A.* **95**, 7293–7298
36. Jean, F., Thomas, L., Molloy, S. S., Liu, G., Jarvis, M. A., Nelson, J. A., and Thomas, G. (2000) *Proc. Natl. Acad. Sci. U. S. A.* **97**, 2864–2869
37. Snellman, A., Keranen, M. R., Hagg, P. O., Lamberg, A., Hiltunen, J. K., Kivirikko, K. I., and Pihlajaniemi, T. (2000) *J. Biol. Chem.* **275**, 8936–8944
38. Stieneke-Grober, A., Vey, M., Anglikar, H., Shaw, E., Thomas, G., Roberts, C., Klenk, H. D., and Garten, W. (1992) *EMBO J.* **11**, 2407–2414
39. Molloy, S. S., Thomas, L., Van Slyke, J. K., Stenberg, P. E., and Thomas, G. (1994) *EMBO J.* **13**, 18–33
40. Heerklotz, H. (2002) *Biophys. J.* **83**, 2693–2701
41. Shogomori, H., and Brown, D. A. (2003) *Biol. Chem.* **384**, 1259–1263
42. Vaisanen, T., Vaisanen, M. R., and Pihlajaniemi, T. (2006) *J. Biol. Chem.* **281**, 33352–33362
43. Hancock, J. F. (2006) *Nat. Rev. Mol. Cell Biol.* **7**, 456–462
44. Kenworthy, A. K., Nichols, B. J., Remmert, C. L., Hendrix, G. M., Kumar, M., Zimmerberg, J., and Lippincott-Schwartz, J. (2004) *J. Cell Biol.* **165**, 735–746
45. Nichols, B. J., Kenworthy, A. K., Polishchuk, R. S., Lodge, R., Roberts, T. H., Hirschberg, K., Phair, R. D., and Lippincott-Schwartz, J. (2001) *J. Cell Biol.* **153**, 529–541
46. Maretzky, T., Reiss, K., Ludwig, A., Buchholz, J., Scholz, F., Proksch, E., de Strooper, B., Hartmann, D., and Saftig, P. (2005) *Proc. Natl. Acad. Sci. U. S. A.* **102**, 9182–9187
47. Schneider, P., Street, S. L., Gaide, O., Hertig, S., Tardivel, A., Tschopp, J., Runkel, L., Alevizopoulos, K., Ferguson, B. M., and Zonana, J. (2001) *J. Biol. Chem.* **276**, 18819–18827
48. Elomaa, O., Pulkkinen, K., Hannelius, U., Mikkola, M., Saarialho-Kere, U., and Kere, J. (2001) *Hum. Mol. Genet.* **10**, 953–962

³ G. Veit, J. Käpylä, M. Zweers, B. Eckes, J. Eble, M. K. Gordon, J. Hein, and M. Koch, unpublished data.

Immunoglobulin heavy chain gene analysis in bone marrow biopsies and corresponding lymph node specimens: Dependency on pre-treatment, histological subtype and extension of B-cell lymphoma

MARGARETE ODENTHAL^{1*}, UDO SIEBOLTS^{1,2*}, KAREN ERNESTUS¹, DANIEL DISSE¹, HANS PETER DIENES¹ and CLAUDIA WICKENHAUSER¹

¹Institute of Pathology, ²Center for Molecular Medicine (CMMC), University of Cologne, Kerpener Str. 62, D-50924 Cologne, Germany

Received October 17, 2007; Accepted December 14, 2007

Abstract. Bone marrow biopsies (BMB) are the conventional staging method for assessing marrow involvement by lymphoma. Morphological criteria provide basic data determining their dignity, but concerning microfocal infiltrates, these criteria are rather inaccurate. Here, by examination of immunoglobulin H (IgH) receptor rearrangement and comparison of medullar and nodular lymphoma sites, diagnostic reliability was improved. Employing non-nested IgH rearrangement analysis with FR3A and JHa consensus primers, B-cell clonality was assessed on glutardialdehyde fixed, decalcified BMB with and without lymphoma infiltration and on the corresponding lymph node specimens. Malignancy was confirmed when polymerase chain reaction (PCR) generated no more than two peaks and was observed in 60% of the medullar B-cell lymphoma. Comparison of lymph node tissues and BMB revealed an identical pattern in 50% of the probes. In 25% of the cases a single clonal peak derived from the lymph node tissues was also observed in the BMB but was surrounded by additional peaks. Here, direct comparison of the data permitted determination of lymphoma in the BMB. Therefore, IgH FR3 PCR analysis is a suitable tool to examine small lymphoid infiltrates in BMB, and direct comparison with corresponding nodal lymphoma can further facilitate estimation of their dignity.

Introduction

There are still conflicting opinions over the distinction between benign (reactive) focal lymphoid aggregates and focal infiltrates of malignant lymphomas in BMB (1-4). Although in BMB particularly histotopography and cytomorphology of lymphoid infiltrates and an increase in reticulin fibers may lead to a certain suspicion concerning their dignity, the morphological evaluation lacks diagnostic reliability particularly concerning microfocal infiltrates and biopsies with inferior quality (5). In daily routine diagnostics, however, the hematopathologist is frequently confronted with this differential diagnosis especially with respect to lymphoma staging, as well as for assessing treatment response and/or restaging. In addition, in lymphoproliferative diseases without LN involvement, diagnosis can only be ascertained in suitable BMB.

IgH FR3 PCR analysis has already been used by others to check clonality of lymphoid infiltrates in BMB (6-12). However, until now the support of corresponding LN clonality analysis in diagnosis of BM involvement has not been investigated systematically. Therefore, in this retrospective study we evaluated the impact of this assay on glutardialdehyde (GA)-fixed, decalcified BMB especially with regard to small medullar lymphoid infiltrates. Data were then compared with those obtained from corresponding lymphoma-infiltrated LN tissues, and this assay facilitated the interpretation of BMB-derived data. When the histomorphology of the BMB was compared with the clonality data, peritrabecular position and increase of reticular fibers were the most significant features indicating malignancy. Prerequisites for a high quality hematological diagnosis therefore incorporate the optimal histological processing of BMB, IgH rearrangement analysis and, ideally, comparison of nodal and medullar lymphoma sites.

Materials and methods

Tissue samples. Paraffin wax-embedded specimens of BMB and LN tissue were analyzed from a total of 40 patients

Correspondence to: Dr Claudia Wickenhauser, Institute of Pathology, University of Cologne, Kerpener Str. 62, D-50924 Cologne, Germany
E-mail: c.wickenhauser@uni-koeln.de

*Contributed equally

Key words: lymphoma, immunoglobulin H receptor rearrangement, bone marrow biopsy

whose files were archived at the Institute of Pathology of the University of Cologne, Germany.

Selection of BMB occurred in a three-step procedure. Firstly, patients with nodal ascertained chronic lymphatic leukemia of B-cell type (B-CLL), mantle cell lymphoma (MCL) and follicular lymphoma (FL) grade 1 to grade 2 were selected employing the WHO classification system. From these patients, BMB drawn from our files were stained, and specimens with lymphoid infiltrates were subdivided according to the proportion of the infiltrates with respect to the hematopoietic area. Groups with infiltrate densities of 5, 10, 15, 30, and 80% were chosen. Each group consisted of five patients. LN specimens of the selected patients were analyzed separately. Histological appraisal including immunohistochemistry was performed independently by two experienced hematopathologists.

In addition, we chose each of five BMB infiltrated by malignant plasma cell myeloma (MM) and immunocytoma (IC). In these cases, monotypic light chain expression was ascertained by immunohistochemistry. The biopsies were subdivided according to their proportion of tumor cell population. Finally, five BMB fixed in buffered 4% formalin fixative were analyzed.

Negative controls comprised five LN specimens with follicular hyperplasia as well as ten BMB from patients with lymphoid infiltrates and well-known immunomodulatory/infectious diseases like autoimmune thyroiditis and hepatitis C or unclear anemia. As a further positive control we chose the L1236 Hodgkin's lymphoma cell line (13).

Processing of BMB and histological staining. The main group of BMB was fixed in a solution of 30 ml formalin (at least 35%, Merck, Darmstadt, Germany), 20 ml glutaraldehyde 25% (Merck) and 15.8 g calcium acetate (Merck) and 1000 ml Aqua dest (Schaefer fixative). Decalcification was conducted for 3-4 days in 10% Tris-buffered ethylenediaminetetraacetic acid (EDTA; Merck) pH 7.2-7.4. The second group of BMB was fixed in buffered 4% formalin fixative while decalcification was also conducted in EDTA. Sections were stained with Giemsa, naphthol-AS-D-chloroacetate esterase and Gomori's stain for reticulin fibers. Five BMB (2 patients with MCL, 2 with B-CLL and 1 patient with FL grade I) were fixed in buffered 4% formalin fixative.

Processing of LN specimens and histological staining. All lymph node specimens were fixed in buffered 4% formalin fixative and paraffin embedded. Slides were stained with H&E and Giemsa.

Immunohistochemistry. Deparaffinized 3 to 5 mm sections were rehydrated, and heat-induced epitope retrieval was performed by microwave method in 0.1 M sodium citrate buffer (Merck), pH 6.0. Monoclonal antibody collection included L26 against CD20 (Dako, Hamburg, Germany; dilution 1:100) as a pan-B-cell marker, F7.2.38 against CD3 (Dako; 1:100) as pan-T-cell marker, R10-21-F3 against light chain κ and N10/2 against light chain λ (both from Dako). The specimens were immunostained according to the ABC method. The secondary biotinylated antibody and the streptavidin/alkaline phosphatase conjugate were applied

according to the manufacturer's instructions (BioGenex, San Ramon, CA, USA). New fuchsin (Serva, Heidelberg, Germany) and naphthol-AS-BI phosphate (Sigma) were used as chromogens. Appropriate positive and negative control stainings were run simultaneously.

Extraction of DNA from tissue sections. Extraction of DNA was performed as described previously (14). In brief, one to three 8 μ m paraffin wax-embedded sections were dewaxed in xylene by incubation at 65°C for 5 min. After vortexing, samples were centrifuged at 13,000 rpm. The procedure was repeated three times. The dewaxed sections were then washed in 500 μ l 100% ethanol. After lysis in 200 μ l proteinase K buffer [500 μ g/ml proteinase K (Gibco, Gaithersburg, MD, USA), 50 mM Tris/HCl, pH 7.4, and 5 mM EDTA, pH 8.0], nucleic acids were extracted by phenol/chloroform and subsequently precipitated with 300 mM sodium acetate and isopropanol. Each series of DNA extractions included sections taken from blocks of pure paraffin wax, which were cut between. The isolated DNA was dried, re-suspended in 25 μ l H₂O and stored at -20°C.

Primers for β -globin PCR analysis. The quality of the DNA was evaluated by amplifying fragments of the human β -globin locus (forward, ACA-CAA-CTG-TGT-TCA-CTA-GC and reverse, CAA-CTT-CAT-CCA-CGT-TCA-CC; length of the amplicon, 109 bp).

Primers for IgH PCR. PCR analysis of the IgH gene involved the use of a consensus primer pair with the upstream primer being homologous to a V segment and the downstream primer annealing to a J segment. In detail, performing a non-nested PCR, a consensus FR3A primer was used as upstream primer (15), and a consensus JHa primer as downstream primer (16,17): FR3A primer (5' IRD 800 fluorochrome end-labeled), 5'-ACA CGG C(CT) (GC) TGT ATT ACT GT-3'; JHa primer, 5'-ACC TGA GGA GAC GGT GAC C-3'.

PCR approach and analysis. A hot start PCR approach was chosen. Analysis was performed in a thermocycler (Biometra). The reaction mix (50 μ l) contained 1.5 μ l, 10 μ M of each primer, 10 μ l, 1 mM each of dNTPs, 5 μ l 10X concentrated PCR buffer (25 mM MgCl₂ in 100 mM Tris-HCl and 500 mM KCl pH 8.3, 20°C) 0.2 μ l of Taq DNA polymerase (5 units/ μ l) and 1.5 μ l genomic DNA and 50 μ l H₂O (Merck). A PCR cycle consisted of annealing for 1 min at 52°C, extension for 1 min at 72°C, and denaturation for 1 min at 94°C. Preceding each round, the PCR reaction was heated to 94°C for 5 min, and after each round a final extension step of 5 min at 72°C was performed (40 cycles). Each experiment was replicated and contained a tube without DNA template (as a negative control), a tube whose template was DNA from a patient with ascertained MM, and native material from the L1236 cell line (positive controls).

Agarose gels. Electrophoresis was performed with PCR-amplified material (10 μ l) in 3% agarose gels in TAE buffer at 125 volts for 40 min, and the DNA was visualized under short wavelength ultraviolet light after ethidium bromide staining of the gel.

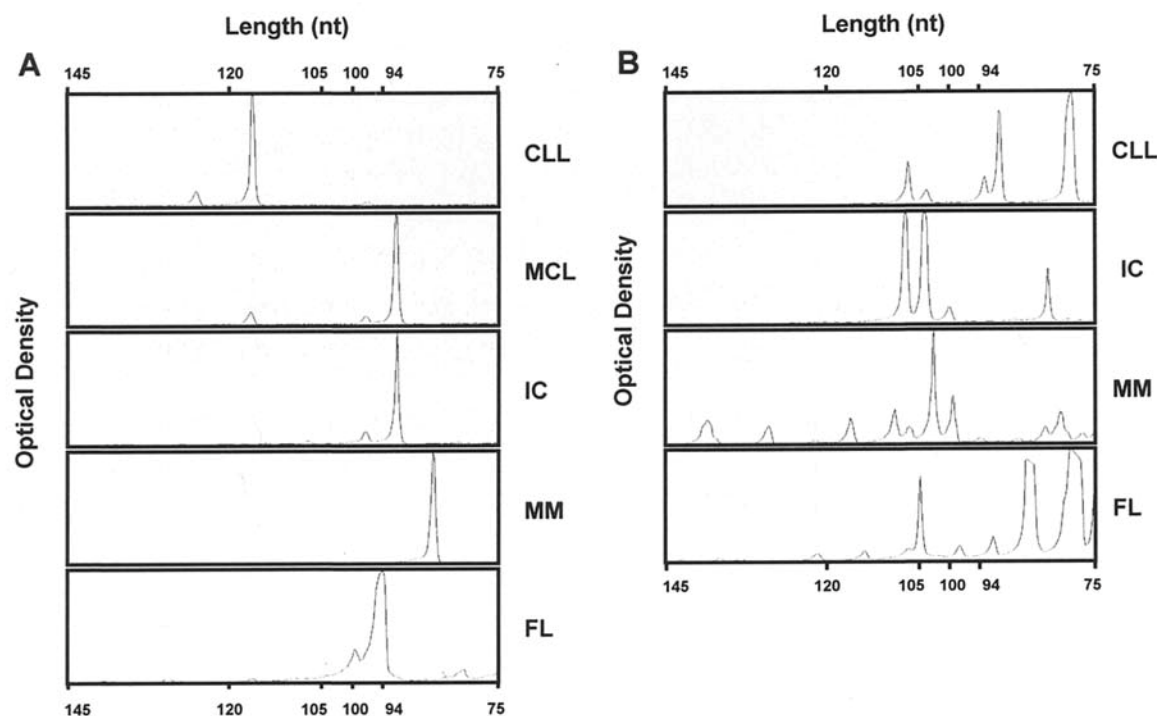


Figure 1. Computer-assisted fragment length analysis of IgH FR3 PCR amplification products from bone marrow biopsies (BMB). (A) A clear peak at defined nucleotide length indicating monoclonality of lymphoid infiltrates is visible for the different lymphoma entities. CLL, chronic lymphatic leukemia; MCL, mantle cell lymphoma; and IC, immunocytoma; MM, multiple myeloma; and FL, follicular lymphoma. (B) A multi-peak pattern indicates several B-cell subclones. The abscissa indicates the length of the amplicons in nucleotides (nt); the ordinate displays relative optical density.

Polyacrylamide gels. PCR products were run on 6% non-denaturing polyacrylamide gel electrophoresis (PAGE) overnight at 50°C and 1500 V/41 cm employing an automated sequencer (LI-COR DNA-Analyzer Gene Reader 4200, MWG-Biotech, Ebersberg). The resolution of the PAGE was sufficient for detection of one base differences of amplicons, and genescan analysis of all samples was performed for assessment of IgH-specific PCR products. Illustration of the PAGE results as electropherograms was realized by measurement of optical densities within the gels employing the Scion Image Software release alpha 4.0.3.2 software (Scion Corp., Frederick, MD, USA).

Sequencing of the PCR products. PCR results with consensus primers were validated using sequence-specific primers labeled with the IRD 800 fluorescence dye (MWG-Biotech). DNA bands of amplicons were cut from the gel and extracted using the Qiaex Kit (Qiagen, Hilden, Germany). The 100 µl eluates were precipitated with 300 µM sodium acetate, glycogen, and two volumes of ethanol, and the DNA was redissolved in 10 µl H₂O. Two microliters of each sample was taken for PCR sequencing using the IRD 800-labeled JHa-seq primer: 5'-IRD 800-ACC TGA GGA GAC GGT GAC C-3'. Sequence analysis was carried out on a LI-COR DNA analyzer Gene Reader 4200. The sequence products were compared with the published data of the NCBI database by BLAST analyses to exclude amplification of a false amplicon.

Results

IgH rearrangement analysis in GA-fixed decalcified BMB. Prior to clonality analysis, PCR analysis for human β-globin

was performed as a control for DNA extraction and delivered definite bands in all samples under study. Performing non-nested IgH rearrangement analysis with FR3A and JHa consensus primers, analysis of all ten BMB with reactive lymphoid infiltrates and 15 out of 25 (60%) GA-fixed BMB with either medullar ascertained B-cell lymphoma or nodular ascertained B-cell lymphoma and suspicious lymphoid infiltrates in the corresponding BMB, resulted in a distinct band in the agarose gels, respectively. In the latter group 18 out of 25 cases (72%) presented definite amplicon visible by polyacrylamide gel electrophoresis. Of these cases, in 14 out of 18 BMB, employing electropherogram analysis, IgH rearrangement analysis resulted in no more than two main peaks (Fig. 1A). Specifically, in two cases out of five FL, in five cases out of five MCL, in two cases out of five B-CLL, in two cases out of five MM and three cases out of five IC a clonal rearrangement with no more than two bands was detected. The other four cases, two cases of FL, one case of B-CLL and one of MM presented three and more irregularly arranged peaks according to electropherogram analysis (Fig. 1B). In 7 out of 25 BMB with ascertained infiltration by B-cell lymphoma no peaks were visualized (Table I). In all cases with reactive lymphoid infiltrates a typical Gaussian distribution of the peak pattern was observed.

In individual cases, distinct amplicons visible in the agarose gels were cut out, extracted, and sequenced. The sequences achieved were compared with the published data of the NCBI database by BLAST analyses, and known VDJ regions were detected in all cases.

Outcome of IgH rearrangement analysis is independent of lymphoma extension in BMB. When reliability of the method

Table I. Correlation between proportion of medullar B-cell infiltrates and clonality.

	5%	10%	15%	30%	>80%
FL	1/1	0/1	0/1	1/1	0/1
MCL	1/1	1/1	1/1	1/1	1/1
B-CLL	1/1	0/1	0/1	1/1	0/1
MM	0/0	1/1	0/1	0/2	1/1
IC	0/0	1/1	1/1	0/1	1/2

Medullar infiltration of nodal ascertained low-grade malignant B-cell lymphoma and each of five cases of malignant plasma cell myeloma (MM) and of LP-immunocytoma (IC). The outcome of clonality analysis depends on histological subtype of lymphoma but not on the density of lymphoma infiltrates within the bone marrow. FL, follicular lymphoma; B-CLL, chronic lymphatic leukemia of B-cell type; MCL, mantle cell lymphoma. The degree of infiltrate per hematopoietic area is labeled horizontally. Cases with one or two peaks/overall cases are described for the various subgroups.

was evaluated, dependency of lymphoma extension in BMB on the significance of IgH rearrangement analysis was tested. Lymphoma infiltrates ranging from 5 to 80% lymphoid cells per hematopoietic area were compared. As described in Fig. 2 IgH rearrangement analysis of medullar mantle cell lymphoma infiltrates always indicated malignancy. Concerning BM infiltration by ascertained germinal center or post-germinal center lymphoma, malignancy was proved in a subset of cases, irrespective of the lymphoma extension (Table I). In all assays, clonality was detectable even in medullar infiltrates representing less than 5% of the hematopoietic area.

Peritrabecular position and aggregation of reticular fibers are the most important histological parameters indicating microfocal B-cell lymphoma infiltration in BMB. When data of IgH rearrangement analysis were obtained, histology and specific peculiarities of lymphoid infiltrates within the BMB were reevaluated. In MM biopsies and in most biopsies infiltrated by IC, immunohistochemistry of light and heavy chain expression turned out to be a very valid marker indicating malignancy (Fig. 3A and B). However, immunohistochemical analysis of B- and T-cell distribution failed to be a clear-cut parameter as did evaluation of cytological details in B-CLL, FL and MCL (Fig. 3C and D). Concerning small infiltrates (<15%) the most significant histological parameters were peritrabecular position and aggregation of reticular fibers (Fig. 3E and F).

Comparison of IgH rearrangement analysis in nodal and medullar lymphoma infiltrates facilitates interpretation of clonality curves. Of all patients suffering from B-CLL, MCL and FL, nodal involvement was histologically ascertained. In this approach IgH rearrangement of each of the five cases was analyzed in the LN tissue as well as in the affected BMB. Clonality curves were compared and initially most conspicuous difference resulted in the clear peaks derived from LN tissue and more shaky peaks of minor quality in

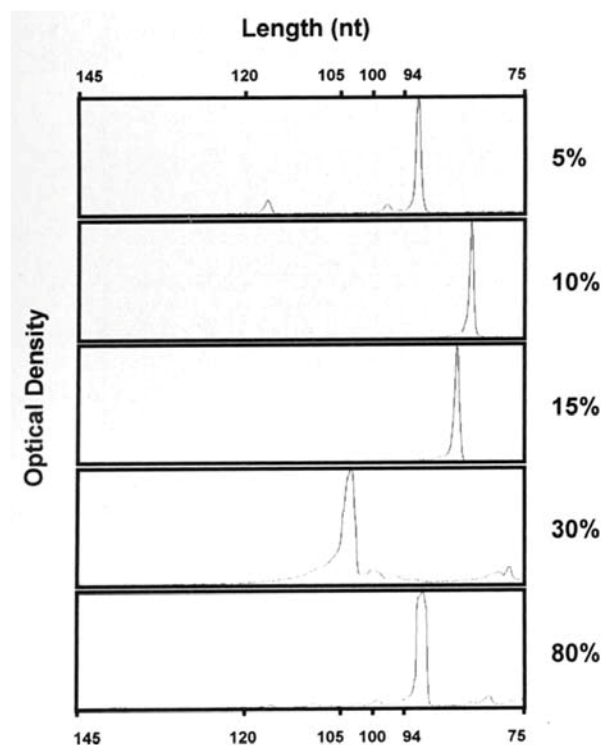


Figure 2. Computer-assisted fragment length analysis of IgH FR3 PCR amplification products from bone marrow biopsies (BMB). Five cases of nodular ascertained mantle cell lymphoma (MCL) with bone marrow infiltration were analyzed. Clonality of small infiltrates (5%) was also detected. The extent of lymphoma infiltrates is indicated on the right side of the figure. The abscissa indicates the length of the amplicons in nucleotides (nt); the ordinate displays relative optical density.

most of the GA-fixed BMB (Fig. 4A and C). In all cases where IgH PCR did not produce definite amplicons, this result was observed congruently in BMB and the corresponding LN tissues (4 out of 15 cases). A congenic pattern with no more than two peaks was observed in 4 out of 15 cases (Fig. 4A). In 4 out of 15 cases, peaks appeared at the same position in both sources, but prominence of these peaks was different and additional peaks appeared in the BMB-derived lymphoma tissues (Fig. 4B). In 3 out of 15 cases the curve progression was largely different when both tissues were compared, although a slightly congenic accordance still occurred (Fig. 4C; Table II).

Concerning non-neoplastic lymphoid tissue, a typical Gaussian distribution was observed in all of the 5 LN tissues under study and in all 10 BMB with non-neoplastic lymphoid infiltrates (Fig. 4D).

Replacement of GA fixation by buffered formalin improves quality of IgH rearrangement analysis. To evaluate whether the shaky peaks following PAGE analysis of IgH rearrangement analysis were induced by GA fixation or decalcification, GA fixation was replaced by fixation in buffered formalin in a small collection of BMB. With the application of this procedure, the quality of the peak pattern increased. Following this procedure, as demonstrated in Fig. 5, curve progression in BMB and the corresponding LN tissues was of identical quality in these cases.

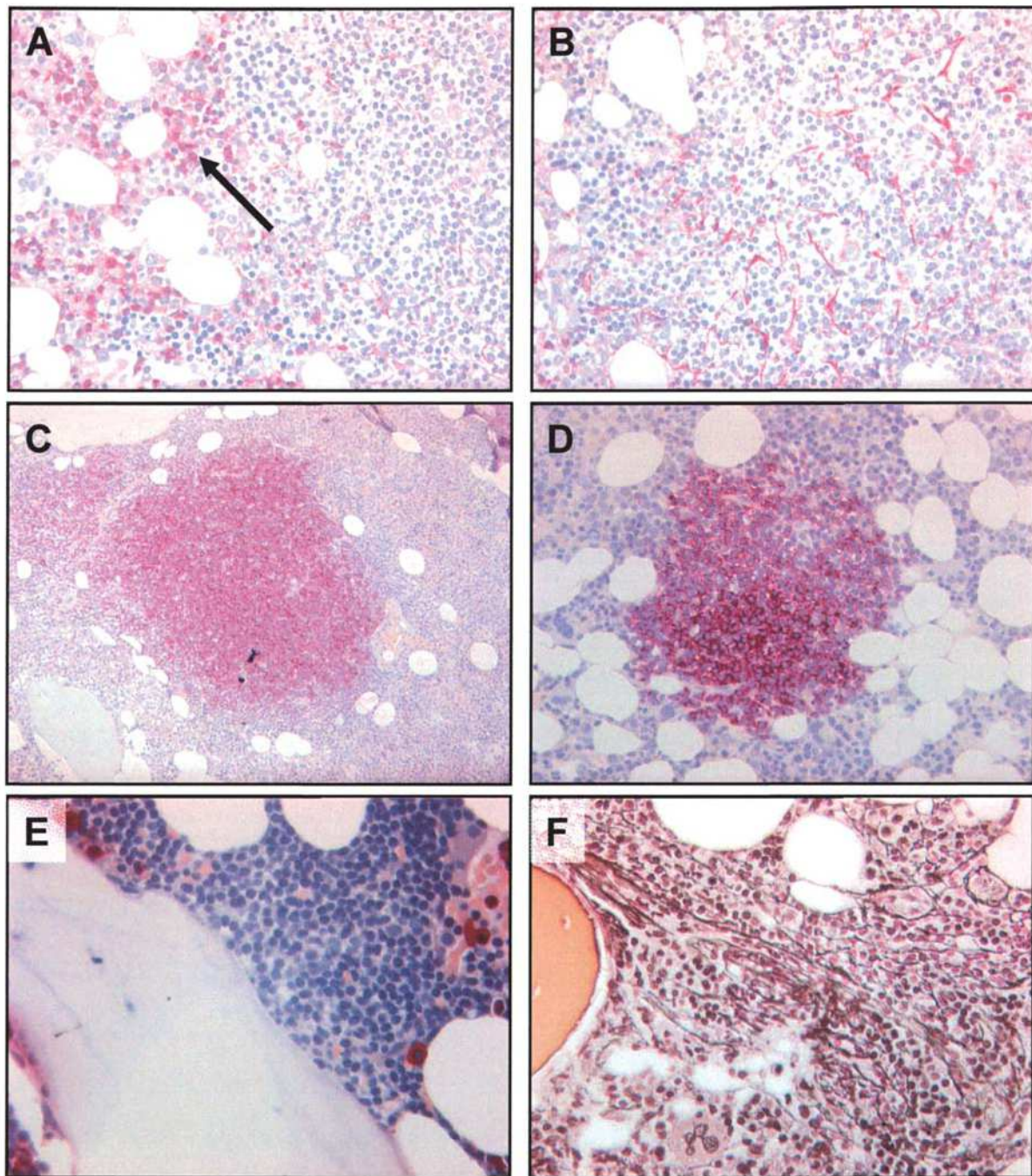


Figure 3. Histochemical analysis of lymphoid infiltrates in bone marrow biopsies (BMB). Detection of κ (A) and λ (B) light chain expression clearly indicates monoclonal plasma cell population within the infiltrate (arrow). Lymphonodular infiltrate of chronic lymphatic leukemia (B-CLL) with a mixed pattern of (C) CD20-positive B-cells and (D) CD3-positive T-cells. Here, immunohistochemistry does not contribute to the determination of dignity. (E) Chloracetate esterase staining of BMB reveals a small lymphoid infiltrate in peritubercular position indicating malignancy in a patient with nodular ascertained mantle cell lymphoma (MCL). (F) Gomori silver staining of the same case. The increase in reticular fiber density also discloses malignancy.

Table II. Comparison of the clonality pattern between nodal and medullary lymphoma.

	Congeneric pattern	Identical peaks, different background	Different pattern	No amplificon
FL	0/5	1/5	2/5	2/5
MCL	4/5	1/5	0/5	0/5
B-CLL	0/5	2/5	1/5	2/5

Comparison between IgH rearrangement analysis of the nodal and medullary lymphoma sites of individual patients. FL, follicular lymphoma; B-CLL, chronic lymphatic leukemia of B-cell type; and MCL, mantle cell lymphoma. Cases per overall cases are described for the various subgroups.

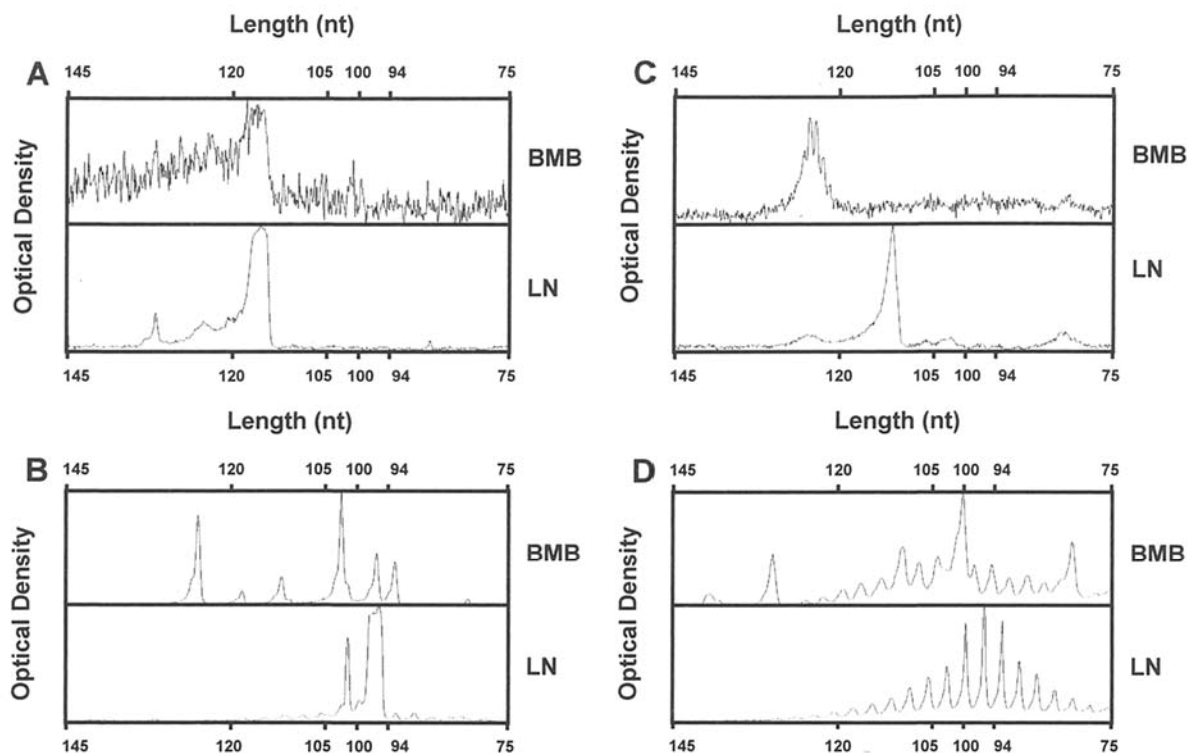


Figure 4. Computer-assisted fragment length analysis of IgH FR3 PCR amplification products. Analysis of corresponding bone marrow (BMB) and lymph node (LN) infiltrates. (A) Congruent pattern in a case of B-CLL. Shaky pattern in the BM analysis indicates inferior DNA quality following glutardialdehyde fixation. (B) Multi-peak pattern in the BMB-derived lymphoid tissue while analysis of the LN tissue revealed two clear peaks indicating clonality (case with FL). In this case, comparison of both curves facilitates interpretation of the data. (C) In other samples (here case with B-CLL) peaks at different nucleotide length indicate dominance of diverse clones at different tumor sites, although a slight elevation at the position of the main peak at the BMB is also seen in the LN analysis. (D) Gaussian distribution of amplification products in normal LN tissue (below) and also a multi-peak pattern in the BMB with reactive lymphoid infiltrates. The abscissa indicates the amplicon length in nucleotides (nt); the ordinate displays relative optical density.

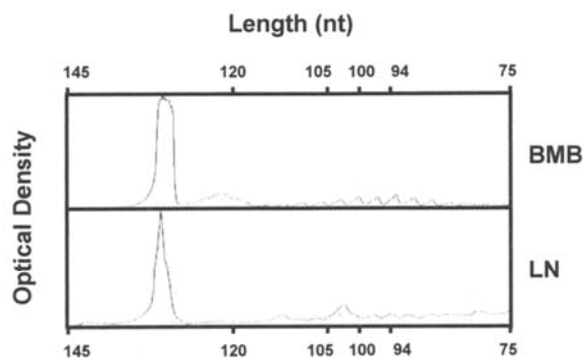


Figure 5. Computer-assisted fragment length analysis of IgH FR3 PCR amplification products. When glutardialdehyde fixative was replaced by buffered formalin, comparison of electropherograms from lymph node (LN) tissues and bone marrow biopsies (BMB) revealed identical quality of the curves in a case with chronic lymphatic leukemia (B-CLL). The abscissa indicates the amplicon length in nucleotides (nt); the ordinate displays relative optical density.

Discussion

Morphologic examination is the generally accepted method for determining bone marrow involvement by lymphoma in patients evaluated for extent of disease at diagnosis and after therapy. A clear-cut distinction between benign lymphoid infiltrates and focal infiltration by low-grade B-non-Hodgkin's

lymphoma is possible in many cases when histotopography of lymphoid aggregates together with cytomorphology and density of reticular fibers are evaluated (5). Unfortunately, immunophenotyping in these cases is only of limited use because GA-containing fixatives allow the usage only of a limited panel of antibodies and because immunohistochemical determination of light or heavy chain restriction is only possible in a subset of lymphoma entities (5). A diagnostic grey zone therefore affects primarily very small lymphoid infiltrates and BMB of inferior quality.

Molecular methods for determining clonality provide alternative techniques for evaluating suspicious or indeterminate lymphoid infiltrates and have the advantage of increased specificity and decreased subjectivity. The consensus PCR protocols can be effectively used in routine molecular diagnostic laboratories and yield highly reproducible results with no reported false-positive results. However, their major drawback is an increased false-negative rate. Possible technical reasons for false-negative results have been reviewed (18,19). In certain clonal populations, despite optimal reaction conditions, the consensus primers may lack sufficient homology to anneal with the pertinent IgH regions because of somatic hypermutation or ongoing mutations. Other reasons include competitive amplification of DNA from rearranged reactive bystanders, interfering chromosomal translocations or deletions. Although increasing the number of amplification cycles may enhance detection in some specimens, excessive cycling can result in increased polyclonal back-

ground smearing and nonspecific bands that complicate assay interpretation, because the polyclonal smear may mask a monoclonal band or a nonspecific band may mimic a clonal band (18). Quantitative mRNA analysis of light chain expression via real-time PCR assay is well suitable for the analyses of highly mutated germinal centre/post-germinal centre lymphoma (20). However, the diagnostic impact is restricted due to poorly preserved RNA and susceptibility to the extent of clonal medullar expansion and reactive background. Furthermore, only the discrimination of distinct rearrangement length distribution enables the investigator to directly compare medullar and nodular clonality profiles.

Performing non-nested IgH rearrangement analysis with FR3A and JHa consensus primers in GA-fixed BMB, a clonal rearrangement could be detected in 60% of the probes with lymphoma involvement, dependent on the lymphoma subtype. This finding is within the normal range as described by others when analyzing neoplastic LN tissues. When BMB were reevaluated with regard to the results of the clonality data, peritrabecular position of lymphoid infiltrates and increases in fiber density were the most significant parameters indicating clonal processes. In this context, as described before, the adoption of the naphthol-AS-D-chloroacetate esterase is a prerequisite for the detection of rather small infiltrates (5). Hence, the careful morphological examination of BMB will continue to be valuable in the future, although the diagnostic certitude decreased when lymphoma extension was low. Therefore, evidence of monoclonality in BMB with a lymphoma extension of <5% clearly indicates that IgH rearrangement analysis must be implemented in high quality hematological diagnostics. In this context it is important to state that patients with autoimmune diseases might also reveal clonal B-cell proliferation in the bone marrow due to auto-antigen stimulation (10). Therefore BMB-derived clonality data from patients with autoimmune diseases have to be interpreted with utmost care and in context with clinical and histomorphological data.

When lymphoma infiltrates of LN tissues and the corresponding BMB were compared, the inferior quality of DNA derived from GA-fixed BMB was apparent. In contrast, concurrent molecular testing of bone marrow lymphoid infiltrates derived from biopsies fixed in buffered formalin identified DNA with identical quality as observed in the corresponding nodal lymphoma tissues.

Our data further indicate that a direct comparison of clonality data from LN tissues and BMB can facilitate the interpretation of the analysis, irrespective of the processing of the BMB. Particularly the appraisal of additional peaks derived from polyclonal B-lymphoid background in BMB is much clearer when employing this comparative method.

Using bone marrow aspirates, false-negative results in clonality analysis are rather frequent due to the failure to aspirate sufficient lymphoma cells (21-23). Therefore the method presented here is clearly superior to the strategy of others examining the BMB solely for morphological analysis and smears for further molecular clonality analysis (18,24,25).

With an overall sensitivity of non-nested IgH rearrangement analysis of 60% in the BMB the values are slightly worse than described for the analysis of nodal lymphoma, probably

due to the inferior DNA quality of this GA fixative and also the decalcified material (26). Adaptation of the BIOMED-2 approach at this point has the potential to further increase sensitivity (27).

With an excellent specificity, our data clearly show that IgH FR3 PCR analysis of BMB is a reliable tool to analyze small lymphoid infiltrates of uncertain dignity which can be further improved by comparison with the corresponding nodal lymphoma. A systematic adoption of this approach must be endorsed in high quality hematological diagnostics.

References

- McKenna RW and Hernandez JA: Bone marrow in malignant lymphoma. *Hematol Oncol Clin North Am* 2: 617-635, 1988.
- Salisbury JR, Devereil MH and Cookson MJ: Three-dimensional reconstruction of benign lymphoid aggregates in bone marrow trephines. *J Pathol* 178: 447-450, 1996.
- Faulkner-Jones BE, Howie AJ, Boughton BJ and Franklin IM: Lymphoid aggregates in bone marrow: study of eventual outcome. *J Clin Pathol* 41: 768-775, 1988.
- Schmid C and Isaacson PG: Bone marrow trephine biopsy in lymphoproliferative disease. *J Clin Pathol* 45: 745-750, 1992.
- Thiele J, Zirbes TK, Kvasnicka HM and Fischer R: Focal lymphoid aggregates (nodules) in bone marrow biopsies: differentiation between benign hyperplasia and malignant lymphoma - a practical guideline. *J Clin Pathol* 52: 294-300, 1999.
- Brinckmann R, Kaufmann O, Reinartz B and Dietel M: Specificity of PCR-based clonality analysis of immunoglobulin heavy chain gene rearrangements for the detection of bone marrow involvement by low-grade B-cell lymphomas. *J Pathol* 190: 55-60, 2000.
- Lassmann S, Gerlach UV, Technau-Ihling K, Werner M and Fisch P: Application of BIOMED-2 primers in fixed and decalcified bone marrow biopsies: analysis of immunoglobulin H receptor rearrangements in B-cell non-Hodgkin's lymphomas. *J Mol Diagn* 7: 582-591, 2005.
- Pittaluga S, Tierens A, Dodoo YL, Delabie J and De Wolf-Peeters C: How reliable is histologic examination of bone marrow trephine biopsy specimens for the staging of non-Hodgkin lymphoma? A study of hairy cell leukemia and mantle cell lymphoma involvement of the bone marrow trephine specimen by histologic, immunohistochemical, and polymerase chain reaction techniques. *Am J Clin Pathol* 111: 179-184, 1999.
- Kremer M, Cabras AD, Fend F, *et al*: PCR analysis of IgH-gene rearrangements in small lymphoid infiltrates microdissected from sections of paraffin-embedded bone marrow biopsy specimens. *Hum Pathol* 31: 847-853, 2000.
- Engels K, Oeschger S, Hansmann ML, Hillebrand M and Kriener S: Bone marrow trephines containing lymphoid aggregates from patients with rheumatoid and other autoimmune disorders frequently show clonal B-cell infiltrates. *Hum Pathol* (In press).
- Fend F, Gschwendtner A, Gredler E, Thaler J and Dietze O: Detection of monoclonal B-cell populations in decalcified, plastic-embedded bone marrow biopsies with the polymerase chain reaction. *Am J Clin Pathol* 102: 850-855, 1994.
- Weirich G, Funk A, Hoepner I, *et al*: PCR-based assays for the detection of monoclonality in non-Hodgkin's lymphoma: application to formalin-fixed, paraffin-embedded tissue and decalcified bone marrow samples. *J Mol Med* 73: 235-241, 1995.
- Wolf J, Kapp U, Bohlen H, *et al*: Peripheral blood mononuclear cells of a patient with advanced Hodgkin's lymphoma give rise to permanently growing Hodgkin-Reed Sternberg cells. *Blood* 87: 3418-3428, 1996.
- Koehler CI, Mues MB, Dienes HP, Kriegsmann J, Schirmacher P and Odenthal M: *Helicobacter pylori* genotyping in gastric adenocarcinoma and MALT lymphoma by multiplex PCR analyses of paraffin wax embedded tissues. *Mol Pathol* 56: 36-42, 2003.
- Brisco MJ, Tan LW, Orsborn AM and Morley AA: Development of a highly sensitive assay, based on the polymerase chain reaction, for rare B-lymphocyte clones in a polyclonal population. *Br J Haematol* 75: 163-167, 1990.

16. Segal GH, Jorgensen T, Scott M and Braylan RC: Optimal primer selection for clonality assessment by polymerase chain reaction analysis: II. Follicular lymphomas. *Hum Pathol* 25: 1276-1282, 1994.
17. Segal GH, Jorgensen T, Masih AS and Braylan RC: Optimal primer selection for clonality assessment by polymerase chain reaction analysis: I. Low grade B-cell lymphoproliferative disorders of nonfollicular center cell type. *Hum Pathol* 25: 1269-1275, 1994.
18. Coad JE, Olson DJ, Christensen DR, *et al*: Correlation of PCR-detected clonal gene rearrangements with bone marrow morphology in patients with B-lineage lymphomas. *Am J Surg Pathol* 21: 1047-1056, 1997.
19. Coad JE, Olson DJ, Lander TA and McGlennen RC: Molecular assessment of clonality in lymphoproliferative disorders: I. Immunoglobulin gene rearrangements. *Mol Diagn* 1: 335-355, 1996.
20. Lehmann U, Bock O, Langer F and Kreipe H: Demonstration of light chain restricted clonal B-lymphoid infiltrates in archival bone marrow trephines by quantitative real-time polymerase chain reaction. *Am J Pathol* 159: 2023-2029, 2001.
21. Crescenzi M, Seto M, Herzig GP, Weiss PD, Griffith RC and Korsmeyer SJ: Thermostable DNA polymerase chain amplification of t(14;18) chromosome breakpoints and detection of minimal residual disease. *Proc Natl Acad Sci USA* 85: 4869-4873, 1988.
22. Martens AC, Schultz FW and Hagenbeek A: Nonhomogeneous distribution of leukemia in the bone marrow during minimal residual disease. *Blood* 70: 1073-1078, 1987.
23. Schwonzen M, Pohl C, Steinmetz T, *et al*: Immunophenotyping of low-grade B-cell lymphoma in blood and bone marrow: poor correlation between immunophenotype and cytological/histological classification. *Br J Haematol* 83: 232-239, 1993.
24. Crotty PL, Smith BR and Tallini G: Morphologic, immunophenotypic, and molecular evaluation of bone marrow involvement in non-Hodgkin's lymphoma. *Diagn Mol Pathol* 7: 90-95, 1998.
25. Kang YH, Park CJ, Seo EJ, *et al*: Polymerase chain reaction-based diagnosis of bone marrow involvement in 170 cases of non-Hodgkin lymphoma. *Cancer* 94: 3073-3082, 2002.
26. Lust JA: Molecular genetics and lymphoproliferative disorders. *J Clin Lab Anal* 10: 359-367, 1996.
27. Evans PA, Pott C, Groenen PJ, *et al*: Significantly improved PCR-based clonality testing in B-cell malignancies by use of multiple immunoglobulin gene targets. Report of the BIOMED-2 Concerted Action BHM4-CT98-3936. *Leukemia* 21: 207-214, 2007.

High diagnostic value of morphologic examination and molecular analysis of bone marrow biopsies in a case of BCR-ABL⁺ CML with clusters of blasts

Eva Markert · Udo Siebolts · Margarete Odenthal ·
Karl-Anton Kreuzer · Claudia Wickenhauser

Received: 23 October 2008 / Accepted: 16 January 2009 / Published online: 20 February 2009
© The Japanese Society of Hematology 2009

Abstract We report a clinical case of chronic myelogenous leukaemia (CML) with regional B-lymphoblastic transformation. Peripheral leukocytosis of $160 \times 10^9/L$, splenomegaly and fatigue suggested CML. In peripheral blood and bone marrow smears, white blood cells in all maturation stages and only few blasts were seen and therefore the diagnosis of chronic phase CML was proposed. Cytogenetics performed on peripheral blood cells revealed the characteristic t(9;22)(q34;q11) translocation as solitary abnormality. Analyzing the bone marrow biopsy a focal nodular B-lymphoid blast component was additionally seen. BCR-ABL FISH analysis demonstrated 31% atypical split signals in the B-lymphoid blasts and in the maturing myeloid cells, furthermore, BCR-ABL fusion transcripts were seen in the RT-PCR assay. Imatinib-based therapy led to temporary regression of peripheral leukocytosis. Bone marrow examination 3 weeks after therapy

induction demonstrated considerably reduced cellularity and the proportion of B-lymphoid blasts had decreased to 20% of the nuclear cells. BCR-ABL FISH analysis still presented 21% atypical split signals but levels of BCR-ABL transcripts had significantly fallen indicating a rather favourable prognosis. However, 3 months after diagnosis the patient relapsed and developed an immunodeficiency with soor esophagitis and aspergillus pneumonia. A therapy with dasatinib was not successful and the patient died in consequence of immunodeficiency. This report demonstrates the high diagnostic value of bone marrow biopsy in the evaluation of CML. Besides morphology investigation of diverse methods including RT-PCR and FISH performed on diagnostic bone marrow biopsies are obligatory for ideal monitoring of drug response.

Keywords CML · Bone marrow biopsy · B-ALL · FISH · RT-PCR

Eva Markert and Udo Siebolts contributed equally to this work.

E. Markert · M. Odenthal · C. Wickenhauser
Institute of Pathology, University Hospital of Cologne,
50924 Cologne, Germany

U. Siebolts · C. Wickenhauser (✉)
Institute of Pathology, University of Leipzig,
Liebigstrasse 26, 04103 Leipzig, Germany
e-mail: claudia.wickenhauser@uniklinik-leipzig.de

K.-A. Kreuzer
Department I of Internal Medicine,
University of Cologne, 50924 Cologne, Germany

U. Siebolts
Center for Molecular Medicine,
University of Cologne (CMMC),
50924 Cologne, Germany

1 Case report

Due to fatigue, weight loss and night sweat, a 65-year-old female patient visited her family doctor. Here, she presented a total leukocyte count of $160 \times 10^9/L$ with an absolute neutrophil count of $98 \times 10^9/L$, platelets of $186 \times 10^9/L$ and an erythrocyte count of $3.6 \times 10^{12}/L$. The patient was then transferred to the Department I of Internal Medicine, University of Cologne, with estimated diagnosis of chronic myelogenous leukaemia (CML). Here, the patient presented a moderate splenomegaly. Clinical chemistry detected elevated lactate dehydrogenase (LDH) (1,077 U/L). The peripheral blood smear confirmed strong elevation of the neutrophils in different stages of maturation, with peaks in the percentages of myelocytes

and of segmented neutrophils, blasts counted for 5% of the white blood cells. Bone marrow smears revealed hypercellular hematopoiesis with dominance of the left-shifted granulopoiesis. Megakaryocytes were small with hypolobated nuclei. A slight increase in myeloblasts was seen (8%). The bone marrow biopsy was hypercellular and micromegakaryocytes as well as Pseudo-Gaucher cells were visible (Fig. 1). However, also areas of blastic cells were seen (nodules with up to 60% of the hematopoietic area, Fig. 1) and diagnosis of blast phase CML was proposed. Immunohistochemically, these blasts were highly proliferative (Ki67 >90%) and stained for CD10, CD34, CD79a, and TdT while myeloid antigens were not coexpressed (see also Fig. 1). RT-PCR performed on the bone marrow biopsy revealed BCR-ABL fusion transcripts with a b2a2 junction (Fig. 2). Cytogenetic analysis of peripheral blood probes revealed the characteristic t(9;22)(q34;q11) translocation as solitary abnormality; no duplication of the Ph chromosome, trisomy 8, or isochromosome 17 was observed. Performing FISH on the bone marrow biopsy (DAKO cytation), BCR-ABL fusion gene was seen in the maturing neoplastic myelopoiesis as well as in the lymphoid blasts.

A treatment constituting of imatinib (Glivec® 400 mg/d) was administered. Three weeks after initiation of this therapy regimen leukocyte count decreased and thrombocytopenia and anemia were regressive. A second trephine biopsy was performed and revealed a marked decrease in cellularity. Also, an imposing regeneration of left-shifted erythropoiesis was seen accompanied by a significant reduction of granulopoiesis and megakaryopoiesis as well as a slight edema. Some micromegakaryocytes and few Pseudo-Gaucher cells were still seen (Fig. 1). The proportion of TdT positive blasts had decreased to 20% and a more diffuse infiltration pattern was now visible (Fig. 1). Consistent with these findings levels of BCR-ABL transcripts had significantly fallen (Fig. 2) and, analyzing FISH data, with 21% split signals a significant reduction of BCR-ABL positive cells was seen. The BCR-ABL positive cells still included lymphoid blasts as well as maturing myeloid cells (Fig. 2). In the further course a complete molecular remission could not be achieved and the Glivec® dose was raised to 600 mg/d. However, the patient again entered the hospital 3 months later with a B-lymphoid blast crisis. Despite a therapy with dasatinib the patient developed a severe pneumonia and died in an aspergillus sepsis.

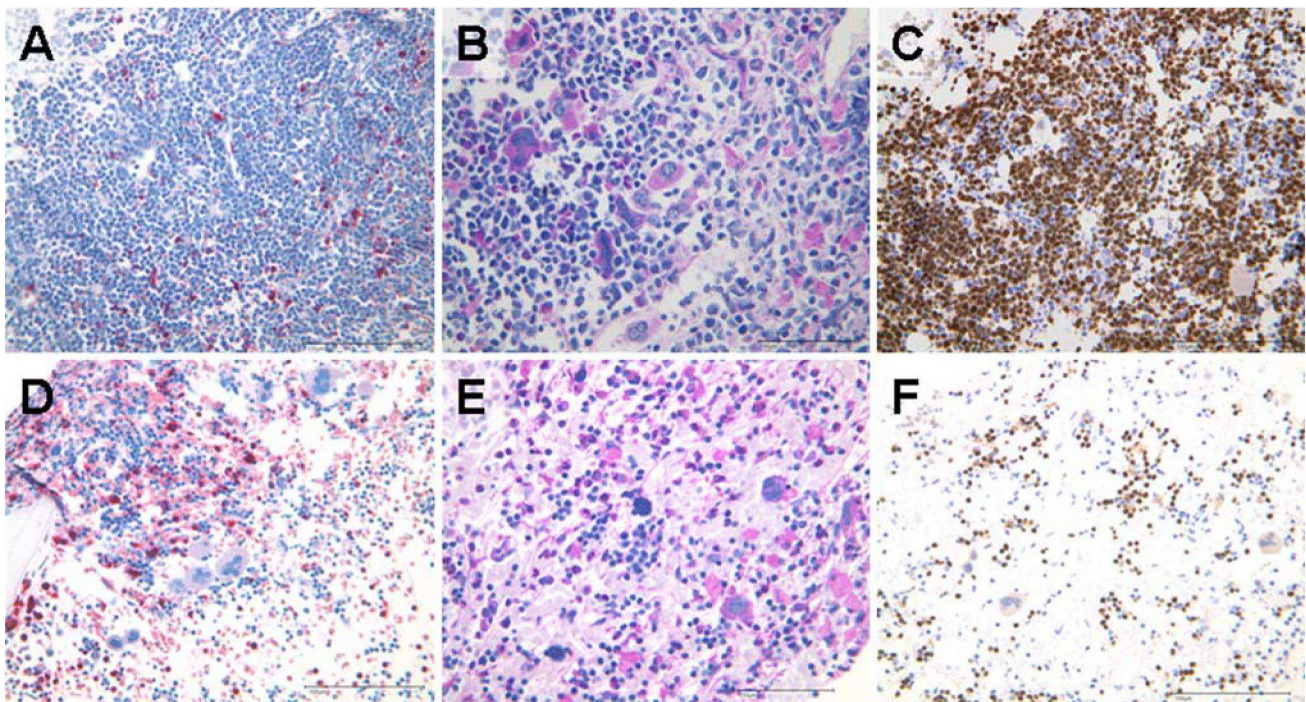


Fig. 1 Histomorphology of bone marrow biopsies. **a–c** Initial biopsy, **d–f** bone marrow biopsy taken 3 weeks after initiation of imatinib treatment (Glivec® 400 mg/d). **a, d** Chloracetatesterase staining. In **a** hot spots with only few cells of the granulopoietic lineage and an imposing blastic infiltrate are seen in some areas of the biopsy. After therapy induction (**d**) overall cell density decreased. Here, the blast density significantly decreased in all parts of the biopsy. Also, regeneration of left-shifted erythropoiesis is seen while granulopoiesis

is rather reduced. **b, e** PAS staining marking the pleomorphic megakaryopoiesis including micromegakaryocytes and Pseudo-Gaucher cells. In **e** number of Pseudo-Gaucher cells is diminished. **c, f** TdT immunohistochemistry with strong nuclear staining of nodular lymphoblasts were dominating areas of the first biopsy. After induction of imatinib therapy the proportion of TdT positive blasts had decreased to 20% and a more diffuse infiltration pattern is now visible (**a, c, d, f** magnification $\times 200$; **b, d** magnification $\times 400$)

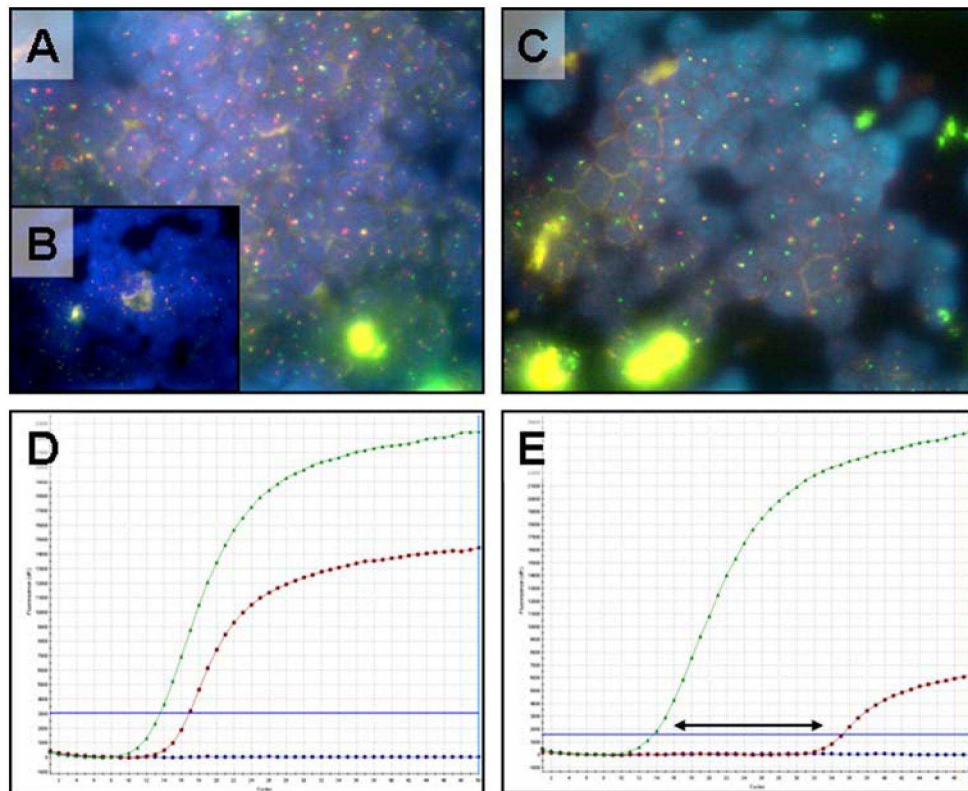


Fig. 2 Fluorescence in situ hybridization (FISH) employed to detect BCR-ABL t(9;22) translocations. The dual-color BCR-ABL probe enables the visualization of transformed cells by the appearance of red and green split signals while non-neoplastic cells typically present an unique yellow signal. In **a** a dominant proportion of split signals is visible (31%). Not only lymphoblasts but also the neoplastic elements of the CML granulopoiesis and megakaryopoiesis are BCR-ABL positive (see also **b**). In **c** the situation after initiation of imatinib treatment is demonstrated. Still, a significant number of 21% split

signals is detectable (**a–c** magnification $\times 600$). **d, e** Quantitative RT-PCR amplification plots demonstrating b2a2 BCR-ABL fusion transcripts (red). The internal control tubulin is presented as a green curve. As expected the allelic burden of the BCR-ABL fusion transcript decreased profoundly, clearly demonstrated by the increase of cycles (highlighted by arrow bar in **e**) between the amplification curves of the internal control compared to the BCR-ABL amplification

2 Discussion

Imatinib mesylate (Glivec[®]) and also a series of other small molecules designed to inhibit the tyrosine kinase activity of the Bcr-Abl oncoprotein have proven to be active in all phases of Ph⁺ CML [1–3]. While all of these molecules can induce complete cytogenetic remissions in the majority of patients with chronic phase CML, complete cytogenetic remission can be missing in the vast majority of advanced stages of the disease. This might be due to genomic instability and indeed clonal evolution and duplication of the Philadelphia chromosome as well as BCR-ABL kinase domain mutations are seen in 30–50% of blast crisis patients [4]. In imatinib-naïve patients with CML blast crisis, imatinib may provide encouraging hematologic and cytogenetic benefits [5, 6]. t(9;22)(q34;q11) translocation as solitary cytogenetic abnormality and also decrease of BCR-ABL transcript level by at least 3 log under imatinib therapy—as seen in the present report—are therefore indicating a basically favorable prognosis [6]. Nevertheless, any

lymphoblast population in CML must be a cause for concern indicating a potentially evolution of an ALL and so far the prognosis of blast crisis appears ominous independent of its rate of onset [7].

In our report, the dimension of the lymphoid blast population was only seen in the bone marrow biopsy—probably due to the more focal infiltration pattern and the slight increase of reticular fibers in the areas with high blast density. In this situation it is very helpful when molecular techniques, especially FISH and RT-PCR, can be performed on decalcified bone marrow biopsies in a specialized molecular laboratory. More precisely, only the parallel removal of a trephine biopsy additional to the bone marrow smears offers the necessary flexibility to provide belated molecular analysis. In addition, careful examination of BCR-ABL translocation performing FISH on bone marrow biopsies is an ideal tool to estimate vulnerability of the blast tumor component under imatinib therapy. Bearing in mind that patients who achieve undetectable BCR-ABL transcript levels or major molecular responses with imatinib appear a

quite low risk for further progression of the disease, FISH and RT-PCR are most important techniques for the estimation of the individual prognosis of patients [8].

The present report clearly demonstrates the high diagnostic value deriving from the close interplay between analysis of diverse hematological compartments and diagnostic techniques. This approach clearly is a prerequisite for a concluding synoptical diagnosis. Herein, despite new molecular techniques, hematopathological analysis on bone marrow biopsies is of outstanding importance for the diagnosis of chronic myeloid leukemia.

References

1. Sawyers CL, Hochhaus A, Feldman E, Goldman JM, Miller CB, Ottmann OG, et al. Imatinib induces hematologic and cytogenetic responses in patients with chronic myelogenous leukemia in myeloid blast crisis: results of a phase II study. *Blood*. 2002;99(10):3530–9.
2. Talpaz M, Silver RT, Druker BJ, Goldman JM, Gambacorti-Passerini C, Guilhot F, et al. Imatinib induces durable hematologic and cytogenetic responses in patients with accelerated phase chronic myeloid leukemia: results of a phase 2 study. *Blood*. 2002;99(6):1928–37.
3. Kantarjian H, Sawyers C, Hochhaus A, Guilhot F, Schiffer C, Gambacorti-Passerini C, et al. Hematologic and cytogenetic responses to imatinib mesylate in chronic myelogenous leukemia. *N Engl J Med*. 2002;346(9):645–52.
4. Ilaria RL, Jr. Pathobiology of lymphoid and myeloid blast crisis and management issues. *Hematol Am Soc Hematol Educ Program* 2005;188–94.
5. Scharenberg CW, Harkey MA, Torok-Storb B. The ABCG2 transporter is an efficient Hoechst 33342 efflux pump and is preferentially expressed by immature human hematopoietic progenitors. *Blood*. 2002;99(2):507–12.
6. Druker BJ, Guilhot F, O'Brien SG, Gathmann I, Kantarjian H, Gattermann N, et al. Five-year follow-up of patients receiving imatinib for chronic myeloid leukemia. *N Engl J Med*. 2006;355(23):2408–17.
7. Kantarjian H, O'Brien S, Cortes J, Giles F, Thomas D, Kornblau S, et al. Sudden onset of the blastic phase of chronic myelogenous leukemia: patterns and implications. *Cancer*. 2003;98(1):81–5.
8. Hughes TP, Kaeda J, Branford S, Rudzki Z, Hochhaus A, Hensley ML, et al. Frequency of major molecular responses to imatinib or interferon alfa plus cytarabine in newly diagnosed chronic myeloid leukemia. *N Engl J Med*. 2003;349(15):1423–32.

Evolution of PTLD following renal transplantation in a child

Markert E, Siebolts U, Habbig S, Odenthal M, Dienes HP, Stippel DL, Hoppe B, Wickenhauser C. Evolution of PTLD following renal transplantation in a child.

Pediatr Transplantation 2008. © 2008 Wiley Periodicals, Inc.

Abstract: We report the case of an eight-yr-old child with early onset PTLD half a year after renal transplantation. The patient developed gastrointestinal pain and bowel biopsies revealed imposing lymphoid infiltrates with small spots of lymphoid blasts in the colonic mucosa. These findings were interpreted as transplantation associated B-cell stimulation. However, the persistent severe abdominal pain led to the resection of a jejunal segment. Here, gut wall perforation caused by a tumor mass was seen. Histologically, a blastic lymphoid cell proliferation of B-cell origin with high proliferation rate and EBV association could be demonstrated. IgH rearrangement analysis and *in situ* hybridization revealed an oligoclonal B-cell pattern. Reduction of immunosuppression and treatment with rituximab led to lymphoma remission and conversion of EBV serology four wk later. The report presented herein demonstrates the evolution of an oligoclonal lymphoproliferation with direct disease progression towards EBV associated PTLD by analyzing different stages of the disease.

Eva Markert¹, Udo Siebolts^{1,2}, Sandra Habbig³, Margarete Odenthal¹, Hans Peter Dienes¹, Dirk L. Stippel⁴, Bernd Hoppe³ and Claudia Wickenhauser¹

¹Institute of Pathology, ²Center for Molecular Medicine, ³Division of Pediatric Nephrology, University Children's Hospital and ⁴Visceral and Vascular Surgery, University of Cologne, Cologne, Germany

Key words: PTLD – EBV – oligoclonality

Dr. Claudia Wickenhauser, Institute of Pathology, University of Cologne 50924 Cologne, Germany
Tel.: +49 221 478 6320
Fax: +49 221 478 6360
E-mail: c.wickenhauser@uni-koeln.de

Accepted for publication 19 March 2008

PTLD are a heterogeneous group of lymphoid and plasmacytoid neoplasms caused by iatrogenic immunosuppression following solid organ and bone marrow/stem cell transplantation. Most PTLD are of B-cell origin and frequently arise in extranodal sites. Early onset PTLD are mainly regarded as EBV-driven disorders that are frequently, although not always, polyclonal or oligoclonal, whereas most late onset PTLD are true monoclonal lymphoid malignancies with autonomous proliferation not necessarily associated with EBV infection and related with a rather adverse outcome (1). Furthermore, early onset PTLD have the potential to progress to malignant lymphoma. This process is thought to be triggered by dominance of few

lymphoid subclones and consecutive autonomous proliferation.

In this article, we report about a child with early onset intestinal and nodal PTLD following renal transplantation. Biopsies taken at different time points and different sites impressively demonstrate the evolution of oligoclonal lymphoproliferative disorder with direct disease progression towards EBV-associated PTLD.

Case report

In August 2006, an eight-yr-old boy with chronic renal failure secondary to bilateral kidney hypoplasia received a deceased donation renal allograft. Immunosuppression was accomplished with daclizumab for induction, methylprednisolone for five days and maintenance immunosuppression was conducted with tacrolimus (target blood level: 8–10 µg/L) and mycophenolate mofetil (TWIST study protocol, FG-02-43). The patient as well as the donor kidney were negative for CMV and EBV antibodies (EBV-VCA-IgM, EBV-VCA-IgG, EBV-EA-IgG). Increasing polyuria (up to 6 L/day) led to left nephrectomy in

Abbreviations: B-NHL, B-cell non-Hodgkin lymphoma; CISH, chromogenic *in situ* hybridization; CMV, cytomegalovirus; EA, early antigen; EBER, EBV-associated small RNAs; EBV, Epstein-Barr virus; IgH, immunoglobulin heavy chain; LMP, latent membrane protein; PCR, polymerized chain reaction; PTLD, post-transplant lymphoproliferative disorders; VCA, viral capsid antigen.

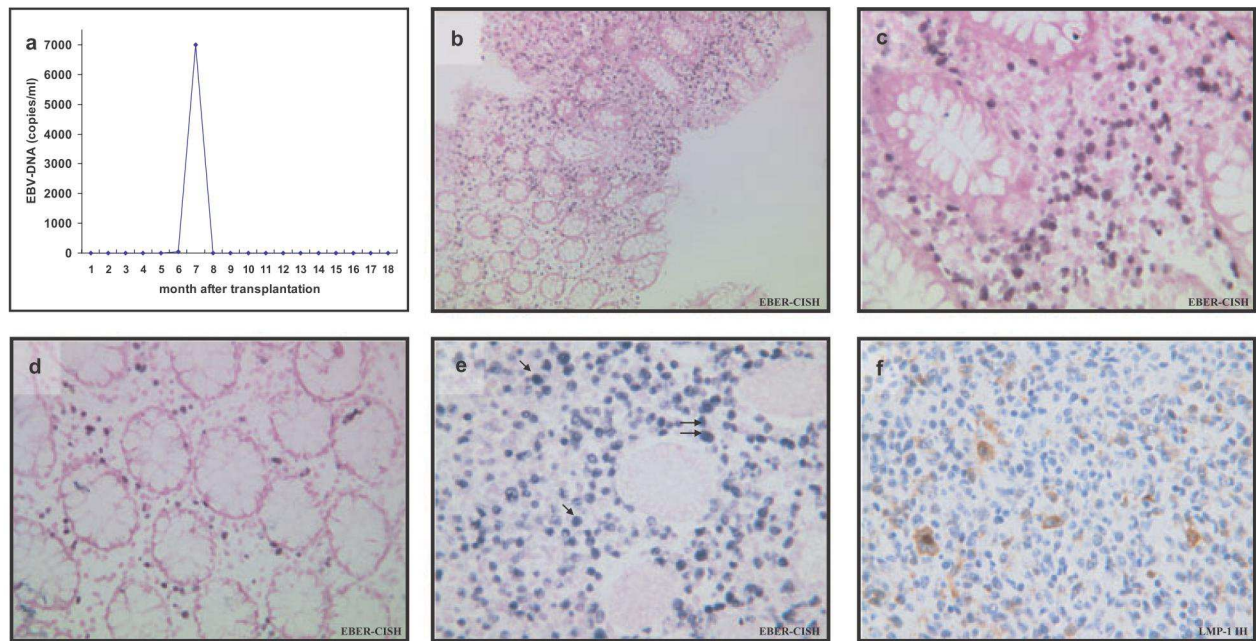


Fig. 1. CISH with EBV-specific RNA probes (EBER1 and 2) and LMP-1 for EBV investigation of colonic and jejunal lymphoid infiltrates. (a) EBV monitoring: after transplantation there was no evidence of EBV infection until month 6 after transplantation. Concurrent EBV infection of both siblings of the patient probably led to primary infection of the initially EBV antibody-negative patient with a rapid increase of EBV-DNA copies and seroconversion at the time of jejunal perforation because of monoclonal PTLT. When therapy was started with a rituximab induction phase of a three-wk course of weekly infusions EBV-DNA PCR resulted negative. However, EBV-VCA-IgG is still detectable, representing post-EBV infection status. (b) CISH analysis (EBER1 and 2) of the colonic biopsy revealing blotchy accumulation of EBV-infected lymphocytes (100 \times). (c, d) Higher magnification (400 \times) of the same specimen demonstrating a dense population of EBV-positive lymphocytes (c) near areas of normal colonic mucosa with solitary spread EBV-infected lymphocytes (d). (e) CISH analysis of the lymphoma showing a high load of EBV in infiltrating lymphoid cells (arrows; 400 \times , nucleoli faintly counterstained with nuclear fast red). (f) Immunohistochemical (IH) staining with evidence for single LMP-1 positive lymphoma cells.

October 2006. Two months later, the patient developed recurrent abdominal pain and diarrhea. Bacterial enteritis (*C. difficile*) was successfully treated with antibiotics, but a Norovirus infection was also present. In January, the patient's siblings developed acute infectious mononucleosis proven by high EBV IgM titers. The patient was clinically unaffected at this time. However, for the first time EBV monitoring (Fig. 1a) now resulted positive with a low EBV-DNA copy number (39 copies/mL), but EBV antibodies were not yet detected. In February 2007, six months after transplantation, the child again suffered from severe abdominal pain. Several bowel biopsies, gained by colonoscopy, revealed considerable lymphoid infiltration at several sites of the colonic mucosa with a variable amount of lymphoid blasts but without clear evidence for a lymphoproliferative disease. Chest radiography was performed because of aggravation of the symptoms and disclosed free intra-abdominal air. At that time, EBV-DNA copy number had increased to 7000 copies/mL and EBV sero-conversion had occurred (EBV-VCA-IgM, IgG and EBV-EA-IgG positive). Surgery

revealed a tumor mass in the jejunum with a circumscribed intestinal perforation. Histological evaluation of this jejunum segment now clearly presented a monomorphic blastic B-cell lymphoma. In addition, celiac lymph nodes were partially affected while cerebral fluid and bone marrow biopsy were tumor free. Immunohistochemistry and molecular techniques revealed EBV association of the lymphoma. Therapy was started with a rituximab induction phase of a three-wk course of weekly infusions of 375 mg/m², while immunosuppression now with tacrolimus and methylprednisolone was continued but reduced to serum levels of 2–4 μ g/L for tacrolimus. As complete remission according to the WHO criteria was achieved, consolidating therapy with rituximab was performed for three months in the same dosage. Because of persisting gastrointestinal symptoms, a further laparotomy with lymph node resection was performed in March 2007. Abdominal lymph nodes were free of tumor at that time, and EBV DNA in serum could not be detected by PCR.

At present, 18 months after transplantation, the boy is well, the donor kidney is perfectly

working under conditions of immunosuppression with tacrolimus (target level 3 µg/L) and methylprednisolone with no signs of rejection, and the lymphoma is in stable remission.

Pathological findings

Biopsies of the large intestine revealed a prominent lymphoplasmacellular infiltrate with variable number of lymphoid blasts and a slight lymphofollicular hyperplasia (Fig. 2a). The jejunal tumor mass was composed of a lymphoid infiltrate destroying the bowel wall with consecutive perforation (Fig. 2b). In contrast to reactive lymphoid bystander cells, this tumor population was composed of large, transformed blastic cells with relatively pale nucleoli and basophilic cytoplasm (Fig. 2c). Immunohistochemically, the blasts were positive for CD20 and, in part, for MUM1P (Fig. 2d,e). A high proliferation rate could be ascertained by nuclear Ki67 expression (Fig. 2f). CISH with EBV specific RNA probes (EBER1 and 2, Zytomed

Systems) demonstrated infection of the majority of tumor cells (Fig. 1e). These findings were in line with data derived from PCR analysis with EBV-specific primers, where a clear band proved EBV infection and data from immunohistochemistry with evidence for EBV-LMP1 staining. The same tumor population was seen in the lymph nodes resected from abdominal sites. Four wk later, control lymph node biopsies from celiac sites presented normal histomorphology and EBV-LMP as well as molecular analysis for EBV infection were negative. Retrospectively, CISH (EBER1 and 2) was also performed in the colonic biopsies. Here, a variable amount of EBV-infected lymphoid cells was present (Fig. 1b–d).

Further molecular findings

IgH rearrangement analysis employing FR3-JH primers was performed from diverse tumor sites of the jejunum (Fig. 3a–c), from different sites of the colonic mucosa (Fig. 3d,e) and from the

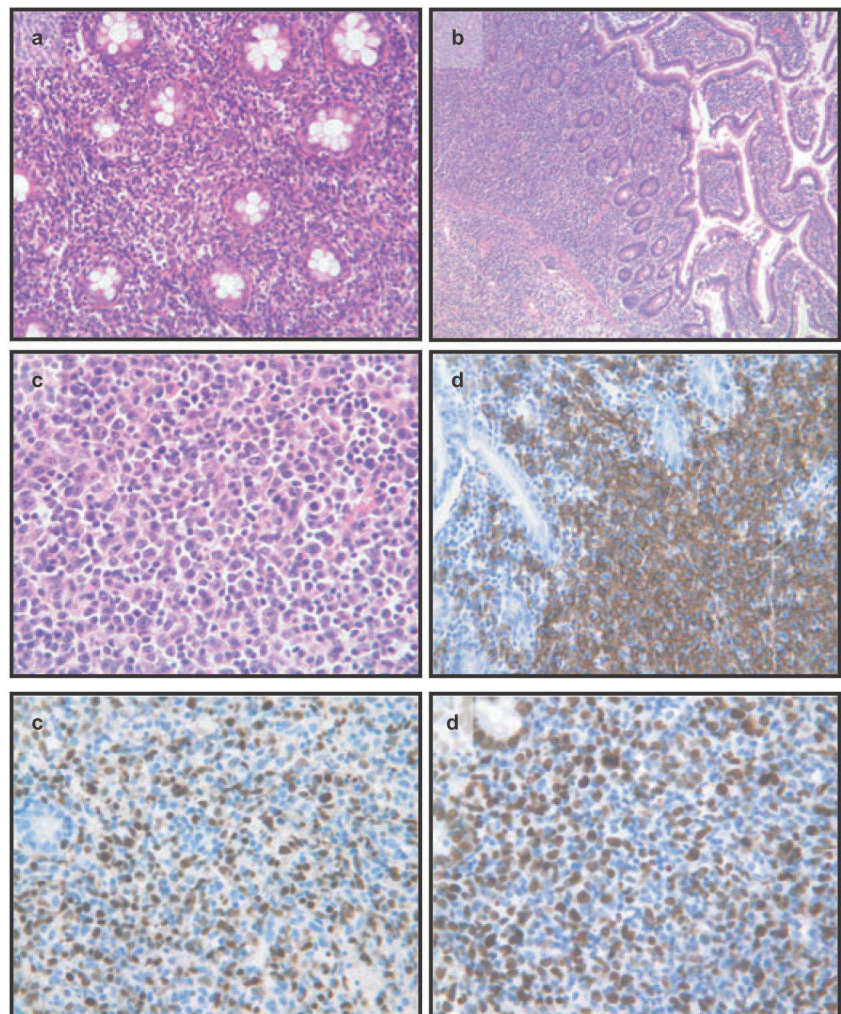


Fig. 2. Histochemical and immunohistochemical analysis of intestinal lymphoid infiltrates. (a) Hematoxylin and eosin staining (250×) of a colonic biopsy showing a dense lymphatic infiltrate. (b) Hematoxylin and eosin staining (100×) of jejunum specimens revealing a prominent lymphoid infiltrate overgrowing and destroying the mucosa and submucosa. (c) Higher magnification (400×) of the same area demonstrates a blastic lymphoid tumor mass corresponding to Fig. 2b. (d) CD20 immunostaining of the same area displays strong membranous staining of the blasts surrounding regular intestinal glands (200×). (e) Distinct pattern of nuclear MUM1P expression in a subpopulation of the tumor cells (400×). (f) Nuclear Ki67 staining in 50% of the tumor cells indicating high proliferation rate.

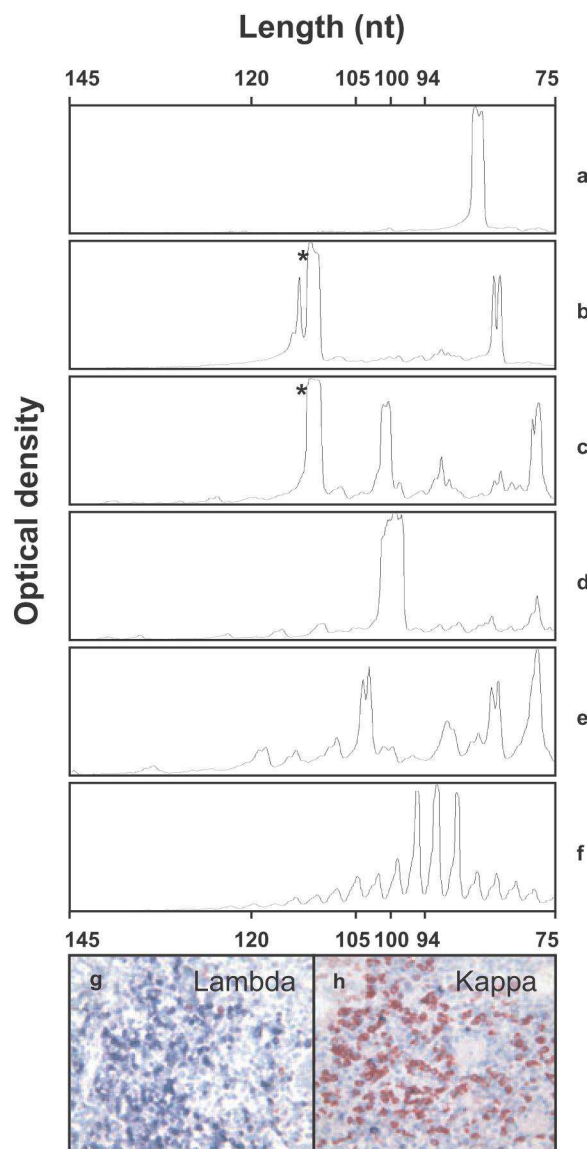


Fig. 3. Computer-assisted fragment length analysis of IgH FR3 PCR amplification products from intestinal lymphoid infiltrates. (a) Clear peak at defined nucleotide length indicating monoclonality of the lymphoid infiltrate in a tumor probe of the small intestine. (b) A double-peak pattern indicates two additional main B-cell subclones in another region of this small intestine tumor. (c) A multi-peak pattern in a third region of this tumor. Here, IgH FR3 analysis fails to indicate clonality. In direct comparison with the pattern in (b) a main peak of identical fragment length is seen (asterisk). (d) Clear monoclonal peak of a different fragment length than described in (a–c) is seen in a colonic biopsy leading to the assumption of a different B-cell clone. (e) Multi-peak pattern of a colonic lymphoid infiltrate revealing polyclonal derivation. (f) Typical Gaussian distribution of amplification products in a lymph node with partial infiltration by B-cell lymphoma. In this analysis molecular data mimic reactive lymph node composition. The abscissa indicates length of the amplicons in nucleotides (nt); the ordinate displays relative optical density. (g, h) CISH reveals monoclonality of B-cells by exclusive mRNA immune light chain expression of kappa or lambda, respectively, emphasizing the finding of different B-cell subclones.

affected lymph nodes (Fig. 3f). In Fig. 3a, a clear monoclonal pattern is seen in the tumor mass of the small intestine while in other regions of the same tumor site (Fig. 3b,c) a different picture is visible. Here, a molecular relationship of one B-cell subclone is present (asterisk, Fig. 3b,c) but the background of additional B-cell clones is different in these two probes. In Fig. 3d, a definite dominant clone is seen in one probe of the colonic mucosa. In contrast to another colonic site, where molecular data indicate B-cell polyclonality (Fig. 3e), although the histological picture of both tissue probes was identical. Clonality analysis of a lymph node with definite histological infiltration by B-cell lymphoma indicated a rather polyclonal pattern (Fig. 3f). In addition to IgH FR3 PCR, CISH was performed for simultaneous visualization of light chains kappa and lambda RNA expression (Zytomed). As seen in Fig. 3g,h, fields of monoclonal cell clusters, sharply demarked one from the other, were seen in the tumor mass of the small intestine. Therefore, the oligoclonal growth of the lymphoma can be underlined through the patchy distribution of kappa and lambda light chain expression.

Discussion

The majority of early PTLD cases are associated with EBV infection (1). In healthy individuals, expression of the LMP-1 by EBV-infected cells leads to activation of cytotoxic T cells (2). Immunosuppression, however, hinders this reaction of EBV elimination and leads to B-cell proliferation. The histopathological spectrum of these B-cell proliferations ranges from early lesions with polyclonal proliferations (plasmacytic hyperplasia or infectious mononucleosis-like pattern) to Hodgkin lymphoma, Hodgkin lymphoma-like PTLD and B-NHL (1).

Diagnosis of PTLD is often challenging and any clinical symptom including lymphadenopathy, fever of undetermined origin, pulmonary infiltrates, unexplained allograft dysfunction, abdominal pain or persisting headache should prompt lymphoma to be included in the differential diagnosis. Here, the surveillance of the EBV status may be an important tool for the clinical monitoring, but an increase of the EBV copy number does not necessarily precede PTLD. In our case, the development of intestinal PTLD went along with a rapid increase of EBV-DNA in blood, without typical symptoms of EBV infection. In this context, it is important to stress that in the histopathologically not affected colonic mucosa retrospective performance of

CISH (EBER 1 and 2) but not immunohistochemistry for LMP-1 already revealed numerous EBV-infected lymphoid cells. This timesaving method therefore provides important data enabling clinicians to reduce immunosuppression in good time. Also, the patchy distribution of EBV-positive lymphocyte areas next to unaffected lymphatic infiltrates can give first hints on initial EBV triggered lymphoma development—even if a typical histological PTLD pattern is not seen at that time because of the pleomorphous character of the lymphoid picture. In this combination, IgH rearrangement analysis—which here indicated monoclonality in one of the probes—can provide the crucial clue for diagnosis of PTLD (Fig. 3d).

Taken together, IgH rearrangement analysis should be added to the diagnostic spectrum of early PTLD in all cases where clinical symptoms are unclear and histomorphology is unspecific. This consensus PCR protocol can be effectively used in routine molecular diagnostic laboratories and is yielding highly reproducible results with no reported false-positive data. However, its major drawback is an increased false-negative rate. Possible technical reasons for false-negative results as somatic hypermutation or ongoing mutations in the binding regions of the consensus primers have already been reviewed (3, 4). Recently, an increase in sensitivity to up to 85% has been reported when the BIOMED-2 approach was adapted (5).

In this report, diversity of B-cell clones at different tumor sites impressively reveal the role of EBV triggered evolution from reactive lymphoid hyperplasia to B-cell lymphoma following organ transplantation (6). The clinical course with jejunal perforation induced by tumor infiltration, histomorphology of the blastic infiltrates, and dominant B-cell clones here demonstrates a rapid disease progression with transformation into a true malignant process.

Considering children with abdominal pain following organ transplantation, this case report underlines that intestinal biopsies should be thoroughly investigated to exclude initial PTLD. Although the reduction of immunosuppression, immunotherapy (rituximab) and surgery, well described as first line therapy regimen (7), led to tumor elimination, the clinical course with jejunal perforation here nevertheless was a life-threatening event.

In this context, the report presented here confirms that the application of a broad spectrum of diagnostic methods on histologic biopsies has the potential to enforce diagnosis of initial PTLD already at a very early moment and therefore can prevent severe complications.

References

1. HARRIS NLSS, FRIZZERA G, SWEDROW SH, et al. Post-transplant lymphoproliferative disorders. In: JAFFE ESHN, STEIN H, VARDIMAN JW, eds. *Pathology and Genetics of Tumours of Haematopoietic and Lymphoid Tissues*. Lyon: IARC Press, 2001: pp. 264–269.
2. RICKINSON AB, MOSS DJ. Human cytotoxic T lymphocyte responses to Epstein–Barr virus infection. *Annu Rev Immunol* 1997; 15: 405–431.
3. COAD JE, OLSON DJ, CHRISTENSEN DR, et al. Correlation of PCR-detected clonal gene rearrangements with bone marrow morphology in patients with B-lineage lymphomas. *Am J Surg Pathol* 1997; 21: 1047–1056.
4. COAD JE, OLSON DJ, LANDER TA, et al. Molecular assessment of clonality in lymphoproliferative disorders: I Immunoglobulin gene rearrangements. *Mol Diagn* 1996; 1: 335–355.
5. EVANS PA, POTT C, GROENEN PJ, et al. Significantly improved PCR-based clonality testing in B-cell malignancies by use of multiple immunoglobulin gene targets. Report of the BIOMED-2 concerted action BHM4-CT98-3936. *Leukemia* 2007; 21: 207–214.
6. HOLMES RD, SOKOL RJ. Epstein–Barr virus and post-transplant lymphoproliferative disease. *Pediatr Transplant* 2002; 6: 456–464.
7. SVOBODA J, KOTLOFF R, TSAI DE. Management of patients with post-transplant lymphoproliferative disorder: The role of rituximab. *Transpl Int* 2006; 19: 259–269.

Review

Immunologic hurdles of therapeutic stem cell transplantation

Olaf Utermöhlen^{1,2,*}, Nikola Baschuk¹, Zeinab Abdullah^{1,a}, Afra Engelmann^{3,b}, Udo Siebolts^{4,c}, Claudia Wickenhauser^{4,c}, Carol Stocking³ and Martin Krönke^{1,2,*}

¹Institute for Medical Microbiology, Immunology and Hygiene, Medical Center, University of Cologne, D-50935 Cologne, Germany

²Center for Molecular Medicine of the University of Cologne (CMMC), D-50935 Cologne, Germany

³Heinrich Pette Institute, University of Hamburg, D-20206 Hamburg, Germany

⁴Institute for Pathology, University of Cologne, D-50935 Cologne, Germany

*Corresponding authors

e-mails: m.kroenke@uni-koeln.de;

olaf.uterhoehlen@uk-koeln.de

Abstract

Detailed knowledge of the immunologic properties of embryonic stem (ES) cells is a prerequisite for safe applications of ES cell-based regenerative medicine. Recently, the long-standing assumption that ES cells are ignored by immunocompetent hosts was disproved. Instead, it is becoming increasingly clear that ES cells actively protect themselves via several immunomodulatory and immunoevasive mechanisms against cytotoxic T-lymphocytes and natural killer cells. Here we review current knowledge about the immunologic properties of ES cells and discuss the implications for ES cell-based regenerative medicine, for the immunobiology of the embryo as a semi-allogeneic graft, and for the regenerative capacity of adult stem cells.

Keywords: cytotoxic T-lymphocyte; embryonic stem cell; natural killer cell; teratoma.

Introduction

Besides ethical issues, there are at least two major practical hurdles to overcome before embryonic stem (ES) cells can be used as a cellular source for regenerative medicine. One hurdle is the rejection of transplanted allogeneic ES cells or their derivatives by the recipient's immune system. The second is teratoma outgrowth from

undifferentiated ES cells, regardless of whether these cells were injected on purpose or as contaminants of more differentiated derivatives. These two obstacles pose a serious dilemma for clinical application of ES cells. Low immunogenicity would allow grafting of therapeutic cells but immunologically uncontrolled teratoma growth. Alternatively, an effective recognition and immune response to ES cells would prevent teratoma formation but would lead to rejection of the therapeutic ES cell graft.

The implications of these immunologic problems inherent in ES cell-based medicine were recognized only recently (Bradley et al., 2002; Utermöhlen and Krönke, 2007) and we are still far from an in-depth understanding of the immunologic properties of ES cells. This is highlighted by recent studies in various laboratories that yielded contradictory results on the fate of transplanted ES cells *in vivo* under simple experimental conditions (see below).

The difficulties in understanding the immunology of ES cells might have been anticipated from our problems in comprehending the closely related immunologic phenomena during pregnancy. The obvious fact that embryos as true semi-allogeneic implants are tolerated by the mother's immune system during pregnancy is still largely enigmatic (Koch and Platt, 2007; Riley, 2008). In fact, unraveling the immunologic properties of ES cells will contribute to a better understanding of the immunologic mechanisms accompanying and allowing pregnancy, as discussed below.

Here, we review present knowledge about the immunologic behavior of ES cells in the light of recently identified immunomodulatory and immunoevasive mechanisms of ES cells.

ES cells: immunogenic or tolerogenic, ignored or immunoprivileged?

Initially, it was hypothesized that ES cells were immunoprivileged in a recipient organism for at least two major reasons (Burt et al., 2004; Li et al., 2004). (i) ES cells express no or low levels of MHC class I molecules on their surface, so that they might be ignored by allospecific cytotoxic T-lymphocytes (CTLs). (ii) ES cells are derived from pre-implantation embryos, which are usually not rejected by the mother's immune system despite being true semi-allogeneic implants with half of their proteins being foreign paternal antigens (Rukavina and Podack, 2000).

Remarkably, the immunoprivileged state of ES cells still is highly controversial. To date, various laboratories have reported contradictory results on the acceptance versus rejection of transplanted ES cells or teratoma growth

Present addresses:

^a Institute of Molecular Medicine and Experimental Immunology, University of Bonn, D-53105 Bonn, Germany.

^b Children's Medical Research Institute, Westmead, NSW 2145, Australia.

^c Institute for Pathology, University of Leipzig, D-04103 Leipzig, Germany.

after transplantation of ES cells or their early differentiated tissue-specific derivatives. Teratomas are embryonic tumors that can naturally emerge either from pluripotent stem cells within the ovaries and testicles or from spontaneously dispersed pluripotent embryonic cells at extrauterine sites. Experimentally, they can grow out of ES cells implanted into various sites of the body. In addition to the initiating embryonic cells, teratomas contain variable mixtures of differentiated cells and tissue-like structures derived from all three germ layers. Immunologically, teratomas can be viewed as simplified models of embryonic implants and/or of stem cell-derived tumors, making them valuable tools in basic research (Andrews et al., 2005).

The first report of murine ES (mES) cells giving rise to teratomas in syngeneic mice was 25 years ago (Wobus et al., 1984), an observation independently confirmed with various ES cell lines (Damjanov, 2004; Nussbaum et al., 2007; Koch et al., 2008).

In allogeneic recipients, transplants of mES cells are usually infiltrated by various immune cell types of the recipient and, if the study design included sufficiently long observation times, are eventually rejected (Kofidis et al., 2005; Swijnenburg et al., 2005; Nussbaum et al., 2007; Robertson et al., 2007). However, this simple scenario was recently challenged. Magliocca et al. (2006) reported that intraportally injected mES cells gave rise to multiple miliary hepatic teratomas in approximately 90% of immunocompetent allogeneic mice, and intravenously or intramuscularly injected ES cells also led to teratoma in allogeneic recipients. Because the aim of this study was to induce tolerance of allogeneic cardiac transplants by intraportal injection of allogeneic ES cells, the teratomas were neither analyzed for an inflammatory infiltrate nor monitored for longer periods of time. Therefore, it is not clear whether the teratomas would have eventually been rejected. However, the size of the multinodular teratomas strongly argues against control of these allogeneic tumors by the immune system of the recipients, even though the allogeneic neonatal cardiac transplants in the same mice were rejected.

Koch et al. (2008) monitored the fate of graded doses of mES cells transplanted subcutaneously into syngeneic, semi-allogeneic, or fully allogeneic hosts. As expected, a standard injected dose of 1×10^6 mES cells did not lead to teratoma formation in allogeneic mice. However, 5×10^6 ES cells gave rise to teratomas in 100% of semi-allogeneic and 30% of allogeneic recipients. Moreover, 20×10^6 ES cells led to teratoma formation in 90% of allogeneic mice. The teratomas were first detected approximately 2 weeks after transplantation and grew rapidly, so that the mice had to be euthanized 3–4 weeks later for ethical reasons. The steady growth of the teratomas over this observation period argues against control of the allogeneic tumors by the recipient's immune system, although considerable numbers of host $CD3^+$ T-lymphocytes infiltrated both semi-allogeneic and allogeneic teratomas. In further support of the acceptance of transplanted mES cells by non-syngeneic hosts, the survival of mouse ES cells in rats (Min et al., 2003) and sheep (Menard et al., 2005) has been reported.

These data highlight the need for caution in interpreting results obtained under specific experimental conditions.

The entire experimental setting (e.g., the type of ES cell line and its dependence on feeder cells, the number of cells transplanted and the injection route, the species and strain of the recipient, or the end-point parameters of the study) should be carefully considered before generalized conclusions can be drawn. Clearly, an in-depth understanding of the mechanisms of interaction between ES cells and immune cells of the host is required before ES cell-based therapy will become a valuable approach in regenerative medicine.

Response of cytotoxic effector cells to ES cells

The most prominent cytotoxic effector cells directed against transplants are natural killer (NK) cells and $CD8^+$ CTLs belonging to the innate and adaptive immune system, respectively. Each of these cell types recognizes its target cells by specific and sensitive receptors. It should be remembered that for both cell types recognition of a target cell does not necessarily result in delivery of a lethal hit against the target. Rather, depending on several conditions (e.g., the previously achieved activation state, the signal strength, the type and combination of receptors involved) the cytotoxic effector cell might be transiently or permanently inactivated, or induced to secrete cytokines, to proliferate or to deliver membrane-bound or soluble cytotoxic effector molecules against the target cell. Therefore, the multiple consequences ensuing from contact of cytotoxic effector cells with ES cells need to be characterized in greater detail.

Low susceptibility of ES cells to lysis by $CD8^+$ CTLs

It has long been known that early embryonic cells express very low levels of MHC class I molecules (Morello et al., 1985; Ozato et al., 1985; David-Watine et al., 1987). Correspondingly, human and mES cells express low or undetectable levels, respectively, of surface MHC class I molecules (Tian et al., 1997; Draper et al., 2002; Drukker et al., 2002; Bonde and Zavazava, 2006; Magliocca et al., 2006; Koch et al., 2008) and would thus be poorly recognized by MHC class I-restricted $CD8^+$ CTLs. Therefore, it was not surprising that human ES cells loaded with a HLA-A2-restricted peptide of influenza virus are not lysed by peptide-specific $CD8^+$ CTLs (Drukker et al., 2006) and that mES cells are not lysed by allospecific $CD8^+$ CTLs (Bonde and Zavazava, 2006). However, it was suspicious that after strong upregulation of MHC class I surface molecules by pretreatment with $IFN-\gamma$, human ES cells, either loaded with peptide or infected with the influenza virus, were not at all or only poorly lysed by CTLs (Drukker et al., 2006).

Immunomodulatory and immunoevasive activities of ES cells against T-lymphocytes

The lack of destruction of ES cells by CTLs does not necessarily indicate a lack of recognition by the effector

cells. Indeed, more detailed analysis of the interaction between ES cells and CD8⁺ CTLs revealed that rather than being ignored or not recognized, ES cells actively inhibit T-cell responses and evade the effector functions of CTLs.

Human and mES cells do not stimulate the proliferation of allospecific T-lymphocytes *in vitro* (Li et al., 2004; Bonde and Zavazava, 2006) and mES cells suppress the maturation of dendritic cells (Koch et al., 2008). Furthermore, mES cells suppress T-cell proliferation *in vitro* in response to various strong stimuli, e.g., third-party allogeneic dendritic cells (DC), immobilized anti-CD3 and anti-CD28 antibodies and Concanavalin A (Li et al., 2004; Koch et al., 2008). These inhibitory effects were shown to be mediated by ES cells via membrane-bound FasL (Fabricius et al., 2005) or via secretion of TGF- β (Koch et al., 2008), resulting in inhibited induction of cellular immune responses against ES cells. Beyond impairing the induction of cellular immune responses, ES cells use mechanisms to inactivate cytotoxic effector mechanisms of fully activated CD8⁺ CTLs. Fabricius et al. (2005) reported that mES cells abrogate the cytotoxic activity of allospecific CD8⁺ CTLs in a dose-dependent manner by inducing CTL apoptosis via FasL. We have shown that lymphocytic choriomeningitis (LCM) virus-specific CD8⁺ CTLs fully respond to mES cells either loaded with synthetic peptide epitopes or infected with the LCM virus (Abdullah et al., 2007). Despite low-level expression of MHC class I on the ES cells, CTLs specifically responded to these target cells by proper polarization and secretion of their cytotoxic granules, but the ES cells were not lysed *in vitro*. We found that mES cells express specific inhibitors of both perforin and granzyme B, i.e., cathepsin B and serine protease inhibitor (serpin or SPI) 6, respectively. Knockdown of SPI-6 by shRNA fully restored the susceptibility of mES cells to lysis by CD8⁺ CTLs.

Taken together, ES cells use several immunomodulatory and immuno-evasive mechanisms that inhibit the induction of a cellular immune response or counteract the cytotoxic effector activities of fully activated CD8⁺ CTLs. What might be the physiological relevance of these mechanisms? Half of the embryonic genome is derived from the father, so that approximately 50% of the embryonic proteins are foreign material for the mother's immune system. Therefore, from the very moment of first contact with the mother's uterine epithelium, the blastocyst faces the challenging task of establishing a true semi-allogeneic implant in the uterus of a principally immunocompetent host. The implantation-stage blastocyst consists of the outer zona pellucida, the single cell layer of the trophoblast and, innermost, the embryoblast, which is an accumulation of ES cells. If a single maternal allospecific CTL were able to penetrate through the delicate zona pellucida and trophoblast, this single cytolytic effector cell could rapidly eradicate the embryonic cells. Thus, the autonomous protection of ES cells against accidental destruction by maternal CTLs is a teleologically reasonable mechanism preventing rejection of the semi-allogeneic embryo.

Formal proof has yet to be delivered as to which of the immunoprotective and immuno-evasive mechanisms contribute to immunoprotection of the embryo and to what

extent. However, very impressive evidence in support of the hypothesis that SPI-6 contributes to protection of the embryo against maternal CD8⁺ CTLs comes from expression patterns of SPI-6 in the murine embryo. At day 4.5 post conception (p.c.) we observed a concentric pattern of high levels of expression SPI-6 in the outer cell layers of the embryo, whereas cells in the deeper embryonic regions were devoid of SPI-6 (Figure 1A). Remarkably, during later stages of embryonic development (e.g., day 12 p.c.) only the placenta, which at this time is the only remaining site of direct contact between the embryo and the mother, stained highly positive for SPI-6 (Figure

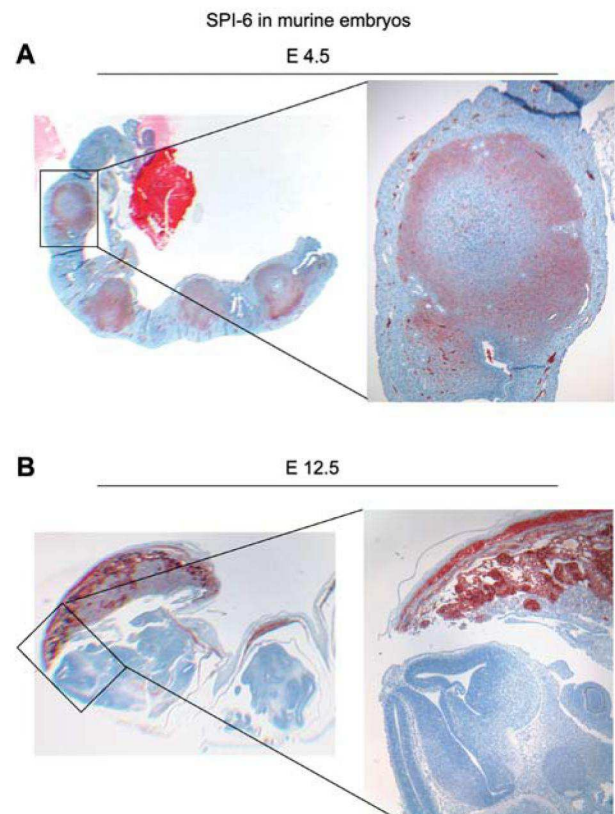


Figure 1 Localization of SPI-6 in murine embryos at days 4.5 and 12.5 post conception.

Pregnant C57BL/6 mice were sacrificed on day 4.5 (A) or 12.5 (B) post conception (p.c.) to prepare the uteri for immunohistochemistry by standard procedures. SPI-6 expression was detected using a mAb (MBL International, Woburn, MA, USA, Cat. No. JM-3544-100) specific for human PI-9 cross-reacting with the murine ortholog SPI-6 (Medema et al., 2001b). Immunohistochemistry was performed on paraffin-embedded tissues. Samples were deparaffinized and rehydrated and microwave heat-induced epitope retrieval was performed in 0.1 M sodium citrate. Following incubation with anti-SPI-6 mAb, samples were treated with a biotinylated secondary antibody and HRP-streptavidin and stained with diaminobenzidine. (A) On day 4.5 p.c. SPI-6 was highly expressed in four individual embryos in outer embryonic cell layers in close contact with the maternal tissue. (B) On day 12.5 p.c. SPI-6 expression was limited to the placenta of two neighboring embryos, whereas somatic embryonic tissue were negative. Pictures were recorded on a Zeiss Axio-phot microscope (Zeiss, Oberkochen, Germany; magnification, overviews 4 \times 10, inserts 20 \times 10) using a JVC KY-F75U digital camera (JVC Germany, Friedberg, Germany) and the acquisition software DISCUS version 4.6.0.342 (Diskus, Koenigswinter, Germany). No further image processing was performed.

1B). These data suggest that expression of SPI-6 at the contact site between the embryo and the mother might contribute to toleration of the semi-allogeneic embryo by the mother's immune system. Expression patterns for other immunomodulatory and immunoevasive molecules remain to be investigated. Many facets contribute to maternal-fetal tolerance, including species-specific anatomical structures at the placental-decidual interface, the local expression pattern of immunologically active molecules in both fetal trophoblast cells and maternal decidual and uterine endothelial cells, and gestation-related local and systemic changes in the mother's immunoreactivity (Moffett and Loke, 2006; Koch and Platt, 2007; Laskarin et al., 2007; Riley, 2008). Therefore, the physiological relevance of SPI-6 and SPI-CI for reproductive success remains to be determined. Furthermore, the complex physiological constellation at the maternal-fetal interface obviously differs from the artificial conditions ensuing from transplantation of ES cells or their derivatives, so additional efforts are required to elucidate the relevance of immunomodulatory and immunoevasive molecules for stem cell-based regenerative medicine.

A significant price to pay for the immunoprotection of ES cells may reside in the conservation of these mechanisms in tumor stem cells. For example, in large teratomas derived from mES cells, we detected small islets of SPI-6-expressing cells interspersed between large areas of more differentiated cells (Figure 2). Apparently, the small nests of SPI-6-expressing cells are ES cells, which are known to remain within ES cell-derived embryoid bodies for long times (Teramoto et al., 2005). In murine tumors, as well as in several clinically relevant hematopoietic and solid human tumors, expression of SPI-6 or its homolog PI-9 has been detected within the entire tumor mass (Medema et al., 2001a; Bladergroen et al., 2002; Barrie et al., 2004; van Houdt et al., 2005). Systematic analysis of tumor stem cells already identified for clinically relevant tumor entities will soon provide clues as to whether anti-cytotoxic immunoprotective molecules comprise mechanisms widely used by tumor stem cells. These mechanisms would add another layer of complexity to the known resistance of tumor stem cells to various therapeutic treatments, e.g., the expression of multidrug-resistance (MDR) transporters, which renders tumor stem cells resistant to chemotherapeutic drugs.

Low susceptibility of ES cells to NK cells

The major fraction of lymphocytes infiltrating the decidua of the pregnant uterus are NK cells (Rukavina et al., 1995; Rukavina and Podack, 2000). According to the missing self hypothesis (Ljunggren and Karre, 1990), a major trigger for release of cytotoxic effector molecules by NK cells is a lack or low level of MHC class I molecules on target cells. Thus, ES cells expressing no or low levels of MHC class I molecules should be ideal targets for NK cells in syngeneic hosts. However, we and others reported that human (Drukker et al., 2002) and mES cell lines (Bonde and Zavazava, 2006; Dressel et al., 2008; Koch

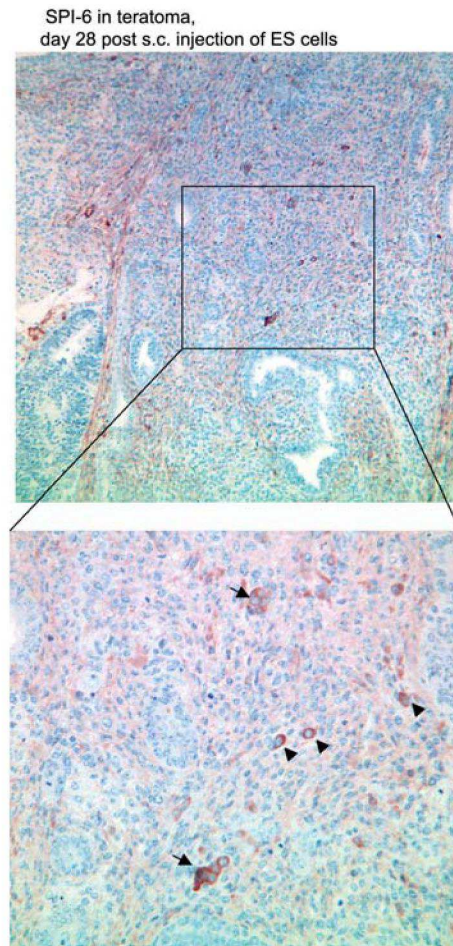


Figure 2 Expression of SPI-6 in CGR8 ES cell-derived murine teratoma on day 28 after cell implantation.

Feeder cell-independent CGR8 cells (1×10^6) were injected subcutaneously into the back of syngeneic 129P2/Ola mice. Teratomas were explanted 28 days later and prepared for immunohistochemistry by standard procedures. SPI-6 was detected using the mAb described for Figure 1. Within the teratoma small groups of cells (arrows) or single cells (arrow heads) with positive SPI-6 staining are visible (magnification, overview 20×10 , enlarged insert 40×10).

et al., 2008; Frenzel et al., 2009) are not at all or very ineffectively killed by NK cells *in vitro*. The variation in the degree of cytolysis of ES cells by NK cells reported in these studies can be easily explained by different experimental conditions, e.g., using resting versus *in vivo*- or *in vitro*-activated NK cells, using syngeneic, allogeneic, or even xenogeneic NK cells, or using different ES cell lines. For example, Dressel et al. (2008) observed that mES cells are not killed by resting murine NK cells, but are lysed by both murine NK cells stimulated *in vitro* with IL-2 and resting splenic NK cells from rats.

The lack or low-level expression of surface MHC class I molecules is only one critical prerequisite for NK cell-mediated lysis. In addition, target cells must express ligands for activation of NK cell receptors and intercellular adhesion molecules (Yokoyama, 2005). Lysis of two different mES lines by naïve rat NK cells or IL-2-activated murine NK cells (Dressel et al., 2008) or poly I:C-activated murine NK cells (Frenzel et al., 2009) was strongly reduced by blocking of the NKG2D receptor with a spe-

cific monoclonal antibody (mAb). Moreover, combined blocking of the NKG2D receptor and the adhesion molecule ICAM-1 completely abrogated cytotoxicity of mES cells (Frenzel et al., 2009). These findings suggest that a better understanding of the variable susceptibility of different ES cell lines to cytotoxicity by NK cells will be achieved by characterizing the expression pattern of ligands for activating NK cell receptors and intercellular adhesion molecules on ES cells.

Immuno-evasive activity of ES cells against NK cells

Both CD8⁺ CTL and NK cells use exocytosis of cytotoxic granules as the major cytolytic effector mechanism, so we wondered whether expression of cathepsin B and SPI-6 might protect ES cells not only against cytotoxicity by CD8⁺ CTLs, but also by NK cells (Abdullah et al., 2007). Neither inhibition of cathepsin B by the specific inhibitor CA047 nor knockdown of SPI-6 by stable lentiviral expression of SPI-6-specific shRNA in ES cells rendered the ES cells more susceptible to cytotoxicity by NK cells (O.U., N.B., Z.A., M.K., unpublished results). However, NK cells express a slightly different set of cytotoxic effector molecules compared to CTLs. A prominent difference is the higher load of granzyme in cytotoxic granules of NK cells (Sayers et al., 2001). We detected expression of the specific inhibitor of granzyme, SPI-1, at both the mRNA and protein level in mES cells. Knockdown of SPI-1 by stable lentiviral expression of specific shRNA rendered ES cells fully susceptible to lysis by resting or activated murine NK cells (O.U., N.B., Z.A., M.K., unpublished results). Thus, ES cells actively and specifically counteract the cytotoxic effector molecules of both CD8⁺ CTL and NK cells.

Adult stem cells express immunoprotective serpins

Protection against lysis by CTL and NK cells might be relevant not only for stem cell-based regenerative medicine and the immunology of pregnancy, but also for stem cells in adult organisms. We found that murine mesenchymal stem cells express SPI-6 and are resistant to CTLs (Utermöhlen and Krönke, 2007). Moreover, analysis of the hematopoietic system as the best-characterized system of stem cells and progenitor cells revealed that murine hematopoietic stem cells express levels of SPI-6 and SPI-1 that are almost as high as in mES cells (Figure 3). One step further along the hematopoietic differentiation process, in common myeloid progenitors, only very low-level expression of these serpins was detectable.

Why do adult stem cells express immuno-evasive molecules protecting them against the cytotoxic activity of CTL and NK cells? Adult stem cells have the capacity for self-renewal and differentiation into any cell type of the respective organ. Therefore, in any tissue or organ, adult stem cells are essentially required for physiologic homeostasis and endogenous regenerative or reparative processes in response to any type of stress or insult. If, for

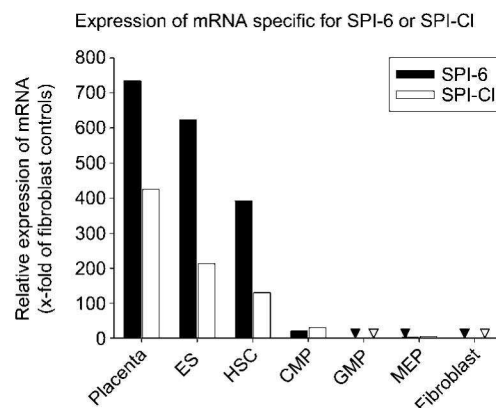


Figure 3 Expression of mRNA coding for SPI-6 or SPI-1 in murine hematopoietic stem and progenitor cells compared to placenta, ES cells, and MEF cells.

Bone marrow cells from male C57BL/6 mice were pooled and depleted of lineage-positive cells using an EasySep progenitor enrichment kit (StemCell Technologies, Vancouver, Canada). Hematopoietic stem cells (HSC; markers Sca1⁺, c-kit⁺; purity 76.3%), common myeloid progenitors (CMP; markers Sca1⁺, c-kit⁺, CD34⁺, CD16/32⁺; purity 58.3%, contaminants mostly MEP), granulocyte progenitors (GMP; markers Sca1⁺, c-kit⁺, CD34⁺, CD16/32⁺; purity 82.6%), megakaryocyte/erythroid lineage-restricted progenitors (MEP; markers Sca1⁺, c-kit⁺, CD34⁺, CD16/32⁺; 87.9%) were stained with mAbs specific for the above differentiation-specific markers and sorted by flow cytometry on a BD FACSARIA™ system (BD Biosciences, Heidelberg, Germany) to the purities indicated. Placenta prepared on day 12.5 p.c. and feeder cell-independent murine CGR8 ES cells were used as controls. Simian virus 40-transformed mouse embryo fibroblasts (C57BL/6-SV) were used as negative controls. Total RNA from 1 × 10⁶ cells of each population was purified using a Qiagen RNeasy Kit (Qiagen, Hilden, Germany) and cDNA was reverse-transcribed using a SuperScript III first-strand Synthesis kit (Invitrogen, Karlsruhe, Germany). qRT-PCR amplification and detection were performed in an ABI Prism 7500 thermocycler using TaqMan universal PCR master mix (Applied Biosystems, Darmstadt, Germany) and primers specific for SPI-6, SPI-1, and β-actin. Data are presented as the fold change in SPI-6 or SPI-1 gene expression normalized to β-actin and relative to the negative control. Triangles represent low SPI-6 values (GMP 0.9, MEP 2.0, fibroblasts 1.0) and SPI-1 (GMP 1.6, MEP 4.4, fibroblasts 1.0).

example, hematopoietic stem cells were easily susceptible to destruction by CD8⁺ CTL or NK cells during an infection with intracellular pathogens, the regenerative capacity of the whole hematopoietic system would be erased. The fatal consequences would resemble the effects of lethal irradiation or chemotherapeutic treatment of the bone marrow. Correspondingly, catastrophic consequences would also occur after destruction of organ-specific stem cells in many other tissues, e.g., intestinal or dermal epithelia.

The dilemma confronting the immune system during infection with intracellular microorganisms of how to eliminate the microorganism within the stem cell without destroying the infected stem cells can apparently be overcome. Indeed, Chisari and co-workers reported virus elimination without lysing of infected host cells several years ago (Guidotti et al., 1994, 1996). However, the effective contribution of immunoprotective mechanisms to prevent accidental elimination of adult stem cells has to be experimentally proven.

Analysis of the immunologic properties of ES cells has increased in momentum over the last few years. Future studies will have implications for our understanding of not only the immunobiology of stem cell-based regenerative medicine and of adult stem cells, but also of reproductive immunology.

Acknowledgments

This work was supported, in part, by a grant (CMMC 5-B7) to O.U. from the Center for Molecular Medicine Cologne, Faculty of Medicine, University of Cologne, Germany.

References

- Abdullah, Z., Saric, T., Kashkar, H., Baschuk, N., Yazdanpanah, B., Fleischmann, B.K., Hescheler, J., Krönke, M., and Utermöhlen, O. (2007). Serpin-6 expression protects embryonic stem cells from lysis by antigen-specific CTL. *J. Immunol.* 178, 3390–3399.
- Andrews, P.W., Matin, M.M., Bahrami, A.R., Damjanov, I., Gokhale, P., and Draper, J.S. (2005). Embryonic stem (ES) cells and embryonal carcinoma (EC) cells: opposite sides of the same coin. *Biochem. Soc. Trans.* 33, 1526–1530.
- Barrie, M.B., Stout, H.W., Abougergi, M.S., Miller, B.C., and Thiele, D.L. (2004). Antiviral cytokines induce hepatic expression of the granzyme B inhibitors, proteinase inhibitor 9 and serine proteinase inhibitor 6. *J. Immunol.* 172, 6453–6459.
- Bladergroen, B.A., Meijer, C.J., ten Berge, R.L., Hack, C.E., Muris, J.J., Dukers, D.F., Chott, A., Kazama, Y., Oudejans, J.J., van Berkum, O., et al. (2002). Expression of the granzyme B inhibitor, protease inhibitor 9, by tumor cells in patients with non-Hodgkin and Hodgkin lymphoma: a novel protective mechanism for tumor cells to circumvent the immune system? *Blood* 99, 232–237.
- Bonde, S. and Zavazava, N. (2006). Immunogenicity and engraftment of mouse embryonic stem cells in allogeneic recipients. *Stem Cells* 24, 2192–2201.
- Bradley, J.A., Bolton, E.M., and Pedersen, R.A. (2002). Stem cell medicine encounters the immune system. *Nat. Rev. Immunol.* 2, 859–871.
- Burt, R.K., Verda, L., Kim, D.A., Oyama, Y., Luo, K., and Link, C. (2004). Embryonic stem cells as an alternate marrow donor source: engraftment without graft-versus-host disease. *J. Exp. Med.* 199, 895–904.
- Damjanov, I. (2004). From stem cells to germ cell tumors and back. *Verh. Dtsch. Ges. Pathol.* 88, 39–44.
- David-Watine, B., Transy, C., Gachelin, G., and Kourilsky, P. (1987). Tissue-specific expression of the mouse Q10 H-2 class-I gene during embryogenesis. *Gene* 61, 145–154.
- Draper, J.S., Pigott, C., Thomson, J.A., and Andrews, P.W. (2002). Surface antigens of human embryonic stem cells: changes upon differentiation in culture. *J. Anat.* 200, 249–258.
- Dressel, R., Schindehutte, J., Kuhlmann, T., Elsner, L., Novota, P., Baier, P.C., Schillert, A., Bickeboller, H., Herrmann, T., Trenkwalder, C., et al. (2008). The tumorigenicity of mouse embryonic stem cells and *in vitro* differentiated neuronal cells is controlled by the recipients' immune response. *PLoS ONE* 3, e2622.
- Drukker, M., Katchman, H., Katz, G., Even-Tov Friedman, S., Shezen, E., Hornstein, E., Mandelboim, O., Reisner, Y., and Benvenisty, N. (2006). Human embryonic stem cells and their differentiated derivatives are less susceptible to immune rejection than adult cells. *Stem Cells* 24, 221–229.
- Drukker, M., Katz, G., Urbach, A., Schuldiner, M., Markel, G., Itskovitz-Eldor, J., Reubino, B., Mandelboim, O., and Benvenisty, N. (2002). Characterization of the expression of MHC proteins in human embryonic stem cells. *Proc. Natl. Acad. Sci. USA* 99, 9864–9869.
- Fabricius, D., Bonde, S., and Zavazava, N. (2005). Induction of stable mixed chimerism by embryonic stem cells requires functional Fas/FasL engagement. *Transplantation* 79, 1040–1044.
- Frenzel, L.P., Abdullah, Z., Kriegeskorte, A.K., Dieterich, R., Lange, N., Busch, D.H., Krönke, M., Utermöhlen, O., Hescheler, J., and Saric, T. (2009). Role of natural-killer group 2 member D ligands and intercellular adhesion molecule 1 in natural killer cell-mediated lysis of murine embryonic stem cells and embryonic stem cell-derived cardiomyocytes. *Stem Cells* 27, 307–316.
- Guidotti, L.G., Ando, K., Hobbs, M.V., Ishikawa, T., Runkel, L., Schreiber, R.D., and Chisari, F.V. (1994). Cytotoxic T lymphocytes inhibit hepatitis B virus gene expression by a noncytolytic mechanism in transgenic mice. *Proc. Natl. Acad. Sci. USA* 91, 3764–3768.
- Guidotti, L.G., Ishikawa, T., Hobbs, M.V., Matzke, B., Schreiber, R., and Chisari, F.V. (1996). Intracellular inactivation of the hepatitis B virus by cytotoxic T lymphocytes. *Immunity* 4, 25–36.
- Koch, C.A. and Platt, J.L. (2007). T cell recognition and immunity in the fetus and mother. *Cell. Immunol.* 248, 12–17.
- Koch, C.A., Geraldes, P., and Platt, J.L. (2008). Immunosuppression by embryonic stem cells. *Stem Cells* 26, 89–98.
- Kofidis, T., deBruin, J.L., Tanaka, M., Zwierchonska, M., Weissman, I., Fedoseyeva, E., Haverich, A., and Robbins, R.C. (2005). They are not stealthy in the heart: embryonic stem cells trigger cell infiltration, humoral and T-lymphocyte-based host immune response. *Eur. J. Cardiothorac. Surg.* 28, 461–466.
- Laskarin, G., Kammerer, U., Rukavina, D., Thomson, A.W., Fernandez, N., and Blois, S.M. (2007). Antigen-presenting cells and materno-fetal tolerance: an emerging role for dendritic cells. *Am. J. Reprod. Immunol.* 58, 255–267.
- Li, L., Baroja, M.L., Majumdar, A., Chadwick, K., Rouleau, A., Gallacher, L., Ferber, I., Lebkowski, J., Martin, T., Madrenas, J., et al. (2004). Human embryonic stem cells possess immune-privileged properties. *Stem Cells* 22, 448–456.
- Ljunggren, H.G. and Karre, K. (1990). In search of the 'missing self': MHC molecules and NK cell recognition. *Immunol. Today* 11, 237–244.
- Magliocca, J.F., Held, I.K., and Odorico, J.S. (2006). Undifferentiated murine embryonic stem cells cannot induce portal tolerance but may possess immune privilege secondary to reduced major histocompatibility complex antigen expression. *Stem Cells Dev.* 15, 707–717.
- Medema, J.P., de Jong, J., Peltenburg, L.T., Verdegaa, E.M., Gorter, A., Bres, S.A., Franken, K.L., Hahne, M., Albar, J.P., Melief, C.J., et al. (2001a). Blockade of the granzyme B/perforin pathway through overexpression of the serine protease inhibitor PI-9/SPI-6 constitutes a mechanism for immune escape by tumors. *Proc. Natl. Acad. Sci. USA* 98, 11515–11520.
- Medema, J.P., Schuurhuis, D.H., Rea, D., van Tongeren, J., de Jong, J., Bres, S.A., Laban, S., Toes, R.E., Toebes, M., Schumacher, T.N., et al. (2001b). Expression of the serine protease inhibitor 6 protects dendritic cells from cytotoxic T lymphocyte-induced apoptosis: differential modulation by T helper type 1 and type 2 cells. *J. Exp. Med.* 194, 657–667.
- Menard, C., Hagege, A.A., Agbulut, O., Barro, M., Morichetti, M.C., Brasselet, C., Bel, A., Messas, E., Bissery, A., Bruneval, P., et al. (2005). Transplantation of cardiac-committed mouse embryonic stem cells to infarcted sheep myocardium: a pre-clinical study. *Lancet* 366, 1005–1012.
- Min, J.Y., Yang, Y., Sullivan, M.F., Ke, Q., Converso, K.L., Chen, Y., Morgan, J.P., and Xiao, Y.F. (2003). Long-term improvement of cardiac function in rats after infarction by transplantation of embryonic stem cells. *J. Thorac. Cardiovasc. Surg.* 125, 361–369.

- Moffett, A. and Loke, C. (2006). Immunology of placentation in eutherian mammals. *Nat. Rev. Immunol.* 6, 584–594.
- Morello, D., Duprey, P., Israel, A., and Babinet, C. (1985). Asynchronous regulation of mouse H-2D and β -2 microglobulin RNA transcripts. *Immunogenetics* 22, 441–452.
- Nussbaum, J., Minami, E., Laflamme, M.A., Virag, J.A., Ware, C.B., Masino, A., Muskheili, V., Pabon, L., Reinecke, H., and Murry, C.E. (2007). Transplantation of undifferentiated murine embryonic stem cells in the heart: teratoma formation and immune response. *FASEB J.* 21, 1345–1357.
- Ozato, K., Wan, Y.J., and Orrison, B.M. (1985). Mouse major histocompatibility class I gene expression begins at mid-somite stage and is inducible in earlier-stage embryos by interferon. *Proc. Natl. Acad. Sci. USA* 82, 2427–2431.
- Riley, J.K. (2008). Trophoblast immune receptors in maternal-fetal tolerance. *Immunol. Invest.* 37, 395–426.
- Robertson, N.J., Brook, F.A., Gardner, R.L., Cobbold, S.P., Waldmann, H., and Fairchild, P.J. (2007). Embryonic stem cell-derived tissues are immunogenic but their inherent immune privilege promotes the induction of tolerance. *Proc. Natl. Acad. Sci. USA* 104, 20920–20925.
- Rukavina, D. and Podack, E.R. (2000). Abundant perforin expression at the maternal-fetal interface: guarding the semiallogeneic transplant? *Immunol. Today* 21, 160–163.
- Rukavina, D., Rubesa, G., Gudelj, L., Haller, H., and Podack, E.R. (1995). Characteristics of perforin expressing lymphocytes within the first trimester decidua of human pregnancy. *Am. J. Reprod. Immunol.* 33, 394–404.
- Sayers, T.J., Brooks, A.D., Ward, J.M., Hoshino, T., Bere, W.E., Wiegand, G.W., Kelly, J.M., and Smyth, M.J. (2001). The restricted expression of granzyme M in human lymphocytes. *J. Immunol.* 166, 765–771.
- Swijnenburg, R.J., Tanaka, M., Vogel, H., Baker, J., Kofidis, T., Gunawan, F., Lebl, D.R., Caffarelli, A.D., de Bruin, J.L., Fedoseyeva, E.V., et al. (2005). Embryonic stem cell immunogenicity increases upon differentiation after transplantation into ischemic myocardium. *Circulation* 112, 1166–1172.
- Teramoto, K., Hara, Y., Kumashiro, Y., Chinzei, R., Tanaka, Y., Shimizu-Saito, K., Asahina, K., Teraoka, H., and Arai, S. (2005). Teratoma formation and hepatocyte differentiation in mouse liver transplanted with mouse embryonic stem cell-derived embryoid bodies. *Transplant Proc.* 37, 285–286.
- Tian, L., Catt, J.W., O'Neill, C., and King, N.J. (1997). Expression of immunoglobulin superfamily cell adhesion molecules on murine embryonic stem cells. *Biol. Reprod.* 57, 561–568.
- Utermöhlen, O. and Krönke, M. (2007). Survival of priceless cells: active and passive protection of embryonic stem cells against immune destruction. *Arch. Biochem. Biophys.* 462, 273–277.
- van Houdt, I.S., Oudejans, J.J., van den Eertwegh, A.J., Baars, A., Vos, W., Bladergroen, B.A., Rimoldi, D., Muris, J.J., Hooijberg, E., Gundy, C.M., et al. (2005). Expression of the apoptosis inhibitor protease inhibitor 9 predicts clinical outcome in vaccinated patients with stage III and IV melanoma. *Clin. Cancer Res.* 11, 6400–6407.
- Wobus, A.M., Holzhausen, H., Jakel, P., and Schoneich, J. (1984). Characterization of a pluripotent stem cell line derived from a mouse embryo. *Exp. Cell Res.* 152, 212–219.
- Yokoyama, W.M. (2005). Natural killer cell immune responses. *Immunol. Res.* 32, 317–325.

Received March 27, 2009; accepted June 5, 2009

10. Acknowledgements

Special thanks to my supervisor Professor Dr. Claudia Wickenhauser. She made this PhD thesis possible and supported me always with best advice and great scientific and also clinical knowledge. She gave me the opportunity to join different scientific working groups to enlarge my skills and every day she supports my clinical training. Furthermore she was and still is my academic mentor and friend.

Many thanks to Professor Dr. Hans-Peter Dienes and Professor Dr. Christian Wittekind, head of the Institutes of Pathology in Cologne and Leipzig, respectively, who gave me the opportunity to work in their institutes. Furthermore, special thanks to Professor Dr. Wittekind for his trust in my skills and for the responsibility of the molecular diagnostics.

I want to thank all the scientific and technical staff of the Institutes of Pathology in Cologne and Leipzig, in particular Priv. Doz. Dr. Kai Breuhahn, Priv. Doz. Dr. Margarete Odenthal, Eva Varus and Silke Kummer. “Without your support this thesis would have never been written.”

Professor Dr. Joachim L. Schultze and Professor Dr. Mats Paulsson, thank you for supervising my thesis during my MD/PhD Program. Furthermore I want to thank Dr. Debora Grosskopf-Kroiher for her uncomplaining and capable help during my MD/PhD Program.

For critical proofreading of this PhD thesis I would like to thank Cathy Purser, Professor Dr. Horst Geilhausen and especially my mother-in-law Dr. Barbara Geilhausen.

Last but not least, I want to thank my family along with Ali Korsch and the most important person at my side, my beloved wife, Kristin Siebolts. They were always there for me and gave me the support only a family can give.

11. Curriculum vitae / List of publications

Personal Data

Name: Udo Siebolts
Birth date: January 15th, 1972
Place of birth: Aurich, Germany
Citizenship: German

Academic Preparation

1992-1994 Pre- Degree in Biology; University of Cologne
1994-1998 Diploma in Biology; Carl von Ossietzky University, Oldenburg
1998-2004 Medical School, University of Cologne
12.2004 Approbation (medical registration), Regierungspräsidium Köln
Since 2005 Interdisciplinary Program Molecular Medicine, University of Cologne
2006 Medical Degree (Dr. med.), University of Cologne

Professional Experience

1999-2004 Lecturer for clinical science, Nursing School, University of Cologne
2004-2008 Lecturer for microscopical anatomy, Medical Technician School, University of Cologne
2004-2008 Resident physician, Institute of Pathology, University of Cologne
Since 2008 Resident physician, Institute of Pathology, University Hospital of Leipzig
Since 2009 Head of molecular pathology diagnostics laboratory, University Hospital of Leipzig
Since 2010 Member of the Working Group Haematopathology, German Association of Pathology
Since 2010 Founding member of the Working Group Molecular Diagnostics, German Association of Pathology

Oberschmid B, **Siebolts U**, Mechtel D, Kreibich U, Beller A, Wickenhauser C. M protein deposition in the skin: a rare manifestation of Waldenström macroglobulinemia. *Int J Hematol*. 2011 Mar;93(3):403-5. Epub 2011 Mar 8. PubMed PMID: 21384096.

Siebolts U, Lange T, Niederwieser D, Wickenhauser C. Allele-specific wild-type blocker quantitative PCR for highly sensitive detection of rare JAK2 p.V617F point mutation in primary myelofibrosis as an appropriate tool for the monitoring of molecular remission following therapy. *J Clin Pathol*. 2010 Apr;63(4):370-2. PubMed PMID: 20354212.

Utermöhlen O, Baschuk N, Abdullah Z, Engelmann A, **Siebolts U**, Wickenhauser C, Stocking C, Krönke M. Immunologic hurdles of therapeutic stem cell transplantation. *Biol Chem*. 2009 Oct;390(10):977-83. Review. PubMed PMID: 19642871.

Markert E, **Siebolts U**, Habbig S, Odenthal M, Dienes HP, Stippel DL, Hoppe B, Wickenhauser C. Evolution of PTLT following renal transplantation in a child. *Pediatr Transplant*. 2009 May;13(3):379-83. Epub 2008 Oct 7. PubMed PMID: 19017284.

Markert E, **Siebolts U**, Odenthal M, Kreuzer KA, Wickenhauser C. High diagnostic value of morphologic examination and molecular analysis of bone marrow biopsies in a case of BCR-ABL+ CML with clusters of blasts. *Int J Hematol*. 2009 Apr;89(3):294-7. Epub 2009 Feb 20. PubMed PMID: 19229589.

Siebolts U, Breuhahn K, Hennecke A, Schultze JL, Wickenhauser C. Imbalance of DNA-dependent protein kinase subunits in polycythemia vera peripheral blood stem cells. *Int J Cancer*. 2009 Feb 1;124(3):600-7. PubMed PMID: 19004005.

Siebolts U, Varnholt H, Drebber U, Dienes HP, Wickenhauser C, Odenthal M. Tissues from routine pathology archives are suitable for microRNA analyses by quantitative PCR. *J Clin Pathol*. 2009 Jan;62(1):84-8. Epub 2008 Aug 28. PubMed PMID: 18755714; PubMed Central PMCID: PMC2603282.

Odenthal M, **Siebolts U**, Ernestus K, Disse D, Dienes HP, Wickenhauser C. Immunoglobulin heavy chain gene analysis in bone marrow biopsies and corresponding lymph node specimens: dependency on pre-treatment, histological subtype and extension of B-cell lymphoma. *Int J Mol Med*. 2008 May;21(5):569-76. PubMed PMID: 18425348.

Siebolts U, Thiele J, Zander T, Ditschkowski M, Beelen DW, Kröger N, Fehse B, Wickenhauser C. Differences in proportion and dynamics of recipient hematopoiesis following hematopoietic cell transplantation in CML and IMF. *Oncol Rep*. 2008 Jan;19(1):287-92. PubMed PMID: 18097609.

Veit G, Zimina EP, Franzke CW, Kutsch S, **Siebolts U**, Gordon MK, Bruckner-Tuderman L, Koch M. Shedding of collagen XXIII is mediated by furin and depends on the plasma membrane microenvironment. *J Biol Chem*. 2007 Sep 14;282(37):27424-35. Epub 2007 Jul 11. PubMed PMID: 17627939.

Thiele J, Varus E, **Siebolts U**, Kvasnicka HM, Wickenhauser C, Metz KA, Beelen DW, Ditschkowski M, Zander A, Kröger N. Dualism of mixed chimerism between hematopoiesis and stroma in chronic idiopathic myelofibrosis after allogeneic stem cell transplantation. *Histol Histopathol*. 2007 Apr;22(4):365-72. PubMed PMID: 17290346.

Gerharz M, Baranowsky A, **Siebolts U**, Eming S, Nischt R, Krieg T, Wickenhauser C. Morphometric analysis of murine skin wound healing: standardization of experimental procedures and impact of an advanced multitissue array technique. *Wound Repair Regen*. 2007 Jan-Feb;15(1):105-12. PubMed PMID: 17244326.

Kappert K, Sparwel J, Sandin A, Seiler A, **Siebolts U**, Leppänen O, Rosenkranz S, Ostman A. Antioxidants relieve phosphatase inhibition and reduce PDGF signaling in cultured VSMCs and in restenosis. *Arterioscler Thromb Vasc Biol*. 2006 Dec;26(12):2644-51. Epub 2006 Sep 21. PubMed PMID: 16990553.

Siebolts U, Ates M, Spitz R, Thiele J, Wickenhauser C. Quantification of clonal hematopoiesis in polycythemia vera. *Virchows Arch*. 2005 Dec;447(6):947-53. Epub 2005 Aug 19. PubMed PMID: 16133363.

Wickenhauser C, Pérez F, **Siebolts U**, Lorenzen J, Varus E, Frimpong S, Thiele J. Structural, antigenetic and transcriptional characteristics in peripheral blood CD34+ progenitor cells from polycythemia vera patients: evidence for delayed determination. Int J Oncol. 2003 Aug;23(2):437-43. PubMed PMID: 12851693.

Leipzig, den 21.04.2011



Dr. Udo Siebolts